Engineering of Polyphenol Metabolism in Tomatoes to enhance Anti-Cancer Activities

Katharina Bulling

A thesis submitted to the University of East Anglia for the degree of Doctor of Philosophy

John Innes Centre
Norwich
September 2013

© This copy of the thesis has been supplied on condition that anyone who consults it is understood to recognise that its copyright rests with the author and that use of any information derived there-from must be in accordance with current UK Copyright Law. In addition, any quotation or extract must include full attribution

Abstract

Anthocyanins are polyphenolic plant pigments that are responsible for much of the attractive colour displays found in many flowers, fruit and vegetables. Anthocyanins are divided into different classes based on the number of hydroxyl groups on their phenyl B-ring and subsequent side chain modifications.

It has been shown in our laboratory that the introduction of the regulatory genes *Delila* and *Rosea*1 activates the biosynthetic pathway leading to accumulation of trihydroxylated anthocyanins in tomatoes. Tomato DFR substrate specificity for trihydroxylated precursors prevents the formation of other anthocyanin classes. By inhibiting the activity of F3’5’H, blocking biosynthesis of trihydroxylated anthocyanins, and introducing a non-specific DFR from *A. majus*, I developed two transgenic tomato lines that produced mono- and dihydroxylated anthocyanins. My work demonstrated that tomatoes could be enriched with different classes of anthocyanins using a metabolic engineering approach.

Dietary consumption of plant secondary metabolites such as anthocyanins and other polyphenols are linked to a reduced risk of developing chronic, non-communicable diseases such as cancer, type 2 diabetes and cardiovascular diseases. High-anthocyanin tomato extracts induced cell death, cell cycle alteration and apoptosis in the human breast cancer cell lines, MCF-7 and MDA-MB-231, whilst WT tomato extracts exerted no biological effects. Purified anthocyanins and polyphenolic compounds had no or little effect on the metabolic status of breast cancer cells, suggesting that anthocyanins exert their biological effects in synergy with other components in the food matrix.

Polyphenolic compounds may act as chemosensitizers for the treatment of tumours with chemotherapeutic agents. Co-treatment of breast cancer cells with the chemotherapeutic agents, doxorubicin or roscovitine, and high-anthocyanin or -resveratrol tomato extracts showed that dietary polyphenols might potentiate the effects of pharmacological agents *in vitro*.

This work demonstrated that the health benefits of dietary plants can be significantly improved through nutritional enrichment with plant bioactives using metabolic engineerin

Acknowledgements

I am dedicating this thesis to my parents, who have always supported me I all my decisions and without whom I never would have been able to pursue my dreams and goals. Everything I achieved, I owe to you, your guidance and knowledge.

Dylan and Cathie, I am grateful for your support and scientific guidance throughout this project. You led me into a field, of which I did not know anything at the beginning but which became a personal passion and interest that has extended way beyond my own research.

A big thanks to all the past and present lab members, many of which became good friends and shared my best and worst lab moments. Research can be solitary at times but thanks to Eugenio, Yang, Kalyani, Daniel(s) and Christian I never felt lonely. A special thanks to Lionel, Dee and everybody else at the John Innes and UEA, who has supported me professionally and personally throughout the years.

Monira, I could not have wished for a better friend. Our friendship has lasted for almost twenty years now, survived many thousands kilometres of separation, the ups and downs of life but there is nothing that will ever come between us. Thank you!

Thanks to all my friends here in Norwich (Caitlan, Olivia, Doreen, Simon, Sarah etc.), the last four years would have not been the same without you. Caitlan, thank you for your friendship and support throughout those challenging and at times, stressful last two years. And thanks to those special people far away. To my friend Mahyar, who I can trust like nobody else and who I will always deeply care for. To Andrés, who reappeared in my life just at the right time and is inspiring me in so many ways.

Very special thanks to my brother, who I can always count on and without whom life just would not be the same

Table of Contents

List of Figures

List of Tables

General Abbreviations

A	Absorbance
A. tumefasciens	*Agrobacterium tumefasciens*
A. majus	*Antirrhinum majus*
ACN	Acetonitrile
ANS	Anthocyanin Synthase
BCA	Bicinchoninic Acid
bHLH	basic Helix-Loop-Helix
bp	base pair
BSA	Bovine Serum Albumin
CHI	Chalcone isomerase
CHS	Chalcone synthase
CVD	Cardiovascular disease
Cy	Cyanidin
°C	Degree Centigrade
DFR	Dihydroflavonol-4-Reductase
DHK	Dihydrokaempferol
DHM	Dihydromyricetin
DHQ	Dihydroquercetin
dH_2O	Distilled Water
DMEM	Dulbecco's Modified Eagle Medium
dNTPs	Deoxyribonucleotide Triphosphates
Dox	Doxorubicin
Dp	Delphinidin
E. coli	*Escherichia coli*
EDTA	Ethylenediaminetetraacetic Acid
EtOH	Ethanol
F3H	Flavanone 3-Hydroxylase
F3'H	Flavonoid 3'-Hydroxylase
F3'5'H	Flavonoid 3',5'-Hydroxylase
FACS	Fluorescent Activated Cell Sorting
FLS	Flavonol Synthase
g	Gravitational Acceleration
g	Gram(s)
h	Hour(s)
HCl	Hydrochloric acid
HPLC	High-Performance Liquid Chromatography
JIC	John Innes Centre
kb	Kilobase pair
kDa	Kilo Dalton
L	Litre
M	Molar
MeOH	Methanol
min	Minute(s)
mL	Millilitre(s)
mM	Millimolar
Mv	Malvidin
ng	Nanogram(s)
nt	Nucleotide(s)

OD	Optical Density
oligo	Oligonucleotide
PAGE	Polyacrylamide Gel Electrophoresis
PBS	Phosphate Buffered Saline
PCR	Polymerase Chain Reaction
PDA	Photo Diode Detector
Pe	Peonidin
Pl	Pelargonidin
Pt	Petunidin
RT-PCR	Reverse-Transcriptase Polymerase Chain Reaction
RNA	Ribonucleic acid
Rosc	Roscovitine
SDS	Sodium Dodecylsulphate
SEM	Standard Error of Mean
S. lycopersicum	*Solanum Lycopersicum*
Taq	*Thermophilus acquarius*
TBST	Tris Buffer Saline Tween
TE	Tris/EDTA
U	Enzymatic Unit
UEA	University of East Anglia
UV	Ultra Violet light
V	Volt
vol	Volume
v/v	Volume per Volume
WST-1	Water-Soluble Tetrazolium Salt-1
WT	Wild type
w/v	Weight per Volume
µ	Micro, 10^{-6} meter
µg	Microgram(s)
µL	Microlitre(s)
µM	Micromolar

1 General Introduction

1.1 Plant secondary metabolism

Plants synthesise a vast range of organic molecules that have been traditionally classified as primary or "essential" and secondary metabolites. Primary metabolites are associated with the survival and reproduction of the plant and have essential roles in photosynthesis, respiration, growth and development. The other group of metabolites, many of which accumulate in high amounts in some species, have been referred to historically as non-essential or secondary metabolites. Initially associated with inessentiality, Williams (1989) summarized some of the historic views regarding the purpose of secondary metabolites as "waste or detoxification products", "a reservoir of non-functional variety out of which new functional processes can emerge" or "designed to permit a network of enzymes that is operative in primary metabolism". However, it is now recognized that many of these compounds are involved in crucial plant metabolic pathways such as lignin biosynthesis, while others play important roles in plant chemical defence mechanisms or act as signalling molecules to attract pollinators and seed-dispersing animals. Secondary metabolites are important for the plant's survival and fitness and represent adaptive traits that were subjected to natural selection and evolution.

Interest and understanding of secondary metabolism in plants has grown steadily, and tens of thousands of structurally different compounds have been identified so far. Despite their structural diversity, secondary plant metabolites can be divided into three, large families: phenolics, terpenes, and alkaloids, of which the phenolics are the most widespread family o metabolites.

Phenolic compounds are ubiquitous in plants and are characterized by their hydroxylated aromatic ring(s). Several thousand phenolic structures have been identified so far, ranging from low molecular weight, single aromatic-ringed compounds, to highly complex tannins and polyphenols. Phenolics are classified according to the number and arrangement of their carbon atoms that are usually decorated with sugars and organic acids, and are divided into two groups: the flavonoids and the non-flavonoids.

Table 1i: Phenolic compound classification.

Compound family	**Basic carbon skeleton**
simple phenols, benzoquinones	C_6
phenolic acids and aldehydes	C_6–C_1
acetophenones, phenylacetic acids	C_6–C_2
hydroxycinnamic acids, coumarins, phenylpropanes, chromones	C_6–C_3
Naphthoquinones	C_6–C_4
Xanthones	C_6–C_1–C_6
stilbenes, anthraquinones	C_6–C_2–C_6
flavonoids, isoflavonoids, neoflavonoids	**C_6–C_3–C_6**
bi-, triflavonoids, proanthocyanidin dimers, trimmers	$(C_6$–C_3–$C_6)_{2,3}$
lignans, neolignans	$(C_6$–$C_3)_2$
Lignins	$(C_6$–$C_3)n$
catechol melanins, phlorotannins	$(C_6)n$
condensed tannins	$(C_6$–C_3–$C_6)n$

1.2 Flavonoid Pathway

The flavonoids are a diverse group of aromatic molecules that are derived from p-coumaroyl coenzyme A (CoA) and malonyl-CoA. Flavonoids comprise fifteen carbons, with two aromatic rings connected by a three-carbon bridge (C_6-C_3-C_6). This large group includes seven major subclasses, of which six (chalcones, flavones, flavonols, flavandiols, anthocyanins, and condensed tannins) are commonly found in higher plants. The aurones form the seventh group and are widespread but not ubiquitous in higher plants. Flavonoids serve as UV protectants, signal molecules in plant-microbe interactions and antibiotics in plant defences responses as well as attractants for pollinators and seed dispersers. Many of the striking colours observed in fruits, flowers and other plant organs can be attributed to the presence of various flavonoids.

Flavonoids are synthesised through the concerted, sequential action of several structural genes encoding enzymes catalysing the biosynthetic steps in the flavonoid pathway (Martin and Gerats, 1993). The pathway is well understood and conserved among seed plants. All flavonoids are produced from malonyl-CoA and 4-coumaroyl CoA, which is derived from the amino acid, phenylalanine. The molecule 4-coumaroyl CoA, is formed through three enzymatic conversions collectively known as general phenylpropanoid metabolism catalysed by phenylalanine ammonia-lyase (PAL), cinnamate 4-hydroxylase (C4H), and 4-coumarate:CoA ligase (4CL; Davies and Schwinn, 2006). The first committed step in flavonoid biosynthesis is the formation of naringenin chalcone catalyzed by chalcone synthase (CHS) which condenses one molecule of 4-coumaroyl CoA and three molecules of malonyl CoA (Figure 1.1). Naringenin chalcone is required for the synthesis of flavones, flavonols and anthocyanins but not stilbenes. Stilbenes such as resveratrol are formed from 4-coumaroyl CoA and malonyl CoA *via* the action of stilbene synthase, an enzyme which is structurally related to CHS. Naringenin chalcone is rapidly isomerized into the colourless flavanone, naringenin, by the enzyme chalcone isomerase (CHI), although this isomerisation can also occur spontaneously. Naringenin is a major branch point in flavonoid biosynthesis: Isoflavone synthase (IFS) directs biosynthesis towards isoflavonoid production, and flavanone 3-hydroxylase (F3H), a 2-oxoglutarate-dependent dioxygenase (OGD), hydroxylates naringenin at the 3-position yielding dihydrokaempferol (DHK), a dihydroflavonol. Using DHK as a substrate two cytochrome P450 enzymes, flavonoid-3'-hydroxylase (F3'H) and flavonoid-3'5'-hydroxylase (F3'5'H), catalyse the hydroxylation of DHK to form dihydroquercetin (DHQ) and dihydromyricetin (DHM), respectively. F3'H and F3'5'H are key enzymes in determining the structure of anthocyanins and thus their colour. They modify the hydroxylation pattern of the B-ring and play key roles in the formation of cyanidin and delphinidin, respectively.

The dihydroflavonols DHK, DHQ and DHM serve as precursors for the formation of the three flavonols, kaempferol, quercetin and myricetin, respectively, through the action of flavonol synthase (FLS). FLS is not required for production of anthocyanin pigments but competes with F3'5'H, F3'H and DFR for common dihydroflavonol substrates and may influence anthocyanin synthesis (de Jong et al., 2004, Luo et al., 2008). Further downstream, dihydroflavonol 4-reductase (DFR) reduces kaempferol, quercetin and myricetin to their corresponding leucoanthocyanidins.

Leucoanthocyanidins are substrates for anthocyanidin synthase (ANS), another member of the OGD family that catalyses the synthesis of the corresponding coloured anthocyanidins, pelargonidin (Pg), cyanidin (Cy) and delphinidin (Dp; Tanaka et al., 2008).

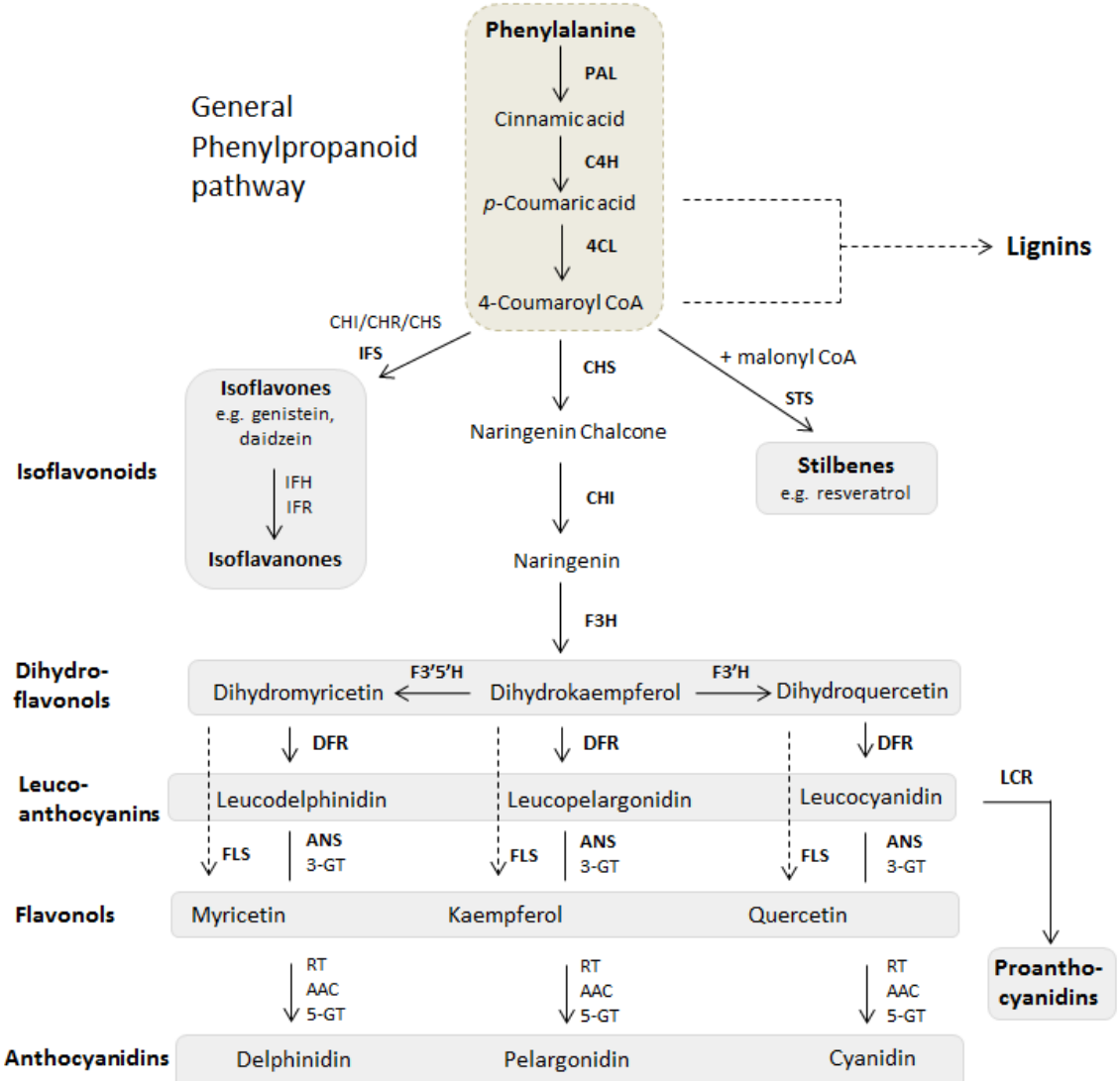

Figure 1.1: Schematic representation of the phenylpropanoid pathway leading to anthocyanin biosynthesis. PAL, phenylalanine ammonia lyase; 4CL, 4-coumarate:coenzyme A ligase; C4H, cinnamate 4-hydroxylase; C3H, 4-coumarate 3-hydroxylase; IFS, isoflavone synthase; IFH, isoflavone hydroxylase; IFR, isoflavone reductase; STS, stilbene synthase; CHS, chalcone synthase; CHI, chalcone isomerase; F3H, flavanone-3-hydroxylase; F3'H, flavonoid-3'-hydroxylase; F3'5'H, flavonoid-3'5'-hydroxylase; FLS, flavonol synthase; DFR, dihydroflavonol reductase; LCR, leucoanthocyanidin reductase; ANS, anthocyanidin synthase; 3-GT, flavonoid 3-O-glucosyltransferase; RT, flavonoid 3-O-glucoside-rhamnosyltransferase AAC, anthocyanin acyltransferase; 5-GT, flavonoid-5-glucosyltransferase; GST, glutathione S-transferase.

Within the family *Solanaceae*, which included the crop species, tomato and potato, one biosynthetic enzyme in the main flavonoid pathway, DFR, shows substrate specificity for DHM and, less effectively, for DHQ but cannot accept DHK as a substrate. *Petunia hybrida* is one of the classical model plant species in which the flavonoid pathway and anthocyanin biosynthesis in particular, has been thoroughly analysed. In *Petunia*, both delphinidin- and cyanidin-derivatives are formed, but no pelargonidin pigments are produced. This is a consequence of the substrate specificity of the *Petunia* DFR, which cannot reduce the pelargonidin precursor molecule DHK (Meyer et al., 1987). Meyer and colleagues showed that by transforming *Petunia* with a DFR gene from maize (*Zea Mays*), which does not have the same strict substrate specificity as the *Petunia* DFR, pelargonidin-type pigments could be produced in *Petunia*. DFR catalyses the conversion of dihydroquercetin into leucocyanidin that can then be further processed into pelargonidin-3-glucosides. Johnson and collaborators (2001a) further investigated the substrate specificity of DFR and identified a 26 amino acid region in the *Gerbera dfr* gene. This was highly variable between different species and likely to determine substrate specificity. *Petunia* and *Gerbera* DFR cannot convert DHK but a site-directed mutation of asparagine 134 to leucine enabled *Gerbera* DFR to accept DHK as substrate, suggesting a crucial role of this amino acid in DFR substrate specificity. The DFR from *Antirrhinum majus* (*A. majus*) can convert DHK to leucopelargonidin as evidenced by the production of pink pelargonidin in the *eos* mutant of *A. majus* (*eos* encodes F3'H).

In tomato, naringenin chalcone, rutin and kaempferol-3-*O*-rutinoside are the main flavonoids and predominantly accumulate in the peel of the fruit. Transcripts of *chs*, *f3h* and *fls*, encoding flavonol biosynthetic enzymes, have been detected in tomato peel. In contrast, *chi* transcript levels are below the levels of detection resulting in the accumulation of the CHI substrate, naringenin chalcone. Flavonoids are virtually absent from the flesh tissue, suggesting that the flavonoid biosynthetic pathway is active only in tomato peel tissue Muir et al. (2001).

1.3 Anthocyanins

Anthocyanins are members of the large group of secondary plant metabolites known as flavonoids. Their name is derived from the Greek; *anthos* (flower) and *kyanos* (blue) based on the blue colour of the corn flower from which they were first isolated (Willstätter and Everest, 1913). They are widespread plant pigments found in most fruit, vegetables and flowers as well as other plant organs. Anthocyanins are responsible for most of the orange-to-blue coloration in pigmented plant tissues. They are thought to act primarily as attractants to pollinators and seed dispersing animals. In addition, anthocyanins are often produced in stem and leaf tissues of young seedlings and some mature plants, indicating a possible role as protectants from UV light, oxidative stress and other environmental stresses (Kubasek et al., 1992). More than 600 naturally occurring anthocyanins have been reported so far, with more structural variants likely to be discovered (Andersen and Jordheim, 2006). Despite their extraordinary variety, just six types of anthocyanins, delphinidin (Dp), cyanidin (Cy), pelargonidin (Pl), peonidin (Pe), petunidin (Pt) and malvidin (Mv), account for most of the total anthocyanin production in plants (Figure 1.2). Glycosides of the non-methylated anthocyanidins Dp, Cy and Pg are the most ubiquitously synthesised variants and are found in 80% of pigmented leaves, 69% of fruits and 50% of flowers (Kong et al., 2003). Modification of the anthocyanins occurs by glycosylation or acylation with the latter resulting in a blue shift and stabilisation of the compounds in solution. Glycosylation leads to a reddening effect (Tanaka et al., 2008).

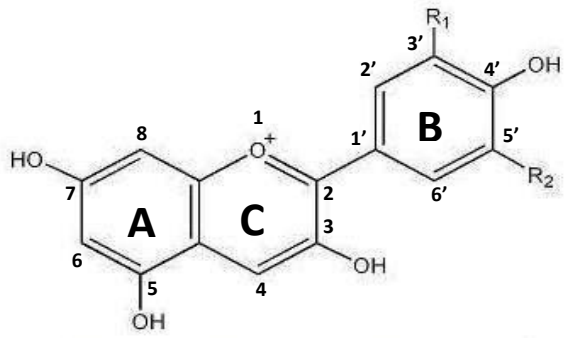

Anthocyanidin	
Pelargonidin	$R_1 = R_2 = H$
Cyanidin	$R_1 = OH$, $R_2 = H$
Delphinidin	$R_1 = R_2 = OH$
Peonidin	R_1 OCH_3, $R_2 = H$
Petunidin	R_1 OCH_3, $R_2 = OH$
Malvidin	$R_1 = R_2 = OCH_3$

Figure 1.2: Chemical structure of anthocyanin aglycones. Anthocyanins differ structurally in their substitutions on the phenyl B-ring and can be further modified by the attachment of sugar residues that may involve acylation with aromatic acids including *p*-coumaric, caffeic, ferulic, sinapic, gallic or p-hydroxybenzoic acids, and/or aliphatic acids such as malonic, acetic, malic, succinic or oxalic acids. These acyl substitutions are commonly, but not exclusively, bound to the C3 sugar.

Anthocyanins are polar, water soluble glycosides and acyloglycosides that are mainly stored in the vacuoles in the epidermal tissues of flowers and fruits as well as in stems and leaves. Due to their long 2-phenylbenzopyrylium (flavylium) chromophore of eight conjugated double bonds carrying a positive charge, they are strongly coloured under acidic conditions, where they behave like pH indicators, being red at low pH, blue at intermediate pH and colourless at high pH (Mazza and Miniati, 1993). In acidic, aqueous solutions, four anthocyanin species exist in equilibrium: the red coloured flavylium cation AH^+, the blue quinoidal base, as well as the colourless carbinol pseudobase and the chalcone (Mazza and Brouillard, 1987, Brouillard and Delaporte, 1977).

1.3.1 Biosynthesis and chemistry

1.3.1.1 Anthocyanin aglycones

All anthocyanin aglycones, also known as anthocyanidins, share a common structure consisting of a C-6 (A ring)-C-3 (C ring)-C-6 (B ring) carbon skeleton (Figure 1.2).

Depending on the hydroxylation and/or methylation pattern on different positions on the A-ring, and the B-ring in particular, 23 naturally occurring anthocyanidins have been identified so far in higher plants (Tanaka et al., 2008, Andersen and Jordheim, 2006). The variation in colouring between the aglycones is due to differences in the hydroxylation pattern on the B ring: An increase in the number of hydroxyl groups causes a shift in the visible absorption maximum to longer wavelengths, leading to a colour change from orange to blue (Mazza and Miniati, 1993). Pg is hydroxylated only in the 4'-position of the B-ring and responsible for orange, salmon, pink and red colours. Cy has hydroxyl groups in the 3'- and 4'-positions providing most magenta and crimson flower colours. Hydroxylation of the Dp molecule occurs at positions 3', 4', and 5' positions giving rise to most purple and blue colours (Forkmann, 1991).

1.3.1.2 Glycosylation and acylation

The extraordinary variation within the anthocyanins results from the substitution of hydroxyl groups by sugar moieties. The nature, number and position of decorating sugar moieties, as well as the acylation patterns, define each of the individual compounds. Glucose, galactose, rhamnose and rabinose and their di- and trisaccharides are the sugars most commonly bound to anthocyanidins. Glycosylation of the C3 hydroxyl group is essential for the stability of anthocyanins in solution (Mazza and Brouillard, 1987). Acyl substituents, such as aromatic acids, including *p*-coumaric, caffeic, ferulic, sinapic, gallic or *p*-hydroxybenzoic acids, and/or aliphatic acids such as malonic, acetic, malic, succinic or oxalic acids are often bound to the C3 sugar. Such modifications affect the physical and chemical properties of the molecule by altering its size and polarity.

Anthocyanin aglycones are very unstable compared to their glycosides. Glycosylation improves the stability of anthocyanins through a network of intramolecular H-bonds within the anthocyanin molecule (Borkowski et al., 2005). Hydroxylation at the C5 position and substitution at the C3 position stabilize the coloured form by protecting the anthocyanin molecule from hydration and subsequent structural transformation into the colourless forms (Mazza and Miniati, 1993). Anthocyanins differ from each other in the number and position of their hydroxyl and/or methoxy groups. Any modifications to the latter can have a marked effect on the colour intensity of the anthocyanins.

The nature and intensity of colouring depends on pigment concentration and also physicochemical conditions, such as pH, temperature and co-pigmentation. The stability of anthocyanins in solution at a given pH may vary significantly between different anthocyanins but the majority of compounds are most intensely coloured under acidic conditions. At very low pH, the red flavylium cation is generally the dominant structure. With increasing pH, its concentration decreases in favour of the blue quinoidal base. As the pH exceeds 5, hydration of the coloured structures leads to the rapid formation of the colourless pseudobase and chalcone species (Castañeda-Ovando et al., 2009, Mazza and Brouillard, 1987).

1.3.1.3 Co-pigmentation

Together with pH, co-pigmentation is the most important factor in determining anthocyanin colouration. Since its discovery in 1931 by Robinson and Robinson (1931), this phenomenon has been extensively studied and has helped to elucidate the structural transformations that anthocyanins undergo in solution. Complexation of the co-pigmentation molecule and the flavylium cation prevents hydration of the anthocyanin molecule and offers protection to the flavylium ring against water attack. Complex formation competes directly with the formation of pseudobases. Most natural anthocyanins form co-pigmentation complexes under suitable conditions and many different kinds of co-pigmentation molecules, including flavonoids, metals, amino acids, polysaccharides or even other anthocyanins, have now been identified (Brouillard, 1988). Co-pigmentation co-factors are generally colourless but upon interaction with the anthocyanin, they produce higher absorbance values (a hyperchromic shift) resulting in an intensification of colouring. Certain pigments may also give a bathochromic shift in the absorption maximum and a blueing of the colour (Boulton, 2001).

1.3.2 Regulation of anthocyanin biosynthesis

Anthocyanin biosynthesis is induced by transcription factors that regulate the expression of the structural genes involved in flavonol biosynthesis. Transcriptional regulation involves three families of proteins that are characterized by their MYB domains, basic helix-loop-helix (bHLH) domains and WD40 repeats (WDR). Regulation of biosynthetic genes late in the biosynthetic pathway leading to the

formation of anthocyanins and condensed tannins is orchestrated by a tertiary MYB-bHLH-WD40 (MBW) complex involving members of all three regulator families. Plant MYB proteins were first identified in 1987 and are the largest family of transcriptional regulators that are characterized by having either one (R1), two (R2 and R3) or three (R1, R2, R3) imperfect repeats of the MYB DNA-binding domain (Martin and Paz-Ares, 1997) that bind to specific *cis*-elements in the DNA, called MYB-binding sites. R2R3-MYB proteins are the most common MYB protein members in plants and are involved in the regulation of flavonoid biosynthesis. Different R2R3-MYB regulators control separate branches in the pathway leading to the formation of different flavonoids. MYB proteins often interact with a 200 amino acid sequence on the N-terminal side of bHLH proteins to alter gene expression. The bHLH proteins are characterized by two α-helices that are involved in DNA-binding which are separated by a loop. The loop is responsible for the three-dimensional conformation and stability of the protein and increases DNA recognition specificity (Nair and Burley, 2000, Toledo-Ortiz et al., 2003). Members of bHLH protein family can bind DNA either alone or in conjugation with MYB proteins. Several functional partnerships between MYB and bHLH transcription factors to coordinate anthocyanin biosynthesis have been identified, including maize *ZmC*1 MYB and *ZmB* bHLH, the *Petunia AN*2 MYB and *AN*1 bHLH, and the *A. majus Ros*1 MYB and *Del* bHLH (Goff et al., 1992, Goodrich et al., 1992, Schwinn et al., 2006, Quattrocchio et al., 1998).

The third group of transcriptional regulators involved in flavonoid biosynthesis are WD40 proteins which belong to a group of proteins characterized by a peptide motif of 44-60 amino acids on the N-terminal side and the WD dipeptide on the C-terminus (Smith et al., 1999). WD40 proteins are thought not have DNA-binding activity but rather enhance gene activation and facilitate protein-protein interactions in the MBW complex because they are able to interact with several proteins simultaneously. Several of the tertiary MBW complexes that regulate anthocyanin biosynthesis have been identified in different plants. In maize for example, *ZmC*1 and *ZmPL*1 (MYBs) interact with *ZmR*1, *B*1, *SN*1 and *HOPl*1 (bHLHs) and *ZmPAC*1 (WD40) to induce anthocyanin biosynthesis and a similarly complex network of transcriptional regulators has been identified in *Arabidopsis* (reviewed by Petroni and Tonelli, 2011).

MBW protein complexes are also known to regulate other branches of the flavonoid biosynthetic pathway such as proanthocyanidins that compete with anthocyanins for the products of the enzymatic reactions catalysed by DFR and ANS. In *Arabidopsis*, *AtTT*2 MYB, *AtTT*8 bHLH and *AtTTG*1 WD40 are necessary for the correct expression of BANYULS (BAN) which encodes the core enzyme of proanthocyanidin biosynthesis in seed coat of *A. thaliana* (Baudry et al., 2004). Similarly, a MBW complex regulating proanthocyanidin biosynthesis during strawberry fruit development involving the functional interaction of *FaMY*B9, *FabHLH*3 and a WD40 *FaTTG*1 was recently identified (Schaart et al., 2013). This suggests that MBW complexes probably regulate all steps in flavonol biosynthesis. To date, only one MYB-like transcriptional regulator of anthocyanin biosynthesis in tomato has been identified (Mathews et al., 2003). *ANT*1 regulates the expression of biosynthetic genes such as CHS and DFR and is involved in the regulation of genes responsible for anthocyanin glycosylation and transportation into the vacuole.

Most transcriptional regulators of anthocyanin biosynthesis are involved in the activation of the enzymatic pathway and so far, only a small number of negative regulators have been identified. Anthocyanin-deficient mutants have helped to shed light on the regulatory processes that control activation and repression of anthocyanin biosynthesis. One of the first repressors of flavonol and anthocyanins biosynthesis identified was the strawberry *FaMYB*1 MYB protein which interacts with bHLH regulators of anthocyanin biosynthesis to repress formation of anthocyanin and flavonols (Aharoni et al., 2001). In *Arabidopsis* a number of negative regulators of anthocyanin biosynthesis have been identified to date. *AtMYBL*2, a MYB protein interacts with the *TT*8 bHLH and negatively controls anthocyanin biosynthesis (Matsui et al., 2008). Similarly, *CPC*, a single-repeat R3-MYB negative regulator, tightly controls anthocyanin accumulation by competing with the R2R3-MYB transcription factor *PAP*1/2 to form the tertiary transcriptional complex required for anthocyanin biosynthesis genes (Zhu et al., 2009).

By understanding the intricate regulation of flavonoid biosynthesis, the pathway can be manipulated to engineer fruits and vegetables with novel enhanced flavonol contents and consequently nutritional content.

1.3.3 Biological roles of anthocyanins in plant

The most important function of anthocyanins is to impact the colour of the flowers and fruit in which they occur. The intense colouration of many plant reproductive and fruiting bodies provides a visual attractant for pollinators and seed-dispersing animals alike. Unsurprisingly, anthocyanins have played an important role in the coevolution of plant-animal interactions and are of substantial relevance to the plant's survival and reproduction.

Most plants also accumulate anthocyanins in their vegetative tissues where they are thought to be involved in protecting plants from herbivore attack, microbial disease and photo-induced damage. Several studies have linked increased accumulation of anthocyanins in the foliage to decreased foraging by herbivores. California maple aphids, for example, have been found to preferentially feed on yellow-orange leaves of the Japanese maple but largely ignore the leaves of red-coloured trees (Furuta, 1986). Similarly, light brown apple moths showed a significant preference for green- over red-foliaged apple trees suggesting a role for anthocyanins as herbivore deterrents (Markwick et al., 2013).

Furthermore, anthocyanins may be produced in the foliage to protect photo-sensitive defence compounds from light-induced degradation. Page and colleagues (2002) found that *Asteraceae* protect photolabile thiarubrines, a group of chemicals with strong antibacterial and antifungal activity, by surrounding them with anthocyanin-containing cells.

Under high-light conditions anthocyanins can serve as optical filters protecting the photosynthetic apparatus from reactive oxygen species (ROS)-induced damage (Gould et al., 2010, Havaux and Kloppstech, 2001, Nielsen and Simonsen, 2011, Zeng et al., 2010). Chloroplasts generate ROS when they receive more light than they can use in the dark reactions of photosynthesis. Anthocyanins in the vacuole may be able to absorb excess high-energy quanta and divert them away from the saturated photosynthetic electron transport chain. The accumulation of foliar anthocyanins has also been implicated in scavenging of free radicals (Gould et al., 2002, Wang et al., 1997) and the acquisition of tolerance to a variety of environmental stresses including chilling and freezing, desiccation and wounding.

Anthocyanins are some of the most versatile and ubiquitous secondary metabolites that are implicated in the survival and adaptivity of higher plants by conferring protection from biotic and abiotic stresses together with enhancing reproductive success by attracting pollinators and seed-dispersing animals.

1.4 Polyphenols: abundance in food

The abundance and diversity of polyphenols in different taxonomic groups is very much a reflection of evolutionary divergence in higher plants. Anthocyanins are absent from non-vascular plants such as mosses and liverworts but are found in some lower vascular plants like ferns (Chai et al., 2012, Harborne, 1965). Whilst some branches of the polyphenol metabolism such as anthocyanins are nearly ubiquitous in gymnosperms and angiosperms, their production may be limited to certain plant organs. Other phenolic compounds such as isoflavonoids in legumes, however, may be unique to a single clade. Thus, it is not surprising that dietary intake of total and different classes of polyphenolic compounds depends dramatically on individual dietary habits as well as cultural food traditions involving geographically unique plant products. For example, the influence of regional dietary habits on total polyphenol intake is evident in the relatively low mean total intake of polyphenols of only 863 ± 415 mg/day in Finnish adults reflecting their low fruit and vegetable consumption (Ovaskainen et al., 2008) compared to 2,500 to 3,000 mg/day in Spanish adults (Saura-Calixto et al., 2007).

1.5 Metabolic fate and bioavailability of anthocyanins

Polyphenols, and particularly anthocyanins, can be present in very large amounts in some dietary components. Average servings of aubergines, black grapes or berries can deliver between several hundred to thousand mg of anthocyanins. In 2005, Manach and colleagues published a comprehensive review of almost 100 studies regarding the bioavailability and bioefficacy of polyphenols in humans. Bioavailability is defined as the fraction of an administered substance that becomes available to the circulatory system or target tissue. Relative urinary excretion of the parental forms of anthocyanins ranged from 0.004% to 0.1% and plasma concentrations were usually in the order of 10 to 50 nmol/L. Similar absorption figures have also been reported in more recent studies

investigating the bioavailability of cranberry and elderberry anthocyanins (American Institute for Cancer Research, 1997, Fernandes et al., 2012). These findings suggest that bioavailability of anthocyanins is very low and often less than 0.1% of the ingested dose. Absorption and elimination of anthocyanins occurred rapidly but absorption took place with poor efficiency, possibly by absorption through the gastric wall.

However, these bioavailability values are largely based on the presence of the parent anthocyanin molecules in plasma and urine and may be significant absorption underestimates when taking anthocyanin metabolites and catabolites into consideration. Only recently, have studies, to determine tissue concentrations of anthocyanins, been conducted. Anthocyanins were recovered from several tissues, including the bladder, prostate, heart, liver, brain and adipose tissue of rats fed a high-anthocyanin diet (Fernandes et al., Serra et al., 2011). By evaluating both circulatory and tissue concentrations of anthocyanins, existing bioavailability estimates may require further review.

For decades, detection methods have focused largely on parental or intact anthocyanins. Indeed, small proportions of intact anthocyanins have been recovered from urine and serum (Serra et al., 2011), but the majority of anthocyanins are likely to undergo extensive modification and metabolism by the colonic microflora upon ingestion. Furthermore, anthocyanins undergo rearrangement in response to pH. The red flavylium cation predominates at pH 1 to 3 but with increasing pH the colourless carbinol pseudobase becomes the major component. Detection methods relying on the sole use of absorbance spectra between 500 and 550 nm (at which coloured anthocyanins show maximum absorbance) will fail to detect anthocyanins in higher pH environments, in which the colourless carbinol pseudobase dominates. Upon passage through the gastrointestinal tract the environment becomes less acidic and this is likely to lead to pH-dependent rearrangements of the anthocyanins. Whether or not this will affect absorption or bioefficacy is not known. Furthermore, anthocyanins will undergo significant post-ingestion modification, including methylation, glucuronidation and sulfation. In fact, several studies have shown that anthocyanin conjugates accounted for the majority of the recovered anthocyanins and are likely to be the predominant forms in which anthocyanins are transported in human serum and urine (American Institute for Cancer Research, 1997, Felgines et al., 2009, Felgines et al., 2007). As the compounds

pass from the small to the large intestine, they will be exposed to the colonic microflora, which are likely to contribute to the degradation and elimination of significant proportions of the ingested anthocyanins. Finally, decoration patterns of individual anthocyanin types may further impact the bioavailability of the compound. Yi and colleagues (2006) demonstrated that glucosylated anthocyanins had significantly higher transport efficiency than galactosylated anthocyanins and that increased numbers of free hydroxyl groups and fewer methoxy groups could significantly reduce bioavailability.

Additional evidence has started to emerge that suggests a beneficial association between polyphenol ingestion and gut bacterial growth. Several *in vitro* and *in vivo* studies have demonstrated that increased polyphenol ingestion may have positive effects on human health through modulation of the composition of the colonic microflora. Most studies have reported an increase in the number of *Bifidobacteria* and *Lactobacilli* which are considered beneficial for intestinal function and a suppression of *Bacteroides*, such as *Staphylococcus aureus*, *Salmonella typhimurium*, *Campylobacter jejuni*, *Listeria* and other pathogenic bacteria such as *Clostridium* and *Propionibacterium* (Dolara et al., 2005, Hidalgo et al., 2012, Park et al., 2013, Parkar et al., 2008). Bacteria such as *Clostridium* have detrimental actions on colonic mucosa and lead to diarrhoea, and subsequently, reduced nutrient uptake. Animal studies have also provided evidence that the microbial community composition differs significantly between obese and lean individuals (Backhed et al., 2004). In obese animals, a shift in the Bacteroidetes-Firmicutes ratio was observed that increased the efficiency to harvest energy from a given diet and deposit fat (Tremaroli and Backhed, 2012). Lipogenesis, and subsequently weight gain, in mice fed a high-fat diet was significantly inhibited by the administration of anthocyanin-rich orange juice but not water (Titta et al., 2010, Salamone et al., 2012). These findings suggest that polyphenolic compounds including anthocyanins can regulate pathways involved in lipid homeostasis as well as playing an important role in maintaining a healthy gut microflora. This provides some evidence for an evolutionary relationship between an ancestral diet high in polyphenol-containing fruit and vegetables and the evolution of the human superorganism.

Current understanding of the bioavailability of anthocyanins remains somewhat inconclusive. While overall bioavailability of anthocyanins is relatively low compared to other flavonoids, most absorption is likely to occur in the stomach, with some

anthocyanins or their metabolites transported to the lower gastrointestinal tract. The mechanisms by which anthocyanins are transported across cellular membranes have not been identified yet but may involve hydrolysis of the glycosides by various hydrolases and absorption of the phenolic aglycones, if similar to absorption of flavonols. Furthermore, bioavailability values reported in the literature should be reviewed in the light of newly identified circulating and excreted metabolites such as methylated and glucuronidated conjugates. Recently it has been demonstrated that the vast majority of ingested anthocyanins are not transported around the human body in their intact form but that it is their metabolites, formed in the small intestine and hepatic cells, or low molecular weight catabolites produced by the gut microflora that reach the circulatory system and body tissues to elicit bioactive effects. A large proportion of the ingested anthocyanins is metabolized to protocatechuic acid by the gut microbiome (Vitaglione et al., 2007, Tsuda et al., 1999, Aura et al., 2005). Protocatechuic acid, a simple phenolic acid, has strong antioxidative activity and potent anti-cancer properties and significantly reduced the progression of skin and liver cell tumours in rats (Tseng et al., 1998, Tanaka et al., 1993).

More research is needed to establish the role of these metabolites and catabolites in exerting health benefits and in the light of this newly emerging data, existing bioavailability values may need to be revised upwards.

1.6 Health benefits of anthocyanins

The abundance of anthocyanins in many plants consumed as foods make them possibly the most important of all dietary flavonoids. They are commonly found in dark-coloured fruits such as berries, plums, grapes, currants and cherries as well as in a number of vegetables including eggplant, red onion, red cabbage, black bean and red-leafed lettuce (Wu et al., 2006). Reports, concerning the average daily intake of anthocyanins in the US, vary significantly, with estimates ranging from as little as 12.5 mg/day reported recently by the United States Department of Agriculture (Wu et al., 2006) to as much as 200 mg/day (Kuehnau, 1976). Compared to the dietary uptake of most other health-promoting phytochemicals, these are relatively large quantities. Total anthocyanin intake depends on individual dietary choices and habits, and there have been no reports of ill effects from excessive anthocyanin consumption.

Numerous studies have shown a strong correlation between an anthocyanin-rich diet and reduced incidence of various chronic diseases, including cancer, cardiovascular diseases (CVDs) and inflammatory diseases, as well as obesity and associated age-related degenerative diseases. Following recognition of their potential health-promoting effects and their applications as natural food colorants in the food industry, research interest in dietary anthocyanins has increased significantly in recent years.

Traditionally, health-promoting effects of anthocyanins have been assigned to their powerful antioxidant capacities observed *in vitro* (Kähkönen and Heinonen, 2003, Wang et al., 1997, Wang et al., 1999). However, more recently, evidence has started to emerge that cellular effects may be mediated not only by radical scavenging but also by direct interactions between the anthocyanins and specific DNA sequences. Many of the proteins these genes encode are involved in intracellular signalling pathways, including protein kinase and lipid kinase signalling cascades (Choe et al., 2012, Hwang et al., 2011a). Inhibitory or stimulatory actions of anthocyanins are likely to be a result of anthocyanin-mediated modulation in the phosphorylation or methylation state of target molecules (Lee et al., 2010, Wang et al., 2013) and/or by alteration in gene expression (Hwang et al., 2011b, Williams et al., 2004, Titta et al., 2010). New molecular targets for anthocyanin-mediated modulation are being identified at an unprecedented speed, many of them with potentially significant implications for the prevention and management of diseases such as cancer or CVDs. The picture that is starting to emerge from both *in vitro* and *in vivo* studies is highly complex: anthocyanins, and other phytochemicals, seem to be able to exert significant regulatory effects on genes involved in cellular signalling pathways. They may be able to maintain and protect cellular homeostasis through regulation of deregulated pathways that are associated with many chronic diseases or inflammatory processes. How anthocyanins exert these remarkable biological effects, whether by direct interaction with the DNA or its translational products, remains still largely unknown. Improvement of our understanding of the molecular mechanisms that cause the observed pharmacological effects, may lead to the formulation of future dietary recommendations or even the use of anthocyanins as adjuvants in pharmacological treatment regimes.

1.6.1 Anthocyanins as anti- or prooxidants

Anthocyanins act as powerful antioxidants *in vitro*. They reduce reactive oxygen species (ROS) such as hydrogen peroxide or peroxyl radicals, scavenge superoxide anions as well as nitric radicals and prevent lipid oxidation (Pietta, 2000). The stability of an anthocyanin in an aqueous solution depends greatly on the pH. Wang and colleagues (1997) investigated the antioxidant properties of fourteen anthocyanins including the five aglycones, delphinidin, cyanidin, pelargonidin, malvidin and peonidin at neutral pH, using an oxygen radical absorbance capacity (ORAC) assay. Cyanidin-3-glucoside showed the highest antioxidant capacity, being 3.5 times more potent than the water-soluble vitamin E analogue, Trolox, a powerful antioxidant. Even pelargonidin, which had the lowest ORAC value, was still as powerful as Trolox. Interestingly, Noda et al. (2001) suggested that anthocyanin antioxidant capacity is not due to direct radical scavenging activity but possibly due to chelation of ferrous ions in the hydroxyl radical generation system. There is a substantial body of evidence from *in vitro* assays that anthocyanins and other polyphenolic compounds may also act as prooxidants through oxidative polymerization and reduction of Cu^{2+} to Cu^{+} with subsequent generation of various ROS (Hadi et al., 2007, Halliwell, 2008, Lambert et al., 2007).

However, there is very limited or highly variable evidence for their antioxidant effects *in vivo* (Halliwell et al., 2005). Even though anthocyanin absorption does occur in the gastrointestinal tract, concentrations in the plasma are usually too low to support significant roles as antioxidation agents in the circulatory system. However, they may work as direct antioxidants in the gastrointestinal tract and thus contribute to the maintenance of gastrointestinal health and modulation of the gut microbial composition (Hidalgo et al., 2012). Furthermore, methylation and glucuronidation in the human body leads to decreased antioxidant (or prooxidant) abilities because of the blocking of the phenolic hydroxyl groups involved in such activities (Williamson et al., 2005).

While their antioxidant properties may be of use and relevance for their application as colorants in the food industry, there is substantial doubt whether they can act as effective antioxidants once absorbed. But through modulation of signalling pathways anthocyanins could induce free radical scavenging pathways in animals (Martin et al., 2011, Martin et al., 2013).

1.6.2 Anticarcinogenic properties

Anthocyanins have potential uses as therapeutics. They occur naturally in significant quantities and display strong pharmacological effects *in vitro*. Numerous studies have demonstrated anthocyanin-induced antiproliferative effects and apoptotic properties in various human cancer cell lines. Anthocyanin extracts from different natural sources, have been shown to effectively inhibit several types of cancers such as colon adenocarcinoma, prostate cancer, breast cancer, cervical, and lung cancer cell lines. The link between cancer-inhibiting effects and anthocyanins in food has led to increased research into dietary chemoprevention as a potential protective and/or inhibiting strategy for some cancers, complementary to conventional pharmacological interventions.

Most pharmacological studies have used purified compounds or anthocyanin extracts from berries or grapes, tart cherries, plums and other fruits (Bagchi et al., 2004, Chen et al., 2006, Kang et al., 2003, Katsube et al., 2002, Seeram et al., 2004) and have reported a positive correlation between the dose-dependent application of anthocyanins and the inhibition of malignant cells or tumours. Anthocyanin-mediated cancer cell death may be the result of activation of apoptotic mechanisms including activation of the caspase cascade (a central element of mammalian apoptosis), cleaving poly (ADP-ribose) polymerase (PARP), inducing p38/p53 and p38/c-jun signalling pathways, depolarizing mitochondrial membrane potential, and releasing cytochrome *c* (Huang et al., 2011, Hui et al., 2010, Lee et al., 2009, Shin et al., 2009). Cancer cells evade programmed cell death through the upregulation of antiapoptotic proteins and inhibition of proapoptotic signals. There is increasing evidence that anthocyanins reduce the expression of oncogenic signalling pathways like Wnt and Notch and their downstream targets like β-catenin, MYC, cyclin D1, cyclin B1, extracellular-signal-regulated kinases (ERKs), and vascular endothelial growth factor (VEGF) proteins (Kausar et al., 2012, Shin et al., 2011, Wang et al., 2013).

Several studies reported anthocyanin-mediated reduction in the invasion and metastasis potential through suppression of matrix metalloproteinase (MMP)-2 and MMP-9 in various cell lines including non-small-cell lung cancer (NSCLC) and cervical cancer HeLa cells (Ho et al., 2010, Lu et al., 2013, Yun et al., 2010). Increasing evidence from animal cancer models suggests that anthocyanins and anthocyanin-rich extracts can

significantly reduce the tumour burden or delay the onset of tumour development *in vivo*. Dietary supplementation with anthocyanins led to a reduction in number and size of intestinal adenoma formation in Apc^{Min} mice, which is used as a genetic model of human familial adenomatous polyposis (Cai et al., 2010, Cooke et al., 2006, Kang et al., 2003). Feed supplemented with anthocyanin-rich tomato extract increased the lifespan of *Trp53*$^{-/-}$ knockout mice, an aggressive cancer model characterized by the spontaneous formation of a wide range of tumour types, by 30% (Butelli et al., 2008). Topical application of anthocyanin-rich pomegranate fruit extract significantly inhibited and delayed skin tumour incidence in a multistage mouse skin (CD-1) carcinogenesis model (Afaq et al., 2005). These findings show that anthocyanins or their metabolites can exert preventative and inhibitory effects *in vivo* against various types of cancer affecting different tissues. Furthermore, these studies confirm that upon ingestion chemopreventive activity is retained, but may be exerted by metabolites or catabolites of dietary anthocyanins.

There is some evidence that the inhibitory effects depend not only on the type of cancer but also on the class of anthocyanin and their chemical modifications. Lazze and colleagues (2004) investigated the effects of the anthocyanin aglycones Dp and Cy on cell cycle progression and induction of apoptosis in human cancer cell lines. The two anthocyanins differ only in the number and position of hydroxyl groups on the phenyl B-ring with three hydroxyl groups on positions 3, 4, and 5 in Dp and two hydroxyl groups on positions, 3 and 4 in Cy. Both anthocyanins exerted antiproliferative effects on normal fibroblast cells, but only Dp showed pro-apoptotic properties in the tumour cell lines. Hou (2004) studied the effects of the six different anthocyanins on the oncogene activator protein 1 (AP-1). Dp, Pt and Cy, but not Pl, Pe and Mv inhibited cell proliferation, transformation, and apoptosis. Data from both *in vivo* and *in vitro* studies revealed significant pharmacological differences between the anthocyanin glycosides and their aglycones (Kang et al., 2003, Seeram et al., 2001, Wang et al., 1999). These findings suggest that hydroxylation, glycosylation and methylation patterns may change the chemical and physical properties of the compound and may affect the therapeutic potential of a particular anthocyanin subclass. However, the results remain somewhat inconclusive as the pharmacological effects reported for an individual anthocyanin type are inconsistent and vary between studies and cell types. *In vitro* studies suggest that aglycones seem to be more bioactive than their corresponding anthocyanins.

Anthocyanins are, however, synthesised by plants in the form of glycosides as they increase compound stability. Aglycones do not really exist in nature as they are very unstable. Anthocyanin glycosides can be absorbed in the stomach or be transformed into aglycones or other metabolites through hydrolysis by intestinal enzymes or by the colonic microflora. Aglycones are more hydrophobic and smaller than their glycosides, factors that may improve their bioavailability by facilitating passive penetration of the epithelial layer in the gut (He and Giusti, 2010). Nonetheless, the microflora does not only transform compounds but also reduces the efficiency of absorption by degradation of the aglycones and production of various simple aromatic acids (Manach et al., 2004, Fleschhut et al., 2006).

More research into *in vivo* bioavailability and absorption is required to determine whether the health-promoting effects can be attributed to the action of anthocyanins or other health-promoting compounds in the food matrix. Some of the effects may be the result of synergistic effects between the anthocyanins, polyphenols and/or other plant compounds.

1.6.3 Disease prevention and diet

In 2004, the World Health Organisation (WHO) adopted the "Global Strategy on Diet, Physical Activity and Health" to reduce the risk factors for chronic diseases associated with unhealthy diets and physical inactivity together with increasing awareness and understanding of the influences of diet and physical activity on health. Disease prevention by improving diet and promoting physical activity was given a central role for formulating and implementing effective strategies for substantially reducing deaths and disease burden worldwide.

Health benefits associated with healthy dietary patterns, like the Mediterranean diet, that are characterized by a high intake of fruit and vegetables, fish, plant protein and fibre together with a low intake of red and processed meats, dairy products and saturated fats, are not at all surprising when viewed in the context of an ancestral hunter-gatherer diet, which significantly shaped our genetic make-up through millions of years of evolution (O'Keefe Jr and Cordain, 2004). Humans emerged as a distinct taxonomic clade 2.6 million years ago heralding the beginning of the Palaeolithic era which came to an end around 10,000 before present time (BP). During the Palaeolithic era, humans grouped

together in small societies leading a nomadic lifestyle characterized by spending long hours gathering plants, hunting or fishing. Diet was highly dependent on regional and seasonal availability but included, as principal components, fibre-rich sweet and ripe fruits and berries, shoots, buds and young leaves, carbohydrate and oil-rich roots, bulbs, nuts, and non-grass seeds and lean muscle meat, organ meats, fish, shellfish, insects, larvae and eggs as important sources of protein and fat. Human dietary patterns evolved rapidly and drastically with the development of agriculture and farming, changing the characteristics of formerly wild food through breeding for increased starch and fat content together with the later development of food-processing (Cordain et al., 2005).

With the onset of the industrial revolution dietary patterns experienced a dramatic shift towards increased consumption of dairy products, cereals, refined sugars, refined vegetable oils, and alcohol which together make up 72% of the total daily energy consumed by people in the United States (Cordain et al., 2000). Such dramatic changes in the dietary patterns of modern humans have had significant effects on the health status of Westernized societies that are now inundated by lifestyle-related chronic disease like CVDs, type 2 diabetes, metabolic syndrome and cancer, which are the leading killers in Westernized society. These diseases are increasing dramatically in developing nations as they adopt Westernized lifestyles. More worryingly, a global obesity pandemic is rapidly spreading in industrialized and emerging economies and led to an estimated 400,000 deaths in 2000 alone (Adams et al., 2006, Masters et al., 2013, Roberts and Barnard, 2005). Mortality from chronic diseases is likely to rise and we are only just beginning to understand the causal relationships between diet, obesity and occurrence of cancer (Calle et al., 2003). Return to a Palaeolithic-style diet, described as the diet to which humans are genetically adapted to, is seen by some as the only solution to prevent and stop the spread of Western chronic diseases (reviewed by Carrera-Bastos et al. 2011, Lindeberg 2012). This idea has been supported by reports of superior health markers in traditional hunter-gatherer societies and reports from a number of clinical trials showing improved glucose tolerance and cardiovascular disease markers in Palaeolithic diet intervention groups (Jönsson et al., 2009, Lindeberg et al., 2007). However, the high costs associated with fresh fruit and vegetables and high-quality animal protein of a biomass-rich Palaeolithic diet together with the global issues of expanding world population and decreasing areas of arable land make the Palaeolithic diet an unrealistic long-term solution for a global population.

Estimates suggest that between 30% and 40% of all cancers could be prevented by appropriate diets, physical activity, and maintenance of appropriate body weight (American Institute for Cancer Research, 1997). This relationship is likely to be even higher for certain cancers like those that affect the gastrointestinal tract. Tsugane and Sasazuki (2007) reviewed several epidemiological studies investigating the link between diet and incidence of gastric cancer and concluded that vegetable and fruit intake, even in relatively low amounts, was associated with a lower risk of gastric cancer and was likely to confer protective effects.

Publications regarding the relationship between diet and overall cancer incidence have been highly heterogeneous and variable in quality and design, leaving many gaps in our current understanding of the different factors that may be involved. Whilst there is overwhelming evidence from *in vitro* test systems that many dietary components, in particular anthocyanins and other polyphenols, can inhibit the growth and proliferation of cancer cell cultures, such clear causal relationships have not been produced by all epidemiological studies.

Some of the most compelling evidence linking a healthy diet rich in different fruit and vegetables and low in fats and red meat, to a lower risk of developing certain chronic diseases came from the European Prospective Investigation into Cancer and Nutrition (EPIC) study, a cohort study involving several hundred thousand participants, studying dietary patterns and chronic disease incidence across European countries. One of the most striking outcomes of the EPIC study was the significantly reduced incidence of certain cancer and CVDs in populations following a Mediterranean dietary pattern. In addition, several other cohort studies have reported a possible inverse relationship between the adherence to a Mediterranean-style diet and prolonged survival of cancer patients indicating potentially protective effects against development of cancer (Benetou et al., 2008, de Lorgeril et al., 1998, Gallus et al., 2004, La Vecchia, 2004, Trichopoulou et al., 2003, Trichopoulou et al., 2000, Stoner, 2009). After analysing the outcomes of several cohort and case-control studies regarding the relationship between the adherence to a Mediterranean diet, mortality and incidences of cancer and other chronic diseases, two meta-analyses also suggested a protective role of the Mediterranean-style dietary pattern towards cancer in general (Sofi et al., 2008, Boffetta

et al., 2010). Most studies observed a trend between healthy dietary patterns and lower incidence of overall cancer but failed to establish a statistically significant correlation. Despite inconsistent outcomes from epidemiological studies investigating the effects of the Mediterranean-style diet on total cancer incidence, strong inverse relationships have been reported from several large cohort studies for certain types of cancer, particularly those of the gastrointestinal tract such as colorectal and gastric (Messina and Hilakivi-Clarke, 2009, Salas-Salvadó et al., 2011, Pritchard, 2010, Tsugane and Sasazuki, 2007).

The study of regional diets across cultures has provided strong evidence that certain dietary patterns can promote health and are associated with a lower risk of developing certain cancers and CVDs. Despite the cultural differences in the cuisines worldwide, there are some shared characteristics of healthy dietary patterns. They are all characterized by high intakes of fruit, vegetables, legumes, whole grains, dietary fibre, fish and are relatively high in ω-3 fatty acids, with low intakes of dairy products, red meats, saturated fats, trans-fats, and dietary cholesterol. Increasing our understanding of dietary patterns and prevalence of non-communicable, chronic diseases may offer crucial clues about how to stop the global pandemic of obesity and lifestyle-related chronic diseases as the global population is shifting towards a Western-style diet.

Nutritional epidemiology has been highly successful in identifying inverse relationships between dietary agents and wide array of epithelial cancer but these observations have often failed to be repeated in randomized clinical trials. A number of cohort studies using controlled intervention trials have investigated the relationship between dietary patterns characterised by either low-fat (Prentice et al., 2006) or high-fruit and vegetables (Pierce et al., 2007) and incidence of invasive breast cancer but did not report any differences between the intervention groups and the control. An analysis of the EPIC cohort assessing relationships between total fruit and vegetables and cancer risk during 1992 and 2000 revealed only a very small inverse association (Verberne et al., 2010).

There are several possible explanations for the apparent lack of association between certain dietary components and cancer progression. A balanced diet rich in fruit and vegetables may deliver the entire biological action package and, subsequently, supplementation with a single dietary compound or food group may be not as effective

as the epidemiological study may have suggested as most of the health benefits are delivered by the combinatorial activity of different components in the diet.

Another possible reason for the inconsistency in the results from dietary intervention and epidemiological studies could be the difficult nature of conducting and reporting medium- to long-term studies. Both study types rely on self-measurement of dietary patterns that are often assessed with considerable measurement errors. Furthermore, clinical intervention trials focus on the diet during adult life and may not acknowledge crucial time windows early in life. Most cancers will result from genetic alterations accumulated over an individual's lifetime and dietary agents may be particularly effective during childhood and puberty when the body is undergoing crucial growth and developmental changes. Many cancers have been associated with epigenetic changes. The accumulation of such disadvantageous alterations may well be influenced by dietary habits throughout childhood and into early adulthood. Also, the follow-up time of most intervention studies is between five and ten years which may simply be too short to capture the role of diet as a preventative or protective factor for cancer. Finally, the role of genetic and epigenetic variations as well as individual differences in the gut microbiota of an individual are still not sufficiently researched but may strongly affect the responsiveness to dietary interventions and subsequently the outcomes of clinical trials.

1.6.4 Dietary changes and the treatment of chronic, non-communicable diseases

Along with the prevention or delayed onset of many chronic diseases, lifestyle intervention studies have demonstrated large reductions in the progression of these diseases and even rendered pharmacotherapy redundant in some cases. Dietary changes have been particularly successful in the treatment of CVDs and type 2 diabetes. Clinical studies have provided evidence that adequate dietary changes can significantly reduce the requirement for antihyperglycemic drug control of type 2 diabetes. The Mediterranean-style diet, for example, with high proportions of fruit and vegetables, and monounsaturated fat, provided significant cardiovascular benefits together with increased insulin sensitivity. A four-year Mediterranean-style intervention diet showed that 56% of patients with newly diagnosed type 2 diabetes did not require antihyperglycemic drug control, lost more weight and experienced greater

improvements in some glycemic and coronary risk measures than the patient control group assigned to a low-fat diet (Lindeberg, 2012). Similarly, adherence to a Mediterranean-style diet decreased the risk of developing type 2 diabetes in individuals at high risk of developing CVDs (Nomura et al., 2008) and reduced the prevalence of metabolic syndrome and its associated CVD risk (Willett, 2010). A meta-analysis of six dietary intervention studies comparing Mediterranean-style and low-fat diets confirmed that the Mediterranean-style diet was more effective than low-fat diets in improving cardiovascular risk factors and inflammatory markers (Manson, 2003).

Adherence to a healthy dietary pattern is likely to reduce the incidence of certain cancers, particular those of the gastrointestinal tract. It is less clear, whether changes in dietary pattern can reduce or even reverse the progression of pre-existing cancers. There are few, highly inconsistent reports of dietary management of cancer. Despite the lack of clinical evidence advocating a diet-assisted cancer therapy, our increasing understanding of how plant bioactive compounds exert their chemopreventive effects could hold some clues to whether these compounds might assist in the therapeutic management of prevalent cancers. It has recently emerged that polyphenols are capable of modulating epigenetic alterations in cancer cells (Link et al., 2010, Vanden Berghe, 2012). Epigenetic mechanisms include changes in DNA methylation, histone modifications and non-coding RNAs that can drive tumour progression by regulating the dynamics of gene expression. Epigenetic modifications occur early and may be reversible, making dietary bioactives potentially interesting agents in the long-term management of chemoprevention and -therapy.

1.6.5 Incidence of cancer worldwide

In 2008, cancer was the leading cause of death worldwide and, according to the World Health Organization (WHO) estimates, accounted for 7.6 million deaths or 13% of all deaths (http://globocan.iarc.fr/). Cancer incidence and mortality is significantly higher in Western countries, accounting for ~20% of all deaths, compared to Eastern countries or emerging economies (Figure 1.3). The difference in cancer prevalence between different geographical regions is most likely the result of different dietary and lifestyle habits together with increased life expectancy in Western countries and, thus, higher incidences of age-related, degenerative diseases.

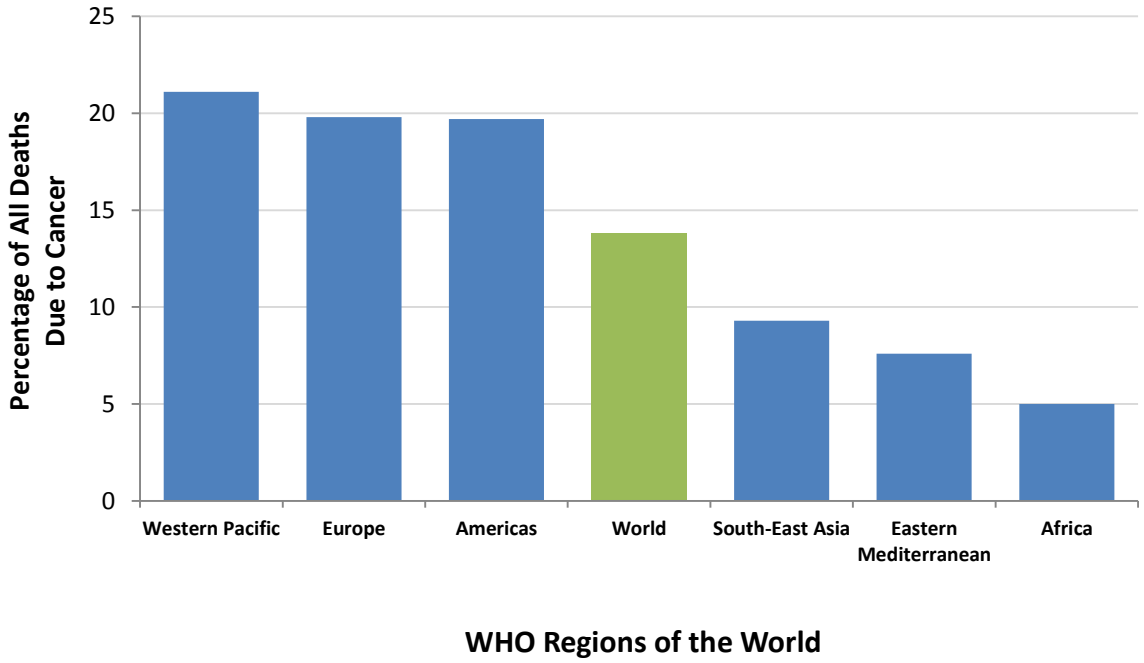

Figure 1.3: 2008 percentages of all deaths due to cancer, as estimated by the World Health Organisation (WHO) for different regions of the world. Cancer was estimated to account for around 14% of all deaths (due to any cause) worldwide in 2008. Cancers includes all malignant tumours excluding non-melanoma skin cancer.

According to GLOBOCAN's 2008 report, more than 304,200 people were diagnosed with cancer every year in the UK. The age-standardised rate (ASR; rate that a population would have if it had a standard age structure) for new cancer cases and cancer deaths was 266.9 and 115.8 per 100,000 people, respectively. The UK has one of highest ASRs, of cancer morbidity in the Western world, which is comparable to that of Croatia (115) and Slovenia (113) and but significantly above that of France (94), Germany (99), Belgium (93), Switzerland (88) and United States (104).

Table 1ii: 2008 estimates of age-standardized rates (ASRs) for regional and gender-specific incidence of cancer, excluding non-melanoma skin cancer. ASRs were highest in the Western countries.

Region	Incidence (ASR)	Gender
North America	**334**	men
Australia/New Zealand	**356.8**	Men
Northern	**288.9**	Men
Western Europe	**335.3**	Men
Middle Africa	< 100	Men
Western Africa	< 100	Men
South-central Asia	< 100	Men
North America	**274.4**	Women
Australia/New Zealand	**276.4**	Women
Northern	**257.8**	Women
Western Europe	**250.5**	Women
Middle Africa	< 100	Women
Northern Africa	< 100	Women

Data from the Internatioal Agency for Research on Cancer GLOBOCAN 2008 report; www. http://globocan.iarc.fr/. ASRs are represented per 100,000.

1.6.6 Breast cancer

Breast cancer is the most frequent cancer among women, accounting for almost a quarter of all cancers with an estimated 1.38 million new cancer cases diagnosed in 2008. It is now the most common cancer both in developed and developing regions. In developing countries, rates have been steadily increasing, and are now approaching those in Westernized countries (GLOBOCAN 2008 report). Breast cancer is the most common cancer in the UK with a lifetime risk of more than 10% and has the second highest mortality rate after lung cancer (Figure 1.4). Overall, breast cancer incidence rates have levelled off since 1990 and most importantly, during this same time period, breast cancer mortality rates have declined by 24%. This reduction in mortality has been attributed to the combination of early detection with screening programmes and the development of more efficacious, systemic chemotherapy agents.

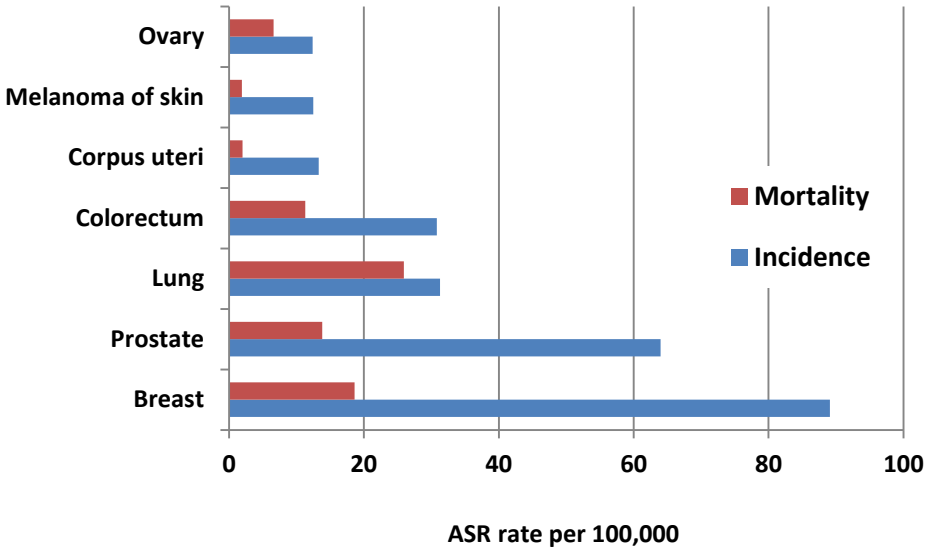

Figure 1.4: Estimated ASRs of incidence and mortality for the seven most common types of cancer in the UK. Rates are shown for both sexes combined. Data from the Internatioal Agency for Research on Cancer GLOBOCAN 2008 report; www. http://globocan.iarc.fr/.

A

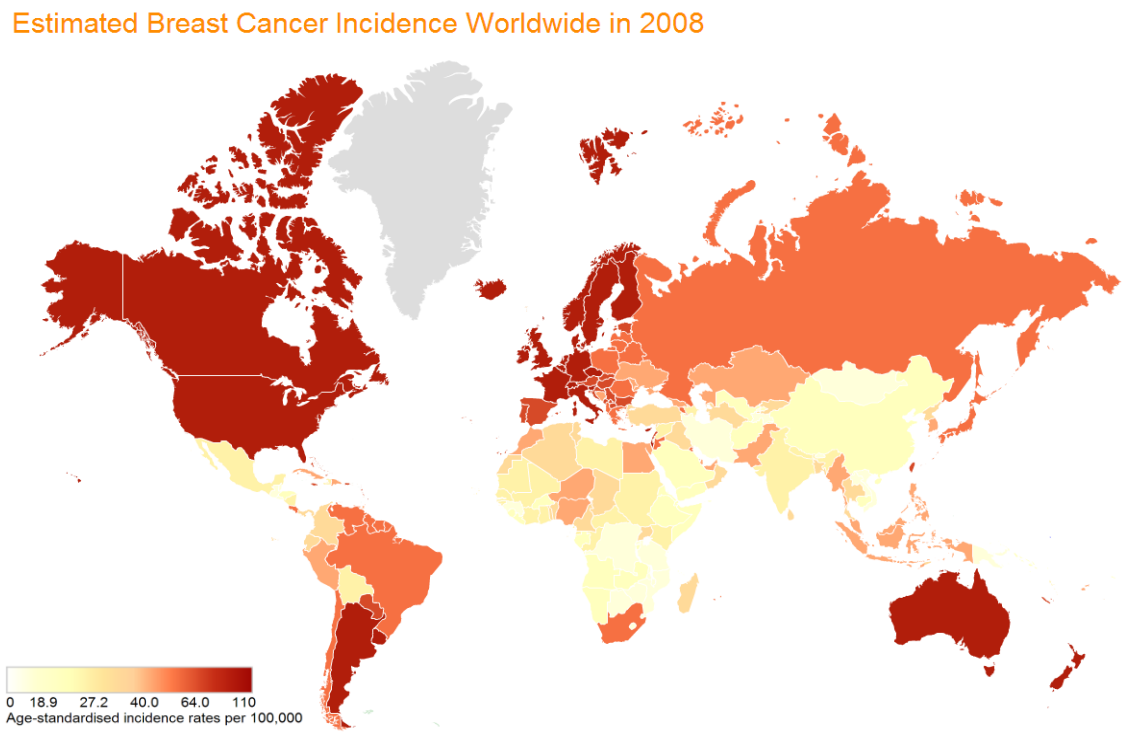

B

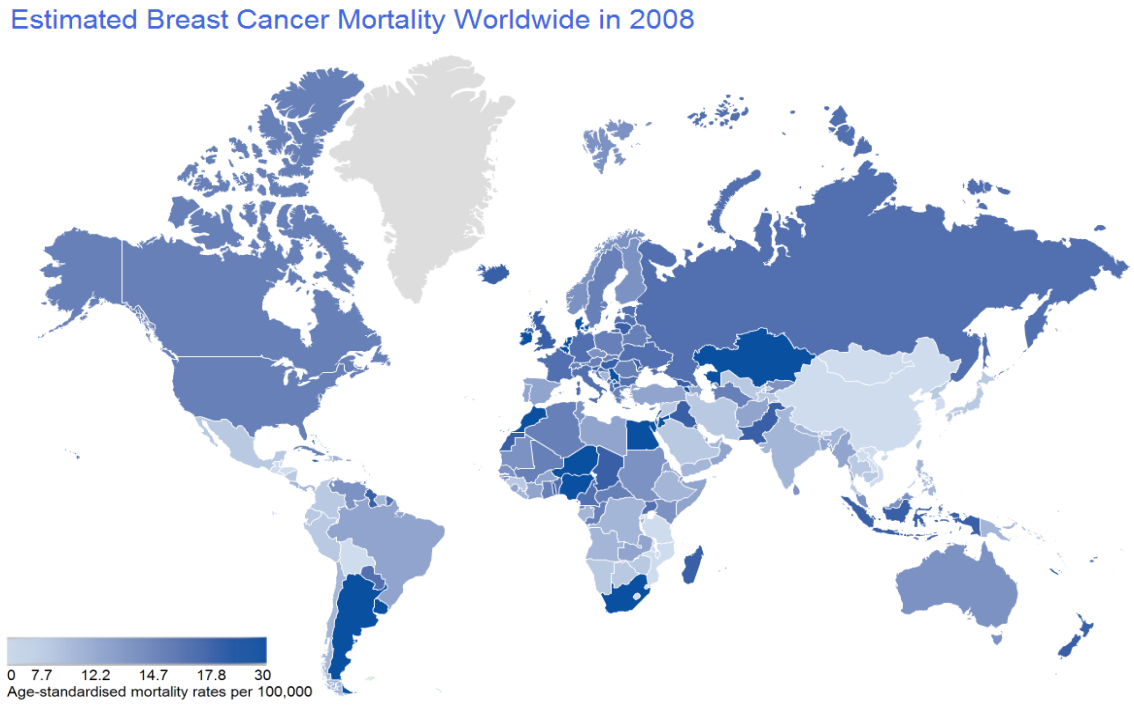

Figure 1.5: 2008 estimates of ASRs for worldwide (**A**) incidence and (**B**) mortality from breast cancer. Data from the Internatioal Agency for Research on Cancer GLOBOCAN 2008 report; www. http://globocan.iarc.fr/. ASRs are represented per 100,000.

However, breast cancer incidence rates remain high, especially in Westernized countries were they have been traditionally several fold higher than in most developing nations (Figure 1.5).

Breast cancer is a highly heterogeneous disease with very diverse, tumour-specific gene expression patterns that have complicated disease prognosis and etiology. However, DNA microarray profiling studies of breast tumours have identified distinct and reproducible subtypes of breast carcinomas that are strongly associated with different clinical outcomes. Based on shared genetic characteristics, invasive breast carcinomas can be divided into five distinct subtypes: luminal A, luminal B, human epidermal growth factor receptor 2 $(HER2)^{+}$/oestrogen receptor $(ER)^{-}$, basal-like ($HER2^{-}$/ ER^{-}), and normal breast-like (Livasy et al., 2006). The basal-like subtype is often associated with mutations in the tumour suppressor genes *BRCA*1 and *p53* and has the highest proliferation rates with poor prognosis and high metastasizing potential (Tsuda et al., 2000). In contrast, the luminal A subtype is associated with the best clinical outcome (Voduc et al., 2010). Given the substantial genetic diversity found in tumours belonging to the same breast cancer subtypes, identification of those genetic alterations shared by tumours of a particular subtype, would greatly facilitate the prognosis of tumorigenic potential and ultimately, the disease outcome for the patient by facilitating the development of multi-targeted, subtype-specific pharmacological treatments.

Most breast cancers develop sporadically as a result of mutations that have accumulated through life or are triggered by exposure to known carcinogens such as radiation or tumorigenic chemicals. Only 5-10% of all breast cancer cases are known to have underlying hereditary factors. Carriers of heritable mutations in the tumour suppressor genes *BRCA*1 and *BRCA*2 have an increased risk of developing breast cancer. Mutations in these genes have been associated with the hereditary breast-ovarian cancer syndrome and affected women have an estimated lifetime risk of breast cancer of >80%, and a lifetime risk for developing ovarian cancer of 40- 65% for *BRCA*1 carriers and 20% for *BRCA*2 carriers (Ford et al., 1998).

Interestingly, a cohort study of carriers of the *BRCA*1 and *BRCA*2 mutation revealed two modifiable risk factors that were significantly associated with delayed onset of breast cancer in these patients: physical exercise as an adolescent and healthy weight (King et al., 2003). Existing data on the relationship between obesity and breast cancer

risk and the clinical outcome is complex and often controversial. Most cohort and case-control studies have reported a distinct, but not always significant, inverse relationship between obesity and breast cancer amongst pre-menopausal women and some studies even suggested that weight gain can increase the risk for pre-menopausal women to develop breast cancer (Protani et al., 2010). Furthermore, obesity at the time of diagnosis is seen as a poor prognostic factor of clinical outcome as there is sufficient evidence that both pre- and post-menopausal women with breast cancer suffering from obesity have poorer survival than normal weight women with breast cancer (Carmichael, 2006). The underlying causes of this inverse relationship between obesity and breast cancer remain speculative but several mechanisms have been proposed: cellular proliferation pathways are upregulated in obese patients (Calle and Kaaks, 2004) which may lead to increased tumour cell proliferation and metastasis. Adipose tissues produce certain growth factors such as leptin, that are known to promote growth of breast cancers (Grossmann et al., 2010) together with increased production of oestrogens which might lead to more aggressive ER^+ breast tumours (Tchernof and Després, 2000).

The role of diet as a modifiable risk factor in the occurrence and management of breast cancer is still debated. In a comprehensive meta-analysis, Michels and colleagues (2007) reviewed nearly 1500 articles, including case-control and cohort studies but failed to establish a clear association between diet and breast cancer. Some possible explanations for the apparent lack of relationship between diet and cancer have already been discussed (Chapter 1.6.3) but studies of total breast cancer incidence may not detect associations between diet and particular types of breast cancer. In fact, Hung et al. (2005) did not observe an association between diet and overall breast cancer occurrence but reported a significant inverse relationship between higher consumptions of fruits and vegetables and reduced risk for ER^- breast cancer. The low incidence of breast cancer (in Asian countries incidence is less than a fifth of that in Westernized countries (Armstrong and Doll, 1975)) has been the subject of considerable scientific interest and speculation (Figure 1.5). The high intake of soy products as a major source of phytoestrogens may play a role in lowering the lifetime risk for breast cancer. The active components in soy products have been suggested to be isoflavones like genistein, which can act as phytoestrogens. However, a meta-analysis of 18 studies regarding soy intake and breast cancer risk failed to establish a clear, inverse relationship between soy

consumption and breast cancer occurrence (Trock et al., 2006). Some of the inconsistencies may be due to variations in the isoflavone contents in the soy products and differences in the responsiveness to oestrogenic stimulants between the types of cancers studied (ER^+ and ER^- subtypes). Nevertheless, cohort studies monitoring the changes in breast cancer risks of Asians migrating to Westernized countries have provided some of the most compelling and significant evidence for an inverse relationship between diet and breast cancer. Both Deapen (2002) and Ziegler (1993) reported that the breast cancer risk of Asians that have migrated to the United States (US) increased by several fold over a few generations, rapidly approaching that among US Whites. Furthermore, breast cancer incidence in Japan, which has traditionally one of the lowest breast cancer rates in the world, has been steadily rising since the 1950s. The trend of increasing breast cancer rates coincides with the increased intake of fats and adoption of a more Western-style diet over the same period (Kato et al., 1987, Tung et al., 1999). The existing epidemiological data from Asian communities are particularly valuable to interpreting the relationship between chronic diseases and certain lifestyle factors, including dietary patterns and known risk factors such as smoking and alcohol. They also offer crucial insight into the consequences of rapid lifestyle changes on the prevalence of chronic diseases within one or few generations.

At present, evidence for an inverse relationship between dietary factors and breast cancer still remain somewhat inconclusive. However, most studies suggest the existence of a beneficial, yet not statistically significant, relationship between healthy dietary patterns and breast cancer risk.

1.6.7 Pathology of cancer

Cancer is, like most non-communicable, chronic illnesses, a disease that is primarily the result of environment and lifestyle choices (Anand et al., 2008). While all cancerous cells harbour genetic alterations, only 5-10% of all cancers can be directly linked to inherited genetic alterations. The causes of cancer are as complex and diverse as the types of cancers and the different tissues they can affect but include known risk factors such as smoking, alcohol consumption, diet and obesity as well as exposure to radiation and mutagenic chemicals.

Cancer cells are characterised by unregulated cell growth and failure to undergo programmed cell death and may invade neighbouring tissue or spread to distant body parts through the lymphatic system or bloodstream. For cells to become cancerous, genetic and regulatory alterations of genes involved in growth regulation and initiation of senescence and cell death, are required to trigger an imbalance between cell proliferation and cell death (Figure 1.6). Mammalian cells have evolved highly sophisticated, interlocking mechanisms to detect and repair DNA lesions that could lead to genomic instability and loss of genomic integrity (Lord and Ashworth, 2012). These mechanisms are collectively known as DNA-damage response (DDR) and encompass a set of coordinated processes, such as DNA damage detection, accumulation of DNA repair factors and repair of damaged DNA fragments. Somatic mutations in the cancer cell genome may include different types of DNA sequence change such as base substitutions, insertions or deletions of small or larger sequences of DNA, rearrangements of broken DNA that has been inserted in a different location in the genome and copy number increases and reductions that may lead to gene amplification or deletion, respectively (Stratton et al., 2009). Mutations in the genes involved in DNA lesion detection and repair which impact the ability of cells to initiate and carry out the DDR, pave the way for additional mutations and the manifestation of alterations in the genome of cancer cells. Furthermore, alterations in the cancer genome often involve gain-of-function mutations, amplifications, and/or overexpression of key oncogenes and the loss-of-function mutations, deletions, and/or epigenetic silencing of key tumour suppressors (Hanahan and Weinberg, 2000). Mutations in the genome are divided into selectively advantageous “driver” lesions, selectively neutral “passenger” lesions and deleterious lesions as well as “mutator” lesions that may accelerate the rate of genetic change. Driver lesions can alter cell behaviour and confer a selective advantage over neighbouring cells that will promote the development of the disease and have also been implicated with reduced sensitivity to anti-cancer agents (Greaves and Maley, 2012, Lord and Ashworth, 2012).

Cancer is an evolutionary process that, by analogy to Darwinian evolution, is characterized by the continuous accumulation of heritable (passed onto the daughter cells) genetic variation by random mutation and natural selection for favourable mutations, which provide an evolutionary advantage to the cancer cells over their neighbouring cells, such as accelerated proliferation and growth. Most of these

evolutionary processes will manifest themselves as benign growths but some of them will acquire further advantageous mutations that will allow them to invade tissues and metastasize (Ewald and Swain Ewald, 2012).

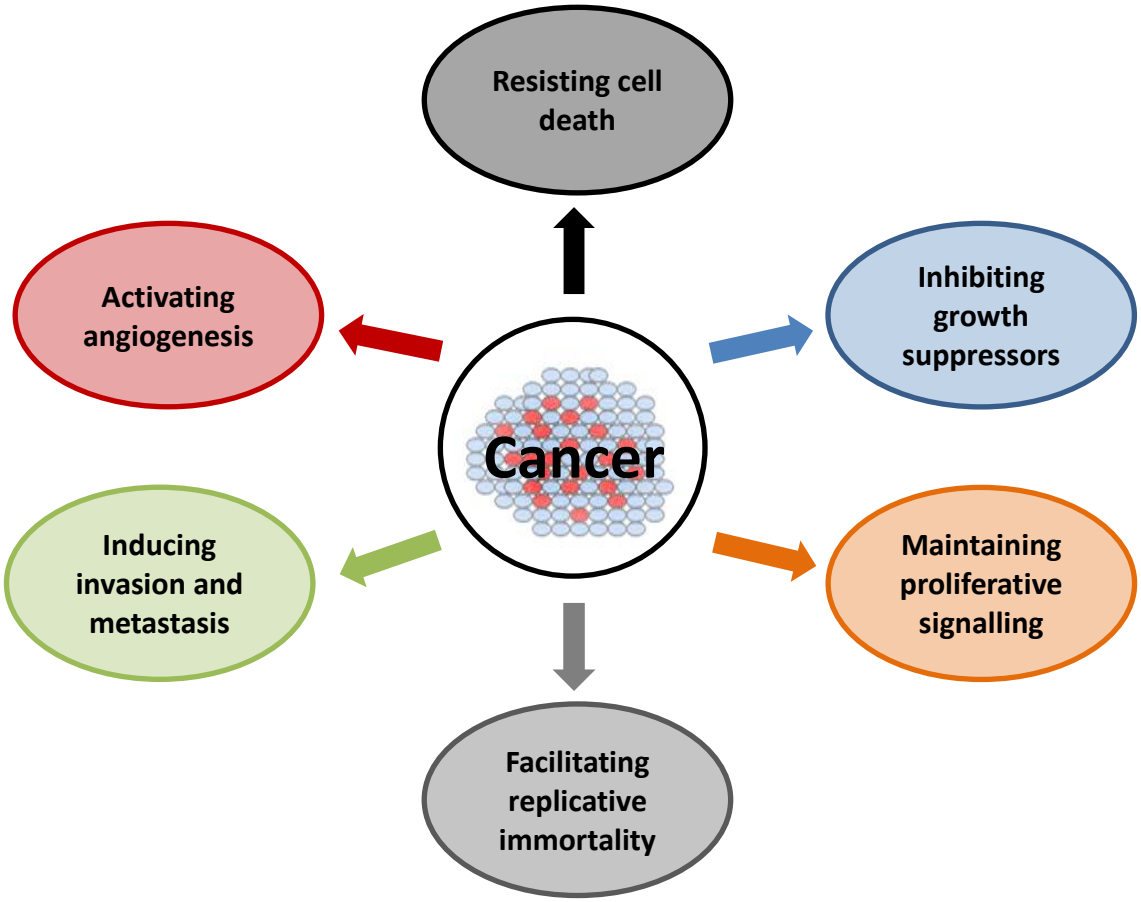

Figure 1.6: The six hallmarks of cancer (modified from Hanahan and Weinberg, 2011).

Tumour suppressor genes such as *p53* provide cellular restraints to prevent deregulated cell growth and survival or genomic instability. The *p53* transcription factor plays a central role in inhibiting cell growth and triggering an apoptotic response to a range of insults including DNA damage, telomere shortening, environmental stresses and oncogene activation. Loss of activity of tumour suppressors removes these restraints and can lead to tumourigenesis. In fact, reactivation of *p53* in mouse tumour models demonstrated that *de novo* activation of tumour suppressor genes can lead to regression of tumours (Martins et al., 2006, Ventura et al., 2007).

Many oncogenes such as extracellular-signal-regulated kinases (ERKs), MYC transcription factor (MYC) and rat sarcoma (Ras) are involved in the regulation of cell growth, differentiation and survival. Permanent activation or overexpression of these proteins in the absence of activated tumour suppressors will inevitably lead to uncontrolled cell growth and, ultimately tumourigenesis (Luo et al., 2009). Owing to their uncontrolled growth, cancer cells require increased uptake and conversion of nutrients but also increased production of nicotinamide adenine dinucleotide phosphate (NADPH) as a reducing agent to maintain the cellular redox balance. Increased energy requirements are met by an enhanced uptake of glucose and glutamine and even *de novo* fatty-acid biosynthesis by some cancer cells (Schulze and Harris, 2012). Extensive metabolic reprogramming is therefore essential to meet the requirements of cancer cells to produce large amounts of precursors for subsequent macromolecular biosynthesis that allows the accumulation of biomass during tumourigenesis (Schulze and Harris, 2012). Oncogenes such as MYC have been associated with regulatory changes in the transcriptional program leading to energy metabolism along with proangiogenic activities, by sustaining the production of vascular endothelial growth factor (VEGF) or enhancing neovascularization (Dews et al., 2006). Tumour growth is often accompanied by increased vascularization that enhances delivery of nutrients and energy to every cell in the solid tumour mass. In fact, lack of vascularity will prevent solid tumours from growing indefinitely as internal cells will fail to gain access to essential metabolites. Angiogenesis is a fundamental process in both embryogenesis and adult development requiring the coordinated action of growth factors and cell adhesion molecules. Key signalling pathways of angiogenesis involve members of the VEGF family and platelet-derived growth factors (PDGFs), which have all been found to activated and upregulated by oncogenes in tumours (Ferrara and Kerbel, 2005). Unsurprisingly,

antiangiogenic agents have been explored extensively, and with growing success, to prevent tumour progression and metastasis (Carmeliet, 2005, Ferrara and Kerbel, 2005).

Traditionally, cancers have been viewed as the result of gradual acquisition of somatic, random mutations in the genome that have accumulated though-out the lifetime. Indeed, the heterogenic nature of tumours representing a mosaic of cells with unique genetic mutation patterns strongly supports the idea that cancer cells have evolved from multiple, gradually occurring genetic alterations rather than a single mutation event (Stratton et al., 2009). However, 2-3% of all cancers appear to have emerged from a one-off cellular catastrophe resulting in tens to hundreds of chromosomal rearrangements (Stephens et al., 2011). The agents that cause such dramatic physical damages to the chromosome remain largely unknown but result in hundreds of double-strand breakages of the chromosomes (likely to occur when they are condensed for mitosis) leading to chromosomal fragments that circulate unhindered in the nucleus, and are pasted together in random order by the DNA repair machinery. Most cells probably do not survive such dramatic cellular events but it only requires one surviving cell to acquire evolutionary advantageous, cancer-causing lesions followed by additional mutations in cancer genes to initiate tumourigenesis.

Our insight and understanding of the highly complex and heterogeneous nature of human tumours has expanded substantially over the last decade, leading to the recognition that new therapeutic approaches are needed to treat cancer effectively and with minimal impact for the patient. Personalized treatments that involve multiple therapeutic agents and the increased awareness of environmental and lifestyle factors that promote and inhibit cancers, will drive significant advances in the prevention and management of the disease in the future.

1.6.8 Mechanisms of mammalian cell death

Multicellular organisms maintain homeostasis by balancing cell proliferation and cell death. Cell death has occurred if at least one of the following criteria has been met: loss of plasma membrane integrity, cell fragmentation and/or engulfment by adjacent cells. Cell death is a multi-stage process and considered reversible until a “point-of-no-return” is passed. In fact, several points-of-no-return have been proposed to define dying cells, including the mass activation of caspases, mitochondrial membrane permeabilization

and phosphatidylserine (PS) exposure. However, several studies have reported caspase activation or PS exposure in non-lethal processes or to have occurred without immediate progression to cell death, highlighting the difficulties of defining universal criteria for cell death (Boya et al., 2005, Green and Kroemer, 2004).

Cell death can occur via different mechanisms and several types of cell death have been described: apoptosis, necrosis, autophagy (characterized by massive autophagic vacuolization of the cytoplasm), cornification (specific to the epidermis and leading to formation of corneocytes containing an amalgam of proteins and lipids that function as a barrier to isolate the body from the external environment) and atypical cell death modalities such as mitotic catastrophe (occurs during or shortly after failed/dysregulated mitosis as a result of micro- or multinucleation) and anoikis (loss of attachment to the substrate or other cells) amongst others. Regardless of the type of cell death, the final fate of any dying or dead cell is engulfment by phagocytes.

Apoptosis and necrosis will be discussed in more detail as they are the two most common forms of cell death (Table 1iii). Apoptosis is defined as programmed cell death. Cells that undergo apoptosis show specific morphological features including the rounding-up of cells, retraction of pseudopods, plasma membrane blebbing, chromatin condensation and nuclear fragmentation but little or no ultrastructural modifications to the organelles. Necrosis occurs following a wide variety of cellular injuries that can be caused by exposure to cytotoxic agents. Necrotic cell death is morphologically characterized by a gain in cell volume, swelling of organelles, rupture of the plasma membrane and loss of intracellular contents. Initially thought to be an uncontrolled or accidental form of cell death, necrosis is now believed to be a finely tuned process, regulated by signal transduction pathways and catabolic mechanisms involving the death domain receptors (Golstein and Kroemer, 2007). Our understanding of the exact molecular processes that trigger necrosis remains fragmented. However, induction of necrotic cell death has been observed in cells in which both apoptosis and autophagy where inhibited, suggesting that necrosis may play a significant role in the highly regulated and sophisticated cell death machinery.

Table 1iii: Characteristics of necrosis and apoptosis.

	Necrosis	Apoptosis
Induction	Non-physiological disturbances (e.g. complement attack, lytic viruses, hypothermia, hypoxia, toxins)	Physiological stimuli (e.g. DNA damage, lack of growth factors, immunomediated)
Tissue effects	Acute inflammatory process; subsequent scarification	Non-inflammatory; phagocytosis induced by adjacent cells; rapid involution without general tissue collapse
	Morphological features	
Onset	Swelling of cytoplasm and mitochondria	Shrinking of cytoplasm and condensation of nucleus
Plasma membrane	Loss of membrane integrity	Membrane blebbing, but no loss of integrity
Chromatin		Aggregation of chromatin at the nuclear membrane
Organelles	Disintegration of organelles	Mitochondria become leaky due to pore formation involving proteins of the bcl-2 family
Vesicles	No vesicles formation; complete lysis of cell	Formation of membrane-bound vesicles (apoptotic bodies)
Terminal	Total cell lysis	Fragmentation of cell into smaller bodies
	Biochemical features	
Regulation	Loss of regulation of ion homeostasis	Tightly regulated process involving activation and enzymatic steps
Energy requirement	No energy input	Energy (ATP)-dependent
DNA	Random digestion of DNA	Non-random mono- and oligonucleosomal length fragmentation of DNA
Timing	Postlytic DNA fragmentation	Prelytic DNA fragmentation
Biochemical events	Involves TNF receptor 1 and the recruitment of Fas-associated death domain; calpain (protease) activation; release of cyclophilin D that results in removal of transmembrane potential of the inner mitochondria	Release of various factors (cytochrome *c*, AIF) into cytoplasm by mitochondria; Activation of caspase cascade; Alterations in membrane asymmetry (i.e., translocation of PS from the cytoplasmic to the extracellular side of the membrane)

Apoptosis is the regulated destruction of the cell and the result of a highly complex process involving a number of different factors and signals. Two key molecular signalling pathways exist that lead to apoptotic cell death (Figure 1.7). The first is the **intrinsic** pathway that is activated from inside the cell by proapoptotic members of the Bcl-2 protein family that governs downstream mitochondrial signals that that may lead to mitochondrial membrane permeabilization. The second is the **extrinsic** or mitochondria-independent death-receptor pathway, that is activated from outside the cell by proapoptotic ligands that interact with members of the death-receptor family such as tumour necrosis factor receptor I (Ashkenazi, 2002).

Many of the morphological changes that characterize apoptosis are linked to the activation of a set of intracellular cysteine proteases called caspases (Kerr et al., 1972). Caspases belong to a large family that has been highly conserved through evolution. They are central executioners of programmed cell death and activated by both the intrinsic and extrinsic apoptotic pathways. Elimination of caspase activity either through mutations or pharmacological inhibitors can rescue cells from their apoptotic fate or at least slow down the apoptotic process. It is not surprising that cancer-associated mutations in caspase-encoding genes have been reported in a number of different cell types. Caspases selectively cleave a set of target proteins that in most cases results in the inactivation of the target protein but may also activate proteins by cleaving off negative regulatory domains or inactivating regulatory subunits.

Caspases are synthesised as zymogens containing three domains (N-terminal prodomain, p20 and p10 domain) that require activation by removal of the N-terminal prodomain. Downstream caspases are activated through proteolytic cleavage by upstream ones, whereas the upstream "initiator" caspases are activated through proximity-induced dimerization (Pop and Salvesen, 2009). Caspases-8, -9 and -10 are considered the key initiator caspases, that activate the downstream effector caspases-3, -6 and -7 and which are usually more abundant and active than the other members of the caspase family. Over 100 caspase substrates have been identified so far, including those inducing chromatin condensation and nuclear fragmentation which are crucial hallmarks of apoptosis, highlighting their importance in the regulation of apoptotic subprogrammes (Liu et al., 1998, Liu et al., 1997, Sahara et al., 1999).

Figure 1.7: Simplefied, schematic representation of the extrinsic and intrinsic apoptosis pathways. Apoptotic cell death can be induced through the extrinsic (also called receptor-mediated) or the intrinsic (mitochondria-mediated) signalling pathways. The extrinsic pathway involves ligation to death receptors (e.g. tumor necrosis factor alpha (TNF-α), TNF-related apoptosis-inducing ligand (TRAIL), FAS receptor (FasR), also known as cluster of differentiation 95 (CD95)) with their ligands through an adaptor molecule, known as Fas-Associated protein with Death Domain (FADD) that bridges death receptors to caspase-8. Death receptors recruit FADD and procaspase-8 to form a death-inducing signalling complex (DISC) that activates procaspase-8 and triggers a cascade of caspase activity that cleave target proteins leading to apoptosis. This pathway is negatively controlled by the anti-apoptotic proteins c-FLIP and Inhibitors of Apoptosis (IAPs). IAPs are a family of functionally and structurally related proteins acting as endogenous inhibitors of apoptosis that block activation of caspase-3. Their activity is blocked by binding to Smac/Direct IAP Binding protein with Low PI (DIABLO). Smac is a mitochondrial protein that promotes cytochrome *c* dependent activation by eliminating the inhibition via IAPs. Intrinsic death stimuli, e.g. reactive oxygen species (ROS), DNA-damaging reagents, or Ca^{2+} mobilization directly or indirectly activate the mitochondrial pathway by inducing release of cytochrome *c* and formation of the apoptosome, composed of Apoptotic protease activating factor 1 (Apaf-1) and caspase-9. Caspase-9 is activated at the apoptosome and, in turn, activates pro-caspase-3. This death pathway is largely controlled by pro-apoptotic (e.g. Bcl-2–associated X protein (Bax), Bcl-2 homologous antagonist/killer (Bak), BH3 interacting-domain death agonist (BID) and Smac/DIABLO) and anti-apoptotic (e.g. B-cell lymphoma 2 (Bcl-2), B-cell lymphoma-extra large (Bcl-X_L), IAPs) proteins. Caspase-8 may also induce cleavage of BID, which induces the translocation of Bax and/or Bak to the mitochondrial membrane and amplifies the mitochondrial apoptosis pathway. Apoptosis inducing factor (AIF) is a mitochondrial protein that triggers chromatin condensation and DNA degradation in a cell in order to induce a caspase-independent pathway of apoptosis. The p53 transcription factor is an essential tumour suppressor and stimulates a wide network of signals that act through the two major apoptotic pathways. In the intrinsic pathway, *p53* responds to stress induction of expression of *Bcl*-2 pro-apoptotic family members like *Bax*. *p53* can activate the extrinsic apoptotic pathway through induction of the genes encoding the transmembrane death receptors proteins: Fas, death receptor 5 (DR5) and PMP-22 (PERP). Red: proapoptotic signals; blue: antiapoptotic signals.

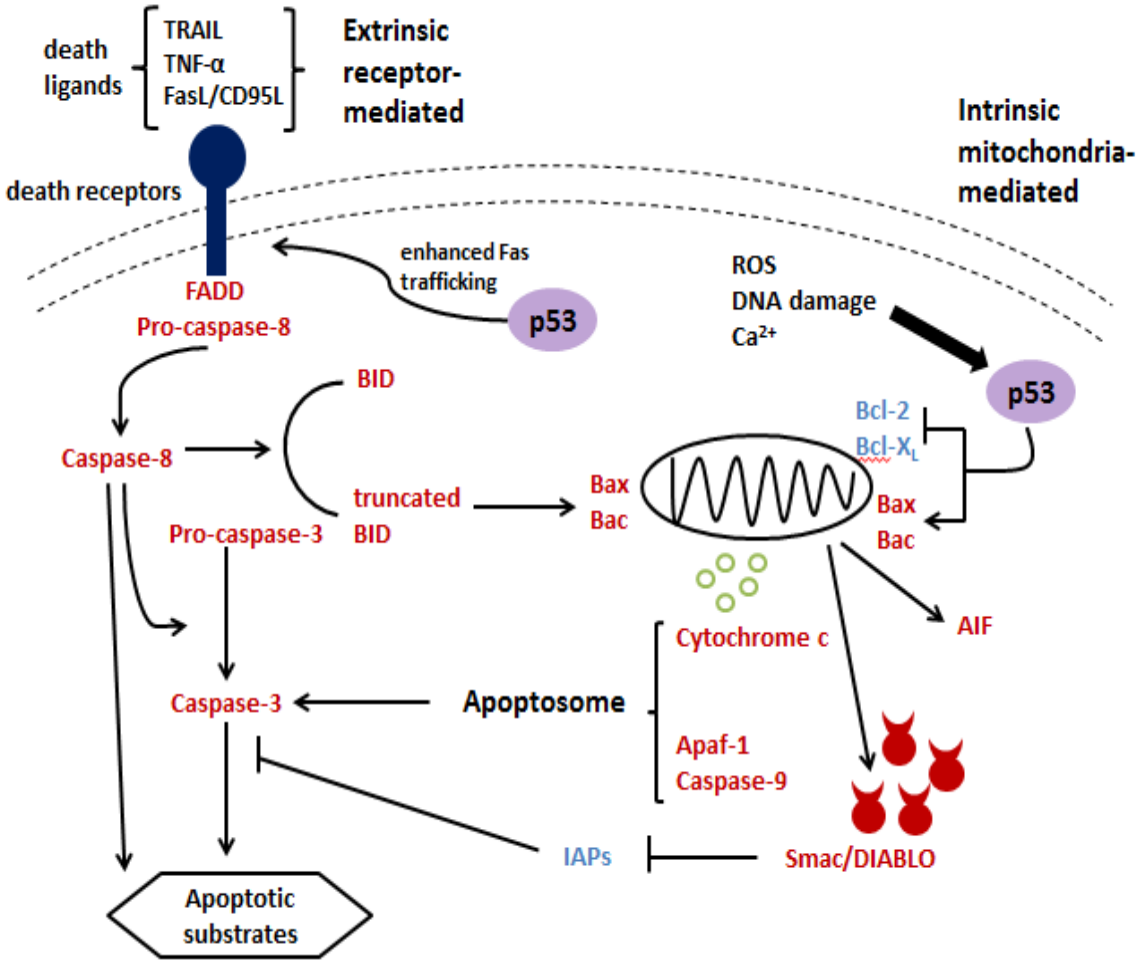
death ligands
TRAIL
TNF-α
FasL/CD95L
Extrinsic receptor-mediated
Intrinsic mitochondria-mediated
death receptors
FADD
Pro-caspase-8
enhanced Fas trafficking
p53
ROS
DNA damage
Ca2+
p53
BID
Caspase-8
truncated BID
Pro-caspase-3
Bax
Bac
Bcl-2
Bcl-XL
Bax
Bac
Cytochrome c
AIF
Caspase-3
Apoptosome
Apaf-1
Caspase-9
IAPs
Smac/DIABLO
Apoptotic substrates

The intrinsic or mitochondrial pathway is triggered by certain extracellular cues and severe internal cell stresses, such as DNA or cytoskeletal damage that induces the transcription or post-translational activation of proapoptotic Bcl-2 family proteins, which constitutes a critical intracellular checkpoint in the intrinsic pathway of apoptosis. Bcl-2 family proteins interact extensively with other proteins and it is likely that the proapoptotic members induce formation of large pore channels or rupture of the mitochondrial membrane either by recruiting other mitochondrial membrane proteins or by controlling directly mitochondrial homeostasis. Pore formation in the mitochondrial membrane leads to the release of cytochrome *c*, an important proapoptotic signalling protein and a universal feature of apoptotic cells. Cytochrome *c* is normally located in the mitochondrial intermembrane space but upon release into the cytosol it binds to the apoptotic protease-activating factor 1 (Apaf-1) whose binding is essential for the formation of the apoptosome (Hüttemann et al., 2011; Figure 1.7).

By disabling the specific mechanism that would normally trigger the initiation of apoptotic pathways, cancer cells survive and proliferate despite harbouring apoptosis-inducing changes. Central to the detection of mutations and misreads in the DNA is the *p53* tumour-suppressor gene. *p53* acts as a transcription factor that interacts with *p53*-responsive sequences of genes such as *p21* and *bax*, a proapoptotic member of the *bcl*-2 family, which, upon activation, induce cell cycle arrest in aberrant cells (Levine, 1997; Figure 1.7). More than 50% of all human tumours harbour missense mutations in at least one allele of *p53* which allow cells to bypass the intrinsic apoptotic pathway in response to their underlying genomic aberrations.

Compounds that can restore apoptosis in cancer cells or increase their sensitivity to chemotherapeutic agents are promising candidates for the treatment of tumours.

1.7 Aims of the project

Metabolic engineering of plants offers a unique opportunity to improve the nutritional value of existing food crops by increasing their content of health-beneficial phytonutrients. During my research for my PhD I aimed to generate two transgenic high-anthocyanin tomato lines that accumulated substantial amounts of cyanidins and pelargonidins in the fruit. A metabolic engineering strategy was developed to modify

the activity of biosynthetic enzymes involved in the formation of separate anthocyanin classes.

Using an *in vitro* breast cancer cell system, I investigated the anti-cancer properties of wild type (WT) and high-anthocyanin tomato extracts in order to establish, whether the nutritional enhancement of crops with bioactive phytochemicals like anthocyanins, could improve their activity against cancer cell proliferation and survival, and whether there were differences between different types of dietary anthocyanins in their anti-cancer properties.

2 Developing novel tomato lines with increased anthocyanin content

2.1 Introduction

Anthocyanins represent an important group of polyphenolic compounds that are derived from the phenylpropanoid biosynthetic pathway (Figure 2.1). Owing to their large structural variability they are one of the largest and most abundant groups in the flavonoid family. Because they are pigments, anthocyanins often act to attract pollinators and seed-dispersing animals but also fulfil other important roles as free radical scavengers or protective screens during stress responses to high irradiance and low temperatures. Due to their high natural abundance, they are important components of the human diet and have been associated with a number of health benefits. Despite their near ubiquitous presence in higher plants (they are missing from the order of the Caryophyllales that includes the amaranth family members, sugar beet and beetroot, which produce betalains instead), anthocyanins are absent from most major food crops. Selective breeding strategies focusing predominantly on traits linked to high yield and high-energetic values (e.g. starch) have resulted in the loss or reduction of many valuable phytonutrients in modern crop varieties. Corn, potatoes, and wheat are some of the most important staple crops worldwide but all major varieties produced for human consumption are anthocyanin-deficient, despite the existence of anthocyanin-rich alternatives. For example, purple corn is a niche crop compared to white, anthocyanin-free corn varieties. Recent advances in our understanding of the dietary importance of these compounds have led to a revival of anthocyanin-pigmented varieties and generated a significant research effort into the improvement of existing crop species.

Commercial tomato plants produce a variety of flavonoids in their vegetative tissues, including low levels of anthocyanins which are mostly produced in the stems of young plants. The fruit contain a number of important phytonutrients, most notably the carotenoid lycopene and the flavonoid, rutin (quercetin-rutinoside). Other flavonols such as naringenin, kaempferol, quercetin and myricetin and their respective dihydroflavonols are produced in small quantities but no anthocyanins are synthesized. Several transgenic approaches to modify polyphenol metabolism in tomato have succeeded in producing plants with improved polyphenol contents. By introducing a *Petunia* chalcone isomerase (CHI) Muir and colleagues (2001) developed transgenic tomato plants with up to 78 fold more flavonols in fruit peel, most notably quercetin glycosides. Similarly, overexpression of other structural genes involved in flavonoid biosynthesis from different plant sources, also resulted in the accumulation of high

levels of deoxychalcones, flavones and flavonols in transgenic tomatoes (Schijlen et al., 2006). Expression of the maize gene encoding the MYB-type transcription factor *C1* and the *LC* gene encoding a bHLH transcription factor that together control the expression of several structural genes in the pathway leading to anthocyanins, also increased accumulation of flavonols in tomato fruit, but not anthocyanins (Bovy et al., 2002).

Despite their absence from tomato fruit, anthocyanins are found in several closely related species such as *Solanum chilense* or *Solanum cheesmanii*, where anthocyanin pigmentation in the fruit has been associated with the genes *Anthocyanin fruit* (*Aft*) and *Aubergine* (*Abg*) (Mes et al., 2008). The introgression of *abg* into tomato resulted in fruit that produced patches of anthocyanin pigmentation in the peel upon exposure to high light (Jones et al., 2003). Introgression is defined as the incorporation of a gene from one species into the gene pool of another through repeated backcrossing of the interspecific ybrid to one of its parents.

Recently, a more uniform anthocyanin pigmentation in the peel of the fruit has been achieved by introgressing *Aft* and the *atroviolaceum* (*atv*) gene into tomato, which influences anthocyanin accumulation in the whole plant (Povero et al., 2011). However, conventional breeding tools have limitations, as illustrated by the inability to generate tomato crosses where anthocyanin pigmentation extends beyond the peel. In 2008, tomato fruit with intense anthocyanin pigmentation of both peel and pericarp were produced using a transgenic approach (Butelli et al., 2008). Two genes encoding transcription factors from snapdragon, Delila (Del) and Rosea1 (Ros1) encoding basic helix-loop-helix (bHLH) and R2R3 MYB transcription factors, respectively, were introduced into tomato (var MicroTom) under control of a tomato fruit-specific promoter (E8). Anthocyanin accumulation in these tomatoes was uniform and light-independent and reached up to 3 mg/g FW. Butelli's work demonstrated that activation of the existing pathway rather than modification or insertion of structural anthocyanin genes was all that was required for anthocyanin accumulation in tomato (Figure 2.1).

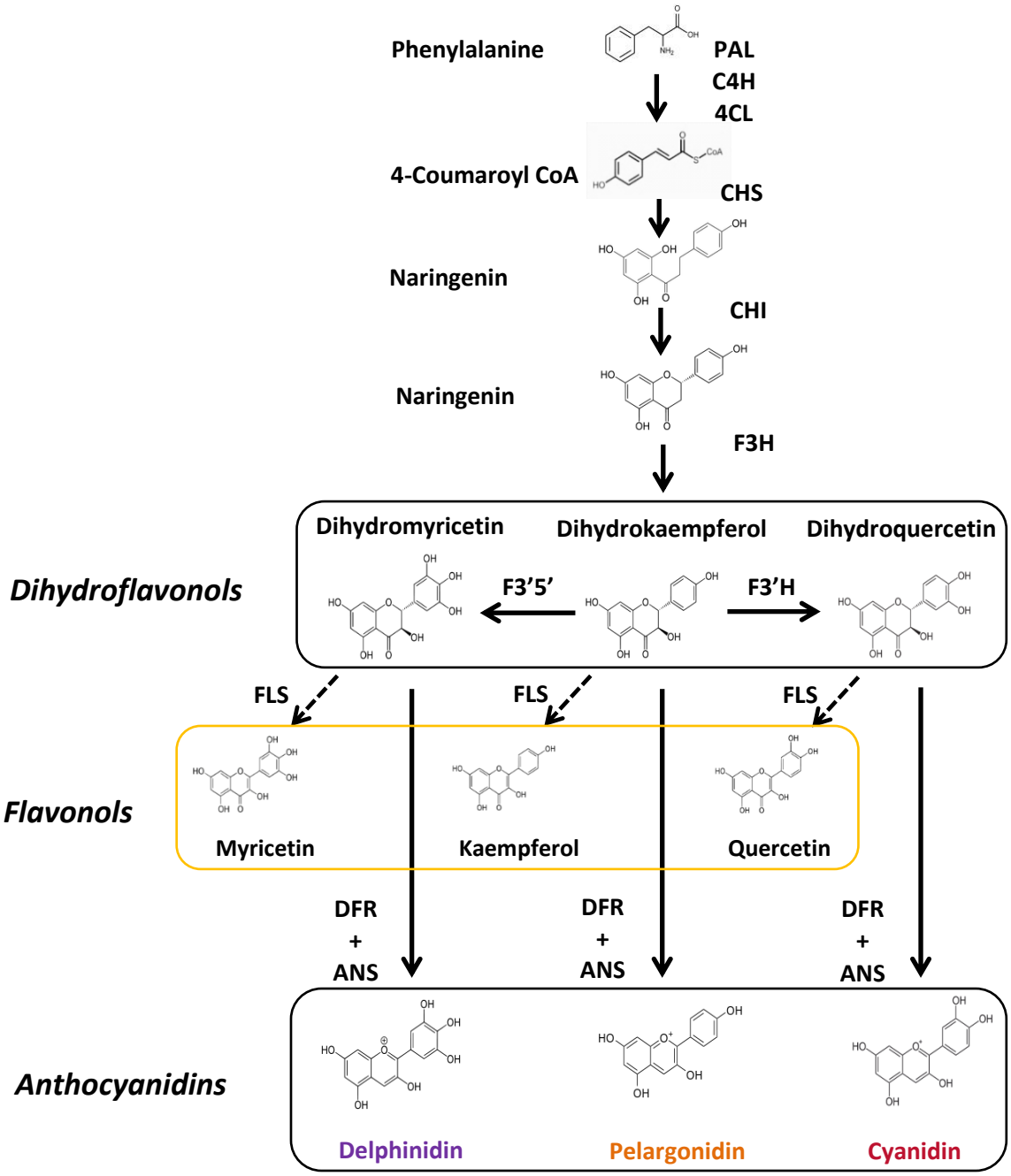

Figure 2.1: Schematic representation of the biosynthetic pathway leading to production of flavonoids. Only the structures of flavonoid classes relevant to this research are shown (boxes). PAL, phenylalanine ammonia lyase; 4CL, 4-coumarate:coenzyme A ligase; C4H, cinnamate 4-hydroxylase; C3H, 4-coumarate 3-hydroxylase; CHS, chalcone synthase; CHI, chalcone isomerase; F3H, flavanone-3-hydroxylase; F3'H, flavonoid-3'-hydroxylase; F3'5'H, flavonoid-3'5'-hydroxylase; FLS, flavonol synthase; DFR, dihydroflavonol reductase; ANS, anthocyanidin synthase.

Biochemical analyses of the tuber skin and flesh of pigmented potato (*Solanum tuberosum* L.) cultivars showed that the anthocyanins are derived mainly from either red, monohydroxylated pelargonidins or purple, trihydroxylated delphinidins but trace amounts of dihydroxylated cyanidins have also been reported (Lewis et al., 1998). Interestingly, anthocyanin-producing tomato varieties and other closely related *Solanaceae* family members produce predominantly trihydroxylated delphinidins indicating the inability to synthesise the other classes of anthocyanins. Dihydroflavonol-4-reductase (DFR) is the first committed step in the anthocyanin pathway and competes with flavonol synthase (FLS) for a group of structurally similar substrates, DHK, DHQ and DHM. Synthesis of the three dihydroflavonols is dependent on the activity of two hydroxylases: F3'H and F3'5'H which catalyses the conversion of DHK to DHQ and DHK to DHM by adding one or two hydroxyl groups, respectively, to phenyl B-ring. Most DFRs can effectively catalyse the reduction of all these colourless precursors since these compounds differ only in the number of hydroxyl groups on the phenyl B-ring, which is not the site of enzymatic action. However, DFRs from some species, such as the solanaceous species *Petunia hybrida* cannot reduce DHK efficiently, and do not produce orange-coloured pelargonidins (Johnson et al., 2001b). In *Petunia*, the substrate specificity of DFR has been associated with a region of approximately 40 amino acids which is highly variable in the DFRs from different species (Johnson et al., 2001b). Similarly, tomato shows a strong DFR substrate specificity for DHM. Tomato DFR may be capable of utilizing DHQ to a lesser extent but the absence of pelargonidin-based anthocyanins in tomato and its close relatives suggest that tomato DFR cannot use DHK as a substrate for the formation of leucopelargonidin and ultimately pelargonidins. Whilst absence of activity of either F3'5'H or F3'H in species like *Ipomea*, *Arabidopsis* and *A. majus* (Hoshino et al., 2003, Ishiguro et al., 2012, Rausher, 2008, Zufall and Rausher, 2004) has accounted for the inability to synthesise all three anthocyanins, the presence of all three dihydroflavonols in WT tomato suggests strongly that it is the specificity of DFR rather than F3'5'H or F3'H activity that is the limiting step in the production of all three anthocyanin classes in tomato.

Failure to produce anthocyanins with less than three hydroxyl group on the phenyl B-ring suggest strongly that tomato DFR has strong substrate specificity for DHM. Increasing the synthesis of DHM through activation of F3'5'H is therefore a prerequisite for making anthocyanin production in tomato possible (Bovy et al., 2002).

Consequently, metabolism of mono- and dihydroxylated anthocyanins could be facilitated by blocking the activity of F3’5’H.

Because tomato is a member of the Solanaceae family, and DFR has been shown to have strong substrate specificity for DHM in other solanaceous species (Johnson et al., 2001b) we hypothesised that in order to generate tomatoes accumulating high levels of monohydroxylated (pelargonidin) or dihydroxylated (cyanidin) anthocyanins we would need to inhibit F3’5’H activity and possibly add a DFR from a species that synthesised cyanidin/pelargonidin to overcome the substrate specificity of tomato DFR for DHM.

We proposed that complementation of tomato plants with DFR from *A. majus*, a species that produces both pelargonidin- and cyanidin-based anthocyanins in its flowers (Sherratt, 1958), could facilitate the *Del/Ros*1 transcription factor-driven production of significant amounts of the two anthocyanins in tomato. In the presence of a functional F3’5’H, tomatoes convert DHK to DHM, and ultimately trihydroxylated delphinidins. In order to generate dihydroxylated cyanidins in tomato, we hypothesised that inhibition of F3’5’H in a *DelRos*1 background was required to induce cyanidin accumulation. We also hypothesised that complementation with DFR from *A. majus* would significantly increase the amount of cyanidins produced in this tomato line by overcoming the potential limitations of the tomato DFR in effectively converting DHQ to leucocyanidin and ultimately cyanidins. Monohydroxylated pelargonidins are not found in the majority of the solanaceous species. The inability of DFR to catalyse the conversion of DHK to leucopelargonidin has been well documented in the solanaceous species *Petunia* (Beld et al., 1989, Johnson et al., 2001b) and is likely to explain the absence of pelargonidins from tomato. We hypothesised that significant accumulation of pelargonidins in tomato could be achieved by following the same approach we proposed to generate large amounts of cyanidin, together with inhibition of tomato F3’H activity (F3’H catalyses the conversion from DHK to DHQ). In the absence of F3’5’H and F3’H activity, DFR from *A. majus* should convert DHK to leucopelargonidins which would ultimately lead to the formation of pelargonidins in tomato.

2.2 Aims

In this chapter the metabolic engineering of steps in the anthocyanin biosynthetic pathway are described. Manipulation of the activity of the hydroxylase, F3’5’H and the reductase, DFR, allowed us to produce structurally different anthocyanins in tomato. A *dfr* gene sequence from *A. majus* known to encode a protein active on DHK and DHQ was used to overcome tomato DFR substrate specificity for DHM and catalyse the production of monohydroxylated pelargonidins and dihydroxylated cyanidins in tomato fruit. Using a transgenic approach all three anthocyanin subclasses, delphinidin, cyanidins and pelargonidins, were generated in different tomato lines. This work confirmed that metabolic engineering is an effective tool for achieving the accumulation of novel compounds in important crop species such as tomato. Furthermore, WT and transgenic tomatoes producing different anthocyanins can be used as models to investigate the health-promoting effects of different anthocyanin classes in the context of the same food matrix in comparative nutrition studies.

2.3 Experimental Procedures

2.3.1 Supplier details

Molecular grade chemicals and kits used in this research were obtained from Amersham (GE Life Sciences), BioRad, Fisher Scientific Ltd, Invitrogen, Life Technologies, Merck Millipore, New England Biolabs, Promega, Roche, Qiagen, Sigma, Thermo Scientific and Waters.

2.3.2 Purified Polyphenolics

The anthocyanin, delphinidin-3-O-glucoside chloride was purchased from Extrasynthase and dissolved in DMSO to a final concentration of 200 mM.

2.3.3 Enzymes

All restriction enzymes used for the generation of constructs for transformation by the insertion or removal of sequences, were purchased from New England Biolabs, Invitrogen or Roche. The polymerases used for the amplification of PCR products were purchased from Qiagen (Taq polymerase) or Thermo Scientific (Phusion® High-Fidelity DNA Polymerase). BP Clonase™ and LR Clonase™, required for the generation of constructs using Gateway® recombination cloning technology were supplied with Gateway® BP Clonase® II Enzyme mix and Gateway® LR Clonase® II Enzyme mix, respectively (Life Technologies).

2.3.4 Antibiotics

Ampicillin, carbenicillin, gentamycin, kanamycin, rifampicin, tetracycline and timentin were used for the selection of bacteria and transgenic plant material as required. Stock and working concentrations for each antibiotic are shown in Table 2i.

Table 2i: Concentrations of antibiotics used.

Antibiotic	**Purpose**	**Working stock concentration**	**Original stock concentration**
Ampicillin	For selection of *E. coli*	100 µg/mL	100 mg/mL
Carbenicillin	Used for selection of *Agrobacterium* AGL-1	50 µg/mL	50 mg/mL
Gentamycin	For selection of *E. coli*	50 µg/mL	50 mg/mL
Kanamycin	For selection of *E. coli*, *Agrobacterium*, transformed plants	50 µg/mL (*E.coli*) 100 µg/mL (plants)	100 mg/mL
Rifampicin	For selection of *Agrabacterium*	50 µg/mL	50 mg/mL
Tetracycline	For selection of *E. coli*	10 µg/mL	10 mg/mL
Timentin	For killing *Agrobacterium* during callus propagation	320 µg/mL	

2.3.5 Plant material

WT tomato (*Solanum lycopersicum* var. MicroTom) and an *f3'5'h*$^{-/-}$ mutant, *a* (anthocyaninless; *Solanum lycopersicum* in VF36 background) were used for plant transformation. Tomato seeds were obtained from the seed bank of the Tomato Genetics Resource Center (TGRC) at the University of California at Davis, USA.

2.3.6 Plant growth conditions

WT and transgenic tomato (*Solanum lycopersicum* var. MicroTom and VF36) plants were grown at 23-25°C under 16 h light and 8 h dark cycle. These conditions were maintained in the growth room, where the plants were grown on MS agar medium, and in the glasshouse. Tomato seedlings were transferred from MS agar medium to soil after approximately 3-4 weeks.

2.3.7 Seed isolation and sterilization

Seeds were extracted from mature tomato fruit and incubated for 10 min in 50% hydrochloric acid (HCl; v/v) on a plate shaker at room temperature to separate the

gelatinous coating and any remaining tomato flesh. After the HCl treatment, seeds were rinsed with water and incubated in 10% trisodium phosphate (TSP) for another 30 min on a plate shaker at room temperature to kill pathogens present on the seed surface. After TSP treatment, seeds were rinsed in water and sterilized in 10% commercial bleach (v/v) for 3 h with vigorous shaking. Seeds were washed three times with sterile, distilled water (dH_2O) before being sown out on MS agar (0.8%) plates with or without selective antibiotic.

2.3.8 Bacterial strains

The bacterial strains used for the expression of genes or maintenance of plasmids were *E. coli* DH5α and the *Agrobacterium tumefasciens* strain AGL-1. All bacteria were grown in medium containing 10g/L tryptone, 5 g/L yeast extract, 5 g/L NaCl and 15g/L agar (optional, for plate growth on solid medium).

2.3.9 Molecular methods

Most methods followed the standard procedures described in MOLECULAR CLONING (Sambrook and Russell, 2001) and were modified according to specific requirements. Additional protocols were followed according to the product supplier's specific instructions and modified when necessary.

2.3.9.1 Extraction of tomato leaf genomic DNA using CTAB and Phenol:Chloroform

DNA was extracted from tomato leaf material using hexadecyl trimethyl-ammonium bromide (CTAB) extraction buffer and purified by phenol:chloroform. CTAB buffer was prepared with CTAB (0.2 g/L, 0.1 M Tris pH 8.0, 0.02 M ethylenediaminetetraacetic acid (EDTA) pH 8.0, 1.4 M NaCl, 1% polyvinylpyrrolidone (PVP 40)) and adjusted to pH 5.0 with HCl.

Fresh, juvenile plant leaf tissue (200 mg) was ground to a fine powder in liquid N_2. 500 µL of CTAB buffer were added to the plant tissue and homogenized. Tubes were transferred to a water bath and incubated for 10 min at 55°C. After incubation, the CTAB/plant extract mixture was centrifuged at 12,000 *g* for 5 min to spin down cell debris. The supernatant was then transferred to clean microcentrifuge tubes. An equal volume of phenol:chloroform was added to the DNA sample and vortexed until an

emulsion formed. The sample was microcentrifuged at 10,000 *g* for 3 min to achieve a separation of the phenol:chloroform and aqueous phase. The aqueous phase from the top was transferred to a fresh tube and the washing steps repeated until all protein and organic matter were removed from the sample.

2.3.9.2 DNA precipitation with ethanol

To precipitate the DNA, 2.3 vol of ice-cold 100% ethanol (EtOH) and 0.1 vol NaAc (3.0 M; pH 5.3) were added to the sample, and mixed well. The DNA solution was incubated at -20°C overnight, before being microcentrifuged for 20 min at 12,000 *g*. The supernatant was removed without disturbing the DNA pellet and the DNA was washed with 1 mL 70% EtOH before being microcentrifuged for another 10 min at 12,000 *g*. The supernatant was removed carefully and the DNA pellet allowed to air-dry to remove all excess EtOH. The DNA pellet was resuspended in sterile, DNAse-free water and stored at -20°C until further use.

2.3.9.3 Primer Design and Supply

For the cloning of genes into various vectors, the confirmation of the presence of genes of interest in vectors, bacteria or plant samples and gene expression studies, specific primers were designed using the following standard guidelines. For the confirmation of gene presence, primers were designed to align at least 100 bp upstream and downstream of the start codon and stop codon, respectively. For restriction cloning, restriction site sequences preceded by a GC clamp to aid primer alignment were carefully added to the gene-specific sequences to ensure the selection of unique restriction sites to avoid insertion in non-target regions in the vector. For Gateway cloning™, *att*B1 and attB2 sites were added to the 5' end of the forward and reverse PCR primers, respectively. All other primers were designed using Primer3Plus© open web software. The primers were synthesized and supplied by Sigma and the PCR T_m values calculated using formula: $T_m = 2(A/T) + 4(G/C)$.

2.3.9.4 Polymerase Chain Reaction (PCR)

PCR reactions were performed using G-Storm and Hybaid Touchdown Thermo Cyclers. Taq DNA polymerase (Qiagen) was used for genotyping and colony PCRs. Phusion® High-Fidelity DNA polymerase (Thermo Scientific) was used for the cloning of

gene/cDNA sequences, where high fidelity and high processivity were required. For a PCR from cDNA, no more than 100 ng of template were transferred to a sterile PCR tube, and 1 µL of each primer (10 mM; synthesised by Sigma-Aldrich, Poole, UK) and 1 µL dNTP mix were added. dNTP mix contained dATP, dGTP, dTTP and dCTP (Promega) each at a final concentration of 10 mM. 5 µL 10x reaction buffer as well as 0.5 U of polymerase and distilled, sterile water to reach a final reaction volume of 50 µL were added. PCR conditions varied depending on the T_m of the primers, the length of the expected product size, and the polymerase used in the reaction.

2.3.9.5 Purification of PCR products

PCR purification was performed using a PCR purification kit (Qiagen) following the protocol provided. This purification procedure allows for the removal of primers, nucleotides, enzymes, salts, detergents and other impurities from DNA samples. Mixing of the PCR solution with binding buffers supplied increases the amount of chaotropic salts which alter the structure of water which is required for optimum adsorption of the DNA to the QIAquick silica membrane resins. Optimum adsorption occurs at a pH ≤ 7.5 and was adjusted with 3 M sodium acetate, pH 5.0 if necessary. During DNA adsorption, impurities do not bind to the silica membrane but will flow through the resin, whilst salts are washed away by an ethanol-containing buffer.

The purified DNA was eluted by adding 30 µL of water directly onto the silica membrane and incubating for 1 min before centrifuging at 13,000 *g* for 1 min.

2.3.10 Methods of construct design

2.3.10.1 Plasmid DNA isolation from *E. coli*

Plasmid DNA was isolated from 1-5 mL of liquid, overnight *E.coli* cultures transformed with the vector of interest and grown with the appropriate antibiotic selection.The bacterial cells were collected by centrifugation at 12,000 rpm for 2 min and resuspended in lysis buffer. Plasmids were isolated using the QIAprep® Spin Miniprep kit (Qiagen) following the instructions provided by the manufacturer. Membrane-bound plasmid DNA was eluted in 25-50 µL of elution buffer (provided).

2.3.10.2 Plasmid and PCR digests

Restriction digestions of PCR products and vectors were performed using suitable restriction enzymes for T4 ligation reactions and the confirmation of cloning. Restriction enzymes with matching buffers where chosen when possible and reaction mixtures set up with 0.5-1.0 µg of plasmid or PCR DNA, 10-20 units of respective restriction enzyme, 1x final concentration of buffer and dH_20 to make up to required reaction volume. Reactions were incubated for 1 h at 37°C or the temperature specified for the enzyme, before loading a small aliquot on a 1.0 % agarose gel to check for successful digestion. If digestion was partial, reactions were re-incubated for up to 4 h before the reaction was either stopped though heat-inactivation at 65°C for 15 min, or the enzyme removed by ethanol precipitation of DNA.

2.3.10.3 Ligation

Ligation reactions were set up with a concentration ratio of 3:1 for insert to vector DNA using approximately 50 ng of insert DNA and 150 ng of vector DNA, 1x ligation buffer, 5-10 units of T4 DNA ligase and dH_20 up to a final volume of 10 µL. The reaction was performed overnight at 4 °C.

2.3.10.4 Agarose gel electrophoresis

PCR and restriction digestion products were run on 1.0 % agarose gels in 1X Tris Borate EDTA (TBE 10X: 0.89 mM Boric Acid and 20 mM EDTA; pH 8) buffer. Prior to casting, ethidium bromide was added to the agarose gel at a final concentration of 0.1 µg/mL. Standard DNA markers (100 bp and 1 kb ladders; NEB) were used to identify the size of fragments and the ethidium bromide-stained DNA was visualized using a long wavelength UV transilluminator.

2.3.10.5 Purification of DNA bands from agarose gels

After running DNA on a 1% agarose gel containing 0.1 µg/mL ethidium bromide, DNA was visualized under UV light and bands of interest cut out using a sharp, sterile scalpel blade and transferred to an Eppendorf tube for subsequent DNA purification.

DNA was eluted and purified from the gel using the Gel Extraction Kit (Qiagen) and the DNA was recovered according to the instruction provided. The DNA was eluted from the Qiagen binding column by adding 25-50 µL of elution buffer (provided with kit).

2.3.10.6 Quantification of DNA or RNA

Purified DNA or RNA samples were quantified using a NanoDrop UV-Vis spectrophotometer (Thermo Scientific). Nucleotides absorb at 260 nm (A260), whilst proteins have a peak absorbance at 280 nm (A280). A ratio of absorbance at 260 nm and 280 nm is used to assess the purity of DNA and RNA. A260/A280 ratio of ~1.8 and higher is typically suitable for further analysis or downstream applications. Protein contamination will lower the A260/A280 ratio.

2.3.10.7 GATEWAY® cloning

The Gateway® recombination cloning technology (Invitrogen) allows for the transfer of DNA sequences between plasmids using a set of recombinant "Gateway® *att*" sites and "BP and LR clonase" enzyme mixes. Cloning is carried out in two steps, requiring the BP clonase-mediated insertion of an "*att*" sequence-flanked DNA fragment into a suitable Gateway® entry vector such as pDONR207. The gene cassette in the entry clone is then transferred into a suitable Gateway® destination vector using LR clonase. Gateway® cloning was performed according to the manufacturer's instructions. The "*att*" sequences and a detailed description for the entry vectors are available from Invitrogen.

2.3.10.8 Sequencing reactions

Plasmids that potentially contained the desired sequence or gene inserts were sequenced using standard Big Dye Sequencing reactions set up with 100-150 ng of plasmid DNA, 0.4 µL of desired primer (10 mM), 1 µL of Big Dye 3.1, 2.6 µL of 5x buffer (supplied with Big Dye), and dH_2O to a final volume of 13 µL. The PCR was performed according to the following conditions: initial denaturation at 96°C for 1 min, followed by 25 cycles of denaturation at 96°C for 10 sec, annealing at 50°C for 10 sec, and elongation at 60°C for 4 min. Samples were commercially sequenced by Genome Enterprise Ltd (Norwich, UK) and data obtained as ABI trace files that were analysed with Vector NTI® Advance Software version 11 (Invitrogen).

2.3.11 Quantifying gene expression

Expression of key anthocyanin pathway genes was detected using quantitative reverse-transcriptase PCR (qRT-PCR).

2.3.11.1 RNA extraction

High quality, intact RNA was essential for analysing the activity of target genes by qRT-PCR. RNA was also required for making first strand cDNA in PCR experiments. Different RNA extraction techniques were used for tomato fruit tissue and tomato leaf tissue.

2.3.11.2 Total RNA extraction from fruit tissue using TRI Reagent®

Tomato fruit were harvested at different developmental stages, sliced and the seeds removed, before being frozen immediately in liquid nitrogen (N_2) and stored at -80°C until further use.

Total RNA was isolated using TRI Reagent® (Sigma) following the recommended protocol with modifications. Tomato fruit tissue (200 mg) was ground in liquid N_2 before adding 1.5 mL of TRI Reagent®. The homogenised sample/TRI Reagent® mixture was incubated at room temperature for 5 minutes shaking, before adding 150 µL 1-Bromo-3-chloropropane (BCP; Sigma) which acts as a phase-separation agent and decreases the possibility of contamination of RNA with DNA. The sample/TRI Reagent®/BCP mixture was homogenized thoroughly and incubated for another 10 min at room temperature. The sample mixture was microcentrifuged for 10 mins at 12,000 *g* at 4°C. Two distinct phases formed and 750 µL of the aqueous, RNA-containing phase were transferred to a sterile, RNAse-free tube and mixed with an equal volume of isopropanol. The RNA was allowed to precipitate for 5 min at room temperature, before being microcentrifuged for 8 min at 12,000 *g* at 4°C. Then, the supernatant was discarded and the RNA pellet washed with 500 µL of isopropanol. Without disturbing the pellet the supernatant was carefully removed and the RNA pellet washed with 1.0 mL of 75% EtOH. The supernatant was discarded and the EtOH washing step was repeated before air-drying the RNA pellet at room temperature for approximately 5 min. Then, the RNA pellet was resuspended in 40 µL sterile, RNAse-free H_20 and allowed to

dissolve for 1 h at 4°C. The sample was centrifuged for 5 min at 12,000 *g* at 4°C to separate the soluble RNA solution from remaining contaminants such as sugar that formed a pellet at the bottom of the Eppendorf tube. RNA-containing supernatant (32 µL) was transferred to a new Eppendorf tube and mixed with 4 µL of DNAse1 and 4 µL of 10x DNAse1 buffer (Invitrogen™) and incubated at room temperature for 45 min. The DNAse reaction was stopped by adding 4 µL of 25 mM EDTA and incubating at 65°C for 10 min.

2.3.11.3 RNA extraction using Qiagen RNeasy mini kit

Total RNA was isolated from plant leaves using the Qiagen RNeasy mini kit following the manufacturer's protocol (Qiagen). Plant material was ground in liquid N_2, lysed and then homogenized with the QIAshredder column.

EtOH was added to the lysate to provide optimum conditions that promote selective binding of the RNA to the RNeasy silica-like membrane. Contaminants were washed away before eluting the membrane-bound RNA with RNase-free water.

2.3.11.4 cDNA synthesis

DNAse-treated RNA (3 µg) was mixed with 1 µL of 10 mM primer mix (1:1 oligo-dT and random primers), 1 µL of 10 mM dNTPs, and RNAse-free H_20 was added to a final volume of 20 µL. The RNA/dNTP/primer mix was incubated for 5 minutes at 65°C and then chilled on ice. Reverse transcription from RNA was performed with Invitrogen's SuperScript® III Reverse Transcriptase kit by adding 6 µL of 5x first strand buffer, 2 µL of 0.1 M dithiothreitol (DTT), 1 µL of SuperScript® III Reverse Transcriptase and 1 µL of RNaseOUT™ (RNase inhibitor, Invitrogen™) to the 20 µL RNA/dNTP/primer mix. Samples were mixed gently and reverse transcription was allowed to take place for 1 h at 50°C. The reaction was inactivated by heating at 70°C for 15 min and samples were stored at -20°C.

2.3.11.5 Quantitative PCR

Three independent biological samples of tomato fruit at breaker stage were pooled and RNA was extracted as previously described in Chapter 2.3.11.2. Expression of

flavonoid biosynthetic pathway genes (primers shown in Table 2ii) was measured by qRT-PCR using SYBR® Green JumpStart™ Taq ReadyMix™ (Sigma) and RNA quantity was normalised to *Solanum lycopersicum* ubiquitin (*S. lycopersicum* ubiquitin). Ubiquitin acts as an internal standard that is required to normalise RNA amount and does not change in expression as tomato fruit undergo development. The qRT-PCRs were performed in white well PCR plates and for each qRT-PCR reaction 50 ng of cDNA were mixed with 5 µM forward and reverse primer (1 µL each) and 10 µL of SYBR® Green JumpStart™ Taq ReadyMix™ and RNAse-free H_20 was added to a final volume of 20 µL. All reactions were performed in triplicate and real-time detection was performed using an Opticon™ DNA Engine 2 thermal cycler (MJ research). The data was acquired and analysed with MJ Opticon Monitor™ 3.1 analysis software.

Table 2ii: Sequences and efficiency values of primers for real-time PCR used to investigate anthocyanin biosynthetis gene expression.

Gene	Primer	Sequence (5' → 3')	Efficiency
SlUBI	F	GCCAAAGAAGATCAAGCACA	1.82
	R	TCAGCATTAGGGCACTCCTT	
SlPAL	F	AATTGCTTCGAGTCGTGGATAG	1.91
	R	ACAAGGACTTGTCTCAGCTTCTG	
SlCHS-1	F	CCTTTATTTGAACTCGTCTCAGC	1.71
	R	CAGGAACATCCTTGAGTAAGTGG	
SlCHI	F	TTGTCAACTCGGTCTAATGTGTC	1.98
	R	TAAAGTGGGACCTTATTGCACAC	
SlF3H	F	ATGGATGAGCCGATTACATTTG	1.98
	R	TGGCCTCTTCAGTTTGTATCTTC	
SlF3'5'H	F	CTCAACGCCACTAAATCTCCCTA	1.93
	R	TTGCCCATATGTTGACACTAAGC	
SlF3'H	F	TATAGCTGGGACAGACACATCCT	2.16
	R	CTACTTTGTCGATCTCCTGTTGG	
SlDFR	F	GACTTGCCGACAGAAGCAAT	1.96
	R	GTGCATTCTCCTTGCCACTT	
SlANS	F	ACGAACAGGATTTTGCTGCT	1.97
	R	TTTGAGCTCAGCAACTGCAT	
SlFLS	F	TGTCCCATATCACCCTTCTTGTC	1.71
	R	TCACCAATGTGGACAATTATAGCA	
AmDFR	F	TGCAACTGTTCGTGATCCTG	1.90
	R	CATGTCTGCCTTCCACAATG	
AmDel	F	AGATTACTTGAGAGGGCTTGAGAGG	2.01
	R	TGGCATCGTGTAGTTTAGTTTTTGT	
AmRos1	F	TGGTCGCTATTGCTGGTAG	1.92
	R	ATCGTTCTCCATCCATCCTCGCCTA	

Am, *Antirrhinum majus*; F, forward; R, reverse; *Sl*, *Solanum lycopersicum*.

2.3.12 Construction of binary vectors for *Agrobacterium*-mediated plant transformation

Stably transformed tomato plants were generated using *Agrobacterium tumefasciens* (*A. tumefasciens*)-mediated transformation. *Agrobacterium*-mediated DNA transfer is an efficient technique to deliver plasmids into many different plant species. *A. tumefasciens* causes crown gall disease and infects plants by transferring virulence genes into the nucleus of infected cells. The disarmed *A. tumefasciens* strains used in plant transformation have lost the genes that cause the symptoms of crown disease but

retained their ability to transfer plasmid DNA into infected plant cells. Binary vectors are shuttle vectors that can replicate in multiple hosts.

2.3.12.1 Construction of binary vector SLJ.E8.DFR

The cDNA sequence encoding for the *A. majus* DFR was cloned into a suitable binary vector allowing for expression in both *E.coli* and *A. tumefasciens*.

2.3.12.1.1 Digestion of binary vector SLJ.E8.60

The binary destination vector SLJ.E8.60 was provided by Eugenio Butelli. SLJ.E8.60 has been modified from the SLJ7292 plant expression vector (generated by Prof Jonathan Jones, The Sainsbury Laboratory, Norwich, UK. Plasmid list available from http://www.tsl.ac.uk/research/jonathan-jones/plasmids.htm) by insertion of sequences encoding the *S. lycopersicum* E8 promoter (GenBank accession: DQ317599.1) and the *A. majus Rosea*1 gene (GenBank accession: DQ866652.1). In order to place the *A. majus dfr* (*AmDfr*) cDNA sequence under control of the E8 promoter, the *Rosea1* gene was removed from SLJ.E8.60 by selecting suitable restriction sites downstream and upstream of the *Rosea*1 sequence and digesting SLJ.E8.60 with *BamH*I and *Sma*I (Figure 2.4 A)

2.3.12.1.2 Addition of restriction sites to AmDfr cDNA

Dfr cDNA from *A. majus* (size 1,341 bp; GenBank accession: X15536.1) was kindly provided by Cathie Martin and reamplified using primers designed to introduce *Bgl*II and *Sma*I restriction sites (Figure 2.2). *BamH*I and *Bgl*II generate compatible cohesive ends that allow for ligation of the *Bgl*II-flanked DFR cDNA sequence into the *BamH*I-digested destination vector. Primer sequences are reported in Table 2iii and their respective positions in the cDNA highlighted in Figure 2.2. The PCR reaction to add these restriction sites was performed with proof-reading Pfu® DNA polymerase (Stratagene) according to the following conditions: initial denaturation at 95°C for 2 min, followed by 30 cycles of: denaturation at 95°C for 45 sec, annealing at 65°C for 45 sec, elongation at 72°C for 90 sec and a final elongation step of 10 min at 72°C.

DfrBglII_FA

CGAGAAGATCTATGAGTCCCACTTCACTAAATACGAGTTCGGAAACCGCACCACCATCCTCAACCACCGT

ATGTGTCACAGGAGCTGCCGGCTTCATAGGCTCATGGCTTGTCATGAGGCTTCTCGAACGTGGCTACACC

GTTCGTGCAACTGTTCGTGATCCTGGTAATATGAAGAAGGTAAAACACCTAATAGAACTGCCAAAAGCAG

ACACGAACTTGACATTGTGGAAGGCAGACATGACAGTAGAAGGAAGCTTCGACGAAGCAATTCAAGGTTG

CGAAGGAGTGTTTCACTTGGCCACGTCTATGGAATTTGATTCCGTGGATCCTGAGAATGAAGTGATCAAG

CCAACAATTGACGGTATGTTGAACATCATTAAATCATGCGTGCAAGCAAAAACCGTCAAGAAATTCATCT

TCACCACATCCGGTGGGACTGTAAATGTTGAAGAACACCAGAAACCAGTCTATGATGAAACAGATTCCAG

TGACATGGATTTCATTAACTCCAAAAAAATGACTGGATGGATGTATTTTGTGTCAAAAATCTTGGCAGAG

AAAGCTGGAATGGAAGCAGCAAAAGAGAATAACATTGATTTTATCAGCATTATACCACCCCTGGTGGTTG

GTCCATTTATCATGCCAACATTCCCACCTAGCCTAATCACTGCACTTTCTCCCATTACTGGGAATGAGGC

TCACTACTCAATCATAAAGCAATGTCAATATGTGCATTTGGATGATCTGTGTGAGGGTCATATATTCTTG

TTTGAGTATCCTAAGGCAGAAGGAAGATACATTTGCTCCTCTCATGACGCAACAATTTATGATATCGCTA

AATTGATCACAGAGAACTGGCCCGAATATCATATCCCTGACGAATTTGAGGGCATTGACAAGGACATACC

GGTGGTGAGTTTCTCCTCCAAGAAAATGATCGGAATGGGTTTTATATTCAAGTACACATTAGAGGACATG

TTCAGGGGTGCGATTGACACTTGCCGCGAGAAAGGAATGCTCCCGTATTCTACTAAGAATAACAAGGGAG

ACGAGAAGGAACCCATTTTGAATTCCCTAGAAAACAATTACAATATTCAAGACAAAGAACTGTTTCCAAT

TTCGGAGGAAAAACACATCAATGGACAAGAGAATGCCCTGCTTTCAAATACTCAAGACAAAGAACTGCTT

CCAACTTCAGAAGAAAAACGTGTTAATGGACTAGAGAGCGCCCTGCTTTCAAAGATTCAAGACAAAGAAG

TGCTTCCAACTTCAGGGGTTAAGCATGCCAACGGACAAGAAAATGCGCTGCTTCCAGACATTGCAAACGA

DfrSmaI_RE

TCATACTGATGGCAGAATCTAGCCCGGGGGACTG

Figure 2.2: *A. majus* pallida cDNA sequence with PCR primer positions and sequences. Restriction site sequences highlighted in red were added to the 3' and 5' end of the cDNA sequence for subsequent cloning into the binary vector SLJ.E8.60.

Table 2iii: Primers for the addition of restriction sites to the cDNA sequence of the DFR cDNA from *A. majus*.

Primer name	**Sequence (5'→ 3')**
DfrBglII_FA	CGAGAAGATCTATGAGTCCCACTTCACTAAATACGAG
DfrSmaI_RE	CGATCATACTGATGGCAGAATCTAGCCCGGGGGACTG

2.3.12.1.3 Ligation of A. majus dfr sequence into binary destination vector

The *Bgl*II/*Sma*I-flanked *A. majus dfr* PCR product was digested with the restriction enzymes *Bgl*II and *Sma*I and ligated into the *BamH*I and *Sma*I digested binary vector SLJ.E8.60 (Figure 2.3 B) using T4 DNA ligase generating the binary vector, SLJ.E8.DFR (Figure 2.3 C). The ligation reaction was incubated overnight at 4°C and was subsequently used to transform *E. coli* Dh5α cells as described in section 2.3.14.1.

Transformed *E. coli* cells containing SLJ.E8.DFR plasmid were selected on agar plates with the selective antibiotic tetracycline. The presence of the *A. majus dfr* gene sequence in the plasmid carried by positive transformed cells was confirmed by colony PCR using the primers DfrBglII_FA and DfrSma1_RE (Table 2iii). With a pipette tip, a small number of *E. coli* cells from individual colonies were transferred into a PCR tube containing the PCR master mix. Colonies containing the *A. majus dfr* gene were selected and grown at 37°C overnight with shaking in 10 mL of L-medium with tetracycline at 10 µg/mL. Plasmid DNA from SLJ.E8.DFR containing *E. coli* was extracted using the Qiagen Spin Miniprep kit following the instructions in section 2.3.10.1. In order to confirm the correct sequence of the *A. majus dfr* gene, a sequencing reaction using the primers shown in Table 2iii was performed following the instructions in 2.3.10.8.

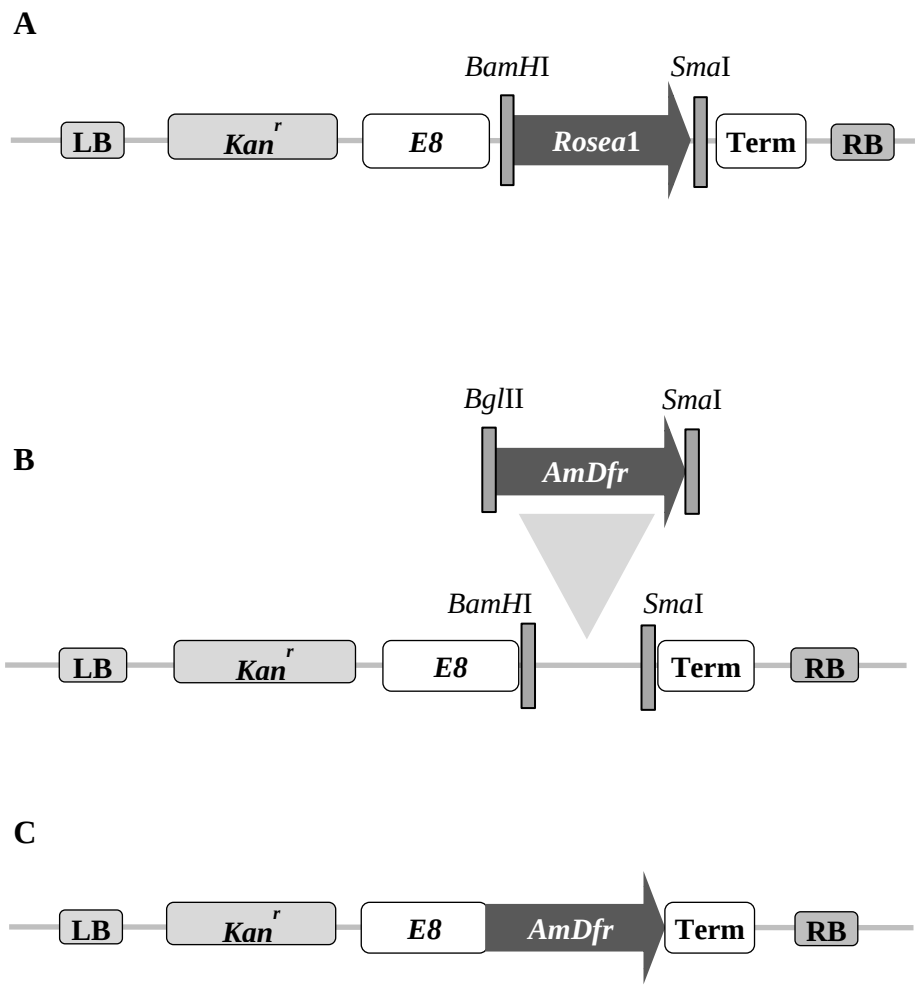

Figure 2.3: Cloning strategy to generate SLJ.E8.DFR. (**A**) Map of T-DNA region of the binary vector SLJ.E8.60 with restriction sites *BamH*I and *Sma*I. (**B**) Cloning of *Bgl*II/*Sma*I flanked *A. majus dfr* sequence into SLJ.E8.60 after removal of *Rosea*1. (**C**) Map of T-DNA region of the binary vector SLJ.E8.DFR used for transformation of tomato plants. *AmDfr*, *A. majus dfr* cDNA sequence; E8, ethylene-responsive fruit ripening E8 promoter; Kan^r, LB, left T-DNA border region; nptII gene conferring kanamycin resistance under the control of the nos promoter; RM right T-DNA border region; *Rosea*1, *A. majus Rosea*1 transcription factor cDNA sequence; Term, terminator region of cauliflower mosaic virus.

2.3.12.2 Construction of binary vector pFRN.F3'H.RNAi

Fragments of the *f3'h* gene encoding for the *S. lycopersicum* F3'H was cloned into a suitable binary double-stranded RNA vector allowing for expression in both *E.coli* and *A. tumefasciens*.

2.3.12.2.1 Addition of Gateway® att sites to the f3'h gene sequence fragment

The mRNA sequence of *f3'h* from *S. lycopersicum* (size 1,785 bp; GenBank accession: XM_004235959.1) was obtained from the National Center for Biotechnology Information (NCBI) Genbank and an *f3'h* fragment was reamplified using primers designed to introduce Gateway® *attB1* and *attB2* sites (Figure 2.4 A). The *att*-flanked *f3'h* sequence fragment was inserted into the Gateway® entry clone pDONR207 by Gateway® BP clonase-mediated recombination (Figure 2.4 B). Primer sequences are reported in Table 2iv. The PCR reaction to add these restriction sites was performed with GoTaq™ DNA Polymerase (Promega) according to the following conditions: initial denaturation at 95°C for 2 min, followed by 30 cycles of: denaturation at 95°C for 45 sec, annealing at 65°C for 45 sec, elongation at 72°C for 120 sec and a final elongation step of 10 min at 72°C.

Table 2iv: Primers for the addition of Gateway® *att* sites to the *f3'h* gene sequence fragment from *S. lycopersicum*.

Primer name	**Sequence (5'→ 3')**
Slf3'h_FA_Gateway	GGGGACAAGTTTGTACAAAAAAGCAGGCTGGTGGCGTATGCTAAGGAAA
Slf3'h_RB_Gateway	GGGGACCACTTTGTACAAGAAAGCTGGGTTCTTTCGGGCCTGAACTCTA

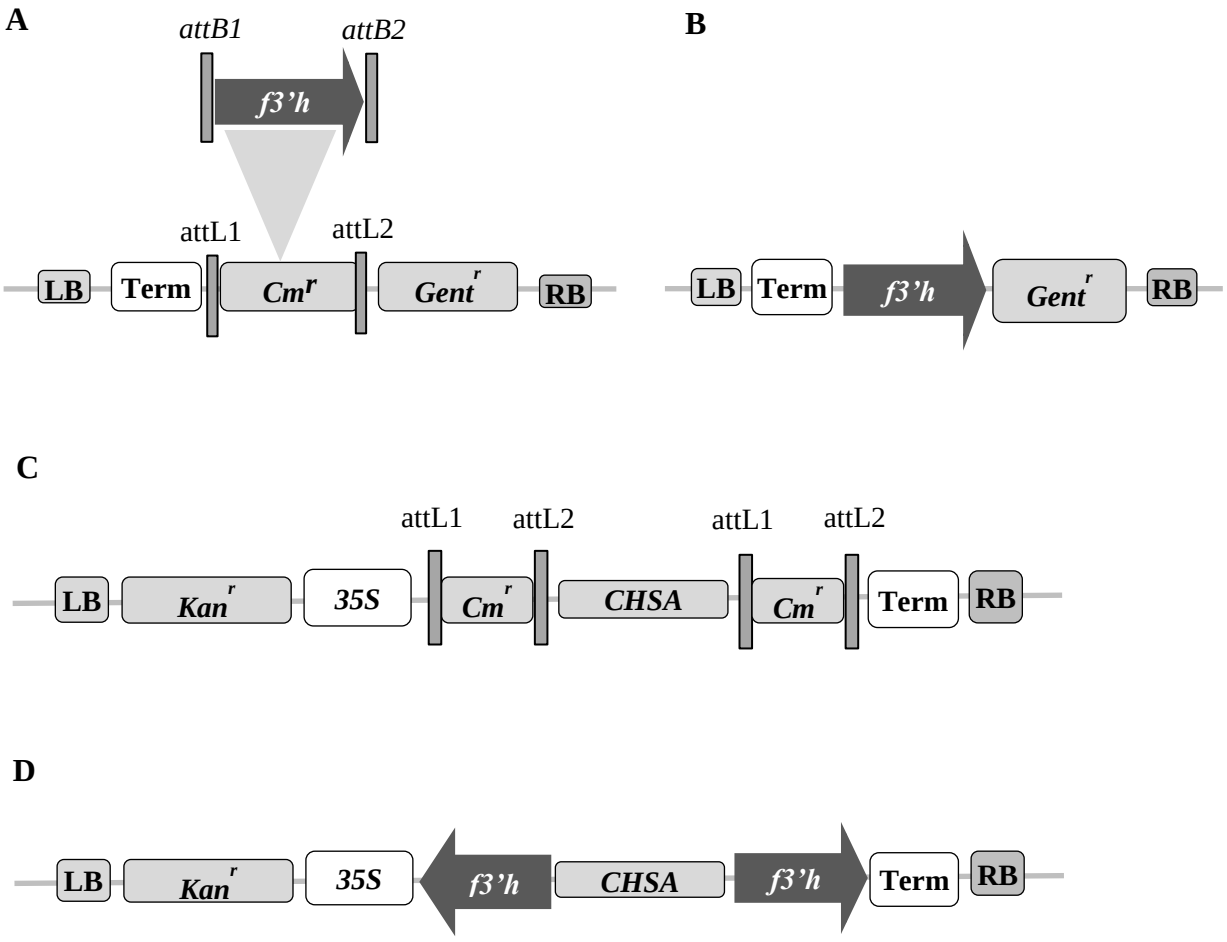

Figure 2.4: Cloning strategy to generate pFRN.F3'H.RNAi. (**A**) Map of T-DNA region of the Gateway® entry clone pDONR207 with entry sites *att*L1/*att*L2 and *attB1/attB2* flanked *S. lycopersicum f3'h* sequence fragment (**B**) Gateway® entry clone pDONR207 containing *S. lycopersicum f3'h* sequence fragment (**C**) Map of T-DNA region of the binary Gateway® destination clone pFRN (modified from the destination clone pFGC5941 expressing dsRNA) containing a 35S promoter (**D**) Map of T-DNA region of the binary vector pFRN.F3'H.RNAi used for transformation of tomato plants. 35S, 35S constitutive promoter sequence of the cauliflower mosaic virus; CHSA, chalcone synthase A intron; Cm^r, chloramphenicol resistance gene; *f3'h*, *S. lycopersicum f3'h* sequence fragment; $Gent^r$, gentamycin resistance gene; Kan^r, nptII gene conferring kanamycin resistance under the control of the nos promoter; LB, left T-DNA border region; RM right T-DNA border region; Term, terminator region.

2.3.12.2.2 Generation of binary destination vector pFRN.F3'H.RNAi

The gene cassette in the entry clone, containing the *f3'h* sequence fragment, was transferred into a suitable double-stranded RNA Gateway® destination vector pFRN (Figure 2.4 C) using Gateway® LR clonase-mediated recombination (see Chapter 2.3.10.7 for description of Gateway® cloning technology). The recombination resulted in the formation of the binary pFRN.F3'H.RNAi vector suitable for silencing of the *f3'h* gene in tomato (Figure 2.4 D).

Transformed *E. coli* cells containing pFRN.F3'H.RNAi plasmid were selected on agar plates with the selective antibiotic kanamycin. The presence of the *S. lycopersicum f3'h* gene sequence fragment in the plasmid, carried by positive transformed cells, was confirmed by colony PCR using the primers Slf3'h_FA_Gateway and Slf3'h_RB_Gateway (Table 2iv). With a pipette tip, a small number of *E. coli* cells from individual colonies were transferred into a PCR tube containing the PCR master mix. Colonies containing the *S. lycopersicum f3'h* gene were selected and grown at 37°C overnight with shaking in 10 mL of L-medium with kanamycin at 50 µg/mL. Plasmid DNA from SLJ.E8.DFR containing *E. coli* was extracted using the Qiagen Spin Miniprep kit following the instructions in section 2.2.10.1. No sequencing reaction confirming the correct insertion of the *S. lycopersicum f3'h* gene fragment into the pFRN.F3'H.RNAi binary vector was carried out because the opposite orientation of the two *S. lycopersicum f3'h* gene fragments made correct alignment and contig assembly very difficult and misreads in the sequence of the *S. lycopersicum f3'h* gene fragment were unlikely to impact the RNA interference (RNAi) leading to the silencing of F3'H in pFRN.F3'H.RNAi-transformed plants.

2.3.13 Sequencing of constructs

All clones designed for transformation of tomato with *AmDfr* cDNA were sequenced before being used for transformation of plants. Several Big Dye (3.1) sequencing reactions with a maximum read length of 500 bp were carried out spanning the whole region of the gene of interest. The sequencing data was analysed using Vector NTI® and contigs generated from sequences obtained with individual primers using ContigExpress. The assembled contigs were aligned with the original sequence obtained from NCBI using AlignX®. Both ContigExpress and AlignX® are part of the Vector

NTI® software package (Invitrogen). The three primer pairs used to confirm the correct sequence of the *AmDfr* clones are reported in Table 2v. Plasmids with the correct *A. majus dfr* sequence were used for subsequent transformation of tomato.

Table 2v: Primers for the sequencing of the *dfr* cDNA sequence of *A. majus* pallida.

Primer name	**Sequence (5'→ 3')**
DFR_F1	ACCACCGTATGTCACAGGA
DFR_F2	GAGAAAGCTGGAATGGAAGCA
DFR_F3	AAGGGAGACGAGAAGGAACC
DFR_R1	GGAAGGCAGACATGACAGTAGA
DFR_R2	TGGATGATCTGTGTGAGGGTCA
DFR_R3	CGTGTTAATGGACTAGAGAGCG

2.3.14 Transformation of organisms

2.3.14.1 Transformation of *E. coli*

E. coli cells were transformed using the heat shock method. Competent Dh5α cells were thawed on ice. After 10 min 1.5 µL of the ligation reaction or plasmid construct containing approximately 300-500 ng/µL DNA were added to 100 µL of thawed, competent Dh5α cells and mixed gently. The competent cell/construct mix remained on ice for 30 min before heat-shock by incubating the cells at 42°C for 45 sec, and then transferring them immediately back onto ice for another 2 min. Pre-warmed LB broth (1 mL) was added and the cells were allowed to recover at 37°C for 1 h shaking in the incubator. Aliquots of transformed cells were the plated on LB agar plates containing appropriate selective antibiotics and incubated at 37°C overnight.

2.3.14.2 Transformation of *A. tumefasciens* by triparental mating

Triparental mating was chosen to transform the binary vectors to *A. tumefasciens* because plasmids ranging from between 25 and 30 kb in size proved too large to enter *A. tumefasciens* by electroporation. Triparental mating relies on the co-cultivation of *A.*

tumefasciens AGL-1 (recipient strain), *E. coli* Dh5α containing the desired construct (donor strain), and *E. coli* pRK2013 (helper strain), which facilitates the transfer of the construct of interest from the transformed *E. coli* to the untransformed *A. tumefasciens*. All three strains were grown separately to an optical density $(OD)_{600}$ of between 0.5-0.9 with their respective antibiotics (*A. tumefasciens* at 28°C with rifampicin 50 µg/mL, *E. coli* Dh5α at 37°C with construct-specific antibiotic, and *E. coli* pRK2013 at 37°C with kanamycin 50 µg/mL).

Aliquots of a the *E. coli* donor, *E. coli* helper and *A. tumefasciens* recipient strains were added to a sterile tube in a ratio of 1:1:2 and mixed thoroughly before spreading 0.5 mL of this mix on L agar plates containing no antibiotics. After incubation of the plate at 28°C for 1 to 2 days, the bacterial film was washed off with 0.5 mL of LB broth. The bacterial solution was plated onto LB agar plates containing the plasmid selective antibiotic, 50 µg/mL rifampicin as well as 100 µg/mL carbenicillin to which *A. tumefasciens* AGL-1 is resistant and which allows selection against *E. coli*. After incubation for 2-3 days at 28 °C individual *A. tumefasciens* AGL-1 colonies were selected and the presence of the desired plasmid was confirmed by colony PCR.

2.3.15 Stable transformation of Tomato

2.3.15.1 Growth media and supplements

Regeneration and shooting medium for the propagation of transformants were prepared freshly on the day of use (recipes can be found in the Appendix).

2.3.15.2 *A. tumefasciens* mediated tomato transformation

A 24 h culture of *A. tumefasciens* AGL-1 containing the binary vector for transformation of tomato was set up at 28°C with shaking. The same day, feeder plates were set up by evenly spreading 1 mL of fine tobacco suspension culture onto plates containing the MS medium with 0.5 mg/L 2,4-dextrose, and 0.6% agarose. Plates were placed unsealed and stacked in the cell culture room in 1ow light, overnight. Cotyledons from ten-day old, sterile grown tomato seedlings were harvested the next morning and placed in sterile water. After removing the outer cotyledon tips with clean, sterile razor blades the cotyledons were cut transversely into 3-4 mm pieces and placed onto sterile

filter paper. Up to 40 cotyledon pieces were then transferred onto a feeder plate with their abaxial surface uppermost. The feeder plates had been covered with a sterile filter paper to prevent direct contact between the tobacco cell culture and the tomato cotyledons. The feeder plates together with the cotyledons were placed at 25°C under low light for 8 h. The 24 h *Agrobacterium* culture was centrifuged to remove the culture medium before resuspending the pellet in MS medium containing 3% sucrose to a final OD_{600} of 0.4-0.5. After the 8 h incubation on feeder plates the cotyledons were immersed in the *Agrobacterium* solution for 1-30 min, before being blotted dry and transferred back onto the original feeder plates. The feeder plates with the cotyledons were then moved back to the culture room and co-cultivated at 25°C under low light for 40 h.

After the co-cultivation period the cotyledon pieces were transferred onto regeneration medium. Twelve cotyledon pieces were placed on each 100 mm Petri dish with the leaf ends curling into the medium to ensure good contact between the leaf and nutrients and antibiotics. The cotyledon pieces were allowed to generate *calli* and leaves and were transferred onto fresh medium every 2-3 weeks for approximately three months. Shoots from each callus structure were then excised and transferred to labelled, individual jars containing fresh rooting medium. Once the shoots had developed a well-branched root system they were removed from the shooting medium and transferred to soil and moved to the glasshouse. Positive transformants were identified by PCR using primers specific for the *npt*II gene conferring kanamycin resistance to explants carrying the transformation construct.

2.3.16 Tomato crosses

Transgenic parental lines were crossed to generate a T1 plant population with the genes of interest. In the T2 plants the allele pairs segregated leading to some T2 plants carrying the desired combination of genes. The Mendelian principle of segregation defines the separation of pairs of alleles in the reproductive cells, resulting in offspring with new allele combinations different from those of the parents'. Tomato crosses were performed by emasculating (removal of stamens) the flowers of the female parents before the flower opened up and the stamens reached full maturity. One day after emasculation the female parents were pollinated by carefully brushing the male parents'

pollen containing stamens against the stigma. Seeds were collected once the developing tomato fruit had reached their full maturity and excess tomato flesh was removed by washing the seeds for 10 min with 50% HCl. Clean seeds were stored in a dry, cold place.

2.3.16.1 Generation of E8::*Del/Ros*1/*f3'5'h*$^{-/-}$

Tomatoes (*Solanum lycopersicum* var. MicroTom) expressing *Delila* (*Del*; GenBank accession: M84913.1) and *Rosea*1 (*Ros*1) under the control of an ethylene-responsive, fruit-specific E8 promoter (E8) were referred to as *Del/Ros*1 (see Figure 2.5 for map of T-DNA region of the binary vector pDEL.ROS; a detailed description of the primers and cloning strategy are available in the supplementary materials of Butelli et al., 2008) and crossed to an *f3'5'h* (*a*) mutant (*f3'5'h*$^{-/-}$, *Solanum lycopersicum* var. VF36) carrying a stop codon mutation in the gene encoding F3'5'H (de Jong et al., 2004). The seeds were obtained from the Tomato Genetics Resource Centre at the University of California, Davis, California and had been generated through chemical-induced mutation. *Del/Ros*1 were used as male parents to pollinate emasculated flowers of *f3'5'h*$^{-/-}$/*a* mutant plants. The resulting cross developed purple-coloured fruit from which seeds were extracted and sown on kanamycin-containing selective medium. The seedlings of the T2 generation were selected by visual analysis, as lack of pigmentation in the seedling stem base was a visual characteristic of *f3'5'h*$^{-/-}$/*a* mutant plants. Therefore, seedlings with two mutated alleles of the F3'5'H/A gene were easily distinguished from plants with functional copies of the F3'5'H/A gene by their unpigmented stems. These seedlings were selected and allowed to mature and set fruit. The presence of *Delila* and *Rosea*1 transcription factors was confirmed by PCR. The resulting plants developed normally and produced plants of orange/red hue.

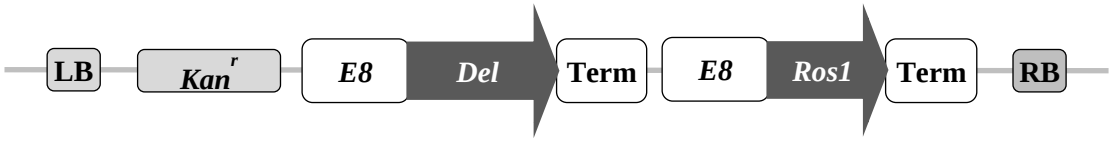

Figure 2.5: Map of T-DNA region of the binary vector pDEL.ROS used for the transformation of tomato plants to induce activation of the anthocyanin biosynthetic pathway (Butelli et al., 2008). LB, left T-DNA border region; Kan^r, nptII gene conferring kanamycin resistance under the control of the nos promoter; E8, ethylene-responsive fruit ripening E8 promoter; *Del*, *A. majus Delila* transcription factor; *Ros*1, *A. majus Rosea*1 transcription factor; Term, terminator region of cauliflower mosaic virus; RM right T-DNA border region.

2.3.16.2 Generation of E8::*Del/Ros*1/E8::*AmDfr*/*f3'5'h*$^{-/-}$ tomato plants

Del/*Ros*1 tomato plants were used as male parents to generate progeny with pelargonidin and cyanidin accumulation. A minimum of ten independent transgenics expressing E8::*AmDfr* (T0 generation) were used as female parents. In order to generate tomato lines producing high levels of mono- and dihydroxylated anthocyanins, *Del/Ros*1 transcription factors mediated activation of the anthocyanin biosynthetic pathway was required. *Del*/*Ros*1 plants (carrying two functional alleles of F3'5'H/A) were selected as male parents and crossed to E8::*AmDfr/f3'5h*$^{-/-}$ plants. The resulting T1 generation seeds were sown out on MS agar medium containing 100 µg/mL kanamycin and the plants were analysed for the presence of *Del*, *Ros*1 and *AmDfr*. All T1 plants carried at least one functional allele of the F3'5'H/A gene resulting in the production of delphinidins and purple colouration of the fruit. In the T2 generation, plants with different genotypes emerged as a result of allelic segregation, with some carrying the desired E8::*Del/Ros*1/E8::*AmDfr*/*f3'5'h*$^{-/-}$ genotype.

2.3.17 Analysis of T2 transgenic tomato plants

Before transferring kanamycin-resistant seedlings to soil, plants were screened by genotyping to confirm the presence of *AmDfr* and *Del/Ros*1. Positive seedlings were transferred to soil and allowed to develop fruit, from which seeds were collected and sown out on agar containing 100 µg/mL of kanamycin. The resulting T2 generation seedlings underwent an initial visual screen. A functional allele of the F3'5'H/A gene is

required for delphinidin production and seedlings with at least one functional copy of F3’5’H/A gene were easily recognized by the purple pigmentation in the roots and base of the stem of young seedlings. Seedlings with unpigmented roots and stems were selected and analysed by PCR for the presence of *AmDfr* and *Del/Ros*1. Seedlings carrying *AmDfr* and *Del/Ros*1 were allowed to mature and develop fruit. Plants with the target genotype E8::*Del/Ros*1/E8::*AmDfr*/*f3’5’h*$^{-/-}$ were easily identified by their distinctly dark red, brick coloured fruit and referred to as *AmDfr*/*Del/Ros*1/*f3’5’h*$^{-/-}$. Tomato fruit were harvested at the ripe stage and further analysed by HPLC-MS to confirm the identity of the anthocyanins present.

2.3.18 Metabolite analyses

2.3.18.1 Anthocyanin and flavonoid extraction

Tomato fruit samples (fresh or frozen) from which anthocyanin samples were extracted were either homogenized using a commercial blender (fresh fruit) or ground to a fine powder using liquid nitrogen (frozen samples). The extraction solution, 50% MeOH (v/v) with 0.7% HCl, was added to the fruit samples at 1 mL per 1 g tomato fruit material, vortexed and incubated overnight at 4°C with shaking. After overnight incubation the tomato fruit samples were centrifuged at 4,000 *g* for 15 min at 4 °C. The supernatant was collected and stored at -20 °C for further analysis.

2.3.18.2 HPLC-LC-MS analysis and quantification of polyphenolic compounds

Tomato extracts were run on a 100 x 2 mm internal diameter Phenomenex® 3 µm Luna C18 column using a Surveyor HPLC attached to DecaXPplus ion trap MS (Thermo Fisher). Separation was achieved using a linear gradient (Table 2vi) of acetonitrile (ACN) versus 0.1% formic acid (FA) in water, run at 300 µL/min and 30 ºC. The elution products were monitored with a photo diode array (PDA) detector over the range of 200-600 nm. Anthocyanins or flavonoids were detected by light absorbance using collecting channels at 500-550 nm or 340-360 nm, respectively. They were also detected by positive mode electrospray MS, collecting full spectra from *m/z* 100-2000. The runs were performed by Dr. Lionel Hill. Polyphenol masses and fragmentation patterns were determined using Quant browser. Anthocyanins and other flavonoids were

quantified using the standards kaempferol-3-rutinoside, rutin, cyanidin-3-glucoside, delphinidin-3-glucoside and chlorogenic acid. For the quantification of resveratrol in the high-resveratrol tomato fruit, flavonoid standards and the stilbenes, resveratrol and resveratrol-glucoside (polydatin), were used. Calibration curves were run before and after the samples. The quantification of polyphenolic compounds was performed by Dr. Lionel Hill.

Table 2vi: Solvent gradient for separation of polyphenolic compounds.

Time (min)	**% ACN**
0	1
4	1
23	30
30	70
30.5	1
37	1

2.3.18.3 Purification of anthocyanins from *Del/Ros*1 tomato fruit

Anthocyanins were purified from delphinidin-producing *Del/Ros*1 tomato fruit using preparative HPLC as part of a collaborative project with Prof Hans-Peter Mock in the department of Applied Biochemistry at the Leibniz Institute of Plant Genetics and Crop Plant Research (IPK) in Gatersleben in Germany.

2.3.18.3.1 Pre-purification of anthocyanins on a solid phase C18 column

Polyphenolic compounds were extracted from tomato fruit by adding 25 ml of 2% FA in 50% MeOH (v/v) to 1 g lyophilized tomato fruit material, followed my ultrasonication for 20 min. Tomato debris was removed using Whatman paper No. 1 or comparable filter system. Filtered polyphenol extracts were transferred to a rotary evaporator to remove all MeOH for subsequent transferral to a solid phase 5000 mg Chromabond® C18 column (Machery-Nagel). Removal of MeOH was required as MeOH interferes with the retention ability of the C18 material and may prevent the polyphenolic compounds from binding to the C18 resin. Solid phase C18 columns were

equilibrated with acidified H_2O before addition of the aqueous polyphenol extract. The polyphenol extract from up to 15 g of lyophilized tomato fruit was loaded onto a 5000 mg Chromabond® C18 column. Polyphenols, but not sugars, were bound by the C18 silica material allowing for the removal of sugars by the addition of water (30 mL). Flavonols and anthocyanins were eluted in a sequential manner: First, flavonols (yellow-coloured) were eluted with 2% FA in 60% MeOH (v/v; 60 mL), followed by the elution of anthocyanins with 10 mL of 2% FA in 100% MeOH. The separation of anthocyanins from other polyphenols on a solid phase C18 silica column was necessary in order reduce contamination of anthocyanin fractions with other polyphenols obtained by subsequent preparative HPLC.

2.3.18.3.2 Separation of total anthocyanins from other polyphenols by medium-scale preparative HPLC

Tomato extracts were run on a 250 x 30 mm internal diameter Phenomenex® 5 µm Gemini® NX-C18 110 Å column using a Varian ProStar 210 preparative HPLC (Agilent Technologies) connected to a Varian ProStar 410 AutoSampler (Agilent Technologies). Separation was achieved using a linear gradient (Table 2vii) of ACN versus 1.9% FA and 0.1% ammonium formate in water, run at 10 mL/min and 25 ºC. The elution products were moitored with a photo diode array PDA detector over the range of 200-600 nm. Anthocyanins and flavonoids were detected by light absorbance using collecting channels at 535 nm and 280 nm, respectively.

Table 2vii: Solvent gradient for separation of polyphenolic compounds on the Phenomenex® 5 µm Gemini® C18 column using a Varian ProStar 210 preparative HPLC.

Time (min)	**% ACN**
0	3
8.5	3
100	20
133.5	30
150	30
153.5	97
165	97
167	3
170	3

The anthocyanins eluted after 50 min and 10 mL fractions were collected every min between minute 50 and 120. A representative HPLC chromatogram of the separation of polyphenolic compounds of *Del/Ros*1 tomato fruit obtained by Varian ProStar 210 preparative HPLC equipped with a 250 x 30 mm internal diameter Phenomenex® 5 µm Gemini® NX-C18 110 Å column is shown in Figure 2.6 A.

2.3.18.3.3 Identification of individual anthocyanins by LCT analysis

All anthocyanin fractions were analysed on a liquid chromatography (LC)/mass spectrometer (MS)/TOF mass spectrometer (LCT premier; Waters) in order to determine the purity and type of the anthocyanins present in the individual fractions collected by preparative HPLC (Chapter 2.2.18.3.2). Samples were run on a Waters 2.1 mm X 100 mm internal diameter ACQUITY UPLC® 1.7 µm BEH Phenyl column, 130 Å, using a LCT premier mass spectrometer. Separation was achieved using a linear gradient (Table 2viii) of 0.1% FA in ACN versus 0.1% FA in water, run at 500 µL/min and 25 ºC.

Table 2viii: Solvent gradient for separation of polyphenolic compounds on the LCT premier.

Time (min)	**% (ACN + 0.1% FA)**
0	0
10	40
10.1	95
10.6	95
10.7	0
13.5	0

Single peak fractions containing only one major anthocyanin were considered as highly pure. However, some anthocyanins coeluted or eluted very closely together and resulted in fractions containing two or more anthocyanins. After LCT analysis of each fraction, Varian ProStar 210 preparative HPLC fractions containing the same anthocyanins were pooled together and concentrated using a nitrogen evaporator.

2.3.18.3.4 Separation of individual anthocyanins by smale-scale preparative HPLC

Anthocyanin fractions obtained by Varian ProStar 210 preparative HPLC were further purified using a small-scale preparative HPLC equipped with a smaller C18 column to achieve better separation. Samples were run on a 19 mm x 150 mm internal diameter Waters 5 µm XBridge™ BEH C18 prep column, 130Å connected to a Prep 2000 HPLC system (Waters) with a UV/Vis detector (Waters).

Separation was achieved using a linear gradient (Table 2ix) of ACN versus 1.9% FA and 0.1% ammonium formate in water, run at 4 mL/min and 25 ºC. The elution products were monitored with a photo PDA detector over the range of 200-600 nm. Anthocyanins were detected by light absorbance using the collecting channel at 535 nm.

Table 2ix: Solvent gradient for separation of polyphenolic compounds on the Waters 5 µm XBridge™ C18 prep column using a Waters Prep 2000 HPLC system.

Time (min)	**% ACN**
0.01	3
5	3
60	20
80	30
90	30
92	97
99	97
100	3

The Waters 5 µm XBridge™ C18 prep column allowed a very good separation of anthocyanin fractions that had previously run too closely together to be separated on the Phenomenex® 5 µm Gemini® C18 column (Figure 2.6 B). However, the different purifications steps were important in order to remove other polyphenols effectively from the fractions. The purified anthocyanins were concentrated using a nitrogen evaporator and resuspended in 50% MeOH (v/v) at 200 mM and stored at -80 °C until further use to investigate their biological efficacy on human breast cancer cells *in vitro* (Chapter 3).

A

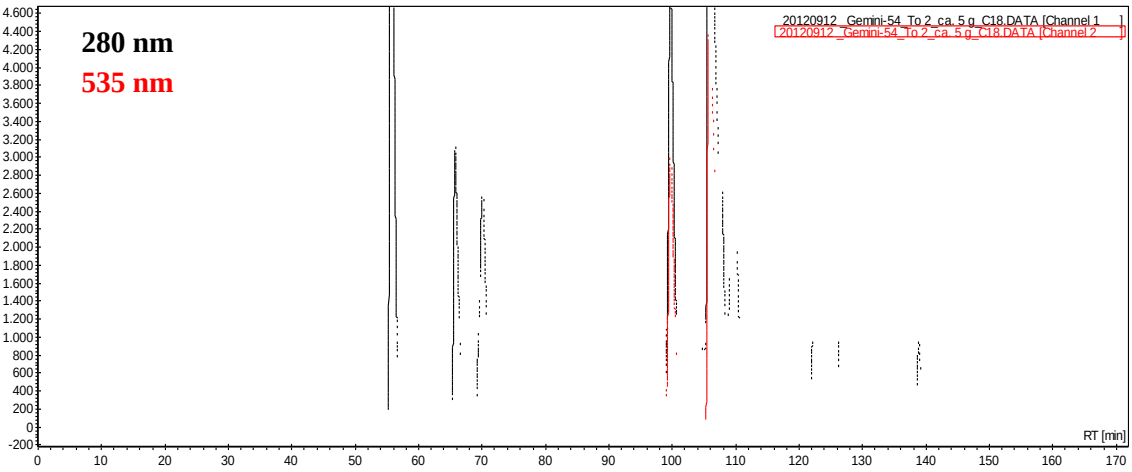

B

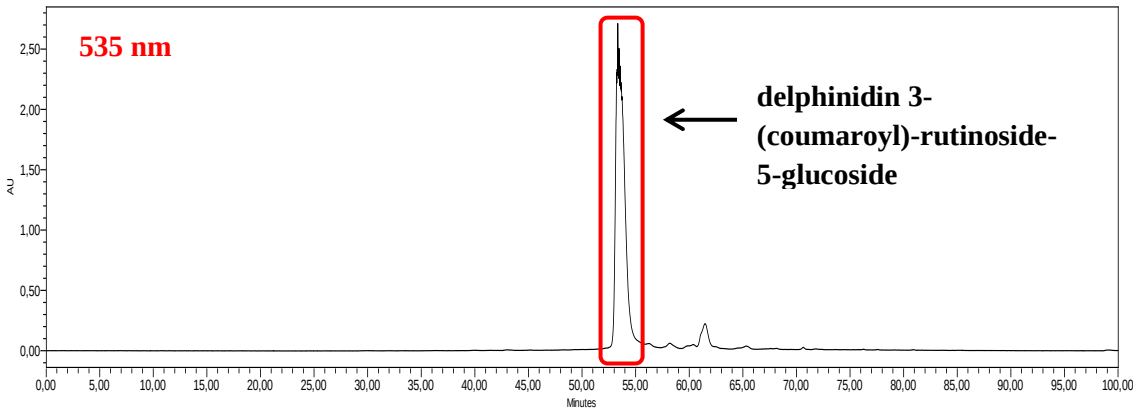

Figure 2.6: Preparative HPLC to purify anthocyanins from the fruit of delphinidin-producing *Del/Ros*1 tomatoes. (**A**) Chromatogram of the preparative HPLC of total anthocyanins (535 nm) and other polyphenols (280 nm) run on the Phenomenex® 5 µm Gemini® C18 column using a Varian ProStar 210 preparative HPLC. (**B**) Chromatogram of the preparative HPLC of a single anthocyanin fraction previously separated in (**A**) and corresponding to delphinidin 3-(coumaroyl)-rutinoside-5-glucoside with a mass of 919 run on the Waters 5 µm XBridge™ C18 prep column using a Waters Prep 2000 HPLC system.

2.3.19 TEAC antioxidant assay

The Trolox equivalent antioxidant capacity (TEAC) measures the antioxidant capacity of substances by comparing them to the standard, 6-hydroxy-2,5,7,8-tetramethylchroman-2-carboxylic acid (Trolox). Antioxidant capacity is measured using the 2,2'-azino-bis(3-ethylbenzothiazoline-6-sulphonic acid) (ABTS) decolourisation assay (7 mM ABTS and 2.45 mM potassium persulfate in dH_2O). ABTS, a blue-green chromophore with a characteristic absorption at 734 nm, is quenched by antioxidants resulting in decolourisation of the solution. The ABTS working solution was obtained by diluting the stock solution in EtOH to an absorbance of 0.70 ± 0.02 AU at 734 nm. A standard curve was obtained by mixing 1 mL ABTS working solution with 10 µL Trolox (0.2 mM, 0.4 mM, 0.6 mM, 0.8 mM, 1.0 mM, 1.2 mM, 1.4 mM, 1.6 mM 1.8 mM, 2mM; see Figure 2.7) and measuring the absorbance after 5 min at 734 nm at room temperature using a 8453 Diode Array spectrophotometer (Hewlett-Packard).

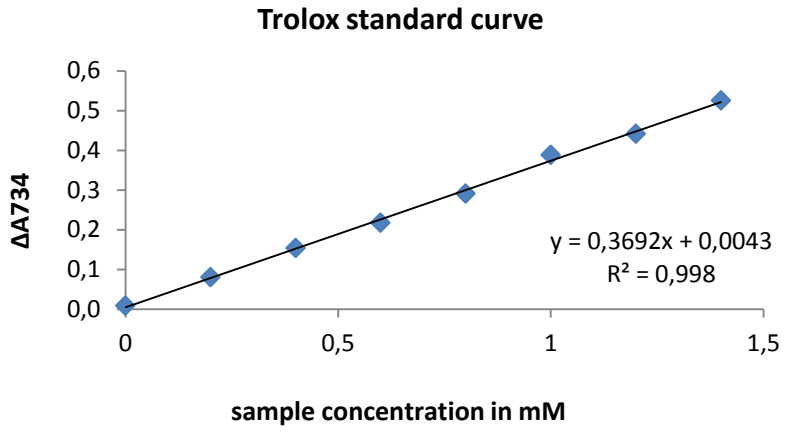

Figure 2.7: Standard curve for the measurement of the Trolox total antioxidant capacity according to is concentration (mM). Conditions: 1000 µL ABTS, 10 µL Trolox, 25 °C, time of reaction: 5 minutes.

2.3.19.1 Polyphenol extraction for TEAC analysis

Polyphenols were extracted from tomato fruit using water and acetone in a sequential manner. Ripe tomato fruit were ground to a fine powder using liquid N_2. Water-soluble polyphenols were extracted from 1 g of tomato powder using 6 mL of dH_2O and TEAC measured following the procedure used to obtain the standard curve. To determine the

TEAC of any remaining, water-insoluble compounds the extraction was repeated with 6 mL ACN. The antioxidant capacity of the polyphneol fraction was measured by mixing 900 µL ABTS working solution with 100 µL polyphenol extract before measuring the absorbance after 5 min at 734 nm at room temperature. The TEAC of each polyphenol fraction was expressed as mmol Trolox per kg FW.

2.3.20 Statistical methods

The statistical significance was determined using Student's t-test. P-values ≤ 0.05 were considered statistically significant.

2.4 Results

2.4.1 Production of cyanidins in tomato through inactivation of f3'5'h

Delila (*Del*) and *Rosea*1 (*Ros*1) are two genes from snapdragon (*Antirrhinum majus*) that encode for a basic helix-loop-helix and a MYB-like transcription factor, respectively. Both *Del* and *Ros*1 are crucial in regulating anthocyanin production in snapdragon flowers (Goodrich et al., 1992, Schwinn et al., 2006). Work by Butelli *et al*. (2008) showed that these two transcription factors, placed under the control of a fruit-specific E8 promoter, can be used to induce production of trihydroxylated anthocyanins (predominantly delphinidins and petunidins) in tomato. These plants were referred to as *Del/Ros*1 plants, and displayed an intense purple colouration of the fruit but not of the vegetative tissue. The substrate preference of the native tomato DFR for DHM results in the production of trihydroxylated anthocyanins only. The production of other classes of anthocyanins in tomato therefore, requires inhibition of the synthesis of the delphinidin precursor DHM combined with an engineering strategy to overcome the DHM substrate specificity of the native tomato DFR. F3'5'H is the key enzyme that catalyses the formation of DHM from DHK through the addition of two hydroxyl groups at the 3' and 5' position on the phenyl B-ring. To determine, whether *Del*/*Ros*1-induced production of anthocyanins other than delphinidins is possible, *Del/Ros*1 plants were crossed with an *f3'5'h*$^{-/-}$ (*a*$^{-/-}$) double mutant. The resulting plants had the E8::*Del/Ros*1/*f3'5'h*$^{-/-}$ (*a*$^{-/-}$) genotype and were referred to as *Del/Ros*1/*f3'5'h*$^{-/-}$. The plants developed normally but produced few fruit that contained few seeds compared to WT or *Del/Ros*1 plants. This observation was already made in the *f3'5'h*$^{-/-}$ homozygous parental plants suggesting that F3'5'H may play a role in pollen development. *Del/Ros*1/*f3'5'h*$^{-/-}$ fruit had orange/red skin colour with red to pink flesh displaying a distinctive purple venation that originated at the fruit stalk base (Figure 2.8 B). HPLC analysis confirmed the presence of five major peaks in the absorbance range of 500-550 nm, at which anthocyanins absorb most strongly (Figure 2.8 A). Mass spectrometry (MS) identified the peaks labelled as 1, 2 (merged peak corresponding to two compounds), 3, 4 and 5 in Figure 2.8 A as cyanidin 3-(caffeoyl)-rutinoside-5-glucoside (*m/z* 919), peonidin 3-(caffeoyl)-rutinoside-5-glucoside (peak 2; *m/z* 933), cyanidin 3-(coumaroyl)-rutinoside-5-glucoside (peak 2; *m/z* 903), cyanidin 3-(feruloyl)-rutinoside-5-glucoside (*m/z* 933), peonidin 3-(coumaroyl)-rutinoside-5-glucoside (mass 917) and peonidin 3-(feruloyl)-rutinoside-5-glucoside (*m/z* 947), respectively. The mass spectra

of the fragmentation pattern of the two predominant anthocyanin compounds identified as cyanidin 3-(coumaroyl)-rutinoside-5-glucoside with a corresponding *m/z* of 903 (part of peak 2 in Figure 2.8 A) and peonidin 3-(coumaroyl)-rutinoside-5-glucoside with an *m/z* of 917 (peak 4 in Figure 2.8 A) are shown in Figure 2.8 C1 and C2. HPLC-MS data, including fragmentation patterns, are summarized in Table 2x. The total anthocyanin content in the fruit of *Del/Ros*1/*f3'5'h*$^{-/-}$ was ~40 fold lower than the amount reported for the *Del/Ros*1 tomatoes (2-3 mg/g FW).

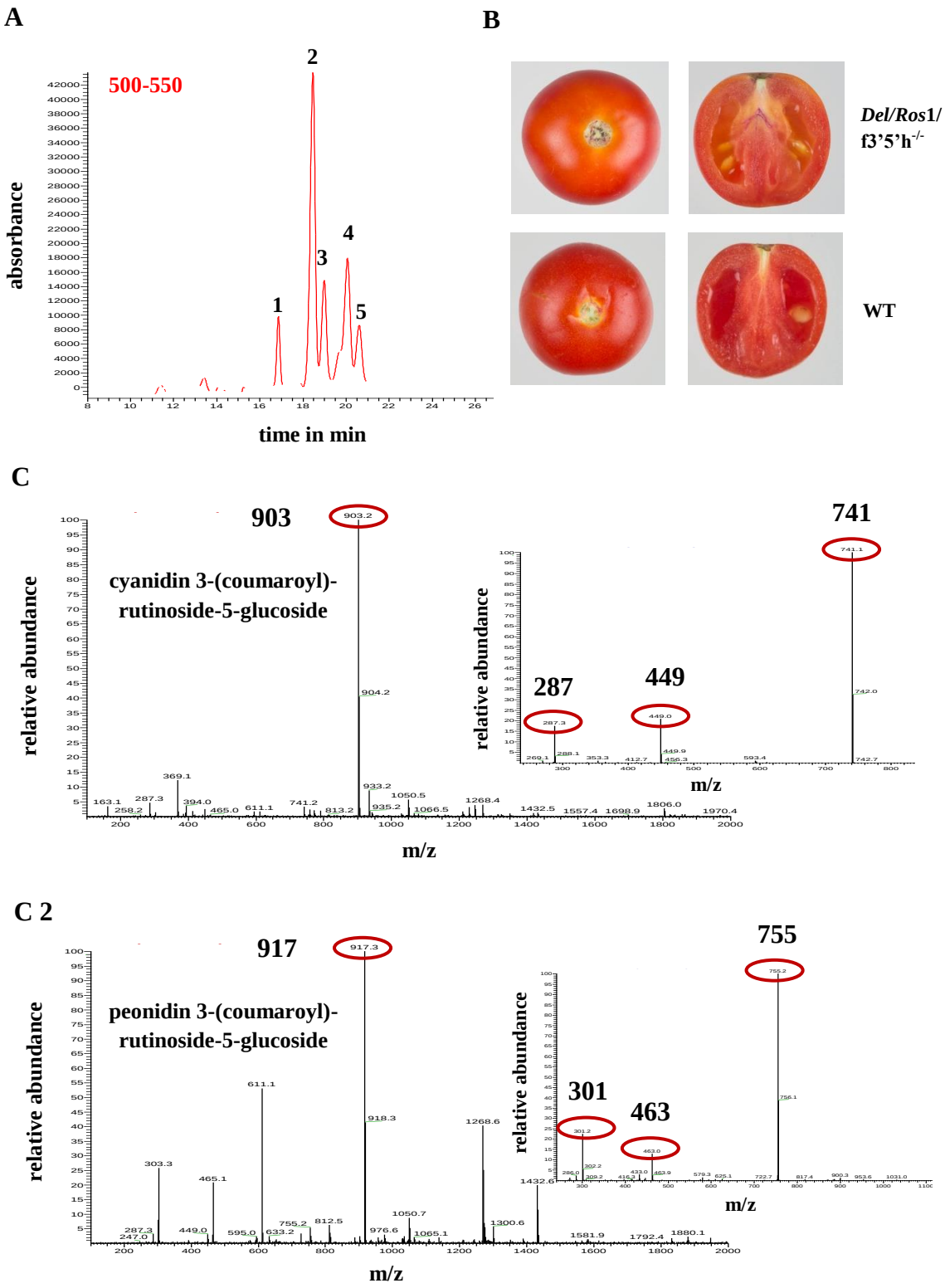

Figure 2.8: Analysis of anthocyanins from the fruit of cyanidin-producing E8::*Del/Ros*1*/f3'5'h*$^{-/-}$ line. (**A**) HPLC analysis of anthocyanins of E8::*Del/Ros*1*/f3'5'h*$^{-/-}$ shows the presence of five major new anthocyanin compounds. (**B**) Fruit of WT and cyanidin-producing E8::*Del/Ros*1 */f3'5'h*$^{-/-}$ line. (**C**) Mass analysis of new products at corresponding to peak 2 and 4 were identified as (**1**) cyanidin 3-(coumaroyl)-rutinoside-5-glucoside and (**2**) peonidin 3-(coumaroyl)-rutinoside-5-glucoside, respectively.

Table 2x: Characterisation of anthocyanin peaks identified in the fruit of the E8::*Del/Ros*1/*f3'5'h*$^{-/-}$ tomato line.

Rt (min)	peak	ESI-MS (m/z)	MS/MS fragments	Compound
16.87	1	919	757[Cy+Rut+Glc], 449[Cy+Glc], 287 [Cy]+	cyanidin 3-(caffeoyl)-rutinoside-5-glucoside
18.47	2	933	771[Pe+Rut+Glc], 463[Pe+Glc], 301 [Pe]+	peonidin 3-(caffeoyl)-rutinoside-5-glucoside
18.47	2	903*	741[Cy+Cou+Rut], 449[Cy+Glc], 287[Cy]+	cyanidin 3-(coumaroyl)-rutinoside-5-glucoside
18.98	3	933	771[Cy+Fer+Rut], 449[Cy+Glc], 287[Cy]+	cyanidin 3-(feruloyl)-rutinoside-5-glucoside
20.07	4	917	755[Pe+Cou+Rut], 463[Pe+Glc], 301[Pe]+	peonidin 3-(coumaroyl)-rutinoside-5-glucoside
20.6	5	947	785[Pe+Fer+Rut], 463[Pe+Glc], 301[Pe]+	peonidin 3-(feruloyl)-rutinoside-5-glucoside

Rt, retention time; Cy, cyanidin; Pe, peonidin; Glc, glucose; Cou, coumaroyl; Rut, rutinoside; Fer, feruloyl; ESI-MS, Electro spray ionization mass spectra; *m/z*, molecular mass of compound.
* Peak 2 corresponds to two compounds of which cyanidin 3-(coumaroyl)-rutinoside-5-glucoside (mass 903 and RT 18.47) is the most abundant.

2.4.2 Towards engineering tomatoes with increased cyanidin content

2.4.2.1 Overcoming DFR substrate specificity

The levels of anthocyanins reported from the *Del/Ros*1/*f3'5'h*$^{-/-}$ tomato plants were extremely low. In order to increase the amount of cyanidins in tomato, we hypothesised that overcoming the substrate specificity of the native tomato DFR was essential. By generating tomato plants with a E8::*Del/Ros*1/E8::*AmDfr*/*f3'5'h*$^{-/-}$ genotype that also expressed a DFR from *A. majus*, a species that does produce both cyanidin and pelargonidins, we expected to increase cyanidin content in these tomatoes. Screening of ~ 200 plants resulted in twenty-four positive T2 plants expressing the three transgenes *Del*, *Ros*1, *AmDfr* and that were homozygous for *f3'5'h*$^{-/-}$ (*a*$^{-/-}$). Of these twenty-four plants, five independent transgenics showed the accumulation of a distinctive, brick red colour in their fruit indicating the presence of novel anthocyanins (Figure 2.9 B). The other transgenic individuals resembled a WT. As previously observed in *f3'5'h*$^{-/-}$ double mutant plants, E8::*Del/Ros*1/E8::*AmDfr*/*f3'5'h*$^{-/-}$, referred to as *AmDfr/Del/Ros*1/*f3'5'h*$^{-/-}$

, produced less fruit and set less seeds compared to WT tomatoes. HPLC-MS analysis and identification of the anthocyanins present in *AmDfr/Del/Ros*1/*f3'5'h*$^{-/-}$ fruit are shown in figure 2.9.

2.4.3 *AmDfr* triggers pelargonidin production in tomato

The HPLC analysis of the *AmDfr/Del/Ros*1/*f3'5'h*$^{-/-}$ fruit revealed the presence of several novel anthocyanin peaks in addition to the peaks found in *Del/Ros*1/*f3'5'h*$^{-/-}$ tomato fruit (Figure 2.9 A). The identity of these anthocyanin peaks was confirmed by mass spectrometry and revealed the presence of several monohydroxylated pelargonidin-type anthocyanins in addition to the dihydroxylated cyanidin-type anthocyanins found in *Del/Ros*1/*f3'5'h*$^{-/-}$ tomato fruit. More than ten anthocyanins were identified in the fruit of *AmDfr/Del/Ros*1/*f3'5'h*$^{-/-}$ and a full list of anthocyanins identified is presented in Table 2xi. The most abundant peak, labelled as peak 9, was identified as pelargonidin 3-(coumaroyl)-rutinoside-5-glucoside with an *m/z* value of 887. MS analysis of this compound revealed a major fragment of *m/z* 725, corresponding to pelargonidin 3-(coumaroyl)-rutinoside due to the loss of glucose with *m/z* 162. Further fragmentation of pelargonidin 3-(coumaroyl)-rutinoside (*m/z* 725) resulted in fragments of *m/z* 433 due to the loss of coumarate and rhamnose and *m/z* 271 due to the loss of glucose. Pelargonidin has a molecular weight of 271 confirming that the compound corresponding to peak 9 and identified as pelargonidin 3-(coumaroyl)-rutinoside-5-glucoside is indeed a pelargonidin derivative (Figure 2.9 C1). The second most prevalent anthocyanin in the fruit of *AmDfr/Del/Ros*1/*f3'5'h*$^{-/-}$ was labelled as peak 7 and corresponded to cyanidin 3-(coumaroyl)-rutinoside-5-glucoside with an *m/z* of 903 (Figure 2.9 C2). This compound was also the most abundant dihydroxylated anthocyanin found in the fruit of *Del/Ros*1/*f3'5'h*$^{-/-}$ (peak 2; Figure 2.8 A). Whilst all the cyanidins originally identified in the *Del/Ros*1/*f3'5'h*$^{-/-}$ (Chapter 2.3.1) were also present in *AmDfr/Del/Ros*1/*f3'5'h*$^{-/-}$, the total amount of cyanidins did not change dramatically in response to *A. majus* DFR activity. The presence of large amounts of novel pelargonidins in the fruit of *AmDfr/Del/Ros*1/*f3'5'h*$^{-/-}$ show that in tomatoes lacking F3'5'H function, *A. majus* DFR drives the production of predominantly monohydroxylated anthocyanins, suggesting a substrate preference for the pelargonidin precursor DHK.

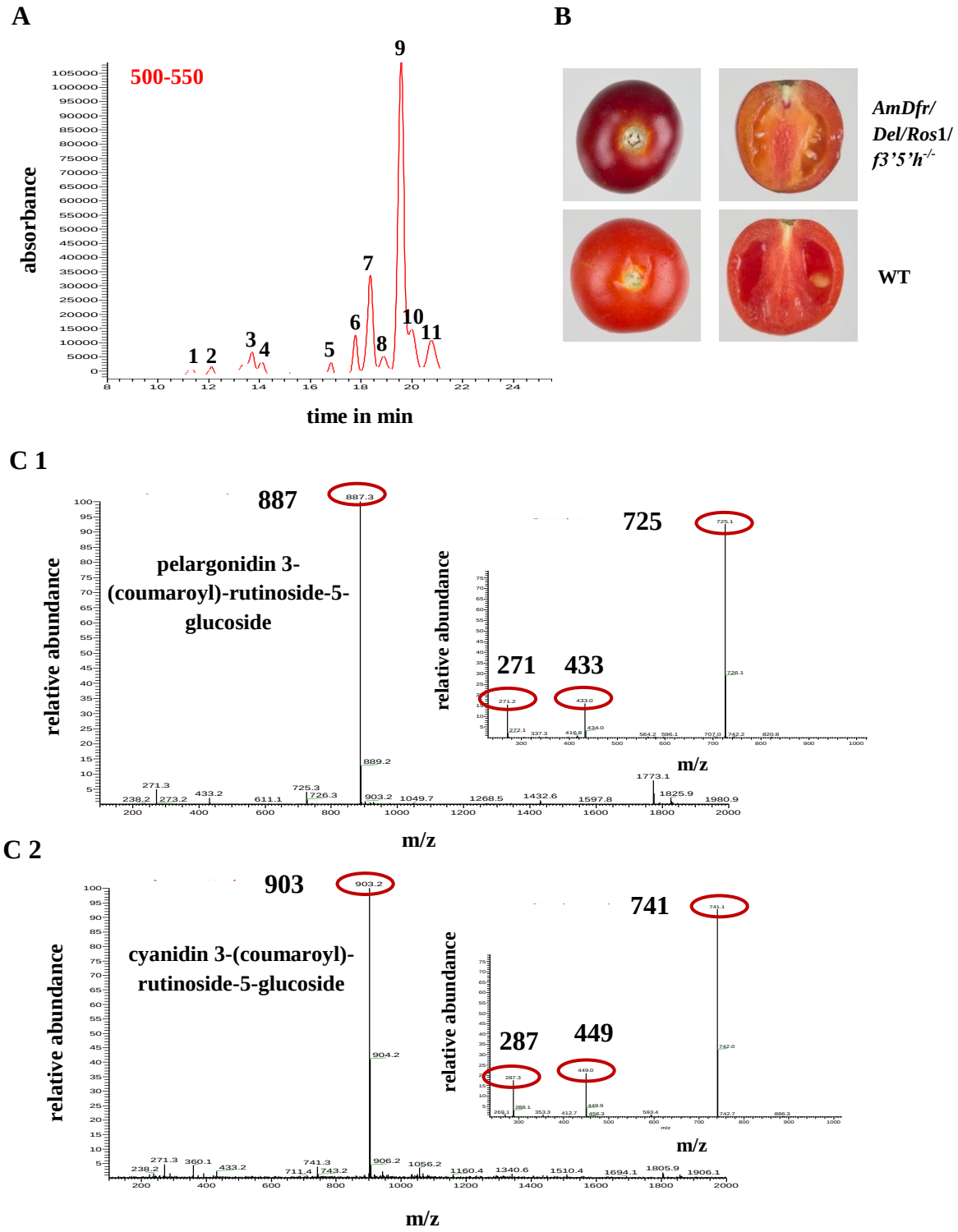

Figure 2.9: Analysis of anthocyanins from the fruit of the E8::*Del/Ros*1/E8::*AmDfr/f3'5'h*$^{-/-}$ line producing predominantly pelargonidins and low amounts of cyanidins. (**A**) HPLC analysis of anthocyanins of E8::*Del/Ros*1/E8::*AmDfr/f3'5'h*$^{-/-}$ shows the presence of at least 11 new anthocyanin compounds. (**B**) Fruit of WT and pelargonidin- and cyanidin-producing E8::*Del/Ros*1/E8::*AmDfr/f3'5'h*$^{-/-}$ line. (**C**) Mass analysis of new products corresponding to peak 9 and 6 were identified as (1) pelargonidin 3-(coumaroyl)-rutinoside-5-glucoside and (**2**) cyanidin 3-(coumaroyl)-rutinoside-5-glucoside, respectively.

Table 2xi: Characterisation of anthocyanin peaks identified in the fruit of the E8::*Del/Ros*1/E8::*AmDfr*/*f3'5'h*$^{-/-}$ tomato line.

Rt (min)	Peak	ESI-MS (m/z)	MS/MS fragments	Compound
11.27	1	757	595[Cy+Rut], 449[Cy+Glc], 287[Cy]+	cyanidin 3-rutinoside-5-glucoside
12.03	2	741	579[Pl+Rut], 433[Pl+Glc], 271[Pl]+	pelargonidin 3-rutinoside-5-glucoside
13.63	3	433	271[Pl]+	pelargonidin 5-glucoside
14.02	4	579	433[Pl+Glc], 271[Pl]+	pelargonidin 3-rutinoside
16.77	5	919	757[Cy+Rut+Glc], 449[Cy+Glc], 287 [Cy]+	cyanidin 3-(caffeoyl)-rutinoside-5-glucoside
17.77	6	903	741[Pl+Rut+Glc], 433[Pl+Glc], 271[Pl]+	pelargonidin 3-(caffeoyl)-rutinoside-5-glucoside
NV		933	771[Pe+Rut+Glc], 463[Pe+Glc], 301[Pe]+	peonidin 3-(caffeoyl)-rutinoside-5-glucoside
18.35	7	903	741[Cy+Cou+Rut], 449[Cy+Glc], 287[Cy]+	cyanidin 3-(coumaroyl)-rutinoside-5-glucoside
18.35	8	933	771[Cy+Fer+Rut], 449[Cy+Glc], 287[Cy]+	cyanidin 3-(feruloyl)-rutinoside-5-glucoside
19.57	9	887	725[Pl+Cou+Rut], 433[Pl+Glc], 271	pelargonidin 3-(coumaroyl)-rutinoside-5-glucoside
19.98	10	917	755[Pe+Cou+Rut], 463[Pe+Glc], 301[Pe]+	peonidin 3-(coumaroyl)-rutinoside-5-glucoside
NV		947	785[Pe+Fer+Rut], 463[Pe+Glc], 301[Pe]+	peonidin 3-(feruloyl)-rutinoside-5-glucoside
20.77	11	N/A	N/A	unknown pelargonidin derivative

Rt, retention time; N/A, not applicable; NV, not visible in UV; Cy, cyanidin; Pe, peonidin; Pl, pelargonidin; Glc, glucose; Cou, coumaroyl; Rut, rutinoside; Fer, feruloyl; ESI-MS, Electro spray ionization mass spectra; *m/z*, molecular mass of compound.

2.4.4 Cyanidins but no pelargonidins are produced in the peel of E8::*Del/Ros*1/E8::*AmDfr*/*f3'5'h*$^{-/-}$ tomato fruit

Analysis of the anthocyanins in peel and flesh of anthocyanin-enriched transgenic tomato lines revealed differences in the classes of anthocyanins produced in the tissues of *AmDfr/Del/Ros*1/*f3'5'h*$^{-/-}$ (Figure 2.10). Cyanidin 3-(coumaroyl)-rutinoside-5-glucoside and peonidin 3-(coumaroyl)-rutinoside-5-glucoside, corresponding to peaks b 1 and b 3 (Table 2xii) were the most abundant compounds in the peel, and no monohydroxylated anthocyanins were detected in the peel of *AmDfr/Del/Ros*1/*f3'5'h*$^{-/-}$.

In the flesh, pelargonidin 3-(coumaroyl)-rutinoside-5-glucoside (peak b 6, Table 2xii) was the predominant anthocyanin but we also identified all dihydroxylated anthocyanins that were also present in the peel. Equal amounts of freeze-dried plant material were used for the anthocyanin extraction procedure and it was evident that the skin accumulated approximately four times more anthocyanins than the flesh (Figure 2.10 B). The peel of the tomato fruit accounts for less that 5% of the total fresh weight of the fruit. Therefore, the monohydroxylated anthocyanins found in the flesh, even at lower relative concentrations, still account for the majority of anthocyanins present in the whole fruit.

There was no significant difference in the amount of anthocyanins that accumulated in the peel or flesh of *Del/Ros*1 tomato fruit, in which petunidin 3-(coumaroyl)-rutinoside-5-glucoside (peak a 2) and delphinidin 3-(coumaroyl)-rutinoside-5-glucoside (peak a 1) were the most and second most abundant compounds in that tomato line (Table 2xii). *Del/Ros*1/*f3'5'h*$^{-/-}$ fruit contained three- to fourfold more anthocyanins in the peel than in the flesh and both tissues accumulated the same dihydroxylated anthocyanins (Figure 2.10 C and Table 2xii). The dihydroxylated anthocyanins found in *Del/Ros*1/*f3'5'h*$^{-/-}$ were identical with those identified in the peel of *AmDfr/Del/Ros*1/*f3'5'h*$^{-/-}$.

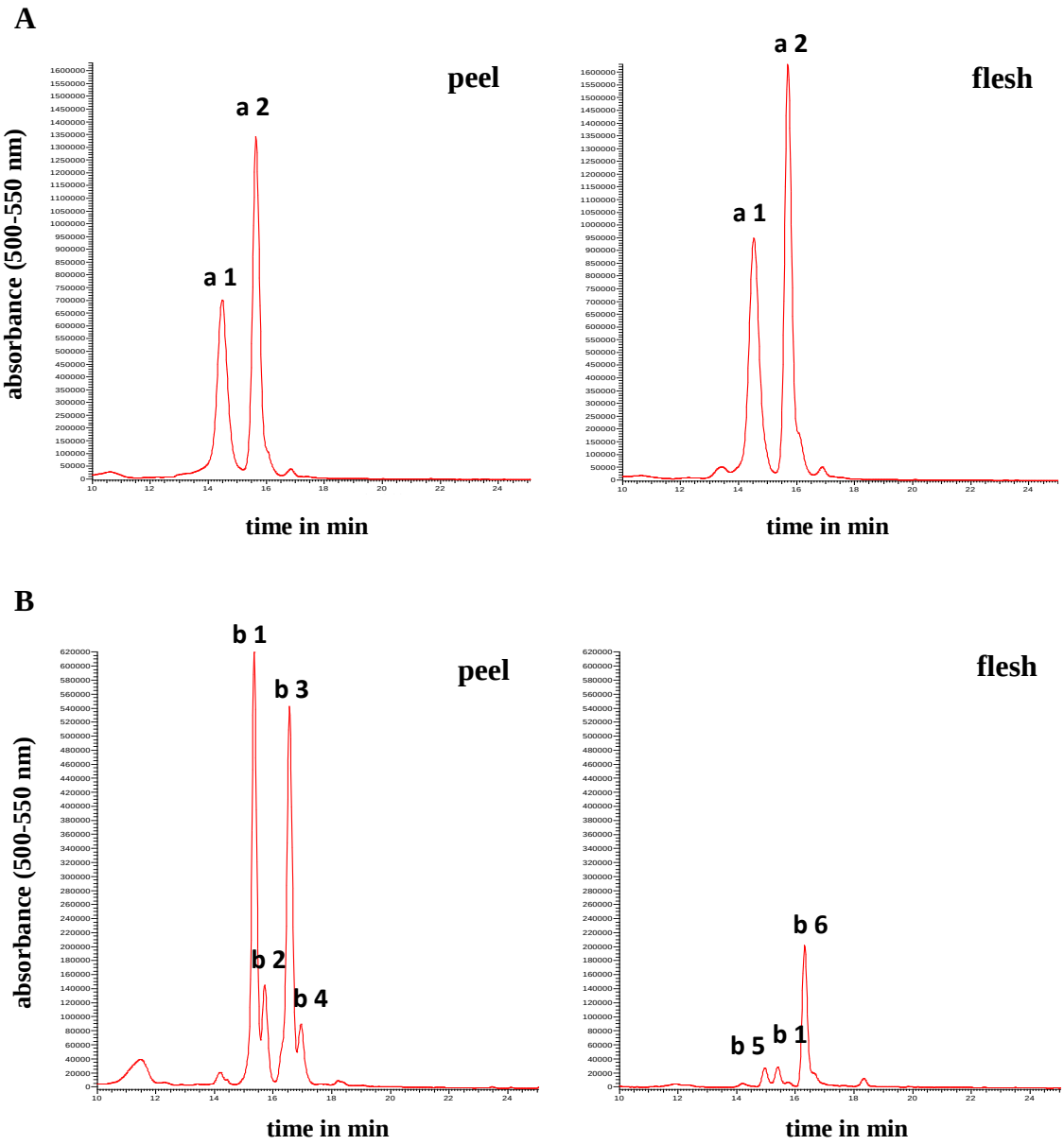
A
peel
flesh
a 1
a 2
absorbance (500-550 nm)
time in min
B
b 1
b 2
b 3
b 4
b 5
b 6

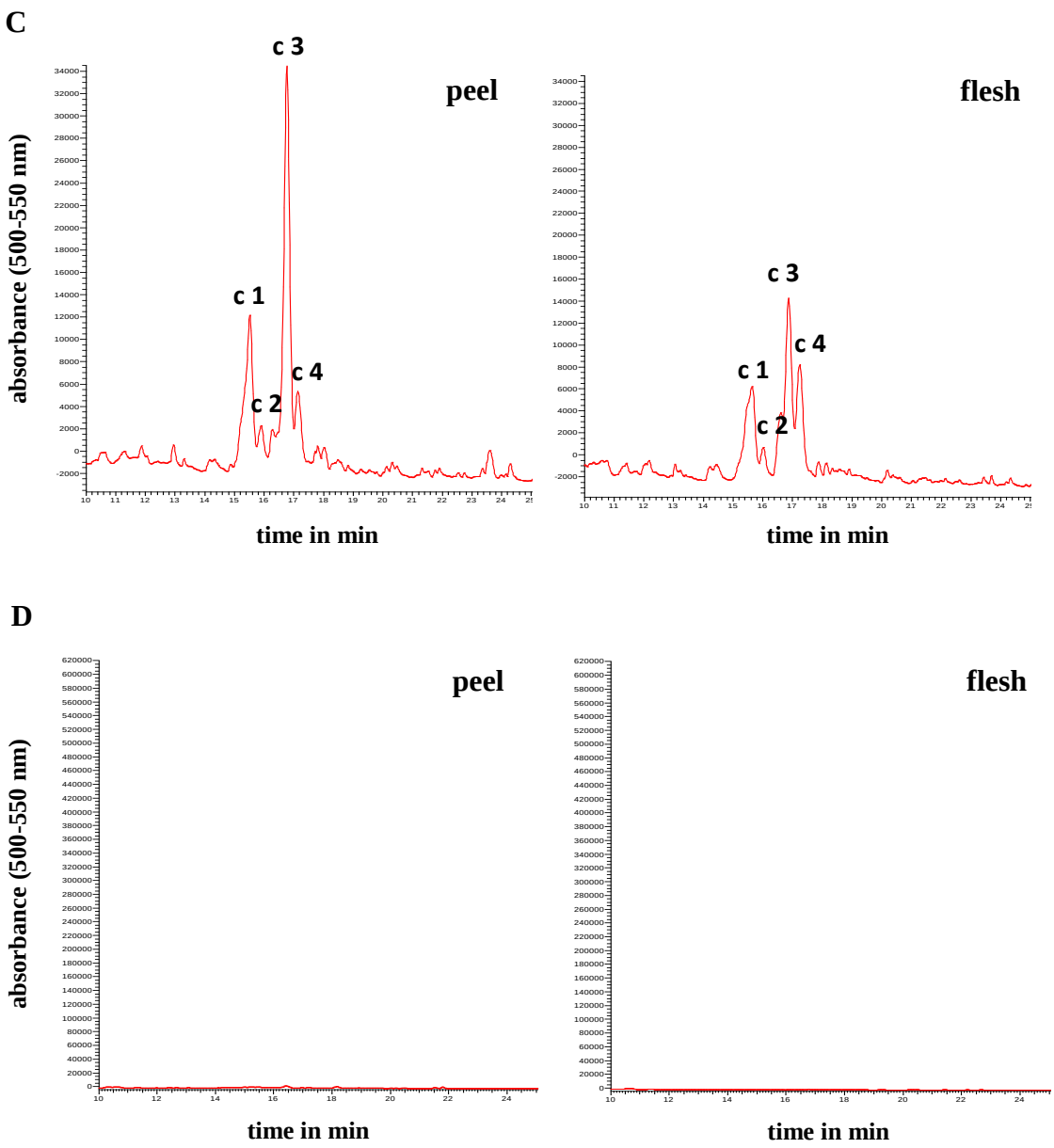

Figure 2.10: HPLC analysis of anthocyanins in the peel and flesh of fruit of (**A**) delphinidin-producing E8::*Del/Ros*1, (**B**) cyanidin- and pelargonidin-producing E8::*Del/Ros*1/E8::*AmDfr*/*f3'5'h*$^{-/-}$, (**C**) cyanidin-producing E8::*Del/Ros*1/*f3'5'h*$^{-/-}$ line, (**D**) WT. HPLC analysis of anthocyanins of E8::*Del/Ros*1/*f3'5'h*$^{-/-}$ shows the presence of five major new anthocyanin compounds. Peaks corresponded to the following compounds: **a 1**, delphinidin 3-(coumaroyl)-rutinoside-5-glucoside; **a 2**, petunidin 3-(coumaroyl)-rutinoside-5-glucoside; **b 1**, cyanidin 3-(coumaroyl)-rutinoside-5-glucoside; **b 2**, cyanidin 3-(feruloyl)-rutinoside-5-glucoside; **b 3**, peonidin 3-(coumaroyl)-rutinoside-5-glucoside; **b 4**, peonidin 3-(feruloyl)-rutinoside-5-glucoside; **b 5**, pelargonidin 3-(caffeoyl)-rutinoside-5-glucoside; **b 6**, pelargonidin 3-(coumaroyl)-rutinoside-5-glucoside; **c 1**, cyanidin 3-(coumaroyl)-rutinoside-5-glucoside; **c 2**, cyanidin 3-(feruloyl)-rutinoside-5-glucoside; **c 3**, peonidin 3-(coumaroyl)-rutinoside-5-glucoside; **c 4**, peonidin 3-(feruloyl)-rutinoside-5-glucoside.

Table 2xii: Characterisation of major anthocyanin peaks identified in the peel and flesh of the fruit of three anthocyanin tomato lines.

Tomato line	Peak	ESI-MS (m/z)	Peel	Flesh	Compound
E8::*Del/Ros*1	a 1	919	yes	yes	delphinidin 3-(coumaroyl)-rutinoside-5-glucoside
E8::*Del/Ros*1	a 2	933	yes	yes	petunidin 3-(coumaroyl)-rutinoside-5-glucoside
E8::*Del/Ros*1/E8::*AmDfr/f3'5'h*$^{-/-}$	b 1	903	yes	yes	cyanidin 3-(coumaroyl)-rutinoside-5-glucoside
E8::*Del/Ros*1/E8::*AmDfr/f3'5'h*$^{-/-}$	b 2	933	yes	yes*	cyanidin 3-(feruloyl)-rutinoside-5-glucoside
E8::*Del/Ros*1/E8::*AmDfr/f3'5'h*$^{-/-}$	b 3	917	yes	yes*	peonidin 3-(coumaroyl)-rutinoside-5-glucoside
E8::*Del/Ros*1/E8::*AmDfr/f3'5'h*$^{-/-}$	b 4	947	yes	yes*	peonidin 3-(feruloyl)-rutinoside-5-glucoside
E8::*Del/Ros*1/E8::*AmDfr/f3'5'h*$^{-/-}$	**b 5**	**903**	**no**	**yes**	**pelargonidin 3-(caffeoyl)-rutinoside-5-glucoside**
E8::*Del/Ros*1/E8::*AmDfr/f3'5'h*$^{-/-}$	**b 6**	**887**	**no**	**yes**	**pelargonidin 3-(coumaroyl)-rutinoside-5-glucoside**
E8::*Del/Ros*1/*f3'5'h*$^{-/-}$	c 1	903	yes	yes	cyanidin 3-(coumaroyl)-rutinoside-5-glucoside
E8::*Del/Ros*1/*f3'5'h*$^{-/-}$	c 2	933	yes	yes	cyanidin 3-(feruloyl)-rutinoside-5-glucoside
E8::*Del/Ros*1/*f3'5'h*$^{-/-}$	c 3	917	yes	yes	peonidin 3-(coumaroyl)-rutinoside-5-glucoside
E8::*Del/Ros*1/*f3'5'h*$^{-/-}$	c 4	947	yes	yes	peonidin 3-(feruloyl)-rutinoside-5-glucoside

Compounds marked with (*) are not annotated in the corresponding chromatogram. Rt, retention time; Cy, cyanidin; Dp, delphinidin; Mv, malvidin; Pt, petunidin; Caf, caffeoyl; Glc, glucose; Cou, coumaroyl; Rut, rutinoside; Fer, feruloyl; ESI-MS, Electro spray ionization mass spectra; m/z, molecular mass of compound.

2.4.5 Inactivation of F3'5'H and F3'H enzyme activity dramatically impacts plant fertility

Silencing of the *f3'h* gene in an *f3'5'h* (*a*) mutant resulted in plants that developed normally but did not produce any fruit that contained viable seeds. The plants developed flowers but most of them did not result in the setting of fruit and the few fruit that developed on these plants did not contain any seeds. Attempts to generate crosses using *AmDfr/Del/Ros*1/*f3'5'h*$^{-/-}$ as a male parent also failed. Several flavonoid metabolism

enzymes have been implicated in plant development and growth. For example, mutations or suppression of the cinnamate 4-hydroxylase (*c4h*) and dihydroflavonol 4-reductase-like gene (*DRL*1) have been reported to lead male sterility in Arabidopsis (Schilmiller et al., 2009, Tang et al., 2009) and co-suppression of *dfr* or *f3'5'h* genes resulted in ovule abortion in *Petunia hybrida* (Jorgensen et al., 2002).

These results show that alterations in the expression of flavonoid biosynthetic genes can impact vital developmental processes in the plant and may pose a limitation to metabolic engineering targeting specific branches in the polyphenol metabolism through inactivation or suppression of key biosynthetic genes.

2.4.6 Comparison of major polyphenolic compound composition and antioxidant capacity between WT and transgenic high-anthocyanin tomato lines

Flavonoid and anthocyanin compositions were compared between the transgenic *Del/Ros*1 and *AmDfr/Del/Ros*1/*f3'5'h*$^{-/-}$ lines and WT fruit (Figure 2.11). The amount of flavonols in ripe fruit did not dramatically differ between the WT and transgenic lines. Total flavonol content was slightly reduced by ~10% in *AmDfr/Del/Ros*1/*f3'5'h*$^{-/-}$ tomatoes and increased by ~20% in *Del/Ros*1 compared to the WT control (Figure 2.11 A). Quercetin-3-O-rutinoside also referred to as rutin was the most abundant flavonol in all three tomatoes but was proportionally more abundant in WT compared to the two transgenic high-anthocyanin tomato lines. The amount of chlorogenic acid (CGA) was increased threefold from 40 µmol/kg FW in the WT control to 120 µmol/kg FW in *AmDfr/Del/Ros*1/*f3'5'h*$^{-/-}$ but reduced to 20 µmol/kg FW in *Del/Ros*1. In the two transgenic lines, levels of kaempferols and quercetins were higher than in the WT fruit. Most notably, kaempferol-3-rutinoside (kae-3-rut) was increased by 2.5 fold compared to WT fruit. Kaempferol-rutinoside-glucoside (Kae-rut-glu) was almost undetectable in both WT and *Del/Ros*1 but was present at 25 µmol/kg FW in the fruit of *AmDfr/Del/Ros*1/*f3'5'h*$^{-/-}$ where F3'5'H was inactive. Levels of quercetin-coumaroyl-rutinoside (que-cou-rut) and quercetin-rutinoside-feruloyl (que-rut-fer) were also higher in the transgenic lines compared to WT.

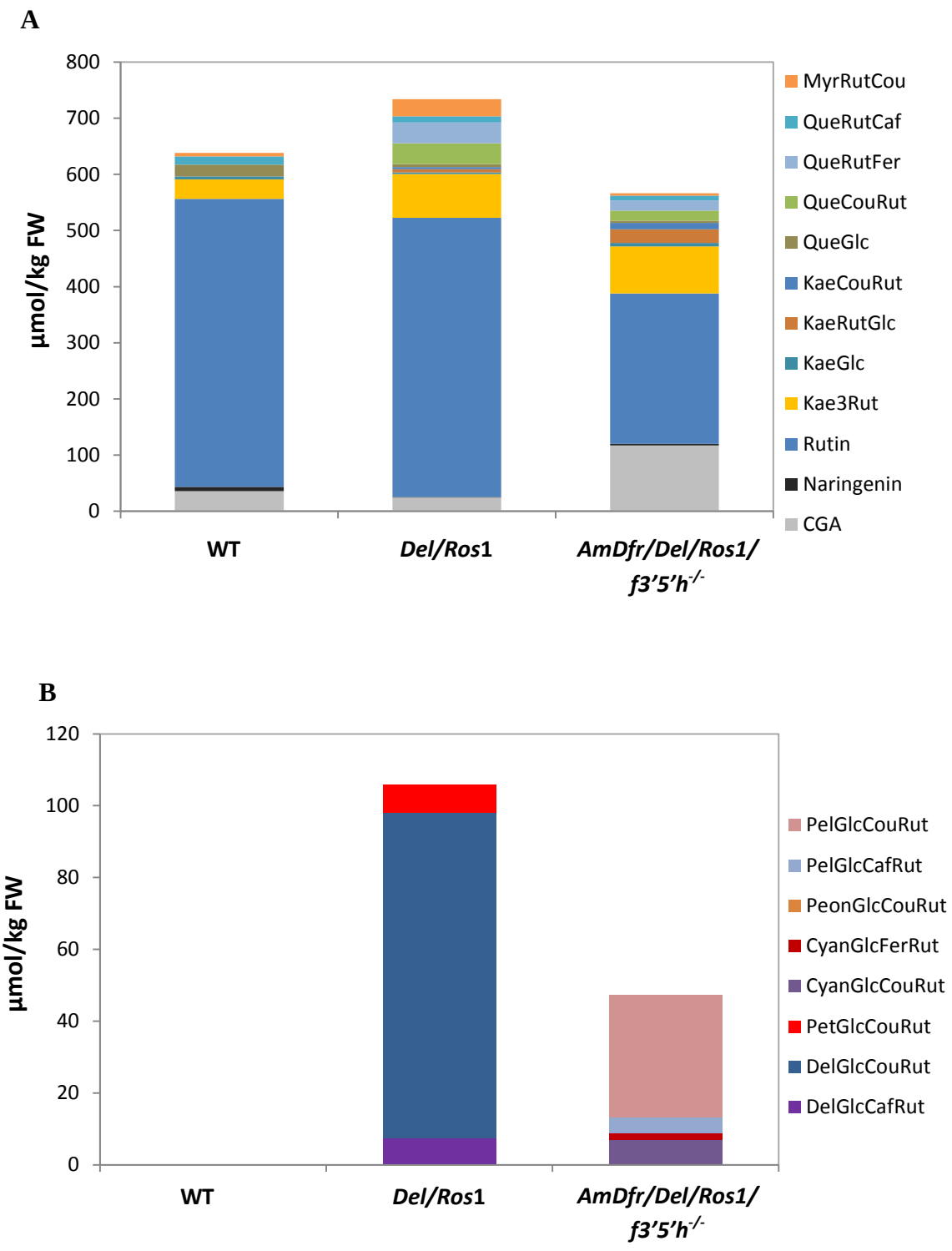

Figure 2.11: Comparative analysis of (**A**) flavonoid and (**B**) anthocyanin content and composition of WT and transgenic lines *Del/Ros*1 and *AmDfr/Del/Ros*1/*f3'5'h*$^{-/-}$. HPLC analysis, recorded at (**A**) 340-360 nm or (**B**) 500-550 nm, of 50% methanol (v/v) extracts of ripe tomato fruit. Classification and identification of compounds was performed on the basis of PDA absorbance and mass spectrometry.

Myricetin-rutinoside-coumarate (myr-rut-cou) was the only trihydroxylated flavonoid that was detected and quantified with fidelity. Myr-rut-cou was present at extremely low levels of ~5 µmol/kg FW in both WT and *AmDfr/Del/Ros*1/*f3'5'h*$^{-/-}$ fruit but increased to 30 µmol/kg FW in *Del/Ros*1.

Similarly, anthocyanins were identified and quantified in the three tomato lines (Figure 2.11 B). As expected, anthocyanins were absent from the WT tomato fruit. The identification of anthocyanins in the fruit of the transgenic high-anthocyanin lines had shown that *Del/Ros*1 produces only trihydroxylated anthocyanins and *AmDfr/Del/Ros*1/*f3'5'h*$^{-/-}$ synthesises predominantly monohydroxylated anthocyanins and low levels dihydroxylated anthocyanins. *Del/Ros*1 contained 2.5 times more anthocyanins that *AmDfr/Del/Ros*1/*f3'5'h*$^{-/-}$. The most abundant anthocyanins found in *Del/Ros*1 fruit was delphinidin-coumaroyl-rutinoside-glucoside (del-glu-cou-rut) and in the fruit of *AmDfr/Del/Ros*1/*f3'5'h*$^{-/-}$ was pelargonidin-coumaroyl-rutinoside-glucoside (pel-glu-cou-rut).

Differences in the antioxidant activity between WT and transgenic anthocyanin tomatoes were measured using the TEAC assay. The activity of the water-soluble fraction (containing anthocyanins) of *Del/Ros*1 tomatoes (var. MicroTom) was fourfold higher than that of WT tomatoes (var. MicroTom; Figure 2.12 A). The water-soluble fraction of *AmDfr/Del/Ros*1/*f3'5'h*$^{-/-}$ tomatoes resulted in a threefold increase in antioxidant activity compared to the WT tomatoes (Figure 2.12 A).

In all three tomato samples, the antioxidant activity observed in the acetone-soluble fraction (containing lipophilic antioxidants) was fourfold lower compared to the water-soluble fractions. In agreement with the results from the hydrophilic fraction, the antioxidant capacity of lipophilic fractions of *Del/Ros*1 and *AmDfr/Del/Ros*1/*f3'5'h*$^{-/-}$ were increased by four- and threefold, respectively, compared to the WT tomato fraction (Figure 2.12 B). Both transgenic anthocyanin tomatoes have significantly higher antioxidant capacities than the WT control with *Del/Ros*1 displaying the most pronounced increase.

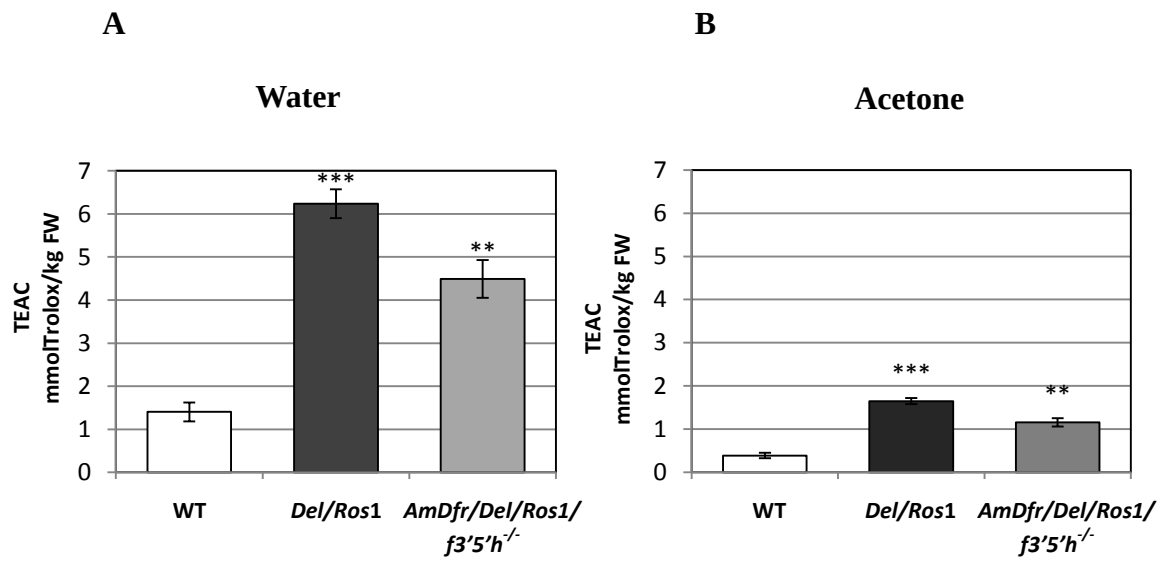

Figure 2.12: Analysis of (**A**) hydrophilic and (**B**) lipophilic antioxidant activity in ripe tomato fruit from WT and transgenic lines *Del/Ros*1 and *AmDfr/Del/Ros*1/*f3'5'h*$^{-/-}$. Values are expressed relative to Trolox antioxidant activity. Histograms represent mean values ± standard error (n=3). * $p<0.05$; ** $p<0.01$; *** $p<0.001$.

2.4.7 Alteration in the anthocyanin pathway gene expression in response to *AmDfr* activity

Expression of the key genes involved in the biosynthetic pathway of anthocyanins in the transgenic, anthocyanin-producing lines *Del/Ros*1 and *AmDfr/Del/Ros*1/*f3'5'h*$^{-/-}$ were investigated by quantitative qRT-PCR and compared to the WT control (Figure 2.14). Fruit were selected at different stages of maturity for subsequent RNA extraction and cDNA synthesis (Figure 2.13). Expression levels for plant polyphenol biosynthetic genes changed dramatically during fruit development, being lowest in ripe fruit and showing highest levels of induction in the early breaker stage. Therefore, I selected fruit at early breaker stage, at which the peel of the fruit would start to turn from green to yellow/orange (Figure 2.13). The expression of the genes was normalized to *SlUbi*, encoding for the tomato ubiquitin and gene expression levels were expressed relative to *SlUbi*. Expression levels of early biosynthetic genes (Figure 2.14 A) varied dramatically between the different tomato lines no general trend between the presence of the transgenes and the changes in gene expression. *pal*, *chs*-1 and *f3'h* were expressed at highest levels in WT fruit, whereas expression of *f3'5'h* and *f3h* was significantly

upregulated in *AmDfr/Del/Ros*1/*f3'5'h*$^{-/-}$ compared to WT and *chi* was most strongly expressed in *Del/Ros*1 tomato.

However, a clear correlation between the presence of the transgenes *Del*, *Ros*1 and *AmDfr* and the upregulation of late biosynthetic genes was observed (Figure 2.14 B). The *fls* gene encoding flavonol synthase which catalyses the conversion of dihydroflavonols to flavonols was expressed most strongly in WT but both *Sldfr* and *Slans*, coding for enzymes that are crucial for performing the structural modifications that are required for the conversion of dihydroflavonols to anthocyanins, were strongly upregulated in the transgenic lines but higher in *AmDfr/Del/Ros*1/*f3'5'h*$^{-/-}$ than in *Del/Ros*1. The transcription factor genes *Del* and *Ros*1 were more strongly expressed in *AmDfr/Del/Ros*1/*f3'5'h*$^{-/-}$ than in *Del/Ros*1, and unsuprsingly showed no expression in the untransformed WT control. High expression of the *AmDfr* transgene expression was detected only in the fruit of *AmDfr/Del/Ros*1/*f3'5'h*$^{-/-}$ and confirmed that *AmDfr* was indeed active in *AmDfr/Del/Ros*1/*f3'5'h*$^{-/-}$ tomatoes and catalysing the formation of predominantly monohydroxylated anthocyanins in the fruit.

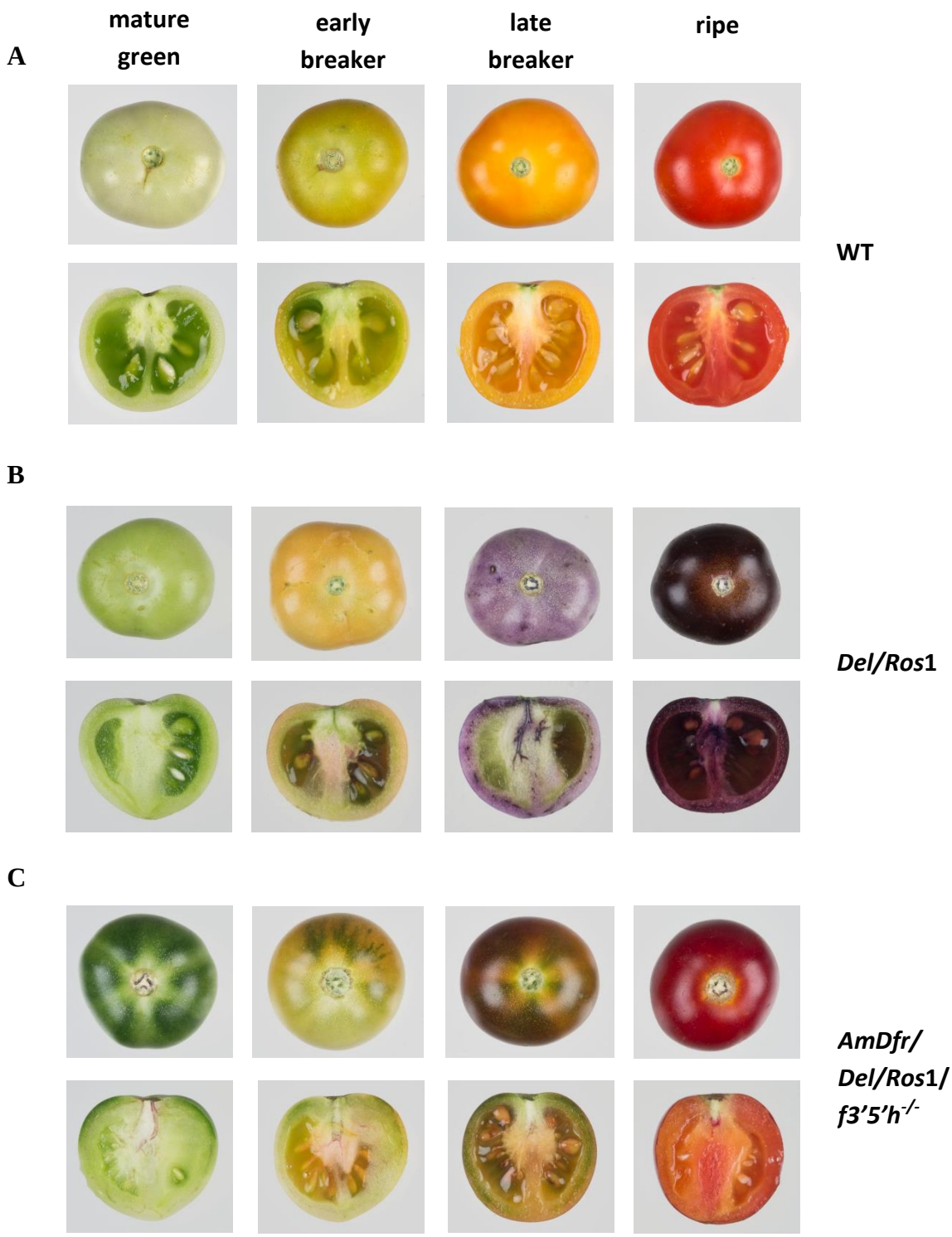

Figure 2.13: Anthocyanin production in various developmental stages of the different anthocyanin tomato genotypes. Photographs of (**A**) WT, (**B**) *Del/Ros*1 and (**C**) *AmDfr/Del/Ros*1/*f3'5'h*$^{-/-}$ tomato fruit.

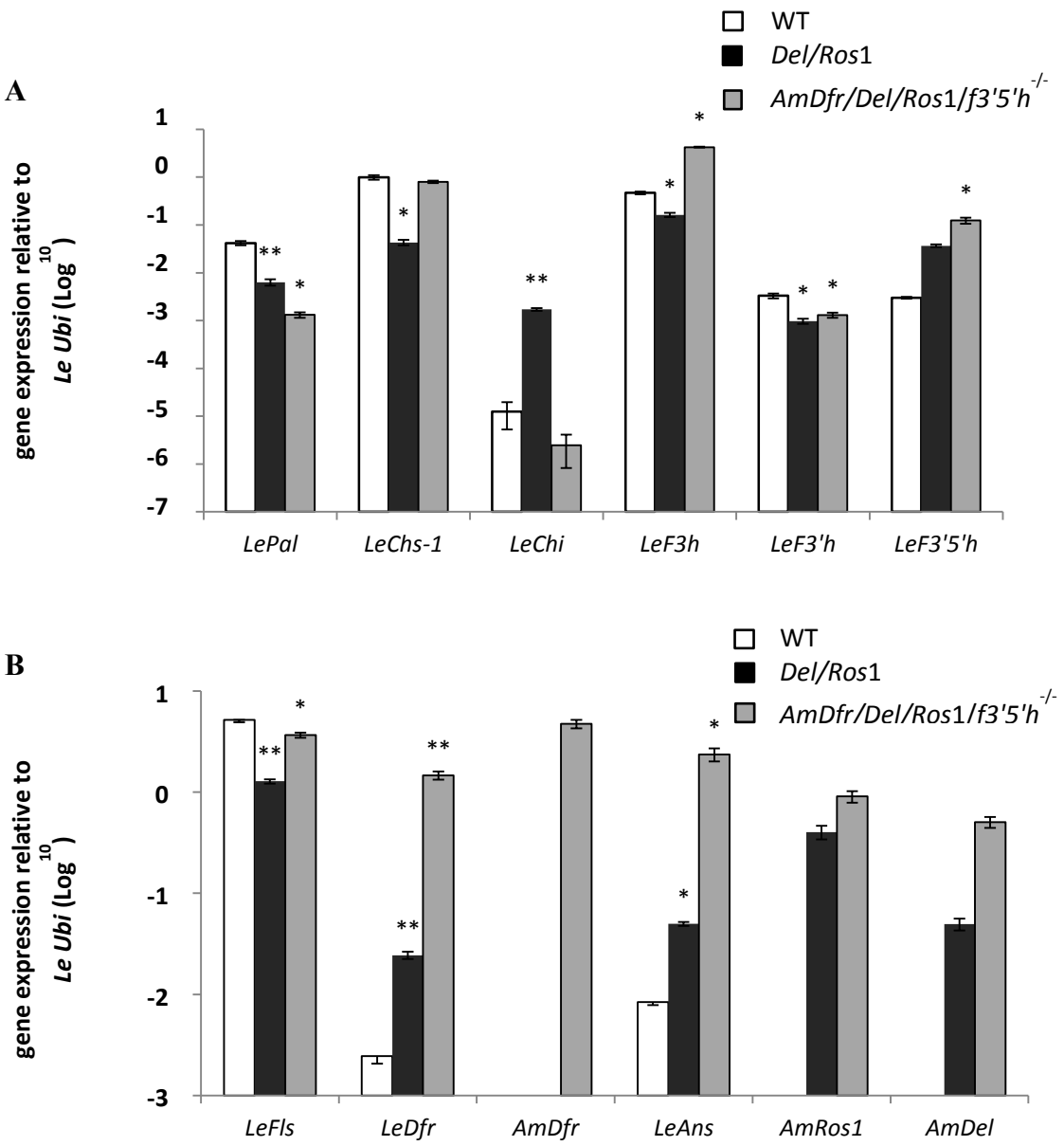

Figure 2.14: Expression profiles of key anthocyanin pathway genes of the transgenic *Del/Ros*1 and *AmDfr/Del/Ros*1/*f3'5'h*$^{-/-}$ tomato lines were compared to WT. Tomatoes were harvested at breaker stage. Expression of (**A**) early biosynthetic pathway genes and (**B**) late biosynthetic pathway genes and transgenes were represented relative to *S. lycopersicum* ubiquitin (*SlUbi*). *A. majus Rosea*1, *AmRos*1; *A. majus Delila*, *AmDel*; *A. majus* dihydroflavonol reductase, *AmDfr; S. lycopersicum* anthocyanidin synthase, *LeAns*; *S. lycopersicum* chalcone synthase-1 (*SlChs-1*); *S. lycopersicum* chalcone isomerase (*SlChi*); *S. lycopersicum* dihydroflavonol reductase; *S. lycopersicum* flavanone-3-hydroxylase (*SlF3h*); *S. lycopersicum* flavonoid-3'-hydroxylase (*SlF3'h*); *S. lycopersicum* flavonoid-3'5'-hydroxylase (*SlF3'5'h*); *S. lycopersicum* flavonol synthase (*SlFls*); *S. lycopersicum* phenylalanine ammonia lyase (*SlPal*). Data shown as mean ± standard error (n=3). * $p<0.05$; ** $p<0.01$.

2.5 Discussion

Plant metabolic engineering is an indispensable tool in molecular biology and has contributed significantly to increasing our knowledge of the fundamental biochemical processes that govern primary and secondary metabolism in plants. By understanding the molecular mechanisms that underlie their development, growth or unique biochemical characteristics, this technology can be applied to modify crop species to improve their nutritional composition or resistance to biotic and abiotic stresses.

Increasing awareness of the health benefits of plant compounds such as carotenoids and polyphenols, has led to increased research efforts using both conventional breeding and transgenic approaches to enhance their content or composition in important crop species including maize, rice, wheat and tomato (Bai et al., 2011, Schijlen et al., 2004). The tissue-specific accumulation of many of these compounds is often regulated by MYB and/or bHLH transcription factors, or their tertiary complexes, that can activate general pathways (e.g. *Vitis vinivera MYB5a*–mediated regulation of anthocyanins, flavonols, tannins, and lignins (Deluc et al., 2006)) or induce highly specific branches in a biosynthetic pathway (proanthocyanidin regulation in strawberry fruit is regulated by *FaMY*B9, *FabHLH*3 and WD40 *FaTTG*1 (Schaart et al., 2013)). The modification of plant secondary metabolism through transcriptional regulation of biosynthetic pathways has resulted in the accumulation of polyphenolic compounds in several crop species (Davies, 2010, Dixon, 2005, Gray et al., 2012).

Commercial tomato varieties accumulate significant amounts of the carotenoid, lycopene, but contain only low levels of flavonols and no anthocyanins in the fruit. Several transgenic approaches have successfully increased the content of carotenoids in in tomato by modulating the expression of regulatory genes (Davuluri et al., 2005) or introducting novel genes (Rosati et al., 2000). Non-transgenic introgression with wild relatives of tomato that accumulate anthocyanins, resulted in tomatoes producing anthocyanins in the peel but not in the flesh (Povero et al., 2011). Transgenic approaches that involved the addition of transcription factors regulating flavonoid biosynthesis in heterogenous species, resulted in tomatoes that accumulated high levels of flavonols (Bovy et al., 2002, Luo et al., 2008) and anthocyanins (Butelli et al., 2008) in peel and flesh. This demonstrates that transcription factors play a critical role in the

regulation of genes implicated with the general flavonoid biosynthetic pathway or specific branches leading to flavonols, anthocyanins and proanthocyanidins.

To date, many transcription factors or MBW complexes regulating flavonoid biosynthesis have been identified in commercially important crops and ornamental plants, but mainly in model species such as *Arabidopsis* and *Antirrhinum* and *Petunia*, which have contributed to most of our understanding of anthocyanin. Our increasing knowledge of the regulatory and structural genes involved in the biosynthetic pathways has allowed targeting of specific branches in the pathway in order to accumulate specific compounds. This has important implications for the development of novel crops with enhanced nutritional qualities through the addition of new compounds, e.g. β-carotene-enriched rice (Paine et al., 2005), or the reduction and elimination of toxic or undesirable compounds like cyanogen in cassava (Siritunga and Sayre, 2003).

Butelli et al. (2008) demonstrated that the addition of the two transcription factors, *Delila* and *Rosea*1, which jointly regulate anthocyanin production in *A. majus*, lead to the accumulation of large amounts of anthocyanins when placed under the control of a fruit-specific E8 promoter. Transgenic *Del/Ros*1 tomatoes accumulated between 2 and 3 mg of trihydroxylated anthocyanins per gram FW. The *Del/Ros*1 tomato line accumulated only trihydroxylated anthocyanins but produced all three classes of flavonols, Kae, Que and Myr (Figure 2.11 A), which strongly suggested that the structural enzymes, required for the conversion of the dihydroflavonol, DHK, to either DHQ or DHM were active in the fruit. These dihydroflavonols act as substrates for FLS, which catalyses the conversion to flavonols or as substrates for DFR that forms leucoanthocyanidins and subsequently, lead to the production of anthocyanins or proanthocyanidins (Figure 2.1). The presence of mono-, di- and trihydroxylated flavonols but absence of mono- or dihydroxylated anthocyanins in *Del/Ros*1 fruit was strongly indicative of the substrate preference of DFR for trihydroxylated DHM.

In order to generate mono- and dihydroxylated anthocyanins we pursued a dual metabolic engineering strategy to overcome DFR substrate-specificity by introducing a non-specific DFR from *A. majus* and controlling the formation different classes of dihydroflavonols by inhibiting the activity of the hydroxylases, F3’5’H and F3’H that catalyse the formation of DHM and DHQ, respectively. The accumulation of low levels

of dihydroxylated anthocyanins in the *Del/Ros*1/*f3'5'h*$^{-/-}$ line confirmed our hypothesis that in the absence of a functional F3'5'H, tomato DFR could bind to the cyanidin precursor DHQ (Figure 2.8 and Table 2x). The low amounts of cyanidin-type anthocyanins indicated however, that tomato DFR could not efficiently convert DHQ to leucocyanidins. In order to overcome the substrate-specific limitations of DFR and increase the amounts of dihydroxylated anthocyanins in the fruit, we introduced a gene from *A. majus* encoding a DFR that produces both mono- and dihydroxylated anthocyanins in the flowers of *A. majus* (Martin et al., 1991).

Somewhat unexpectantly, the resulting line, *AmDfr/Del/Ros*1/*f3'5'h*$^{-/-}$, produced both mono- and dihydroxylated anthocyanins in the fruit and had a total anthocyanin content of 2.5-fold lower than that of the *Del/Ros*1 line (Figure 2.11 B). Separate analysis of the peel and flesh revealed however, that only dihydroxylated cyanidins and peonidins were produced in the peel whereas both dihydroxylated and monohydroxylated anthocyanins were produced in the flesh of ripe tomato fruit of *AmDfr/Del/Ros*1/*f3'5'h*$^{-/-}$ (Figure 2.10 B). This was an interesting observation as no monohydroxylated anthocyanins were detected in the *Del/Ros*1/*f3'5'h*$^{-/-}$ line, which produced low levels of cyanidins in both peel and flesh. The absence of monohydroxylated pelargonidins from the fruit peel of *AmDfr/Del/Ros*1/*f3'5'h*$^{-/-}$ suggests that in the peel, F3'H is active and converts DHK to DHQ, which is then converted by DFR into leucocyanidin. The presence of both mono- and dihydroxylated anthocyanins in the flesh, shows that some DHK is converted to DHQ by F3'H but a substantial proportion of the available DHK is directly converted into leucopelargonidin by the *A. majus* DFR.

This observation might indicate that the transcription factors *Delila* and *Rosea*1 strongly induce expression of F3'H in the peel but less effectively in the flesh of tomato fruit. Gene expression analysis of tomato *f3'h* in the whole fruit at the early breaker stage showed that expression of *f3'h* was lower in the anthocyanin-producing lines, *Del/Ros*1 and *AmDfr/Del/Ros*1/*f3'5'h*$^{-/-}$ compared to WT (Figure 2.14 A). F3'5'H, F3'H and DFR compete for the same substrate, DHK. In the delphinidin-producing *Del/Ros*1 line, F3'5'H is substantially increased in response to *Del/Ros*1, and binds more effectively than F3'H to their common substrate, DHK. This might lead to negative feedback on the expression of F3'H and could explain why expression levels of *f3'h* are reduced in *Del/Ros*1. In the *AmDfr/Del/Ros*1/*f3'5'h*$^{-/-}$ line, activity of F3'5'H has been blocked as a

result of a stop mutation in the gene encoding F3'5'H. Gene expression analysis of *f3'5'h* in the fruit of the *AmDfr/Del/Ros*1/*f3'5'h*$^{-/-}$ line showed that transcript levels of *f3'5'h* were significantly increased (Figure 2. 14 A). However, the absence of trihydroxylated dihydroflavonols or delphinidins in these tomatoes illustrated that *f3'5'h* transcripts were not translated into a functional enzyme due to the stop mutation in its sequence.

In *AmDfr/Del/Ros*1/*f3'5'h*$^{-/-}$, F3'H competes with DFR but not F3'5'H for DHK substrate binding. Whilst tomato DFR cannot use DHK as a substrate, *A. majus* DFR can effectively convert DHK to leucopelargonidin. Both tomato and *A. majus* DFR (*LeDfr* and *AmDfr*; Figure 2.14 B) were significantly upregulated in the fruit of *AmDfr/Del/Ros*1/*f3'5'h*$^{-/-}$ resulting in the production of both di- and monohydroxylated anthocyanins in the fruit. However, the high amounts of cyanidins found in the peel of *AmDfr/Del/Ros*1/*f3'5'h*$^{-/-}$ and the absence of pelargonidins suggest that in this tissue, F3'H is activate and converts all DHK to DHQ. Separate gene expression analysis of F3'H in peel and flesh is required to confirm whether F3'H is differentially regulated in the peel and the flesh of tomato fruit.

Our current observations confirm that in the fruit of transgenic *AmDfr/Del/Ros*1/*f3'5'h*$^{-/-}$ tomatoes, *A. majus* DFR effectively converts both DHK and DHQ to leucopelargonidin- and –cyanidin, respectively. The failure to substantially increase the accumulation of dihydroxylated anthocyanins in the flesh of *AmDfr/Del/Ros*1/*f3'5'h*$^{-/-}$, however, suggests that in this tissue, F3'H is insufficiently activate. The transcription factors, *Delila* and *Rosea1*, effectively activate general phenylpropanoid metabolism and result in the upregulation of late biosynthetic pathway genes, *dfr* and *ans*, which are required for the formation of anthocyanins (Figure 2.14 B). Compared to *f3'5'h*, total expression of *f3'h* in the developing fruit is not increased as a result of *Delila* and *Rosea*1 activation. This indicates that in the flesh, which accounts for most of the DW of the fruit, the *f3'h* gene does not respond effectively to *Del/Ros*1-mediated transcriptional activation. Not all transcriptional regulators may work equally well in every species or some may fail to control expression of all structural flavonoid genes (Schwinn et al., 2006). In maize, for example, the *R* and *C1* genes encode transcription factors that regulated anthocyanin production in the maize kernels. The expression of *R* and *C1* in transgenic tomato fruit resulted in the accumulation of high levels of flavonols but not

anthocyanins (Bovy et al., 2002). *Delila* and *Rosea*1 regulate biosynthesis of mono- and dihydroxylated anthocyanin in *A. majus* and effectively induced the genes such as f3'5'h, required for the production of trihydroxylated anthocyanins in tomato (Butelli et al., 2008). However, the failure to significantly upregulate the expression of *f3'h* in *AmDfr/Del/Ros*1/*f3'5'h*$^{-/-}$ tomatoes might indicate that *Delila* and *Rosea*1 do not activate this structural gene effectively and thus, are unsuitable for increasing the amount of dihydroxylated cyanidins in tomato.

Tissue-specific expression of flavonoid genes in tomato as well as other species is well documented and the amount of major flavonoids such as naringenin that accumulate in the peel may account for around 90% of total flavonoids present in the tomato fruit (Torres et al., 2005). The weak expression of structural flavonoid genes in the flesh has limited previous transgenic attempts to accumulate high amounts of flavonoids in the whole fruit of tomato (Muir et al., 2001) but also explains the skin-specific accumulation of anthocyanins in the fruit of non-transgenic anthocyanin tomatoes (Povero et al., 2011). However, this limitation was overcome by placing transgenes under the control of a fruit-specific E8 promoter, which successfully activated the expression of flavonoid biosynthetic genes that led to the accumulation of flavonols or anthocyanins in all fruit compartments (Bovy et al., 2002, Butelli et al., 2008, Luo et al., 2008).

I demonstrated, that by blocking F3'5'H activity and introducing a substrate-independent DFR, novel branches in the anthocyanin biosynthetic pathways were activated that led to the formation of cyanidins and pelargonidins. My work also demonstrated the complexity and difficulty of controlling several structural enzymes in order to target specific compounds in a pathway.

Failure to upregulate *f3'h* activity significantly and increase cyanidin production in the flesh of *AmDfr/Del/Ros*1/*f3'5'h*$^{-/-}$ tomatoes, could potentially be overcome by introducing a novel F3'H from *A. majus* or *Chrysanthemum*, which both accumulate significant amounts of cyanidins in their flowers under the control of their native promoters (AmF3'H is responsive to Del and Ros1) or an E8 promoter.

The development of a high-pelargonidin line that produces exclusively pelargonidins in both peel and flesh might be even more challenging. The silencing of *f3'h* in the *a*

(*f3'5'h*$^{-/-}$) mutant resulted in plants that were unable to self-fertilise. Cross-pollination attempts also failed in these plants suggesting that both pollen and anther development could be affected in these plants. Flavonoid biosynthesis and metabolism have been implicated with a number of developmental processes such as auxin transport and pollen development (Taylor and Grotewold, 2005). The CHS is the first committed step in the synthesis of flavonoids and *chs*-deficient plants fail to accumulate flavonoids in their tissues and organs. Antisense inhibition of *chs* in *Petunia* resulted in flavonoid-deficient anthers that were male sterile due to an arrest in male gametophyte development (van der Meer et al., 1992). Conditional male fertility was also reported in CHS-deficient maize (Pollak et al., 1995) but *Arabidopsis* plants harbouring a null mutation in their *chs* gene and were deficient in flavonoid biosynthesis but fully fertile (Burbulis et al., 1996). Schijlen et al. (2007) reported the development of parthenocarpic (seedless) fruit with impaired pollen tube growth in a *chs* RNAi tomato lines suggesting that flavonoids are essential for pollen development. CHS and flavonoid accumulation appears to be essential for pollen and anther development in some species such as maize, *Petunia* and tomato but not in others. So far, there are no definite reports of other flavonoid biosynthetic genes to impact male or female fertility. However, Suzuki et al. (2000) reported male and female sterility as a result of co-suppression of CHS and DFR in the ornamental plant *Torenia hybrida* but did not report whether suppression of DFR alone impacted plant fertility. Despite normal flower development, the *f3'h* RNAi (in *a f3'5'h*$^{-/-}$ background) tomato line failed to self-pollinate and set fruit. Similarly, cross-pollination with pollen from fertile tomato lines failed to produce fruit in these plants suggesting that inhibition of both *f3'h* and *f3'5'h* severely impacted male and female fertility in tomato. Compared to WT plants, a reduction in the number of fruit developed was observed in the *a* mutant. Additional loss of F3'H activity resulted in complete failure to self-pollinate. Further studies, investigating pollen tube and anther development, are required to investigate underlying causes of the apparent infertility of F3'H/F3'5'H co-suppressed tomatoes. Inhibition of F3'H and F3'5'H activity is a requirement to generate a tomato line that produces monohydroxylated anthocyanins only. However, generating tomatoes which produce only pelargonidins in both peel in flesh may not be possible if concurrent inhibition of F3'H and F3'5H leads to irreversible sterility.

3 Anthocyanin-enriched tomato extracts induce apoptosis in breast cancer cells

3.1 Introduction

Numerous studies have reported that pure plant polyphenols as well as polyphenol-rich extracts of fruit and vegetables can inhibit the proliferation of multiple cancer cell types *in vitro*. Several studies have provided evidence that exposure to these compounds can alter the apoptotic response through modulation of key components of the apoptotic pathway suggesting that anthocyanins and other plant polyphenols possess certain anti-cancer or chemotherapeutic properties. The mechanisms by which these biological effects are exerted are still not fully elucidated but are thought to be the result of combinatorial induction of the apoptotic program, changes in the cellular oxidative state, alterations in the cell cycle, and reduced DNA synthesis.

Plant polyphenols such as resveratrol and anthocyanins have been shown to induce arrest of the cell cycle in G0/G1 (Bai et al., 2010) or alternatively in the S-phase depending on the individual cancer cell type, through effects on cell cycle regulator proteins such as p53, p21, cyclin D1, cyclin A and others (Joe et al., 2002, Pozo-Guisado et al., 2002, Lazze et al., 2004, Malik et al., 2003). Cell cycling is central to cell division and cell proliferation and cell cycle profiles are often altered or accelerated in cancer cells, making cell division a common target for many chemotherapeutic agents.

The development and growth regulation of normal cells is strongly interlinked with apoptosis, a complex cellular process relying on the coordinated activation and execution of various subprogrammes. Many chemopreventive agents target inducers of apoptosis in malignant cells. A number of studies have shown that anthocyanins and resveratrol along with many other phytochemicals exhibit strong proapoptotic activity through both the intrinsic, mitochondria-dependent (Feng et al., 2007)) and extrinsic, mitochondria-independent pathways. Both apoptotic pathways have unique component mechanisms but almost always involve the activation of caspase proteases.

Caspases are a family of cysteine proteases that play a crucial role in the activation of the morphological changes associated with apoptosis. Loss of function or alterations in caspase activity can prevent cells from assuming their apoptotic fate (Earnshaw et al., 1999). Thus, alterations in caspase functionality, as a result of mutations, are frequently observed in different types of cancer, including MCF-7 breast cancer cells which do not

express detectable levels of caspase-3 due to a partial deletion within exon 3 of the *CASP*-3 gene (Jänicke et al., 1998). Activation of caspases after exposure to anthocyanin-rich extracts has been observed in different cell lines (Hui et al., 2010, Lee et al., 2009, Reddivari et al., 2007). In order to understand the anti-cancer activity of phytochemicals, it is vital to study at least some of the markers indicative of cell death.

Most of our current understanding of the health-beneficial effects of these dietary phytonutrients is derived from studies involving the use of isolated compounds. However, over the last few years, results have emerged suggesting that isolated polyphenols do not have the same health-promoting effects as the same compounds in a food matrix environment (Prior et al., 2008, Titta et al., 2010). It is now believed that the dietary components alone do not explain the health benefits of diets that are rich in fruit and vegetables. Taking the nutritional context into account and assessing the importance of the food matrix are likely to increase our understanding of the mechanisms by which phytochemicals contribute towards reduced disease risks and incidences. Consequently, comparison of high-anthocyanin or high-resveratrol tomato lines with WT tomatoes deficient in these phytonutrients may provide a good model to study the health benefits of these compounds in a food context.

3.1.1 Aims

In this chapter the effects of a high-resveratrol and several anthocyanin-enriched tomato extracts on metabolic activity and apoptosis of MCF-7 and MDA-MB-231 breast cancer cells are described. A comparison of purified, dietary supplements compared to whole tomato extracts containing the same phytochemicals allowed me to study their biological effects in the context of a food matrix. WT tomato extracts provided a matched matrix control in the experiments using high- resveratrol or high-anthocyanin tomatoes. This allowed me to link any differences in the biological effects between the different tomato extracts to the compounds that are unique to the individual tomato lines. A comparative analysis of the chemopreventive effects of a high-delphinidin and a high-pelargonidin tomato extracts was conducted in order to understand whether the structure of different anthocyanin molecules affects their biological activity.

3.2 Experimental procedures

3.2.1 Cell culturing

3.2.1.1 Description of cell lines

All cell lines were purchased from the American Type Culture Collection (ATCC®). Both MCF-7 (Figure 3.1 A) and MDA-MB-231 (Figure 3.1 B) are adherent cell lines that were derived from breast adenocarcinomas. MCF-7 in non-invasive and ER^+ and responds to oestradiol via a cytoplasmic oestrogen receptors. The MDA-MB-231 human cell line has an invasive phenotype and is ER^-.

HMT-3522-S1 or HMT-3522/wt is a human breast epithelial cell subline derived from HMT-3522. The parent line was established from a benign breast tumour. HMT-3522-S1cell line has remained non-tumourigenic for more than 400 passages.

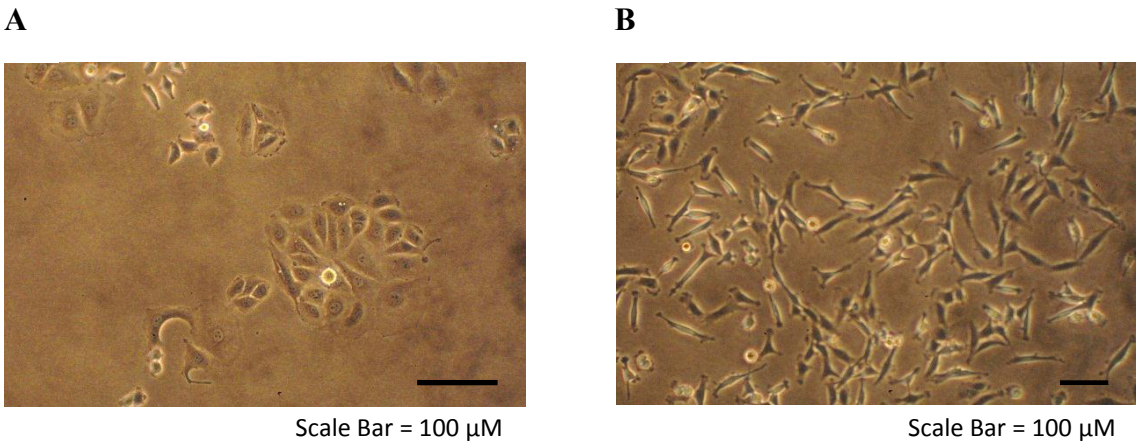

Figure 3.1: Images of (**A**) MCF-7 and (**B**) MDA-MB-231 human breast cancer cell lines.

3.2.1.2 Media and selection

Both MCF-7 and MDA-MB-231 cells were maintained in GlutaMAX™ Dulbecco's Modified Eagle medium (DMEM) cell culture medium (GIBCO, Life technologies) supplemented with 1% non-essential amino acids (GIBCO, Life technologies) and 10% heat inactivated fetal calf serum (FCS; GIBCO, Life technologies) at 37°C and 5% CO_2.

DMEM GlutaMAX^{TM} has a glucose concentration of 1 g/L and contains 110 mg/L pyruvate. Cells were sub-cultured twice a week or when reaching 80% confluence.

HMT-3522-S1 cells were maintained in collagen-coated flasks in serum-free DMEM/Ham's F12 (1:1) cell medium (GIBCO, Life technologies) containing 2 mM glutamine supplemented with 250 ng/mL insulin, 10 µg/mL apo-transferrin, 2.6 ng/mL sodium selenite, 0.1 nM estradiol, 1.4 µM hydrocortisone, 5 µg/mL ovine prolactin and 10 ng/mL Epidermal Growth Factor (EGF). Collagen is an extracellular matrix protein that is used in cell culture to facilitate cell attachment growth, differentiation, migration, and tissue morphogenesis. Cell culture flask were coated with collagen and incubated for 1 h at 37°C and 5% CO_2 before the addition of cells and cell culture medium.

3.2.1.3 Passage and maintenance of cells

For experimental analyses MCF-7 and MDA-MB-231 cells were used at passages between 6 and 20. Passaging or subculturing refers to the transfer of a small numbers of cells into a new culture vessel. Regular subculturing is required to avoid the induction of transcriptional changes or senescence associated with prolonged high cell density.

3.2.1.4 Trypsinisation

Both MCF-7 and MDA-MB-231 cells form monolayers that require dissociation from each other and the culture flasks, in order to be transferred to new culture vessel. Trypsinizing refers to the use of the proteolytic enzyme trypsin to break adhesion proteins in cell-cell and cell-matrix interactions and results in the detachment of cells. Prior to trypsinisation, cell medium was removed and cells were washed twice with PBS. Washed cells were incubated with 2 mL of 0.05% Trypsin-EDTA (Gibco, Life Technologies) for two to three minutes at 37°C and 5% CO_2 or until cells had detached. The proteolytic activity of trypsin was inactivated by addition of complete medium containing FCS that acts as a trypsin inhibitor.

3.2.2 Plant secondary metabolites

All plant secondary metabolites were purchased. The anthocyanin, delphinidin-3-O-glucoside chloride was purchased from Extrasynthase and dissolved in DMSO to a final concentration of 200 mM. The stilbenes, resveratrol (3,4', 5-trihydroxy-*trans*-stilbene)

and polydatin (reservatrol-3-β-mono-D-glucoside) were purchased from Sigma and dissolved to a final concentration of 200 mM in ethanol and DMSO, respectively.

3.2.3 Tomato extract preparation for human cell studies

Crude tomato extracts were prepared from ripe high-anthocyanin, high-resveratrol and WT tomato fruit. Tomatoes were harvested at the ripe stage and immediately transferred into liquid N_2 before being freeze-dried and powdered. The freeze-dried tomato powder was then stored protected from light at -20°C (short term) or -80°C (long term). A crude tomato extract was prepared by extracting water- and methanol-soluble compounds with an 80% methanol (v/v) containing 0.75% HCl from the freeze-dried tomato powder. 1 g of freeze-dried plant material and 50 mL of 80% MeOH (v/v) were incubated overnight at 4°C in the dark with shaking, before being centrifuged at 4,000 *g* at 4°C for 15 min to separate the polyphenol-containing solvent extract from the plant material. The clear extract was then concentrated using a rotary evaporator. The solvent was evaporated at 37°C for approximately 40 min or until extracts were almost dry and had reached a gel-like composition. Tomato-derived extracts were dissolved in 50% MeOH (v/v) at a ratio of 0.67 g (DW) of tomato powder used to 1 mL of 50% MeOH (v/v). The re-solubilized extracts were stored at -20°C for no more than one month. Anthocyanin and resveratrol content was quantified as described in Chapter 2.3.18.

Table 3i: Final concentration of tomato extract and the molar equivalents of their main active compounds.

Extract	Active compound	0.1%	0.3%	0.4%	0.5%	0.6%	0.7%	0.8%	0.9%	1%
high-del	anthocyanin	10 µM	30 µM	40 µM	50 µM	60 µM	70 µM	80 µM	90 µM	100 µM
high-pel	anthocyanin	4 µM	12 µM	16 µM	20 µM	24 µM	28 µM	32 µM	36 µM	40 µM
high-res	resveratrol	2 µM	6 µM	8 µM	10 µM	12 µM	14 µM	16 µM	18 µM	20 µM

3.2.4 Cell viability

3.2.4.1 Trypan Blue exclusion assay

After incubation, cell viability was assessed by Trypan Blue exclusion. Trypan Blue is derived from toluidine. The stain is not absorbed by viable, healthy cells but can enter damaged or dead cells, allowing for them to be counted. 20 μL of cell suspension were mixed with an equal volume of 0.4% Trypan Blue solution (Sigma). Cells were counted on a dual-chamber haemocytometer under the light microscope.

3.2.4.2 WST-1 cell metabolic activity assay

3.2.4.2.1 Assay principle

The water-soluble tetrazolium (WST)-1 assay contains 2-(4-Iodophenyl)-3-(4-nitrophenyl)-5-(2,4-disulfophenyl)-2H-tetrazolium, and is based on the reduction of water soluble, red WST-1 tetrazolium salt to water soluble, orange formazan salt a tetrazolium. Tetrazolium salts are widely used to measure spectrophotometrically the proliferation, growth, viability and chemosensitivity of cell populations. The assay principle relies on the cleavage of tetrazolium salt to tetrazolium by cellular enzymes. Growth and expansion of cells results in an increase in the overall activity of mitochondrial dehydrogenase which leads to an augmentation of formazan dye formed that correlates to the number of metabolically active cells in the sample. The reaction depends on the glycolytic production of NAD(P)H in viable cells and the concentration of orange formazan dye formed correlates to the number of metabolically active cells. The amount of formazan dye produced can be measured using a spectrophotometer with a test wavelength at 450 nm. Although the assay is described as a proliferation assay, I used it to determine the metabolic status, specifically the mitochondrial activity of the cells. The metabolic activity of the cells is related directly to their ability to grow and proliferate (application details can be found on http://www.roche-applied-science.com).

3.2.4.2.2 Wst-1 cell metabolic activity assay: Dose-dependency experiment

Human breast cancer cell lines MCF-7 and MDA-MB-231 and the normal breast epithelial cell line HMT-3522-S1 were grown as described previously (Chapter 3.2.1). MCF-7 and MDA-MB-231 cells were split and seeded into 96-well plates at 5,000 cells per well, whereas HMT-3522-S1 cells were seeded at 12,500 cells per well and cultured

in 100 µL complete medium for 24 h to allow cells to adhere. Cells were then treated for 24 h with complete medium containing various concentrations of purified compounds or tomato extracts. Purified compounds dissolved in EtOH or DMSO were diluted to a final concentration of 0.1% in the culture media. Tomato extracts dissolved in 50% MeOH (v/v) were diluted to a final concentration of 1% in the culture media. After 24 h incubation in complete medium containing the desired treatment conditions, the treatment medium was removed and replaced with 100 µL complete medium containing 10% WST-1 reagent (Roche). The samples were incubated for another 2 h at 37 ° and 5% CO_2 to allow the cells to metabolize the WST-1 reagent. The formazan dye produced was quantified by measuring the absorbance at 450 nm with a reference wavelength of 600 nm using a FLUOstar Omega multi-mode microplate reader (BMG Labtech). Absorbance data were expressed as the percentage of metabolic activity relative to the solvent-treated control.

3.2.5 Flow cytometry

Flow based cytometry or fluorescence-activated cell sorting (FACS) are techniques that allow the analysis, identification and isolation of individual cells in a fluidic channel. Addition of fluorochrome-labelled antibodies or fluorescent dyes to the cell suspension allows targeting of specific markers present in the cell population.

Flow cytometry is based on the principle of light scattering, light excitation, and emission of light from a fluorochrome molecule at a certain wavelength to create multi-parametric data from cells within the size range of 0.5 µm and 40 µm diameter. In the process of single cell analysis, cells pass individually through a highly focused laser beam by a continuous flow of a fine stream of the suspension. The light scattering or fluorescence emission intensity of individual cells labelled with fluorochromes will provide information about the cell's properties. Flow cytometers use separate fluorescence (FL-) channels that are equipped with optical filters that will block certain wavelengths while permitting others and are capable of detecting light emission at specific wavelengths. This allows for simultaneous analysis of more than one cell parameter monitored by different fluorochromes, provided that those fluorochromes emit light at different wavelengths.

3.2.5.1 Flow cytometry data analysis

Histograms represent the intensity of either scatter or fluorescence of a specific parameter per histogram. Dot plots quantify the percentages of cells with various properties. Distinct subpopulations of cells with different properties can be identified with both histograms and dot plots. In a dot plot, each cell is represented by a dot and positioned on the x and y scales according to their intensity. Scatter dot plots (x = forward scatter, y = side scatter) are often useful in assessing the overall state of the cell population. Cell debris often accumulates at the axis intersection and along the y axis. Intact cells usually form a distinct population clearly separated from cell debris and other contaminants (Figure 3.2 A) which can be selected through "gating" and studied separately for other parameters.

Fluorescein (FITC)-conjugated Annexin-V and propidium iodide (PI) are two fluorescent stains that are frequently used to different parameters of apoptosis and cell cycle. They emit light at different excitation wavelengths which requires the use of two distinct fluorescence channels (eg. FL-1 and FL-3). Quadrants allow for the separation and quantification of distinct cell subpopulations based on their light emission intensity (Figure 3.3). Annexin-V is detected by FL1 and Annexin-V positive cells scatter at the far end of the x axis, whereas PI is detected by FL-3 and PI-positive cells accumulate at the top end of the y axis (Table 3ii).

Table 3ii: Interpretation of fluorescence detection of Annexin-V/PI stained cells and the distribution of subpopulations in a gated scatter plot based the light emission intensity of a given cell.

Quadrant	Fluorescence channel	Annexin-V	Propidium Iodide	Cell stage
D--	-	negative	negative	healthy
D+-	FL1	positive	negative	early apoptotic
D++	FL-1/FL-3	positive	positive	late apoptotic
D-+	FL-3	negative	positive	necrotic

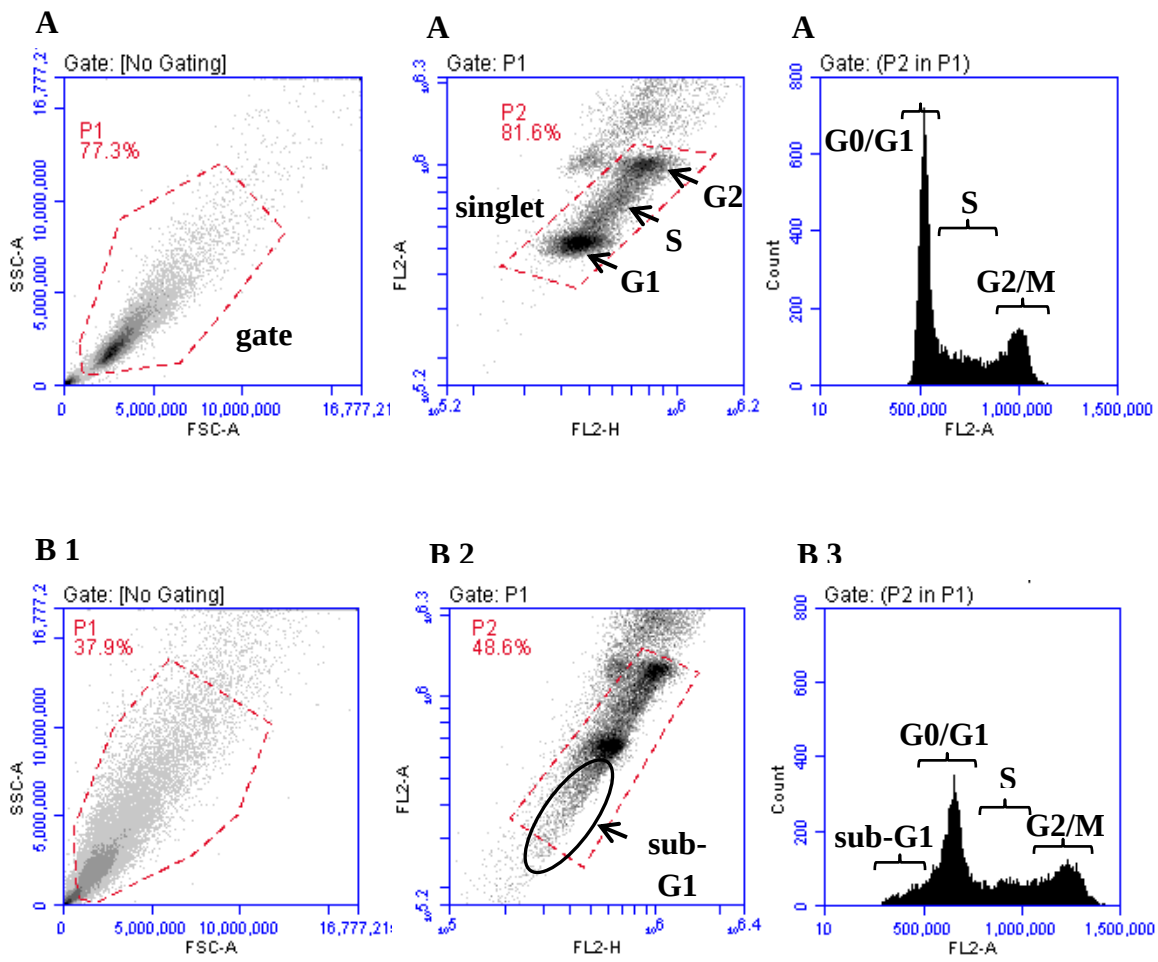

Figure 3.2: Examples of scatter plots and histograms of flow cytometric analysis of the cell cycle of (**A**) a normal cell cycle of MCF-7 cells after 24 h treatment with 1% WT tomato extract and (**B**) an altered cell cycle of MCF-7 cells in response to 24 h treatment with 1% high-pel tomato extract. (**1**) Data acquisition scatter plot demonstrating the selection of intact cells by "gating". (**2**) Scatter plot of the cell population selected through gating in (**1**) and selection of single cells through second gating. (**3**) Histogram representing the distinct cell cycle phases corresponding to the DNA content of individual cells in the population selected through gating in (**2**).

Cell cycle profiles are usually represented as histograms showing the distinct distribution of DNA content within a population of cells measuring the fluorescence intensity per individual cell (Figure 3.2 A3 and B3). Cells in G0/G1 will have one copy of the genomic DNA and therefore 1x fluorescence intensity, cells in G2/M phase of the cell cycle will have two copies of the genomic DNA and 2x fluorescence intensity. Cells in the S phase are synthesizing DNA and will accordingly have fluorescence values between the 1x and 2x. Fluorescence intensity will also double if cells are present as doublets or aggregates. Aggregates and simultaneously read events are unavoidable during the acquisition part of cell cycle analysis but must be omitted from single cells in order to maintain data fidelity. Aggregates will have a higher area to height ratio (FL2-A to FL2-H) and can be excluded from later analysis by gating the singlet population (Figure 2 A2 and B2). A cell cycle histogram representing the DNA content in single cells of a given population which is produced by plotting cell count against total cell fluorescence (FL2-A; see Figure 3.2 A3 and B3).

3.2.5.2 Cell cycle detection by Propidium Iodide

Cell cycle analysis is a method that allows the distinguishing of cells in different phases of the cell cycle. Cell cycle alterations can be the result of cell damage, including DNA damage that causes cells to pause at certain checkpoints in order to prevent the proliferation of aberrant cells. Flow cytometric analysis allows the accurate determination of whether and where drugs or xenobiotic compounds operate in the cell cycle.

PI was one of the first fluorescent dyes to be used in FACS assisted cell cycle analysis and allows for quantification of DNA content and binds in proportion to the amount of nucleic acid present in an individual cell. PI does not discriminate between DNA and RNA, making the removal of RNA prior to cell cycle analysis an essential requirement in order to maintain data fidelity. The DNA content of cells doubles as they progress from G0/G1 to G2/M phase, which is reflected in a doubling in the fluorescent signal emitted by PI-stained cells.

3.2.5.2.1 Sample preparation, data acquisition and analysis

MCF-7 and MDA-MB-231 cells were seeded into 6-well plates at 150,000 cells per well for cell cycle analysis and incubated for 24 h prior to treatment. Cells were exposed

to tomato extracts at a final concentration of 1% in the medium for 0 h, 3 h, 6 h, 12 h or 24 h. After exposure to treatment, cell medium containing detached cells was transferred to a labelled 15 mL tube. Cells that remained attached to the well were washed twice with PBS (PBS washing solution was also transferred to the labelled tube) before being trypsinised and pooled with the detached cells in the 15 mL tube. After centrifuging at 300 *g* for 5 min and washing once with PBS, cells were resuspended in 500 µM 70% EtOH (v/v) to permeabilize the cell membranes and incubated overnight in the dark at -20°C. Samples were centrifuged at 600 *g* for 5 min, EtOH was removed and cells were washed with PBS before being resuspended in 60 µL RNA-degrading solution containing 0.1% Triton X-100, RNAse A 0.5mg/mL in PBS and incubated at 37°C for 30 min. Aliquots of 3 µl of 1 mg/mL PI were added to the cell suspension and samples immediately analysed with a flow cytometer.

Data acquisition was performed with a BD Biosciences Accuri™ C6 Flow Cytometer equipped with a 488 nm laser. 10,000 events were collected in the gated population of single cells for each sample. Figure 3.2 show representative plots of PI stained cells demonstrating the gating strategies and data acquisition procedure. Cell debris was excluded from the analysis. Data acquisition and analysis was carried with BD CFlow® Software.

3.2.5.3 Apoptosis detection by Annexin-V

3.2.5.3.1 Assay principle

Apoptosis is a normal genetic process by which cells undergo a tightly regulated programme leading to controlled cell death. In apoptotic cells, the membrane phospholipid phosphatidylserine (PS) translocates from the inner to the outer membrane leaflet exposing itself to the external cellular environment. Annexin-V is a 35-36 kD phospholipid-binding protein characterized by a high affinity for PS. Annexin-V is conjugated to fluorochromes and acts as a highly sensitive probe for flow cytometry analysis of cells undergoing apoptosis. Translocation of PS precedes the loss of membrane integrity which takes place at the later stages of apoptosis. That loss of integrity results from either apoptosis or necrosis. In order to distinguish between early and late stages of the cell death, Annexin-V is used in conjunction with PI, a fluorescent molecule with a high affinity for nucleic acids. Viable cells exclude PI, whilst the

membranes of damaged or dead cells become permeable to PI. Apoptosis is a gradual process that may take hours to even days to develop; this allows for cells to be tracked over time moving from Annexin-V negative and PI negative (viable cells, with intact membranes) to Annexin-V positive and PI negative (early apoptotic cells, PS becomes exposed but cellular membranes remain impermeable) to Annexin-V positive and PI positive (late apoptotic or dying cells, PS is exposed and membrane permeable to PI). Annexin-V negative and PI positive cells are necrotic. See Table 3ii for summary of the stain combinations and their interpretations.

3.2.5.3.2 Sample preparation, data acquisition and analysis

MCF-7 and MDA-MB-231 cells were seeded into 12-well plates at 50,000 cells per well and treated with tomato extracts as described in Chapter 3.2.5.2.1. After exposure to treatment, cell medium containing detached cells was transferred to a labelled 15 mL tube. Cells attached to the well were washed twice with PBS (PBS washing solution was also transferred to the labelled tube) before being trypsinised and pooled with the detached cells in the 15 mL tube. After centrifuging at 300 *g* for 5 min and washing twice with PBS, cells were resuspended in 97.2 µL of 1x binding buffer before adding 2.5 µL of Annexin-V and 5 µL PI, which were all provided with the Annexin-V FITC assay kit (eBioscience). Samples were incubated for 10 min in the dark prior to analysis with a flow cytometer.

Data acquisition was performed as described in Chapter 3.2.5.2.1. Figure 3.3 A and B show representative scatter plots of Annexin-V/PI stained cells and demonstrate the gating strategies applied to select the intact cells in the population. Cell debris including dead cells was excluded from the apoptosis analysis.

Data acquisition was carried with BD CFlow® Software and data analysed with Kaluza® Flow Analysis Software (Beckman Coulter).

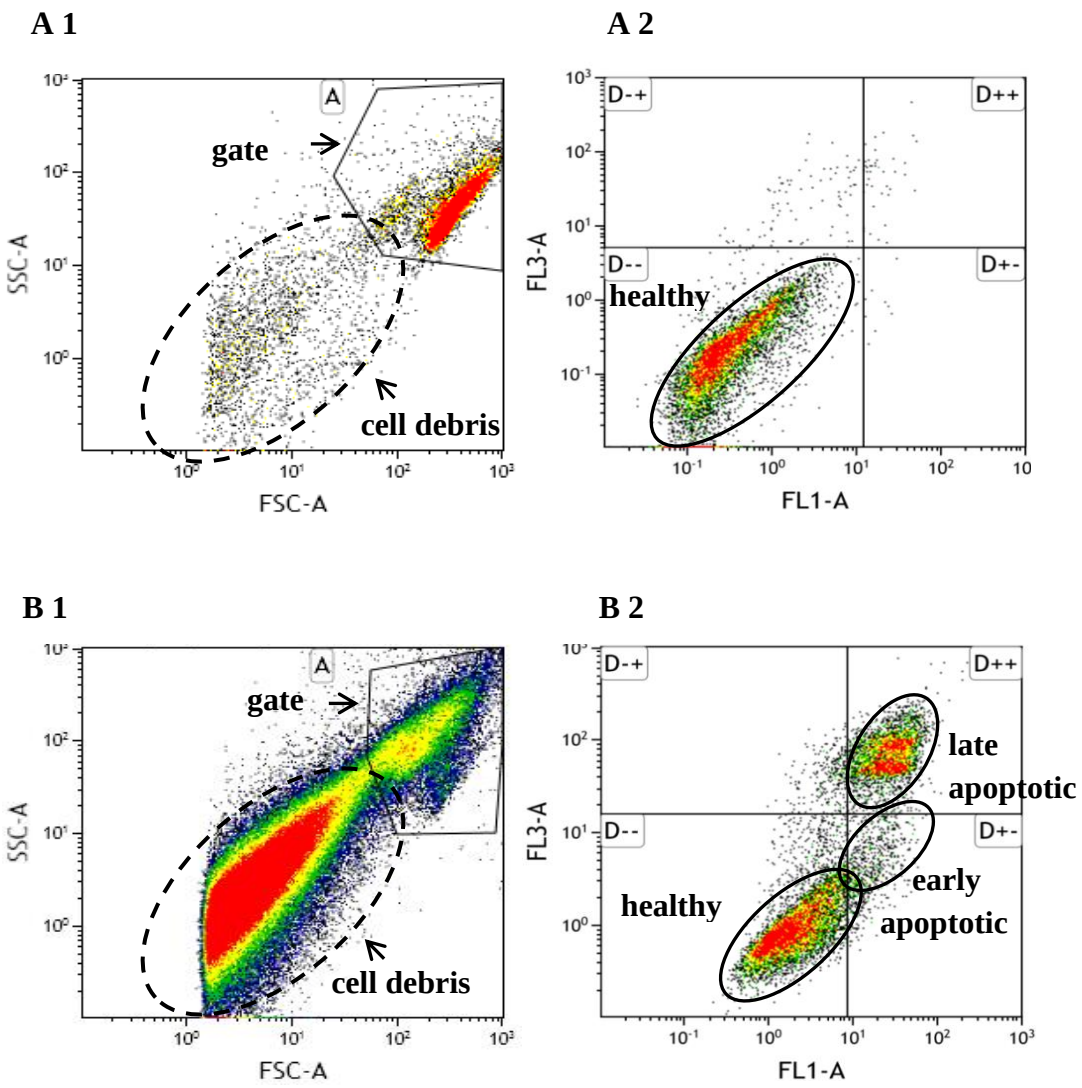

Figure 3.3: Example of scatter plots and gating strategy of the flow cytometry analysis of apoptotic stages in (**A**) healthy MCF-7 cells after 24 h treatment with 1% WT tomato extract and (**B**) apoptotic MCF-7 cells in response to 3 h treatment with 1% high-del tomato extract. (**1**) Data acquisition scatter plot demonstrating the selection of intact cells by "gating". (**2**) Scatter plot of the cell population selected through gating and identification of subpopulations through use of fluorescence channels FL-1 and FL-3.

3.2.6 Detection of protein levels by western blot analysis

3.2.6.1 Antibodies

The primary antibodies caspase-3 (#9662), caspase-7 (#9492) and caspase-9 (#9502) were purchased from Cell Signaling Technology and stored and used according to the manufacturer's instructions. Antibodies were used at a final concentration of 1:1000.
The secondary, HRP-conjugated was purchased from Cayman Chemical stored and used according to the manufacturer's instructions. The secondary antibody was used at a final concentration of 1:10000.

3.2.6.2 Preparation of protein extracts from human cells

MCF-7 and MDA-MB-231 cells were exposed to various stimuli. Cells were washed twice with ice-cold PBS and lysed with ice-cold RIPA buffer (50 mM TrisHCl pH7.4, 150 mM NaCl, 2 mM EDTA, 1% NP-40, 0.1% SDS), supplemented with protease inhibitors (complete mini protease inhibitor cocktail tablet, Roche). Samples were incubated for 20 min on ice, before pelleting the cell debris by centrifugation (20 min, 13,000 *g*, 4°C) and the supernatant protein was collected and stored at -20°C until further use.

3.2.6.3 Gels and running conditions

SDS-PAGE separation of protein samples was performed using 10% precise Tris-Glycine gels Thermo Scientific) or home-made 10% PAGE gels at 185 V in XCell SureLock™ Mini-Cell (Life Technologies) at room temperature. 30 µg of protein, previously quantified using the bicinchoninic acid assay, was mixed with 4x loading dye (Laemmli loading buffer, 250 mM Tris-HCl pH 6.8, 8% SDS, 40% Glycerol, 8% betamercaptoethanol, 0.02% bromophenol blue) and boiled for 3 min before being loaded on the gel along with a prestained, broad range protein marker (7-175 kDa; New England BioLabs).

3.2.6.4 Transfer and blotting conditions

Proteins were transferred from the gel to a nitrocellulose membrane (Whatman™, GE Healthcare). The transfer was performed at 100 V for 1 h at 4°C using the Mini Trans-Blot® Module (Bio-Rad) following the manufacturer's instructions.

3.2.6.5 Immunoblotting and development

The unspecific binding antibodies to the membrane was prevented by incubating the membrane in 20 mL of blocking solution that consisted of 5% (w/v) fat-free milk powder in TBS-T (50 mM Tris-Buffered saline pH 7.5 (TBS) and 0.1% (v/v) Tween-20 (Sigma) for a minimum of 1 h at room temperature. The membrane was then incubated the blocking solution containing the primary antibody specific for the protein of interest. Antibodies were diluted in blocking solution according to the manufacturer's recommendations. Incubation with primary antibody was performed overnight at 4°C with shaking. The next day, the primary antibody solution was removed and the membrane washed three times at room temperature with TBST before being incubated with horseradish peroxidase-conjugated (HRP), secondary antibody diluted 1:10,000 (v/v) in blocking solution, for 1-4 h at room temperature.

Membrane-bound protein bands were visualized on an ImageQuant™ LAS 500 or 4000 camera (GE healthcare) after the addition of Pierce® ECL Western Blotting Substrate (Thermo Scientific), a nonradioactive, highly sensitive luminol-based chemiluminescent substrate for the detection of HRP.

3.2.7 Bicinchoninic Acid Assay

Total protein content was quantified using the bicinchoninic acid assay (BCA) assay kit (Thermo Scientific). The assay relies on the formation of a Cu^{2+}-protein complex under alkaline conditions, followed by reduction of the Cu^{2+} to Cu^{1+}. The amount of the reduction is proportional to the amount of protein present. In alkaline conditions, BCA forms a purple complex with Cu^{1+}. The reduction of Cu^{2+} by proteins can be determined colorimetrically by measuring the at an absorbance maximum of 562 nm.

3.2.8 Statistical methods

The statistical significance was determined using Student's t-test. P-values ≤ 0.05 were considered statistically significant.

3.3 Results

3.3.1 Purified polyphenols have little effect on cell viability

The effects of exposure to resveratrol, polydatin, and rutin on MCF-7 and MDA-MB-231 cell metabolic activity were investigated. After 24 h exposure to resveratrol a significant dose-dependent reduction in cell proliferation was observed in MCF-7 but not in MDA-MB-231 cells (Figure 3.4 A). Incubation with 50 μM and 100 μM resveratrol reduced MCF-7 cell metabolism by 20 % ($p<0.05$) and 40 % ($p<0.001$), respectively, relative to the solvent-treated control (Figure 3.4 A). In contrast, resveratrol induced a metabolism-stimulating effect in MDA-MB-231 cells, increasing cell proliferation significantly in a dose-dependent manner by up to 20% after exposure to 50 μM and 100 μM resveratrol.

Plants produce a significant proportion of their resveratrol in glucosylated forms. In order to compare the biological efficacy of both trans-resveratrol and glucosylated resveratrol we performed the same experimental procedure with the commercially available resveratrol glycoside, polydatin. Polydatin treatment resulted in a decrease in metabolism of both MCF-7 and MDA-MB-231 cells (Figure 3.4 B). At 100 μM, polydatin reduced metabolic status of MCF-7 and MDA-MB-231 cells by ~15%. At the highest concentration tested, 200 μM of polydatin induced a statistically significant inhibition of metabolism of ~30% in both cell types relative to the untreated control (Figure 3.4 B). Interestingly, intermediate concentrations (50 μM) of polydatin resulted in a statistically significant increase in the metabolic status of ~10% in the MCF-7 cells.

We also investigated the inhibitory effect of rutin, a highly abundant flavonoid present in tomatoes. Rutin displayed some weak biological activity in both cell lines; at the highest treatment concentration (200 μM), rutin treatment resulted in a reduced metabolic status of MCF-7 and MDA-MB-231 cells by 10% and 15% ($p<0.05$), respectively (Figure 3.4 C).

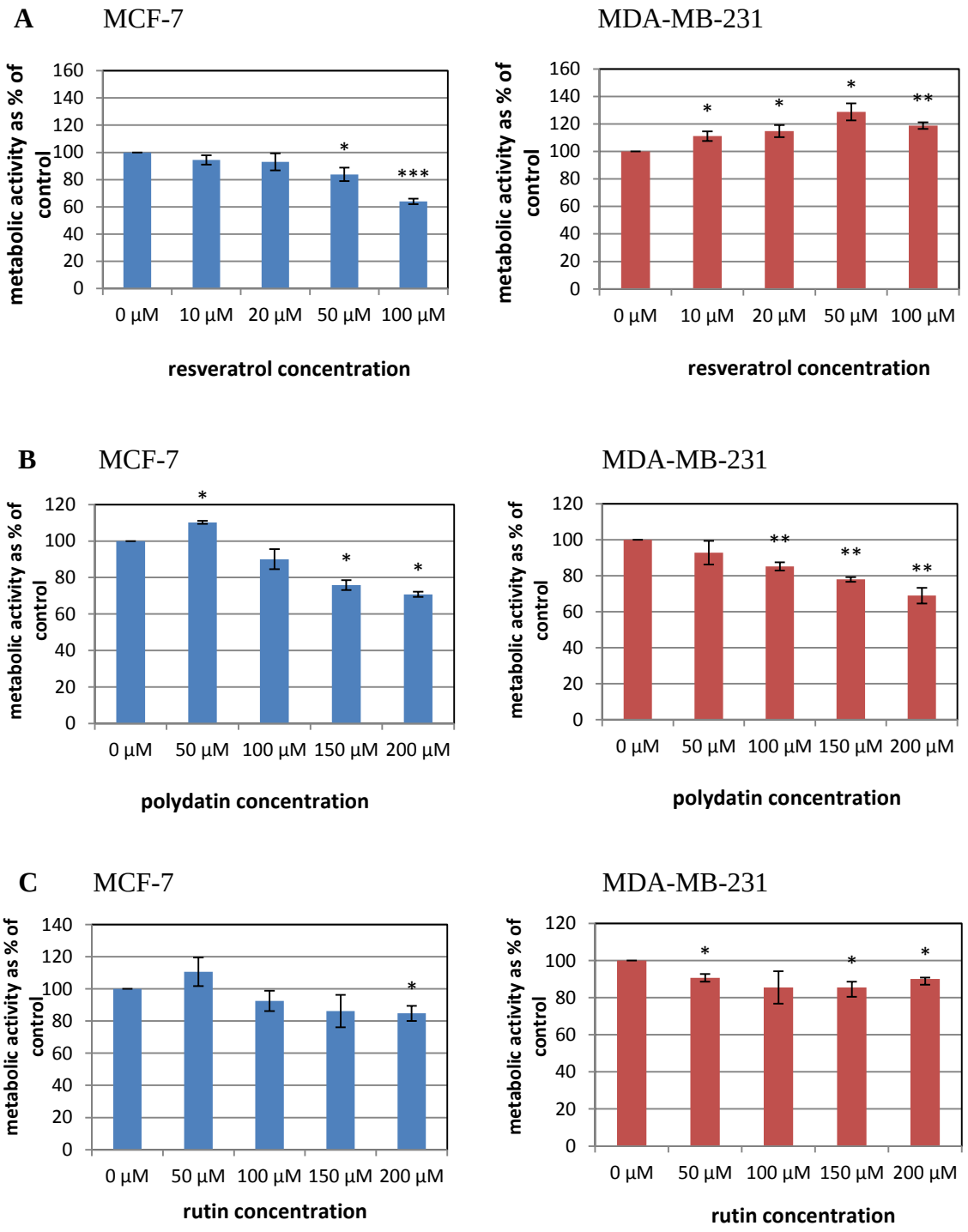

Figure 3.4: Dose response effects on the metabolic status of MCF-7 und MDA-MB-231 cells after 24 hour treatment with polyphenols. Cells were exposed to (**A**) resveratrol at 0 µM, 10 µM, 20 µM, 50 µM and 100 µM, (**B**) polydatin at 0 µM, 50 µM, 100 µM, 150 µM and 200 µM and (**C**) rutin at 0 µM, 50 µM, 100 µM, 150 µM and 200 µM. Results are expressed as a percentage of metabolic activity after treatment relative to the untreated control. Data shown as mean ± standard error (n=3 technical replicates. Experiments were performed at least twice). * $p<0.05$; ** $p<0.01$; *** $p<0.001$.

3.3.2 Commercially available and purified anthocyanins from high-del tomatoes have little effect on the cell metabolic status.

The dose-dependent effects of delphinidin-3-glucoside (del-3-glu), a commercially available anthocyanin, on the cell viability of MCF-7 and MDA-MB-231 cells were studied after 24 h incubation with complete medium containing del-3-glu at different concentrations (Figure 3.5 A). At the maximum concentration of 200 µM, no significant reduction in the metabolic status of either cell line was observed. However, at the respective concentrations 100 µM and 150 µM, the metabolic status of MCF-7 and MDA-MB-231 cells, was significantly ($p<0.05$) reduced by 10% relative to the untreated control. This reduction in cell metabolism was only transient and no longer observed at the highest treatment concentration of 200 µM, leading to the conclusion that del-3-glu does not lastingly affect the metabolic activity of both cell lines at the treatment concentrations and durations chosen.

The effects on MCF-7 and MDA-MB-231 cell survival following exposure to up to 200 µM of the two most prevalent anthocyanins delphinidin 3-(coumaroyl)-rutinoside-5-glucoside (del-3-cou-rut-5-glu) and petunidin 3-(coumaroyl)-rutinoside-5-glucoside (pet-3-cou-rut-glu) in the high-delphinidin tomato (purified as described in Chapter 2.2.18.3) were studied following the same experimental procedure as used for the analysis of del-3-glu (Figure 3.5 A). The purified anthocyanins del-3-cou-rut-5-glu and pet-3-cou-rut-5-glu exerted weak inhibitory effects on the metabolic status in a dose-dependent manner in both breast cancer cell lines.

In response to 24 h treatment with del-3-cou-rut-5-glu, both MCF-7 and MDA-MB-231 showed a ~ 10% decrease in cell metabolic status at the lowest concentration tested (50 µM). After treatment with 200 µM of the compound, metabolic activity was further decreased by 20% and 10% in MCF-7 and MDA-MB-231 cells, respectively (Figure 3.5 B). These data indicate that del-3-cou-rut-5-glu exerts its cytotoxic effects in a dose-dependent manner but administration of relatively high molar concentrations is required to reduce metabolic status significantly.

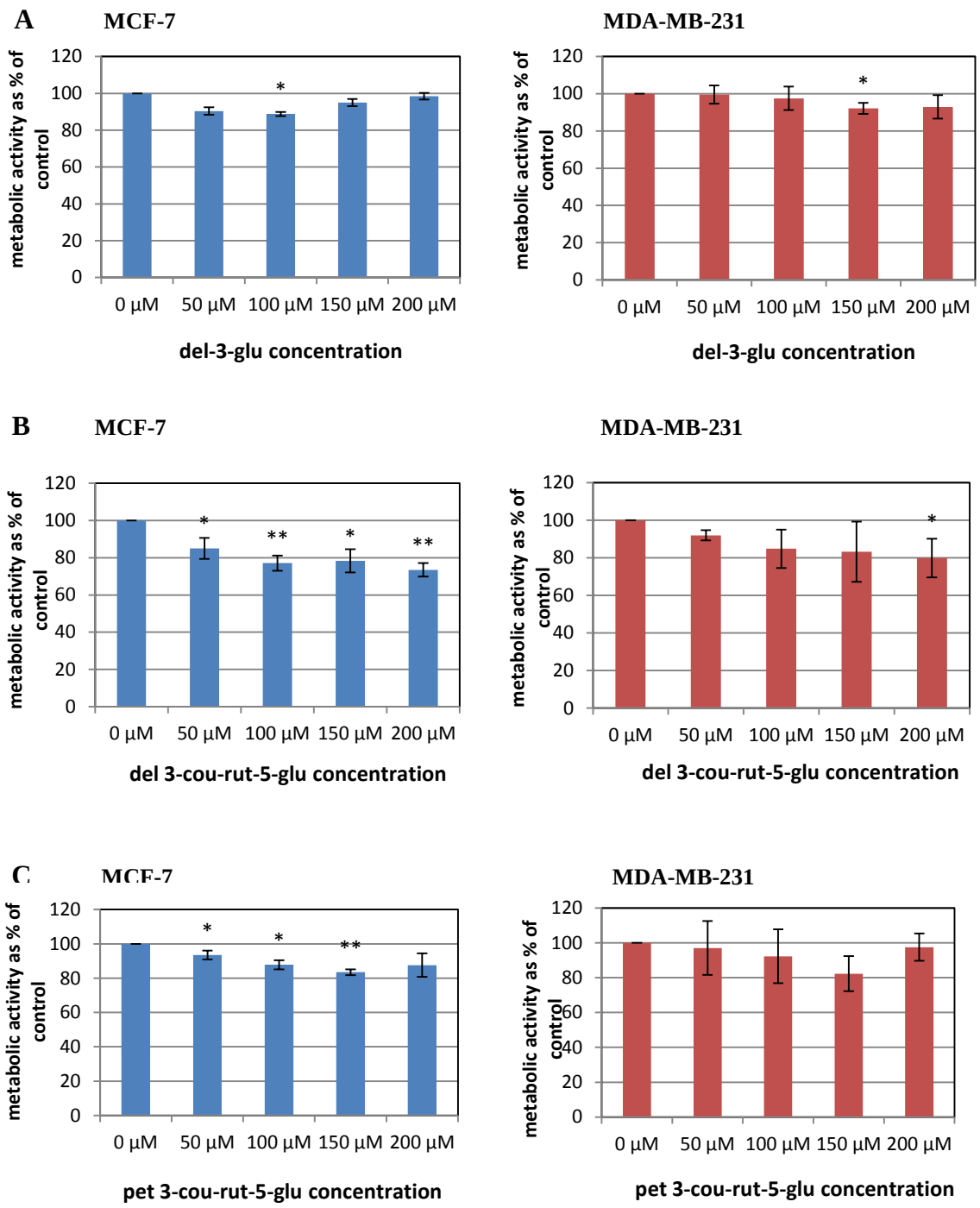

Figure 3.5: Dose response effects on the metabolic status of MCF-7 and MDA-MB-231 cells after 24 hour anthocyanin treatment at 0 µM, 50 µM, 100 µM, 150 µM and 200 µM. Cells were exposed to (**A**) delphinidin-3-glucoside, (**B**) delphinidin 3-(coumaroyl)-rutinoside-5-glucoside and (**C**) petunidin 3-(coumaroyl)-rutinoside-5-glucoside. Results are expressed as a percentage of metabolic activity after treatment relative to the untreated control. Data shown as mean ± standard error (n=3 technical replicates. Experiments were performed at least twice).

* $p<0.05$; ** $p<0.01$.

The second most prevalent anthocyanin in the high-delphinidin tomatoes was pet-3-cou-rut-5-glu. Exposure to purified pet-3-cou-rut-5-glu significantly reduced cell metabolic status of MCF-7 cells by approximately 20% after 24 h treatment with 150 µM ($P<0.01$; Figure 3.5 C). At 200 µM, cell metabolic activity was only 10% reduced (statistically not significant) relative to the untreated control, suggesting that the statistically significant pet-3-cou-rut-5-glu-induced reductions in the cell viability at concentrations lower than 200 µM may have been a result of biological variability rather than lasting growth-inhibitory activity. No statistically significant effects on the metabolic activity of MDA-MB-231 cells were observed as a result of pet-3-cou-rut-5-glu treatment (Figure 3.5 C).

3.3.3 Anthocyanin and high-resveratrol tomato extracts reduce the metabolic activity of breast cancer cells

The dose-dependence of tomato extract effects on the metabolic activity of MCF-7 and MDA-MB-231 breast cancer cells was investigated following the cell culture and metabolic activity assay procedures outlined in chapters 3.2.1.2 to 3.2.1.4. Cells were exposed to different concentrations of various tomato extracts for 24 h before measuring their metabolic activity using Roche's WST-1 cell assay.

No cytotoxic effects on MCF-7 or MDA-MB-231 cells were observed in response to incubation with WT tomato extracts (Figure 3.6 A). On the contrary, the metabolic activity of both breast cancer cell lines increased in a dose-dependent manner in response to increasing WT tomato extract supplementation. At the highest WT tomato extract concentration I observed a statistically significant 20% increase ($p<0.05$) in metabolic status of both cell lines compared to the untreated control.

The dose-dependent effects of high-resveratrol (high-res) tomato extract on the metabolic activity of breast cancer cells were tested. High-res extract dramatically reduced cell metabolic status of MCF-7 and MDA-MB-231 cells (Figure 3.6 B). Cell metabolic activity started to decrease after exposure to 0.4% of extract in the medium. After incubation with 0.8% extract, which contained approximately 16 µM of total resveratrol (Table 3i), the percentage of viable MCF-7 and MDA-MB-231 cells was reduced to almost 0% ($p<0.001$, Figure 3.6 B).

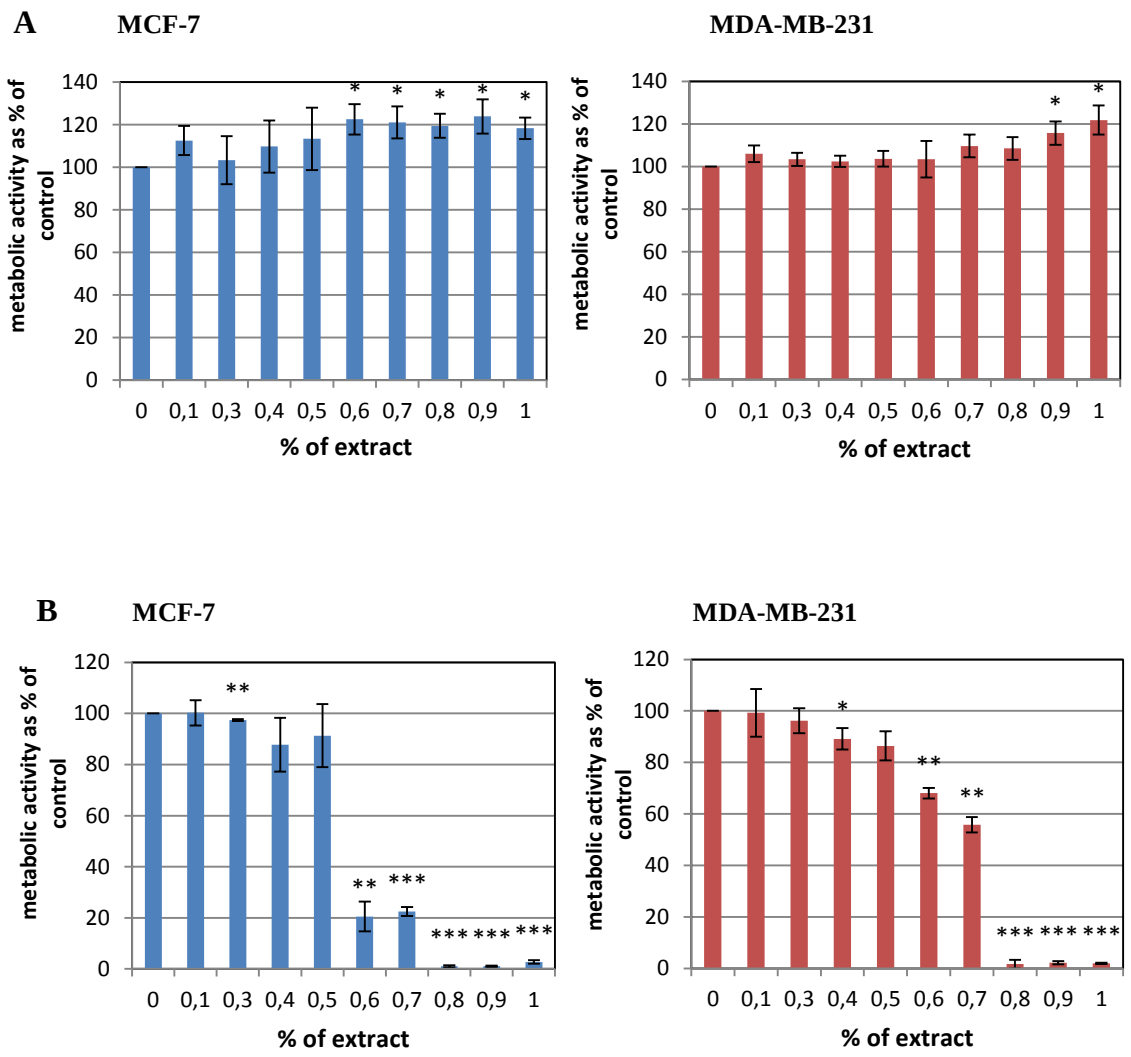

Figure 3.6: Dose response curves for 24 hour treatment of MCF-7 und MDA-MB-231 cells with (**A**) WT tomato extract and (**B**) high-resveratrol tomato extract. Cells were exposed to extract concentrations ranging from 0.1% to 1% of the total medium and results are expressed as a percentage of metabolic activity after treatment relative to the untreated control. Data shown as mean ± standard error (n=3 technical replicates. Experiments were performed at least twice). * $p<0.05$; ** $p<0.01$; *** $p<0.001$.

A dramatic reduction in breast cancer cell metabolic activity was also observed in response to treatment with high-delphinidin (high-del) tomato extracts (Figure 3.7 A). In MCF-7 cells, high-del tomato extract had a statistically non-significant stimulatory effect up to an extract concentration of 0.6%, stimulating cell metabolic activity by up to 30% compared to the untreated control. However, metabolic activity of MCF-7 cells was strongly inhibited once high-del extract concentrations surpassed 0.6% in the medium. At 1% high-del extract concentration in the medium, which contained approximately 100 µM of total trihydroxylated anthocyanins (Table 3i), metabolic activity of MCF-7 cells was significantly reduced to ~5% ($p<0.001$) relative to the activity of the untreated control (Figure 3.7 A).

In MDA-MB-231 cells, a strong correlation between high-del extract concentration and cell metabolic activity was observed (Figure 3.7 A). High-del tomato extract did not stimulate cell growth of MDA-MB-231 cells at low treatment doses but resulted in a gradual concentration-dependent decrease in cell viability. Extract concentrations of 0.8% and higher led to an almost complete inhibition of metabolic activity ($p<0.001$; Figure 3.7 A).

Similarly, the dose-dependence of exposure to extract from the high-pelargonidin (high-pel) tomatoes by MCF-7 and MDA-MB-231 cells was investigated (Figure 3.7 B). The exposure to high-pel extract concentrations of 0.9 % and 1 %, which contained approximately 36 and 40 µM of mono- and dihydroxylated anthocyanins (Table 3i), resulted in a significant reduction ($P<0.05$) of 30 % and 40 % in the metabolic activity of MCF-7 cells.

MDA-MB-21 cell activity was significantly reduced by 20% in response to treatment with 0.5% high-pel extract ($p<0.05$) and cell metabolic activity continued to decrease with increasing concentrations of high-pel extract. After 24 h incubation with 1% extract, metabolic activity of MDA-MB-231 cells had been reduced to only 30% compared to the of the solvent-treated control (Figure 3.7 B).

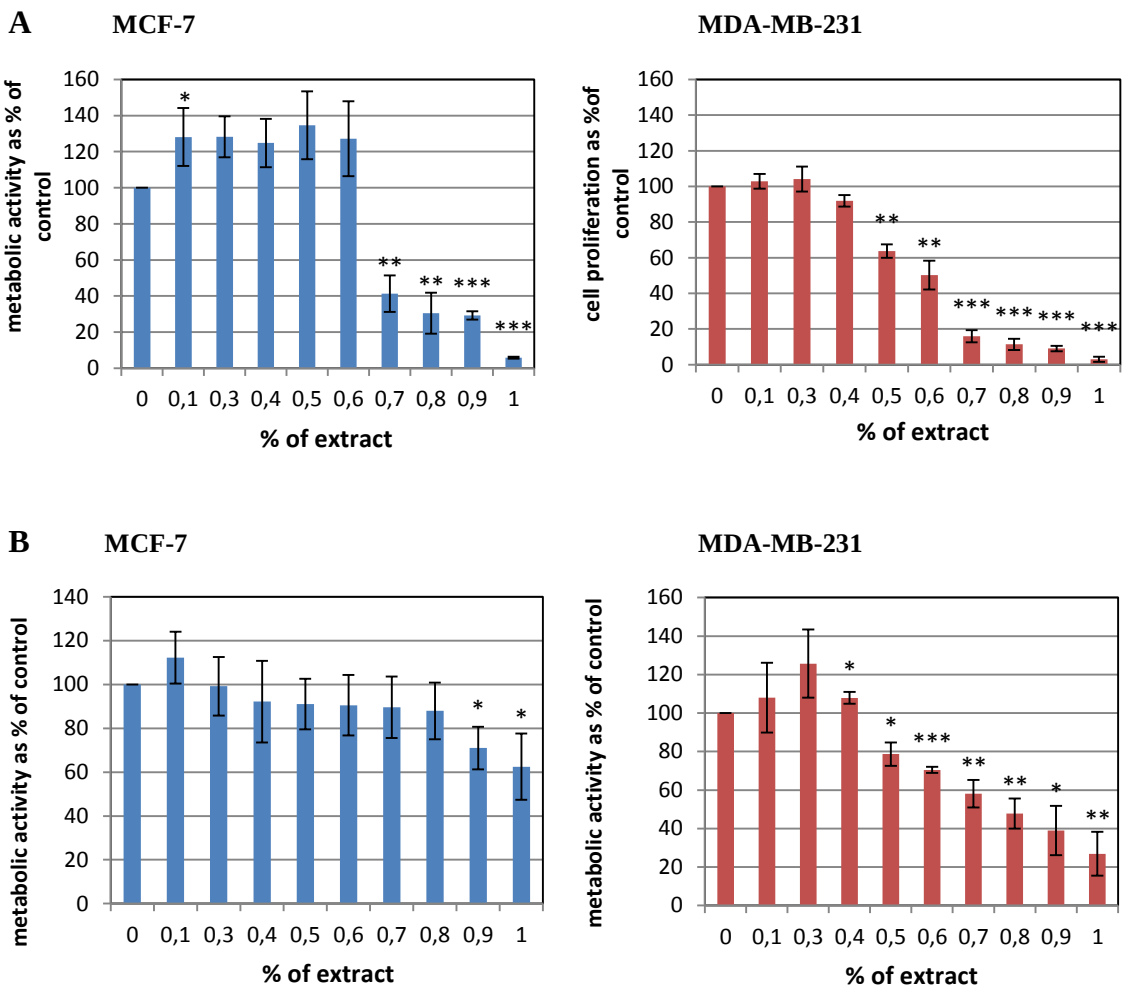

Figure 3.7: Dose response curves for 24 hour treatment of MCF-7 und MDA-MB-231 cells with (**A**) high-delphinidin tomato extract, and (**B**) high-pelargonidin tomato extract. Cells were exposed to extract concentrations ranging from 0.1% to 1% of the total medium and results are expressed as a percentage of metabolic activity after treatment relative to the untreated control. Data shown as mean ± standard error (n=3 technical replicates. Experiments were performed at least twice). * $p<0.05$; ** $p<0.01$; *** $p<0.001$.

3.3.4 Effects of WT and high-del extracts on the viability of normal HMT-3522-S1 breast cells

HMT-3522-S1 cells are derived from a benign breast tumour but are considered a "normal" breast epithelial cell line. They are sometimes used in comparative studies investigating the differential behaviour of normal and cancerous cells (Bissell et al., 2002, Kenny et al., 2007). Dose-dependency effects of either WT or high-del tomato extracts on the metabolic activity of HMT-3522-S1 cells in response to 24 h exposure were investigated (Figure 3.8). WT tomato extract induced a stimulatory effect of up to 20% which is in agreement with the observations made in MCF-7 and MDA-MB-231 cells (Figure 3.6 A).

Exposure to high-del extract reduced metabolic activity of HMT-3522-S1 cells in a dose-dependent manner, resulting in a 70% reduction in cell proliferation at the highest concentration tested (1% extract).

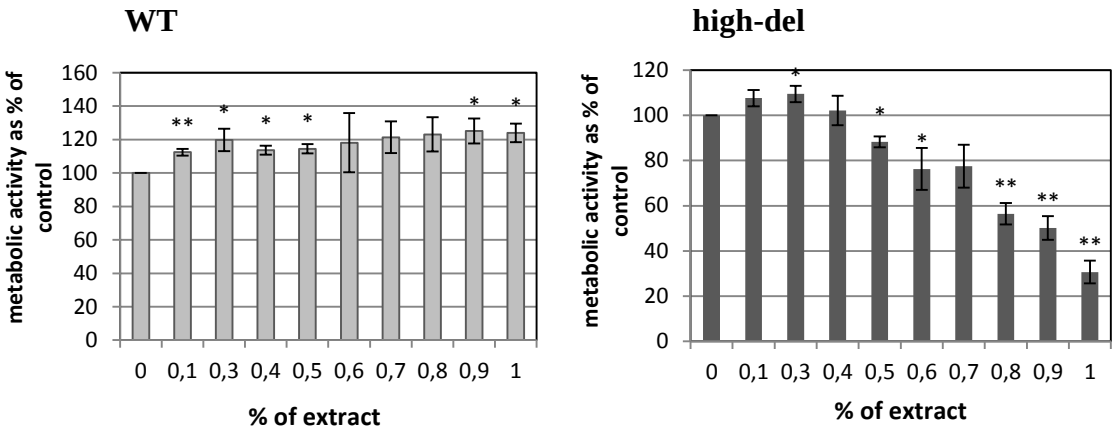

Figure 3.8: Dose response curves for 24 hour treatment of HMT-3522-S1 cells with WT tomato extract or high-delphinidin tomato extract. Cells were exposed to extract concentrations ranging from 0.1% to 1% of the total medium and results are expressed as a percentage of metabolic activity after treatment relative to the untreated control. Data shown as mean ± standard error (n=3 technical replicates. Experiments were performed at least twice). * $p<0.05$; ** $p<0.01$; *** $p<0.001$.

3.3.5 Comparison of the biological efficacy of delphinidin and pelargonidin in food matrix background

In order to determine whether delphinidins and pelargonidins differ in their biological efficacy, a comparative study using delphinidin and pelargonidin tomato extracts was conducted. The high-del tomato extracts contained ~2.5 times more anthocyanins than the high-pel tomato line and their biological efficacy not directly comparable with one another. In order to compare directly the biological effects of delphinidins and pelargonidins, the high-del tomato extracts were diluted 2.5 times with WT tomato extract to achieve an equimolar anthocyanin concentration (40 µM) comparable to that present in the high-pel tomato extracts. Diluted high-del extracts equally reduced metabolic activity of MCF-7 ($p<0.05$) and MDA-MB-231 ($p<0.01$) cells by 40% after 24 h exposure to the highest extract concentration of 1% (Figure 3.9 B). There was no notable difference between the two cell lines in their response to high-del treatment.

MCF-7 and MDA-MB-231 cells responded differently to pelargonidin-containing high-pel extracts (Figure 3.9 A). At the highest concentration tested, 1% of high-pel extract which contained 40 µM of anthocyanins, inhibited the metabolic activity of MCF-7 cells by 40% ($p<0.01$) and of MDA-MB-231 cells by 70% ($p<0.01$). Diluted high-del and high-pel extracts, each containing 40 µM of delphinidins or pelargonidins, induced an equal inhibitory effect in MCF-7 cells, reducing their metabolic activity by 40% (Figure 3.9 A and B). In contrast, high-pel tomato extract was more effective than diluted high-del extract in reducing the metabolic activity of MDA-MB-231 cells (Figure 3.9 A and B). 1% of high-pel extract reduced MDA-MB-231 cell metabolic activity by 70% compared to only 40% after treatment with 1% high-del tomato extract, indicating that MDA-MB-231 cells are more sensitive to pelargonidins than to delphinidins.

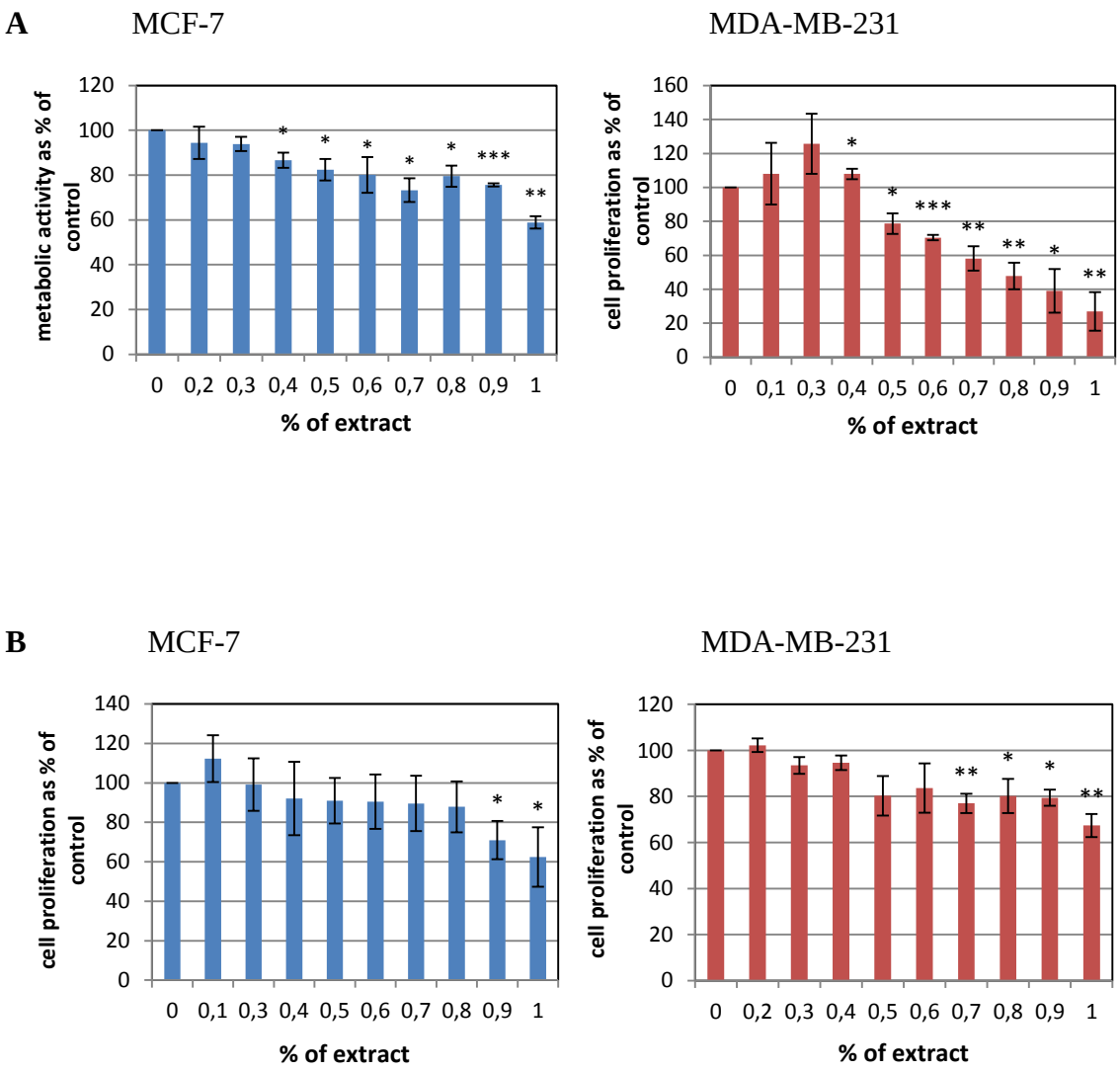

Figure 3.9: Comparative study of the 24 hour exposure effects of (**A**) high-pelargonidin and (**B**) high-delphinidin tomato extracts on the metabolic activity of MCF-7 und MDA-MB-231 cells. High-delphinidin tomato extract was diluted to the equimolar concentration of anthocyanins found in the high-pelargonidin tomato extract. Cells were exposed to extract concentrations ranging from 0.1% to 1% of the total medium and results are expressed as a percentage of metabolic activity after treatment relative to the untreated control. Data shown as mean ± standard error (n=3 technical replicates. Experiments were performed at least twice). * $p<0.05$; ** $p<0.01$; *** $p<0.001$.

3.3.6 Alterations to the cell cycle after exposure to tomato extracts

The cell cycle is a central component of cell proliferation and division in which DNA is replicated, divided and passed on to daughter cells. Many chemotherapeutic agents target the cell cycle by interfering with key genes that participate in and control cell cycle checkpoints and which are often targets of genetic alterations in cancer.

The effects of high-anthocyanin tomato extracts on the cell cycle of the breast cancer cell lines were measured after exposure to 1% tomato extracts between 3 h and 24 h. The 24 h exposure to 1% WT tomato extract had no effect on the distribution of cells in the cell cycle (Figure 3.10 A). This result confirmed the findings of the metabolic status assays where WT tomato extract did not interfere with the survival and growth of MCF-7 and MDA-MB-231 cells.

In contrast, short-term exposure (3 h and 6 h) to 1% high-del extract resulted in a dramatic alteration of the cell cycle profile of both cell lines (Figure 3.10 A). 3 h exposure to high-del extract reduced the MCF-7 cell population in G0/G1 significantly and resulted in an increased population in the S and G2 phases. After 6 h treatment, the cell cycle of high-del extract treated MCF-7 cells was severely disturbed; a sub-G1 population, indicative of highly apoptotic cells, had formed and the populations in the G1, S and G2 phases were significantly decreased. In the 6 h treatment, cell debris accounted for approximately 90% of the cell sample, indicative of the severely cytotoxic effects of high-del. No cell cycle data could be recorded beyond the 6 h time point as no intact cells remained in the sample.

In MDA-MB-231 cells, there was also a significant high-del extract-induced increase in the cells in the G1 population and also led to the formation of a sub-G1 peak, representative of late apoptotic cells (Figure 3.10 A). As a result of the severe cytotoxicity of high-del extracts no more cell cycle data could be collected beyond the 6 h time point due to the absence of sufficient intact cells to generate reliable data. The amount of damaged cells and cell debris increased dramatically with exposure duration to high-anthocyanin extracts and the proportions of cell debris were comparable to those reported in Table 3iii for the Annexin-V/PI apoptosis assay.

Breast cancer cells were also exposed to 1% high-pel extract for 3 h to 24 h (Figure 3.10 B). A reduction in the cell population in the G0/G1 phased was observed in both MCF-7

and MDA-MB-231 after 6 h and was further reduced in a time-dependent manner until the 24 h time point. A sub-G1 population started to form after an incubation period of 12 h in the MCF-7 cells and after 24 h in the MDA-MB-231 cells. At the 24 h time point, the number of cells in the G0/G1 phase had decreased significantly with a simultaneous increase in the G2/M population (Figure 3.10 B).

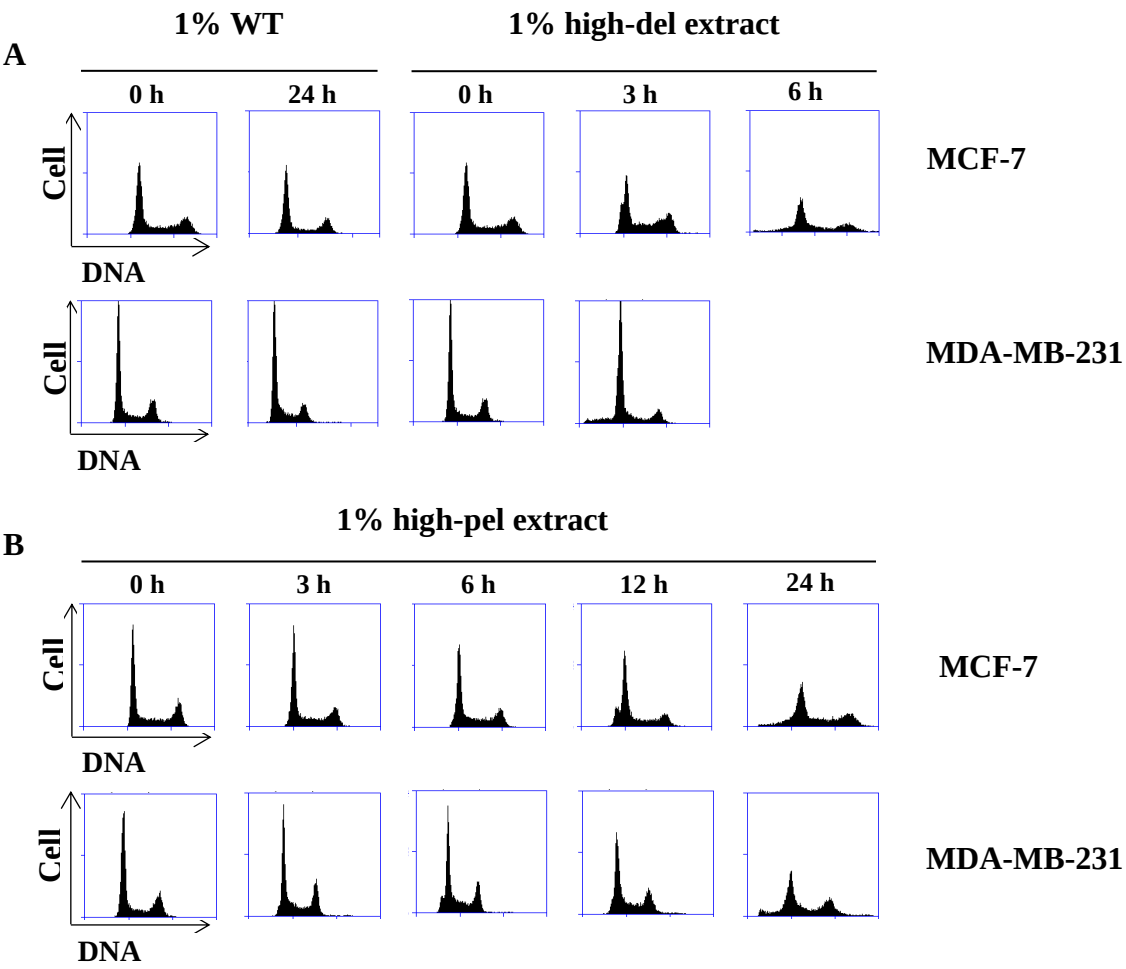

Figure 3.10: Effect of anthocyanin tomato extracts on the distribution of cells in different phases of cell cycle in MCF-7 and MDA-MB-231 cells. The cells were treated with either (**A**) WT tomato extract for 0h and 24 h or high-delphinidin tomato extract for 0 h, 3 h and 6 h, or (**B**) high-pelargonidin tomato extract for 0 h, 3 h, 6 h, 12 h, 24 h, before being collected and stained with PI. Following the FACS analysis, cellular DNA histograms were further analysed by BD CFlow® software. The data are a representative example for duplicate tests.

3.3.7 Time-dependent induction of apoptosis after exposure to high-polyphenol tomato extracts

3.3.7.1 Exposure to extracts of WT tomatoes did not induce apoptosis

The time-dependent effects of WT tomato extracts on apoptosis of MCF-7 and MDA-MB-231 cells after exposure to 1% extract were investigated using Annexin-V/PI staining and FACS analysis. WT tomato extract did not induce apoptosis in either cell line confirming the previous observations made in the metabolic status assays (Figure 3.6 A) that WT tomato extracts do not exert cytotoxic effects on the cell lines. A small, yet statistically significant increase in healthy cells compared to the solvent-treated control was observed in both MCF-7 and MDA-MB-231 cells in response to prolonged exposure to WT tomato extract (Table 3iii A). The amount of cell debris detected in WT extract-treated cell samples was negligible and hence not shown in Table 3iii A.

3.3.7.2 Dependence of induction of apoptosis by high-pel extract on the length of exposure

MCF-7 and MDA-MB-231 cells were treated with 1% high-pel tomato extract for a maximum duration of 24 h to investigate the extract-induced time-dependent effects on apoptosis. High-pel extracts exerted pro-apoptotic effects on MCF-7 and MDA-MB-231 cells in a time-dependent manner, gradually reducing the proportion of healthy cells as they shifted quickly into the late apoptotic stage (Table 3iii B). In the MCF-7 cell population, the effects were most significant after a 24 h exposure when more than 80% ($p<0.001$) of the cells had entered late apoptosis and less than 10% of cells were healthy. A similar, yet less dramatic trend was observed in MDA-MB-231 which responded to increased high-pel exposure with a gradual transition into apoptosis and necrosis. The apoptotic response of MDA-MB-231 was most acute after 24 h treatment exposure where 50% and ~20% of the cell population were undergoing apoptosis and necrosis, respectively (Table 3iii B). The amount of cell debris, representative of severely damaged cells that have been excluded from the apoptosis analysis, increased dramatically with extract exposure times to 88.4% for MCF-7 cells and 91.7% for MDA-MB-231 cells after 24 h exposure.

Table 3iii: Time-dependent effect of different tomato extracts on the apoptosis of MCF and MDA-MB-231 cells. Cells were treated for 0 h, 3 h, 6 h, 9 h, 12 h, and 24 h with 1% extract of (**A**) WT, (**B**) high-pelargonidin and (**C**) high-delphinidin tomatoes before being collected and stained with Annexin-V and PI. Following the FACS analysis and data were further analysed with BD Kaluza software. No cell debris was detected (not applicable; N/A). Results are expressed as the percentage of the cell population in each state. Data shown as mean ± standard error. * $p<0.05$; ** $p<0.01$; *** $p<0.001$.

A MCF-7

extract	duration	Healthy	early apoptotic	late apoptotic	necrotic	cell debris in %
wt	0h	93.4	0.6	1.1	4.9	N/A
wt	3h	95.9	1.4	1.7	**1.1****	N/A
wt	6h	97.0	0.8	0.9	**1.3*****	N/A
wt	9h	96.5	0.8	0.6	2.1	N/A
wt	12h	**96.9***	0.9	1.5	**0.7****	N/A
wt	24h	**97.9***	0.8	0.8	**0.5****	N/A

MDA-MB-231

extract	duration	Healthy	early apoptotic	late apoptotic	necrotic	cell debris in %
wt	0h	94.7	2.3	0.1	2.9	N/A
wt	3h	**99.1****	**0.3****	0.5	**0.1***	N/A
wt	6h	**98.8****	**0.6***	0.3	**0.3***	N/A
wt	9h	**99.0****	**0.5****	0.3	**0.3***	N/A
wt	12h	**98.9****	**0.4****	**0.5****	**0.2***	N/A
wt	24h	95.6	2.7	0.9	**0.9***	N/A

B MCF-7

extract	duration	healthy	early apoptotic	late apoptotic	necrotic	cell debris in %
high-pel	0h	96.0	2.2	1.1	0.7	11.8
high-pel	3h	90.5	0.9**	3.4	5.2	82.7
high-pel	6h	86.4	2.0	8.9	2.8	88.6
high-pel	9h	73.9	5.3	16.2	4.6	85.2
high-pel	12h	68.2*	2.0	22.3*	7.6	84.7
high-pel	24h	9.3***	7.5**	81.2**	1.9	88.4

MDA-MB-231

extract	duration	healthy	early apoptotic	late apoptotic	necrotic	cell debris in %
high-pel	0h	95.4	0.8	3.0	0.9	15.1
high-pel	3h	90.0	5.4	3.5	1.1	75.2
high-pel	6h	83.2*	8.8*	6.2	1.9	87.5
high-pel	9h	71.5*	5.0	20.6*	3.0	82.4
high-pel	12h	62.4*	5.2**	30.9*	1.6	76.0
high-pel	24h	27.6***	3.8*	49.5**	19.1**	91.7

C MCF-7

extract	duration	healthy	early apoptotic	late apoptotic	necrotic	cell debris in %
high-del	0h	89.6	3.0	5.4	2.0	18.3
high-del	3h	56.2	5.4	29.6	8.8**	81.8
high-del	6h	1.9***	25.6***	72.5***	0.0**	93.0
high-del	9h	3.8**	21.3***	75.0**	0.0**	98.7
high-del	12h	0.6***	10.6**	88.7***	0.1**	93.3
high-del	24h	0.7***	8.9	90.4**	0.0**	98.0

MDA-MB-231

extract	duration	healthy	early apoptotic	late apoptotic	necrotic	cell debris in %
high-del	0h	94.7	4.8	1.7	0.2	17.9
high-del	3h	23.0***	16.5*	55.3***	5.3*	87.5
high-del	6h	2.5***	25.9**	71.5***	0.1	94.7
high-del	9h	1.4***	24.2*	74.4*	0.0	92.8
high-del	12h	1.2***	18.1	80.7*	0.0	88.8
high-del	24h	0.7***	6.5	92.8***	0.0	96.6

3.3.7.3 Dependence of induction of apoptosis by high-del extract on the length of exposure

The cell metabolic activity assays and cell cycle analysis demonstrated that high-del tomatoes had the highest cytotoxic effects compared to the other anthocyanin tomatoes. A significant induction of apoptosis in both breast cancer cell lines was observed after as little as 3 h of incubation with medium supplemented with 1% high-del extract (Table 3iii C). MDA-MB-231 responded more quickly to high-del treatment than MCF-7 cells; at the 3 h time point less than 25% ($p<0.001$) of MDA-MB-231 cells were healthy compared to more than 50% ($p<0.05$) of MCF-7 cells. However, after 6 h exposure there was no difference in the apoptotic response between the two cell lines. After 6 h of treatment ~25% of MCF-7 and MDA-MB-231 cells were undergoing early apoptosis and almost 75% of cells had reached a late apoptotic stage. The percentage of cells undergoing cell death was further increased with prolonged incubation periods, and after the maximum exposure period of 24 h, more than 90% of cells were in late apoptosis and the remaining cells in the early stages of apoptosis (Table 3iii C). The amount of cell debris, representative of severely damaged or dead cells that were excluded from the apoptosis analysis, increased dramatically with extract exposure times.

3.3.8 Anthocyanin-rich tomato extracts trigger activation of apoptotic proteins

Levels of select proteins involved in the activation or execution of apoptosis in mammalian cells were assayed by western blot. Members of the caspase family are activated by proapoptotic signals and play a crucial role in the activation of the apoptotic mechanism. Caspase-3, caspase-7 and caspase-9 were selected to shed further light on the possible mechanisms by which the high-anthocyanin lines induce their proapoptotic effects.

MCF-7 cells are known to have an exon mutation in the *Casp-3* gene resulting in the loss of function and expression of caspase-3 in these cells. Staurosporine, a powerful and reliable inducer of apoptosis, was used a positive control for induction of apoptosis. Cells were exposed to 10 µM of staurosporine for 9 h, before collecting protein for western blot analysis. Untreated cells were used as a negative control.

3.3.8.1 Caspase-3 is not activated by exposure to high-anthocyanin tomato extract treatment

Alterations to the expression of caspase-3 in MCF-7 and MDA-MB-231 cells after exposure to tomato extracts for different durations were investigated at the protein level by western blot. MCF-7 cells did not show any expression of caspase-3 in response to any treatment, which is in agreement with previous reports of the total absence of caspase-3 expression in MCF-7 due to an exon mutation in *Casp-3*.

In MDA-MB-231 cells, caspase-3 expression in response to anthocyanin-enriched tomato extracts was measured after 0 h, 3 h, 6 h, 9 h, 12 h and 24 h. Neither treatment with the positive control staurosporine, nor exposure to any of the anthocyanin tomato extracts resulted in activation (cleavage) of caspase-3. Figure 3.11 shows the inactive (uncleaved) caspase-3 expression in MDA-MB-231 cells in response to different exposure times to high-del treatment.

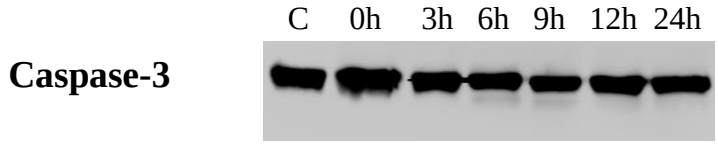

Figure 3.11: Caspase-3 protein levels in MDA-MD-231 cells after a 9 h exposure to 10 µM of staurosporine (positive control; C) or treatment periods of 0 h, 3 h, 6 h, 9 h, 12 h and 24 h with 1% high-del tomato extract.

3.3.8.2 High-del tomato extract activates caspases-7 and -9

Activation of caspase-7 and -9 was induced in both MCF-7 and MDA-MB-231 cells after treatment with high-del tomato extract (Figure 3.12). The 3 h exposure to high-del extract was sufficient to induce cleavage of caspase-7 in MCF-7 cells. No change in the MCF-7 caspase-7 expression signal was observed in response to different treatment exposure times (Figure 3.12 A). In the negative control (0 h) caspase-7 was only present in its inactive, uncleaved form, whilst 9 h exposure to 10 µM staurosporine (positive control; C) also resulted in activation of caspase-7. However, there may have been a problem with the loading of the untreated control as protein bands are severely distorted. Short term (3 h and 6 h) exposure to high-del extract did not activate caspase-

7 in MDA-MB-231 cells. However, there was activation of caspase-7 after prolonged exposure of 9 h and 12 h to high-del extract in MDA-MB-231 cells (Figure 3.12 B). These results indicate that the activation of caspase-7 by high-del treatment is exposure time-dependent in MDA-MB-231 but not in MCF-7.

Activation of the initiator caspase-9 after exposure to high-del extract was observed in both MCF-7 (Figure 3.12 A) and MDA-MB-231 (Figure 3.13 B). In MCF-7, cleavage of caspase-9 was only detectable after the treatment exposure of 24 h, whilst in MDA-MB-231 cells cleavage of caspase-9 was observed at all exposure times (3 h to 24 h) and no significant changes in the levels of active, cleaved caspase-9 were observed in response to increased exposure times.

3.3.8.3 High-pel extract activates caspase-7 and caspase-9

A time-independent activation of caspase-7 was observed in high-pel treated MCF-7 cells (Figure 3.14 A). A weak band corresponding to cleaved caspase-7 was present in the 3 h to 24 h treated cells but absent in the untreated (0 h) samples, indicating the ability of high-pel tomato extract to induce activation of caspase-7.

High-pel tomato extract also induced activation of caspase-9 in both MCF-7 and MDA-MB-231 cells through cleavage of procaspase-9 (Figure 3. 15). High-pel-induced activation of caspase-9 was independent of the duration of extract exposure and appeared after only 3 h and persisted up to the final 24 h time point.

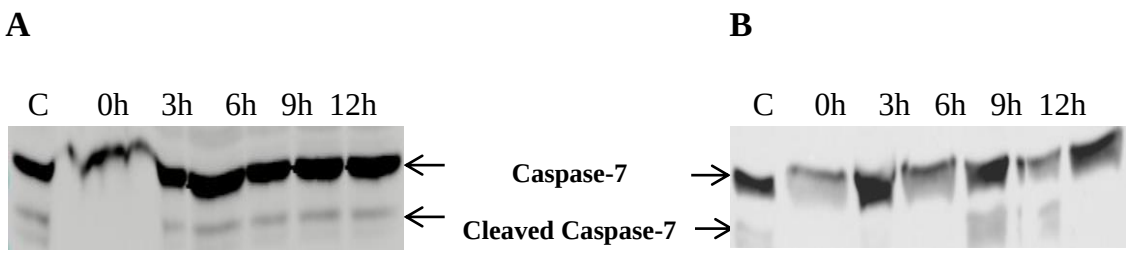

Figure 3.12: Caspase-7 protein levels in (**A**) MCF-7 and (**B**) MDA-MD-231 cells after a 9 h exposure to 10 µM of staurosporine (positive control; C) or treatment periods of 0 h, 3 h, 6 h, 9 h, 12 h and 24 h with 1% high-del tomato extract.

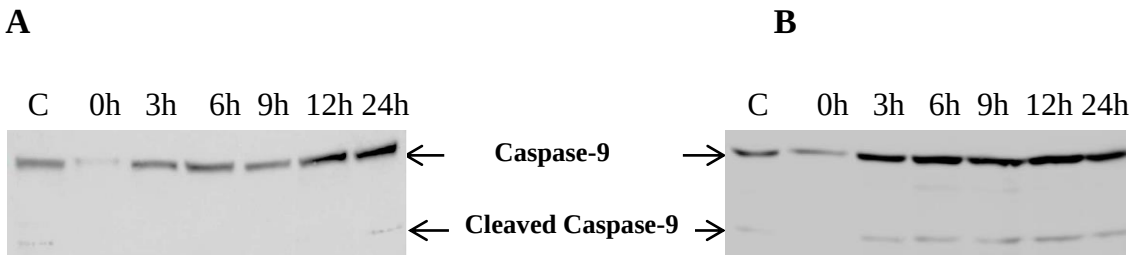

Figure 3.13: Caspase-9 protein levels in (**A**) MCF-7 and (**B**) MDA-MB-231 cells after a 9 h exposure to 10 µM of staurosporine (positive control; C) or treatment periods of 0 h, 3 h, 6 h, 9 h, 12 h and 24 h with 1% high-del tomato extract.

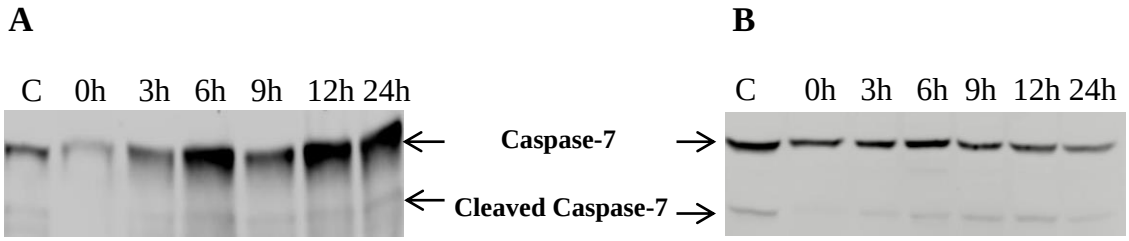

Figure 3.14: Caspase-7 protein levels in (**A**) MCF-7 and (**B**) MDA-MB-231 cells after a 9 h exposure to 10 µM of staurosporine (positive control; C) or treatment periods of 0 h, 3 h, 6 h, 9 h, 12 h and 24 h with 1% high-pel tomato extract.

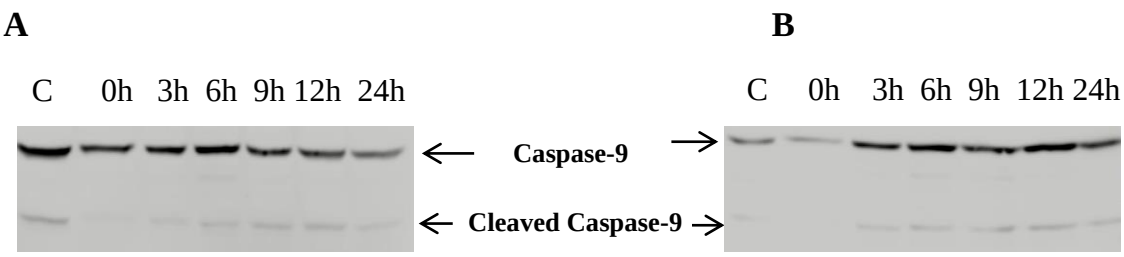

Figure 3.15: Caspase-9 protein levels in (**A**) MCF-7 and (**B**) MDA-MB-231 cells after a 9 h exposure to 10 µM of staurosporine (positive control; C) or treatment periods of 0 h, 3 h, 6 h, 9 h, 12 h and 24 h with 1% high-pel tomato extract.

3.3.8.4 Low-cyan tomato extracts also induce apoptosis in breast cancer cell lines

The low cyanidin (low-cyan) tomato extracts induced similar inhibition of the metabolic status and proapoptotic effects in the MCF-7 and MDA-MB-231 as observed in response to high-del and high-pel extract exposure. The effects were, however, much less pronounced, which may be a consequence of the relative low total anthocyanin content found in the low-cyan line. The results will be summarized here and data are available in Appendix section 3.

Low-cyan tomato extracts induced a modest, growth-inhibitory response in the breast cancer cell lines. Analysis of the cell cycle and revealed that low-cyan extracts induced an increase of cells in the G2/M phase indicative of cells being arrested at the final cell cycle checkpoints.

Low-cyan tomato extracts induced apoptosis in MCF-7 and MDA-MB-231 cells in a time-dependent fashion. A reduction in healthy cells in the population was most pronounced and statistically significant after 24 h exposure ($p<0.05$) to low-cyan extract, when ~50% of MCF-7 cells and ~40% of MDA-MB-231 cells were either late apoptotic or necrotic (Appendix Table 3ii).

Western blot analyses revealed that low-cyan tomato extract treatment induced the activation of caspase-7 in both MCF-7 and MDA-MB-231 cells. Cleaved caspase-7 was detected only at the 9 h and 12 h time points but not at earlier time points.Caspase-9

was not activated in MDA-MB-231 cells in response to treatment with low-cyan tomato extract.

These findings reveal that the low-cyan extract is capable of inducing an apoptotic response in both breast cancer cell lines through activation of proapoptotic proteins and alterations of the cell cycle but the effects are more dramatic for the other two high-anthocyanin tomato extracts.

3.4 Discussion

Regular consumption of fruit and vegetables has been associated with health benefits and protection from many chronic diseases, including certain cancers. Results from both *in vitro* cell and *in vivo* human and animal studies have provided strong evidence that the intake of fruit and vegetables can reduce the incidence of tumour development and progression and inhibit cancer cell proliferation. Different structural and functional classes of phytochemicals have been associated with anticancer activities, which include both chemopreventive and chemotherapeutic properties. The health benefits of purified resveratrol and anthocyanins have been extensively researched with conflicting results and little attention has been given to the possible synergistic or additive effects taking place in the food matrix of whole foods.

In this chapter I investigated the cell metabolic status-inhibiting effects of select purified polyphenolic compounds and compared them to the biological activity of whole tomato extracts. This comparative analysis was intended to shed further light on the question of whether the biological effects of certain phytochemicals are modulated by the food matrix environment and subsequently, whether the inhibitory effects on cell metabolic activity that were observed with the anthocyanin extracts were attributable to the induction of cell death through an apoptotic pathway or necrosis.

Very few comparative analyses of anthocyanins involve whole food products rather than dietary supplements. There is increasing evidence that the health benefits associated with the consumption of phytonutrients could be heavily influenced by their food context that may involve synergistic interactions with other components in the food matrix. The growth-inhibitory effects of a number of commercially available polyphenols (resveratrol, polydatin, rutin and delphinidin-3-glucoside) and the two most abundant anthocyanins purified from the high-del tomatoes were investigated and compared to the biological effects induced by different whole tomato extracts using the WST-1 cell proliferation/metabolic activity assay (Roche) that measures the metabolic activity of viable cells. Our study revealed that whole tomato extracts containing either high amounts of resveratrol (Figure 3.6 B) or anthocyanins (3.7 A and B) had significantly stronger effects on the metabolic activity and exerted their cyto-inhibitory effects at lower equimolar concentrations than the purified compounds (3.4 A-C and 3.5 A-C). No growth-inhibitory effects were associated with WT tomato extracts indicating

that the growth-inhibitory effects observed in the high-anthocyanin and high-resveratrol tomato extract-treated cells were caused by the novel polyphenols present only in those transgenic tomatoes. We observed little reduction in metabolic activity after exposure to the pure polyphenolic compounds. These findings suggest that polyphenolic compounds such as anthocyanins and resveratrol may not be as active when in their purified form but are likely to interact with other components in the food matrix that potentiate their biological effects or increase their bioavailability.

The mechanisms by which these synergistic or additive effects are exerted and whether they involve other plant polyphenols or structurally unrelated compounds remain to be discovered. However, these findings are in agreement with other studies suggesting that whole food products are more efficient in exerting health benefits than dietary supplements alone (Liu et al., 2009, Prior et al., 2008, Titta et al., 2010).

In this Chapter, I investigated the growth-inhibitory and proapoptotic effects of extracts from various transgenic tomato lines, using MCF-7 and MDA-MB-231 breast cancer cells. The main objective of this study was to investigate whether the presence of compounds such as anthocyanins or resveratrol, unique to the transgenic tomato lines, confer enhanced health benefits, such as improved anticancer properties. The metabolic activity studies (Figures 3.7) provide clear evidence that all high-anthocyanin tomato lines as well as the high-resveratrol (high-res) tomato line exhibited antiproliferative activity in the human breast cancer cells MCF-7 and MDA-MB-231. The three high-anthocyanin tomatoes investigated, displayed varying degrees of growth-inhibitory effects that correlated well with the amount of anthocyanins present in the different extracts. High-del tomato extract contained approximately 100 µM total trihydroxylated anthocyanins and exhibited the strongest anti-proliferative effects (Figure 3.7 A), followed by the high-pel tomato extracts containing 40 µM of anthocyanins (Figure 3.7 B). Strong antiproliferative activities were also observed after exposure to high-res extract (Figure 3.6 B).

We also aimed to compare anthocyanin tomato extracts containing different anthocyanin classes to investigate whether anthocyanin structure impacts their biological activity. Cells were treated with whole high-anthocyanin tomato extracts rather than purified compounds in order to assess the biological effects in a food

context. The anthocyanin-containing tomatoes allow for the comparison of trihydroxylated delphinidins with monohydroxylated pelargonidins in similar chemical environments. Anthocyanin levels varied between the different tomato lines, with high-del exhibiting the highest total anthocyanin content, approximately 2.5 and 40 fold higher than that of the high-pel and low-cyan tomatoes, respectively. Direct comparisons between the different tomato extracts were therefore impossible and high-del tomato extracts were diluted 2.5 times with WT tomato extract to match the concentration of total anthocyanins (40 µM) present in the high-pel tomatoes. Due to their comparatively low anthocyanin content, the low-cyan tomatoes were excluded from the comparative experiment. My results showed that MCF-7 and MDA-MB-231 cells responded with different sensitivities to the different high-anthocyanin extracts (Figure 3.9). Cell viability of MCF-7 cells was significantly reduced in response to the highest concentration of both high-pel and high-del extracts that each contained 40 µM of total anthocyanins. This observation suggests that there is no difference in the biological efficacy of tomato extracts containing trihydroxyalated delphinidins or monohydroxylated pelargonidins on MCF-7 cells. In contrast, MDA-MB-231 cells did show an effect of the different anthocyanin classes. 1% of high-pel extract containing 40 µM of monohydroxylated anthocyanins inhibited MDA-MB-231 cell metabolic status by 70% (Figure 3.9 A) compared to only 35% after treatment with equimolar concentration of trihydroxylated anthocyanins (Figure 3.9 B). These findings suggest that pelargonidins are somewhat more effective than delphinidins at mediating anthocyanin-induced MDA-MB-231 cell death.

Both trihydroxylated delphinidins and dihydroxylated cyanidins have been extensively researched with respect to their anti-cancer activities whereas pelargonidins have remained largely unresearched which could be explained by their relatively low natural abundance compared to delphinidin and cyanidin (Chen et al., 2006a, Feng et al., 2007, Lamy et al., 2006, Lazze et al., 2004, Syed et al., 2008, Yun et al., 2009). Several studies have compared the efficacy of individual anthocyanins but have yielded inconclusive results. Cell type dependent differences in the response to individual anthocyanins might be responsible for the reported discrepancies in the results. That highlights the difficulty of comparing these studies in order to draw any conclusion regarding the links between anthocyanin structure and biological efficacy. Some studies have reported that pelargonidins have weaker biological effects than delphinidins or

cyanidin, whereas other findings suggest that the specific type of cells used may impact the biological efficacy observed more than the anthocyanin compound under investigation (Lamy et al., 2006, Zhang et al., 2005b). Wang et al. (2011) reported that trihydroxylated, O-methylated malvidin chloride was more effective than monohydroxylated pelargonidin chloride in inhibiting the growth of Caco-2 colon adenocarcinoma cells but that pelargonidin chloride was more effective than malvidin chloride in reducing the growth of HepG2 liver cells. Pelargonidin-containing tomato extracts were significantly more effective in inhibiting growth of MDA-MB-231 cells than of MCF-7 cells, whilst no differences in the biological efficacy of pelargonidin- or delphinidin-containing extracts was detected in MCF-7 cells. The trihydroxylated delphinidin purified from the high-del tomato seemed to be slightly more effective than its O-methylated form petunidin. At the highest concentration tested the delphinidin induced a significant reduction in metabolic activity of ~20% in both MCF-7 and MDA-MB-231 cells (Figure 3.5 B), whereas the petunidin-induced changes to the cell metabolic status were not statistically significant (Figure 3.5 C). Delphinidin and petunidin are different anthocyanins that share a common trihydroxylated backbone. The decoration of anthocyanins through glycosylation, acylation and methylation increases their stability in the plant but are likely to have an impact on the bioavailability of these anthocyanins by impacting their absorption and metabolism in the human body (Kroon et al., 2004).

My findings support the idea that the biological efficacy of a given compound or structural class may depend strongly on the specific type of cells and that individual cell lines may respond differently to the same agent. Furthermore, these compounds might exert their biological activity by targeting specific molecules in a given cell type rather than being non-selectively cytotoxic. In order to determine whether anthocyanin structure affects biological activity, many cell lines from different tissues as well as a set of structurally diverse anthocyanin compounds should be included in the study.

The use of cell proliferation or cell viability assays allows for a preliminary assessment of a cell population's overall health. Other assays and experiments are required to investigate the mechanisms by which particular treatments induce growth-inhibition or cell death. All anthocyanin extracts induced an apoptotic response independent of the cell line used. The Annexin-V/PI assay allowed cells to be tracked whilst undergoing

different stages of apoptosis and the expression analysis of proapoptotic caspases provided further evidence that these cells undergo apoptotic cell death in response to anthocyanin extract treatment. However, the large amount of cell debris that was detected by FACS analysis upon exposure to the anthocyanin extracts may suggest that a significant proportion of the cell population died trough a different form of cell death.

The induction of apoptosis by anthocyanin-rich extracts measured by Annexin-V/PI assays was confirmed by characteristic morphological changes and activation of proapoptotic proteins such as caspases (caspase-7 and -9). Anthocyanin extract-induced alterations to the cell cycle further confirmed the hypothesis that anthocyanin tomato extracts are potent inducers of cell death *in vitro*. Anthocyanin tomato extracts inhibited growth of MCF-7 and MDA-MB-231 cells and blocked G2/M phase progression. Studies by several different research groups have reported that anthocyanins can inhibit the growth of different tumour cell lines, and have linked this to caspase-dependent apoptosis, activating both the intrinsic and extrinsic apoptotic pathway (Chen et al., 2006b, Lazze et al., 2004, Lee et al., 2009, Reddivari et al., 2007, Sun and Hai Liu, 2006). Results of the Annexin-V apoptosis assay (Table 3iii) demonstrate that high-anthocyanin tomato extracts are powerful inducers of apoptosis in both MCF-7 and MDA-MB-231. This observation is in agreement with the previously reported proapoptotic effects of different anthocyanins and their glycosides in other cancer cell lines (Feng et al., 2007, Shih et al., 2005, Yun et al., 2009). However, anthocyanin concentrations equal or higher than 200 µM were used in these studies, whereas we observed a more dramatic and rapid apoptotic response at much lower anthocyanin concentrations (1% of high-pel and high-del tomato extract contained 40 µM of monohydroxylated anthocyanins and 100 µM of trihydroxylated anthocyanins, respectively). These findings suggest that the use of food supplements may not deliver the same beneficial health effects that are associated with a diet rich in fruit and vegetables.

The FACS analyses of Annexin-V/PI stained cells also revealed that high-del and high-pel extracts induced the very rapid onset of apoptotic cell death of MCF-7 and MDA-MB-231 and also led to the accumulation of a large percentage of dead cells and debris in the samples after prolonged exposure times (Table 3iii B and C). The Annexin-V/PI assay does not discriminate between cells that die as a result of apoptosis or necrosis.

However, the distinct time-dependent migration of cells from early apoptotic (Annexin-V positive and PI positive) to late apoptotic (Annexin-V positive and PI negative), suggests that the intact cell populations analysed by Annexin-V/PI were indeed undergoing apoptosis rather than necrosis.

The accumulation of cell debris increased dramatically with prolonged exposure times to high-anthocyanin tomato extracts. It is important to note, that only the intact cell population was included in the Annexin-V/PI analysis. Cell debris or severely damaged cells show up as false healthy cells (Annexin-V negative and PI negative) and were therefore excluded from the analysis of the apoptotic state in order to maintain data fidelity. The increased amount of cell debris in the high-anthocyanin extract treated cells could be indicative of acute treatment toxicity that may have induced very rapid necrotic cell death. Apoptosis and necrosis are two very distinct routes to cell death that are triggered through different pathways and involve a complex and unique set of pro-death signals (see general introduction). Necrotic cell death is associated with high cytotoxicity and is a consequence of acute disruption of cellular metabolism, leading to mitochondrial and cellular swelling, activation of degradative enzymes, plasma membrane failure and cell lysis. It is possible that within the same population, individual cells responded to the extracts with different cell death mechanisms. Varying degrees of chemosensitivity could explain that those cells that accounted for the cell debris suffered rapid membrane rupture and necrotic cell death in response to the anthocyanin tomato extract treatment, whilst those identified by the Annexin-V/PI assay as undergoing apoptosis were more resilient and responded more slowly through a coordinated induction of proapoptotic signals.

Furthermore, high-anthocyanin tomato extracts induced activation of caspase-7 and caspase-9 in both MCF-7 and MDA-MB-231 but not caspase-3 in MDA-MB-231 (MCF-7 does not produce detectable levels of caspase-3 due a deletion in the exon of *Casp-3*). However, anthocyanin-induced activation of caspase-3 has been reported for U937 human leukaemia cells (Lee 2009), HL-60 human leukaemia cells (Chang 2005), MDA-MB-453 but not MCF-7 or MDA-MB-231 human breast cancer cells (Hui et al., 2010) and in LNCaP prostate cancer cells but not in PC-3 prostate cancer cell (Reddivari et al., 2007). This suggests that anthocyanins differentially induce apoptosis in various cell lines through caspase-3 dependent and independent pathways. Caspase-9

occupies an essential role in the caspase cascade as the upstream activator of caspase-3 and caspase-7 which, in turn, then go on to propagate the caspase cascade by activating caspase-2, -6, and -10 (Slee et al., 1999). Both caspase-7 and -9 were activated in both cell lines after exposure to tomato anthocyanin extracts, demonstrating that even without the activation of caspase-3, anthocyanin extract-induced apoptosis involves the caspase-dependent pathway. The non-discriminatory induction of apoptosis in both MDA-MB-231 and the caspase-3-deficient MCF-7 cells indicated that caspase-3 is not imperative for the anthocyanin extracts to induce fast and sustained alterations to the cell cycle and time-dependent apoptosis. However, it should be noted that sample loading, especially of the untreated control, was an issue in some Western blots, which made it difficult to draw any conclusion regarding *de novo* synthesis of caspases in response to treatment with anthocyanin-enriched tomato extracts. Caspase-corresponding protein bands were often substantially weaker in the untreated control compared to the treated samples which could suggest *de novo* synthesis of procaspases in the treated samples or simply indicated discrepancies in the amount of protein loaded.

My findings do not allow for conclusions regarding the mechanisms by which apoptosis is induced in the breast cancer cells and further experiments would be required to distinguish between the different routes of mammalian cell death induced by the high-polyphenol tomato extracts and their interactions with key effectors in the apoptotic pathway.

Anthocyanins and other polyphenols have been shown, both in *in vitro* test systems and *in vivo* animal models, to induce substantial biological responses associated with the protective effects of diets rich in fruit and vegetables against degenerative and chronic diseases. With the aim of developing dietary recommendations for major phytochemicals, a number of studies have investigated the bioavailability and metabolic fate of those compounds within the human body. Up to now, our understanding of the biological fate of polyphenols, after entering the digestive tract, has remained somewhat fragmented. Only fractions (nanomolar ranges) of several hundred mg of polyphenols are detected after ingestion, whilst the metabolic fate of the remaining anthocyanins remains largely unknown (Scalbert and Williamson, 2000). Polyphenol conjugates are likely to be substantially modified and metabolized during absorption, making the post-digestive detection increasingly difficult.

I exposed breast cancer cells to medium containing a maximum of 100 µM of total anthocyanins (high-del tomato extracts) or 200 µM of purified polyphenols. These concentrations are relatively high and may not be physiologically relevant. I*n vivo,* cells in tissues distal to the digestive system are likely to be exposed to much lower concentration of those compounds in the blood. However, my *in vitro* observations complement the results of a previously conducted preclinical intervention study with *Trp53*$^{-/-}$ knockout mice in which feed, supplemented with high-anthocyanin tomatoes significantly prolonged their average lifespan by delaying tumour development (Butelli et al., 2008). Animals fed on the WT tomato supplemented diet showed no increase in lifespan compared to animals fed standard diet, whereas *Trp53*$^{-/-}$ knockout mice consuming the high-anthocyanin tomato-supplemented diet lived ~ 30% longer. The *p53* tumour suppressor gene plays a key role in cell cycle regulation, tumour suppression and control of apoptosis. Increased cell proliferation and failure to undergo apoptosis are defining criteria of cancerous cells and re-establishing or inducing mechanisms that control these processes, may improve therapeutic treatment significantly. High-anthocyanin tomato extracts strongly inhibited cell metabolic activity which is linked directly to cell proliferation and growth, induced cell cycle alterations and activated pro-apoptotic proteins in breast cancer cells *in vitro*. My findings suggest strongly that the delay in tumour development and subsequent prolongation of lifespan of *Trp53*$^{-/-}$ knockout mice fed on a diet supplemented with high-anthocyanin tomatoes, are the result of an anthocyanin-induced activation of the apoptotic programme, possibly through mechanisms bypassing or compensating for the loss of *p53* function, as well as a modulation of the cell cycle, which reduces the proliferation of aberrant cells.

The results from Butelli's epidemiological study using the well-established *Trp53*$^{-/-}$ knockout mouse cancer model and my *in vitro* breast cancer tests confirmed that anthocyanins confer improved health benefits to the transgenic tomatoes by enhancing their anti-cancer bioactivities.

In order to gain a more complete understanding of the molecular mechanisms underlying the anthocyanin tomato-mediated induction of apoptosis, further investigation of key apoptotic signalling and executing molecules is required, including

expression analysis p53 and p53-regulated genes and other signalling pathways like extracellular signal-regulated kinases (ERKs) or phosphatidylinositide 3-kinases (PI3Ks) which are associated with cell survival.

4 Chemosensitizing effects of high-resveratrol and high-delphinidin tomato extracts

4.1 Introduction

A number of plant polyphenols have been suggested to prevent or reduce the initiation of cancer or suppress its development. These compounds exert their effects through modulation of intracellular cell signalling pathways that are involved in tumourigenesis. Evidence has emerged that these phytochemicals may also play a role in enhancing the tumoricidal effects of pharmacological agents by increasing their systemic availability, abrogating drug resistance or protecting normal cells from therapy-induced damaging and toxic effects (Satoh et al., 2003, Casanova et al., 2012, Jazirehi and Bonavida, 2004, Molnár et al., 2008, Misra and Sahoo, 2011, Younes-Sakr et al., 2012).

Several studies have reported that the combination with drugs or pre-treatment with phytochemicals result in greater inhibition of cancer cell proliferation and enhanced induction of apoptosis, than the drugs alone. Genistein, an isoflavone and phytoestrogen found in many soy products, significantly enhanced the sensitivity of human breast, prostate and pancreatic cancer cells to the chemotherapeutic agents such as adriamycin, cisplatin and docetaxel (Li et al., 2005, Satoh et al., 2003). Furthermore, pre-treatment with genistein enhanced radiation-mediated inhibition of prostate tumour cells (Raffoul et al., 2006, Hillman et al., 2004).

Resveratrol, a stilbene and natural phytoalexin predominantly found in the skin of grapes, has received substantial scientific attention due to its alleged anti-aging, anti-cancer and cardiovascular-protective effects (Park and Pezzuto, 2002). A number of studies demonstrated that resveratrol can also act as powerful chemosensitizer for a number of chemotherapeutic agents. Combinatorial treatment of melphalan, roscovitine or doxorubicin with resveratrol significantly enhanced the effect of drug-induced apoptosis and cell death in various cancer cell lines (Węsierska-Gądek et al., 2008, Fulda and Debatin, 2004, Casanova et al., 2012).

Similarly, improved cytotoxic and pro-apoptotic effects were reported after co-treatment with the plant polyphenolic compound, (-) epigallocatechin-3-gallate (EGCG), a major constituent of green tea, and cyclooxygenase-2 (COX-2) inhibitors targeting prostate cancer cells *in vitro* (Adhami, 2007).

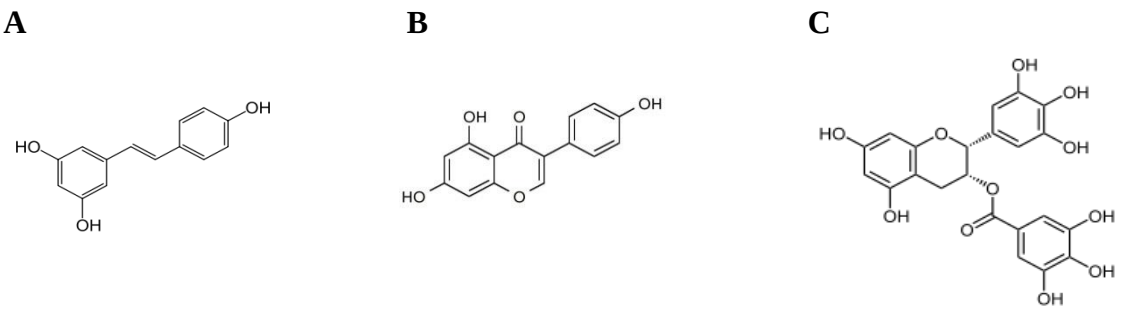

Figure 4.1: Chemical structures of (**A**) resveratrol, (**B**) genistein, and (**C**) (-) epigallocatechin-3-gallate.

The mechanisms by which chemosensitizing effects may be exerted are diverse and could involve the regulation of the NF-κB and Akt cell survival pathways which are involved in drug resistance (Gill et al., 2007, Hillman et al., 2004, Pommier et al., 2004) and the activation of proapoptotic pathways involving the induction of p53, p21 together with caspases (Li et al., 2005, Raffoul et al., 2006, Surh, 2003). Furthermore, polyphenols may increase the endogenous antioxidant defence potential and thus modulate cellular redox state. Oxidants and free radicals are not only implicated in normal intracellular signalling but also in the pathogenesis of chronic inflammatory diseases and cancer. Polyphenols may act as both anti- or pro-oxidants depending on their concentrations and therefore modulate intracellular ROS signalling (Rahman et al., 2006).

Phytochemical-induced immunomodulation or –potentiating effects may also account for some of their chemosensitizing effects. Phytochemicals have been implicated in improving the immune response and reducing chemotherapy-induced side effects by enhancing lymphocyte proliferation, natural killer cell cytotoxicity and cytokine-producing CD4+/CD8+ ratio, which have been associated with immunity against tumours. Plant bioactives also modulated the production of interleukins and interferons that involved in regulating the response of the entire immune system to foreign antigens (Falchetti et al., 2001, Zhang et al., 2005a).

Despite a significant choice of chemotherapeutic agents, the heterogenic nature of tumours and their ability to develop resistance to drugs remains a significant challenge for delivering effective and successful cancer treatments with minimized effects on non-

target tissues. Novel treatment strategies will most certainly involve combinatorial treatments of established drugs and could include compounds that sensitize or decrease the development of resistance to cytotoxic drugs by tumours or confer protection to normal cells from chemotherapy drug damage. The concept of combinatorial drug treatments to treat cancer is not a new one. The idea of combining different agents that act as sensitizers and inducers is, however, novel and promising. So far, little research has been conducted into the potential of plant natural compounds as components of multi-drug chemotherapy treatments. Yet, the many positive health effects attributed to dietary polyphenols and the lack of reported adverse effects on whole organisms from dietary levels of these compounds make them attractive candidates for inclusion in chemotherapy drug regimes. Resveratrol, genistein and curcumin, a phenolic curcuminoid found in the spice turmeric, are among the polyphenolic compounds that have attracted significant scientific and medical attention because of their health benefits as cancer chemopreventive, anti-inflammatory and cardioprotective agents (Park and Pezzuto, 2002). More research into the chemosensitizing effects of these dietary supplements and the underlying mechanisms, by which they are induced, is required to make any recommendations for their use as adjuvants in chemotherapy. Furthermore, the impact of dietary intervention as a strategy to improve the body's resistance against the adverse effects associated with most pharmacological agents has been largely ignored. Changes in dietary habits that involve the increased consumption of plant-based food products, rich in bioactive phytochemicals with confirmed chemosensitizing effects, together with a reduction in food components that have known adverse health effects, like those containing high amounts of sugars and trans fats may reduce the systemic impact of chemotherapy, improve treatment success and ultimately, improve the long-term clinical outcome for chemotherapy patients.

4.2 Aims:

Strong chemosensitizing effects have been associated with a number of dietary supplements, including resveratrol, curcumin and EGCG. In this chapter, we investigated whether co-treatment with high-resveratrol and high-delphinidin tomato extracts potentiated the cytotoxic effects of the chemotherapeutic agents, doxorubicin and roscovitine. Human breast cancer cell lines MCF- and MDA-MB-231 were exposed

to different combinatorial doses of phytochemical-enriched tomato extracts and chemotherapy drugs to test their potential to induce chemosensitizing effects.

4.3 Experimental procedures

4.3.1 Chemicals

Doxorubicin (Dox), also known under the brand name of Adriamycin is an anthracycline antibiotic and chemotherapy drug that acts as a topoisomerase-2 inhibitor blocking cell division and growth. Roscovitine (Rosc) is a small purine-like cyclin-dependent kinase (CDK) inhibitor that preferentially inhibits multiple enzyme targets including CDK1, CDK2, CDK5, CDK7 and CDK9. Doxorubicin and roscovitine were purchased from Sigma and dissolved in DMSO to a stock concentration of 10 mM and 30 mM, respectively. Resveratrol was also purchased from Sigma and dissolved in EtOH to a stock concentration of 100 mM. Small aliquots were stored at -20°C until further use.

4.3.2 Tomato extract preparation

High-res and high-del tomato extracts were prepared as described in Chapter 3.2.3.

4.3.3 Cell culture and treatment

MCF-7 and MDA-MB-231 cells were cultured following the cell culture procedures outlined in Chapter 3. Cells were exposed to Dox diluted in complete DMEM medium at 0.1 µM, 1 µM, 3 µM, 5 µM and 10 µM, Rosc diluted in medium at 1 µM, 5 µM, 10 µM, 20 µM and 30 µM or pure resveratrol diluted in medium at 10 µM, 20 µM, 30 µM, 50 µM and 100 µM. Tomato extracts were diluted in medium to a final concentration of 0.05%, 0.1%, 0.2%, 0.3% and 0.5%. Cells were exposed to treatment media for 24 hours, followed by analysis or incubation with treatment-free, complete medium for another 24 hours. Cell metabolic activity was measured using the WST-1 assay as described in Chapter 3.2.4.2 (Roche).

4.3.4 Statistical methods

The statistical significance was determined using Student's t-test. P-values ≤ 0.05 were considered statistically significant.

4.4 Results

4.4.1 Effect of resveratrol, doxorubicin and roscovitine on cell metabolic status

The effects of resveratrol, Dox and Rosc on the metabolic status of MCF-7 and MDA-MB-231 breast cancer cell lines were investigated (Table 4.i). Cell metabolic status was measured after 24 h exposure to treatment (Table 4i A) or after a total of 48 h (24 h treatment + 24 h incubation in treatment-free medium; Table 41 B). In MCF-7 cells, 24 h incubation with resveratrol induced a dose-dependent reduction in cell proliferation (Table 4i A). At 100 µM, the number of actively metabolising cells relative to the untreated control was significantly reduced by 35%. The 24 h treatment with resveratrol (10 µM to 100 µM) significantly stimulated the metabolic activity of MDA-MB-231 cells by up to 30%.

In a second experiment, cells were incubated with resveratrol-containing medium for 24 h before replacing the medium with treatment-free medium and incubation for another 24 h (Table 4i B). The metabolic activity of MCF-7 cells treated with 100 µM resveratrol was not compromised when 24 h exposure to resveratrol was followed by 24 h recovery in treatment-free medium (Table 4i B). This indicates that the resveratrol-mediated inhibition of metabolic activity of MCF-7 cells may have been the result of cytostatic rather than cytotoxic effects as cells recover in treatment-free medium. The metabolic status of MDA-MB-231 was reduced by 15% in cells that were exposed to resveratrol-containing medium followed by 24 h recovery in treatment-free medium. This observation may be due to experimental variability or indicate that non-toxic doses of resveratrol may compromise the long-term metabolic activity of MDA-MB-231 cells.

Treatment with Dox significantly reduced the metabolic activity of both MCF-7 and MDA-MB-231 cells in a dose-dependent manner ($p<0.001$; Table 4i A). At low concentrations MDA-MB-231 cells were more sensitive to Dox than MCF-7 cells. At the highest concentration (10 µM), Dox-induced inhibition of metabolic activity was 77% and 84% for MCF-7 and MDA-MB-231 cells, respectively (Table 4i A). Incubation with Dox-containing medium followed by 24 h incubation with treatment-

free medium resulted in a weak recovery of MDA-MB-231 cells. Interestingly, the metabolic status of MCF-7 cells was significantly more reduced in cells that received 24 h Dox treatment followed by 24 h Dox-free treatment than those that were exposed to 24 h Dox without 24 h recovery in treatment-free medium (Table 4i B). This observation suggests that Dox induces long-term, cytotoxic effects that persist, even after removal of Dox and is indicative of strong cytotoxicity. In contrast, the metabolic status of Dox-treated MDA-MB-231 cells was slightly higher in those cells that incubated for another 24 h in treatment-free medium, suggesting that the cells started to recover after removal of the Dox.

Treatment with Rosc resulted in the reduction of the metabolic status of both cell lines. (Table 4i) MCF-7 cells were more sensitive to Rosc than MDA-MB-231 and treatment with the highest concentration of Rosc (30 µM) resulted in 70% and 35% in MCF-7 and MDA-MB-231 cells, respectively (Table 4i A).Treatment with Rosc followed by a 24 h incubation in treatment-free medium did not change the metabolic activity of the cells compared to the 24 h Rosc treatment without further incubation in treatment-free medium (Table 4i B)These observations suggest that Rosc is cytotoxic and that cells do not recover following treatment. MCF7 cells appear more sensitive to Rosc than highly metastatic MDA-MB-231 cells Both Dox and Rosc are potent cytotoxic compounds that effectively inhibit metabolic activity of both breast cancer cell lines and continue to exert their inhibitory effects after their removel from the medium (Table 4i).

Resveratrol, at the concentrations tested, induced a moderate reduction in metabolic activity of MCF-7 cells. Compared to Dox and Rosc, higher equimolar concentrations of resveratrol were required to induce biological effects. This is not surprising as resveratrol is a dietary component with little known adverse systemic effects, whereas both Dox and Rosc are highly cytotoxic causing severe disruption the DNA replicative machinery and cell cycle regulation.

Table 4i: Dose response curves for (**A**) 24 h treatment with resveratrol, doxorubicin or roscovitine or (**B**) 24 h treatment + 24 h treatment-free medium containing resveratrol, doxorubicin and roscovitine on the proliferation of MCF-7 and MDA-MB-231 cells.

A			**24 h**			
	Concentration	**10 µM**	**20 µM**	**30 µM**	**50 µM**	**100 µM**
MCF-7	Resveratrol	94.6 ± 3.4	93.1 ± 6.2	94.6 ± 2.8	95.8 ± 2.8	64.0 ± 1.9 ***
MDA-MB-231	Resveratrol	111.1 ± 3.6 *	114.8 ± 4.4 *	116.21 ± 0.2 ***	128.7 ± 6.2 *	118.7 ± 2.4 **
	Concentration	**0.1 µM**	**1 µM**	**3 µM**	**5 µM**	**10 µM**
MCF-7	Doxorubicin	118.5 ± 2.0 **	86.3 ± 0.2 ***	71.9 ± 1.4 ***	60.4 ± 0.4 ***	22.8 ± 0.5 ***
MDA-MB-231	Doxorubicin	95.7 ± 6.3	67.5 ± 3.4 **	40.5 ± 1.6 ***	31.2 ± 1.2 ***	15.9 ± 1.7 ***
	Concentration	**1 µM**	**5 µM**	**10 µM**	**20 µM**	**30 µM**
MCF-7	Roscovitine	105.7 ± 1.5 *	96.5 ± 4.8	95.7 ± 2.1	73 ± 2.5 **	31.4 ± 0.5 ***
MDA-MB-231	Roscovitine	100.6 ± 2.6	92.2 ± 1.8 *	87.4 ± 1.3 **	75 ± 5.2 *	66.1 ± 5.4 **

B			**24 h + 24 h treatment-free**			
	Concentration	**10 µM**	**20 µM**	**30 µM**	**50 µM**	**100 µM**
MCF-7	Resveratrol	96.7 ± 6.2	111.1 ± 4.0 *	101.8 ± 11.4	121.6 ± 3.8 *	104.5 ± 6.5
MDA-MB-231	Resveratrol	105.7 ± 3.4	97.8 ± 4.3	96.7 ± 0.9	88.3 ± 3.7 **	84.8 ± 1.8 **
	Concentration	**0.1 µM**	**1 µM**	**3 µM**	**5 µM**	**10 µM**
MCF-7	Doxorubicin	113.1 ± 6.8	20.1 ± 3.9 ***	8.9 ± 1.3 ***	9.1 ± 2.3 ***	6.1 ± 1.9 ***
MDA-MB-231	Doxorubicin	95.5 ± 6.3	71.4 ± 3.4 **	40.4 ± 1.8 ***	31.2 ± 1.3 ***	25.9 ± 2.1***
	Concentration	**1 µM**	**5 µM**	**10 µM**	**20 µM**	**30 µM**
MCF-7	Roscovitine	108.9 ± 1.4 **	100.5 ± 4.6	91.2 ± 17.6	82.7 ± 8.4	32.9 ± 10.9 **
MDA-MB-231	Roscovitine	98.6 ± 2.9	41.2 ± 3.7 *	91.4 ± 1.9 *	73.0 ± 4.8 *	64.1 ± 5.1 **

Results are expressed as a percentage of metabolically active cells after treatment relative to the untreated control. Data shown as mean ± standard error (n=3 technical replicates. Experiments were performed at least twice). * $p<0.05$; ** $p<0.01$; *** $p<0.001$.

4.4.2 Combinatorial effects of resveratrol and roscovitine and doxorubicin

Having determined the responses of the two cell lines to the chemotherapy agents and the plant polyphenols, the next stage of the experiments was to explore the use of combinations of treatments at submaximal levels, to evaluate potential antagonistic or additive effects. The effects on the metabolic status of cells were investigated following the treatment with combinatorial doses of resveratrol and Rosc and Dox (Figure 4.2).

Neither resveratrol (50 µM) nor roscovitine (5 µM or 10 µM) alone had inhibitory effects on the metabolic activity of MCF-7 cells. However, the combination of resveratrol (10 µM, 25 µM and 50 µM) with either 5 µM or 10 µM roscovitine (Figure 4.2 A) induced a gradual reduction in the metabolic activity of MCF-7 cells which was significant ($p<0.05$) at the combinatorial dosage of resveratrol at 25 µM and 50 µM and Rosc at 10 µM. The reduction in metabolic activity of MCF-7 was weaker but highly significant ($p<0.01$) in the combinatorial treatment of resveratrol and 5 µM Rosc (Figure 4.2 A).

No resveratrol-Rosc-induced inhibitory effects on the metabolic activity were observed in MDA-MB-231 cells. In contrast, combinatorial treatment of resveratrol and 5 µM of Rosc significantly stimulated metabolic activity (Figure 4.2 A).

A similar experiment was conducted to investigate the potential combinatorial effects of resveratrol and Dox on the metabolic status of both cell lines. Treatment with 5 µM or 2.5 µM of Dox alone reduced the metabolic activity of MCF-7 cells by 40% and 30%, respectively (Figure 4.2 B). The combination of resveratrol at 10 µM, 25 µM and 50 µM with doxorubicin (2.5 µM or 5 µM) did not inhibit the growth of MCF-7 cells significantly. The combination of 2.5 µM doxorubicin and different doses of resveratrol resulted in a slight, statistically insignificant decrease in cell proliferation relative to cells treated with 2.5 µM of doxorubicin alone. Co-treatment of 5 µM of doxorubicin and resveratrol (25 µM) resveratrol even increased the proliferation of MCF-7 cells by 10% compared to the drug treatment alone.

Metabolic status of MDA-MB-231 cells was inhibited by 70% and 60%, respectively, after treatment with Dox at 5 µM or 2.5 µM. No pro- or anti-stimulatory effects on the metabolic activity of MDA-MB-231 cells were observed after co-treatment with

resveratrol and Dox (Figure 4.2 B). Consequently, there was no evidence of additive or synergistic effects between Dox and resveratrol in either cell line.

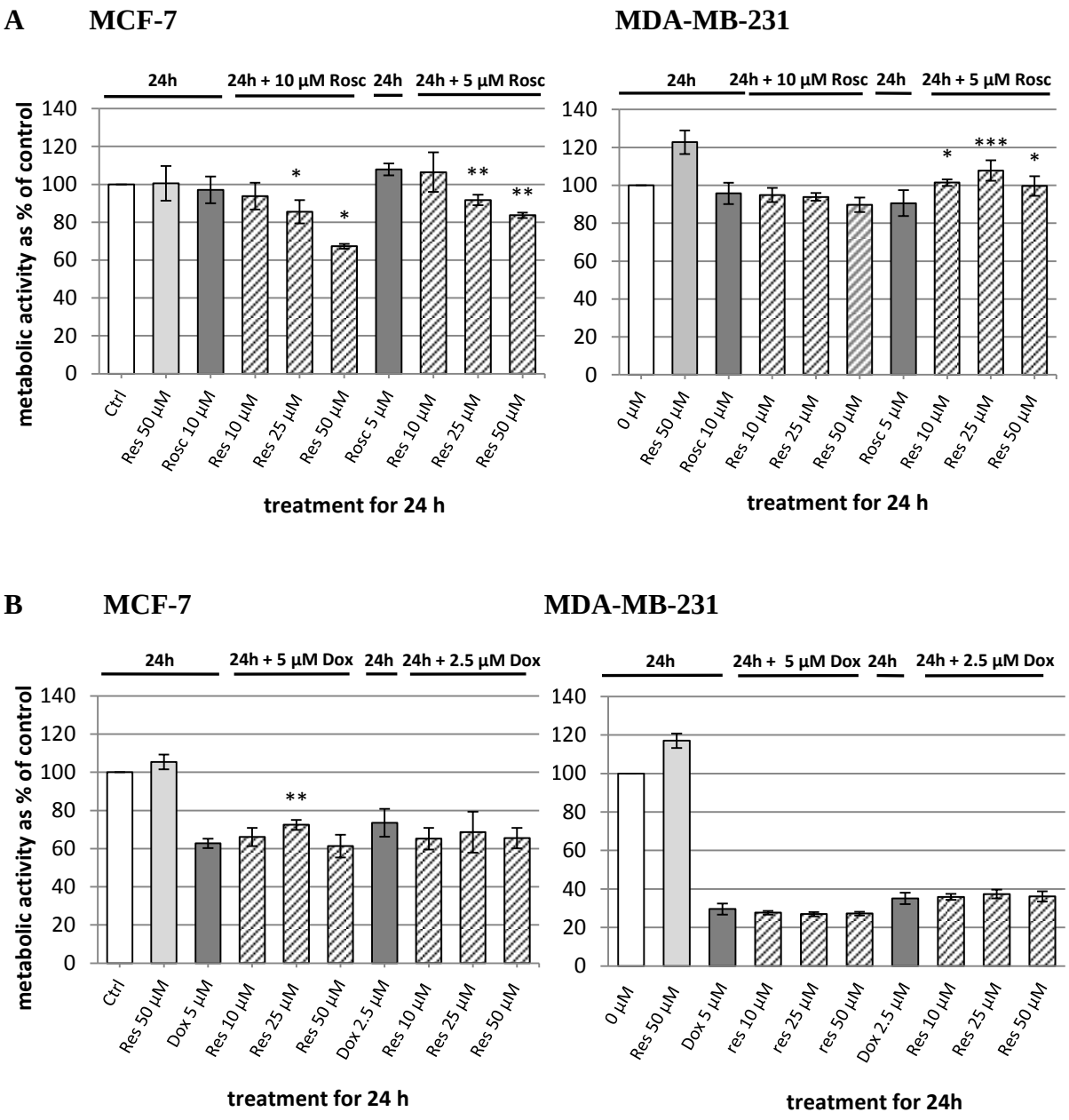

Figure 4.2: Combinatorial effects of resveratrol (Res) and (**A**) roscovitine (Rosc) or (**B**) doxorubicin (Dox) on proliferation of MCF-7 and MDA-MB-231 cells were investigated. Cells were exposed to Res, Rosc or Dox alone, or to a combination of Res and Rosc or Res and Dox to the concentrations indicated. Results are expressed as a percentage of cell metabolic activity after treatment relative to the untreated control. Data shown as mean ± standard error (n=3 technical replicates. Experiments were performed at least twice). The statistical significance of the effect of combined treatment compared to the treatment with 10 µM ROSC alone was determined. * $p<0.05$; ** $p<0.01$; *** $p<0.001$.

4.4.3 Combinatorial effects of tomato extracts and roscovitine and doxorubicin

The effects of whole tomato extracts on the metabolic status of MCF-7 and MDA-MB-231 cells were investigated (Table 4ii). The extracts used were prepared from tomatoes that contained either large amounts of delphinidins (high-del) or resveratrol (high-res) or from unmodified tomatoes (WT) that contained no anthocyanins and very low levels of resveratrol.

Table 4ii: Final concentration of tomato extract and the molar equivalents of their main active compounds.

Extract	Active compound	0.1%	0.3%	0.4%	0.5%	0.6%	0.7%	0.8%	0.9%	1%
high-del	Anthocyanin	10 µM	30 µM	40 µM	50 µM	60 µM	70 µM	80 µM	90 µM	100 µM
high-res	Resveratrol	2 µM	6 µM	8 µM	10 µM	12 µM	14 µM	16 µM	18 µM	20 µM

Extracts were prepared as described in Chapter 3 and cells were exposed to different concentrations of tomato extract in the medium. Final cell medium concentrations of the tomato extract (in %) and their corresponding active compounds (in µM) are summarized in Table 4ii.

As discussed in Chapter 3, WT tomato extract had no effect on the metabolic status of MCF-7 and MDA-MB-231 cells, while both high-del and high-res tomato extracts significantly reduced the metabolic status of both cell lines (Table 4iii).

Table 4iii: Dose response curves for 24 h treatment with WT, high-del and high-res tomato extracts on the metabolic status of MCF-7 and MDA-MB-231 cells.

	concentration	**0.25%**	**0.50%**	**0.75%**	**1%**
MCF-7	WT	111.0 ± 3.1 *	110.8 ± 7.9	113.8 ± 6.4	106.9 ± 6.8
MDA-MB-231	WT	118.2 ± 6.9 *	110.1 ± 7.7	108.0 ± 4.6 *	95.3 ± 3.9
MCF-7	High-del	108.6 ± 6.5	96.9 ± 4.9	40.7 ± 8.7 **	0.0 ± 0.4 ***
MDA-MB-231	High-del	109.0 ± 6.9	64.1 ± 4.9 **	11.6 ± 4.4 ***	6.3 ± 2.2 ***
MCF-7	High-res	102.8 ± 11.0	106.4 ± 12.5	108.9 ± 15.7	29.1 ± 6.3 **
MDA-MB-231	High-res	102.6 ± 6.3	109.8 ± 2.3 *	68.1 ± 7.2 *	7.0 ± 1.8 ***

Results are expressed as a percentage of metabolically active cells after treatment relative to the untreated control. Data shown as mean ± standard error (n=3 technical replicates. Experiments were performed at least twice). * $p<0.05$; ** $p<0.01$; *** $p<0.001$.

4.4.4 Combinatorial effects of tomato extracts and roscovitine

Co-treatment effects between Rosc and and high-del tomato extract were investigated by treating cells with 10 µM of Rosc and different concentrations of high-del extract (Figure 4.3 A). Treatment with either 0.5% high-del extract, corresponding to 50 µM of anthocyanins, or 10 µM of Rosc alone did not impact on the metabolic activity of MCF-7 cells. The co-treatment of 10 µM of Rosc with different concentration of high-del tomato extract did not result in a significant dose-dependent inhibition of cell metabolic activity. A small, significant ($p<0.05$) 10% reduction in the metabolic activity of MCF-7 cells was observed after 24 h combinatorial treatment with 0.2% of high-del extract but not with higher extract concentrations. This observation is probably the result of experimental variation as this reduction in metabolic activity was not observed with increasing combinatorial concentrations of high-del extract.

Treatment with 10 µM of Rosc alone did not inhibit the metabolic status of MDA-MB-231 cells while treatment with high-del extract resulted in a 40% reduction (Figure 4.3 A). Co-treatment of Rosc (10 µM) and high-del tomato extract resulted in a dose-dependent inhibition of MDA-MB-231 cell metabolic activity. Co-treatment with Rosc

(10 µM) and 0.5% high-del extract, which corresponds to 50 µM of total anthocyanins, resulted in a strong inhibitory effect of 60% compared with 40% after treatment with 0.5% high-del alone. The reduction in the metabolic status of co-treated MDA-MB-231 cells compared 0.5 % high-del treated cells was highly statistically significant ($p<0.01$). This suggests that synergistic effects between Rosc, which on its own did not exert inhibitory action, and the active compounds in the high-del extract may play a role in exerting the increased reduction in metabolic activity of MDA-MB-231 cells.

I also tested the combinatorial effects of Rosc (10 µM) and high-res tomato extract on the metabolic status of MCF-7 and MDA-MB-231 cells. 0.5% of high-res tomato extract contained approximately 20 µM of total resveratrol (Table 4ii) and did not affect the metabolic status of either cell line. Co-treatment with Rosc (10 µM) and increasing concentrations of high-res tomato extract resulted in a 15% reduction in the metabolic status of MCF-7 cells that was statistically significant ($p<0.05$) at the highest combinatorial treatment dose of 0.5% of high-res extract and 10 µM of Rosc (Figure 4.3 B).

Combinatorial treatment with high-res tomato extract and 10 µM of Rosc resulted in a weak but statistically significant reduction in metabolic activity in response to treatment with low concentrations of high-res extract (0.1% and 0.2%) and 10 µM of Rosc (Figure 4.3 B). However, co-treatment with the highest dose of high-res tomato extract (0.5%) did not reduce the metabolic activity of MDA-MB-231 cells, which suggests that the putative the co-treatment effects observed with low concentrations of high-res extract might be due to experimental variation.

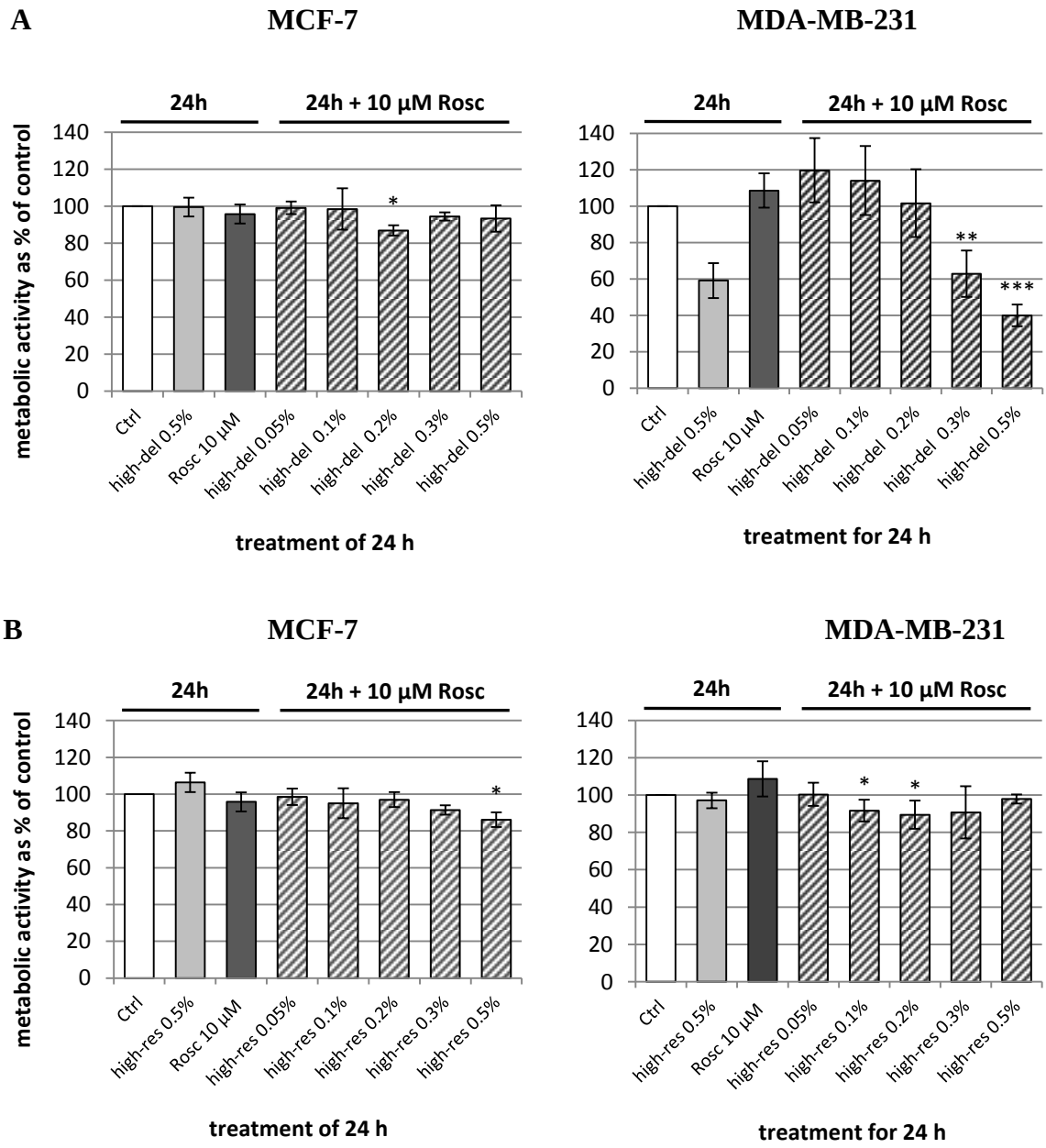

Figure 4.3: Combinatorial effects of roscovitine (Rosc) and (**A**) high-delphinidin tomato extract (high-del) or (**B**) high-resveratrol tomato extract (high-res) on metabolic activity of MCF-7 and MDA-MB-231 cells were investigated. Cells were exposed to Rosc, high-del or high-res alone, or to a combination of Rosc and high-del or Rosc and high-res to the concentrations indicated. Results are expressed as a percentage of cell metabolic activity after treatment relative to the untreated control. Data shown as mean ± standard error (n=3 technical replicates. Experiments were performed at least twice). The statistical significance of the effect of combined treatment compared to the treatment with 10 µM Rosc alone was determined.

* $p<0.05$; ** $p<0.01$; *** $p<0.001$.

4.4.5 Combinatorial effects of tomato extracts and doxorubicin

The co-treatment effects between high-del or high-res tomato extracts and Dox on the metabolic status of MCF-7 and MDA-MB-231 cells were investigated. Treatment with 5 µM of Dox alone resulted in a reduction in metabolic activity of MCF-7 and MDA-MB-231 cells by 40% and 70%, respectively.

Treatment with 0.5% high-del tomato extract inhibited metabolic activity of MDA-MB-231 cells by 40% but had no effect on MCF-7 cells. In MCF-7, the co-treatment with 5 µM of Dox and low doses of high-del tomato extract (0.05%, 0.1% and 0.2%) stimulated metabolic activity significantly ($p<0.01$; Figure 4.4 A). However, at higher combinatorial concentrations of high-res extract the stimulatory effect was lost and metabolic activity was similar to that of Dox alone.

Similarly, stimulatory effects were observed in MDA-MB-231 cells in response to co-treatment with low doses of high-del tomato extract and 5 µM of Dox compared to Dox treatment alone (Figure 4.4 A). However, at increasing co-treatment concentrations of high-del tomato extract (0.3% and 0.5%) cell metabolic activity was significantly reduced compared to treatment with Dox alone indicating potentially synergistic effects, although those were small.

As observed previously, treatment with 0.5% of high-res extract which corresponded to 20 µM of total resveratrol did not inhibit the metabolic activity of either cell line. The metabolic status of MCF-7 cells appeared to be slightly decreased, but not statistically significantly, in response to co-treatment with higher doses of high-res extract compared to treatment with Dox alone (Figure 4.4 B).

In MDA-MB-231 cells, combinatorial treatment of 5 µM of Dox and 0.5% of high-res tomato extract significantly reduced the metabolic activity of MDA-MB-231 cells compared to treatment with Dox alone (Figure 4.4 B) indicating synergistic effects between the two treatments.

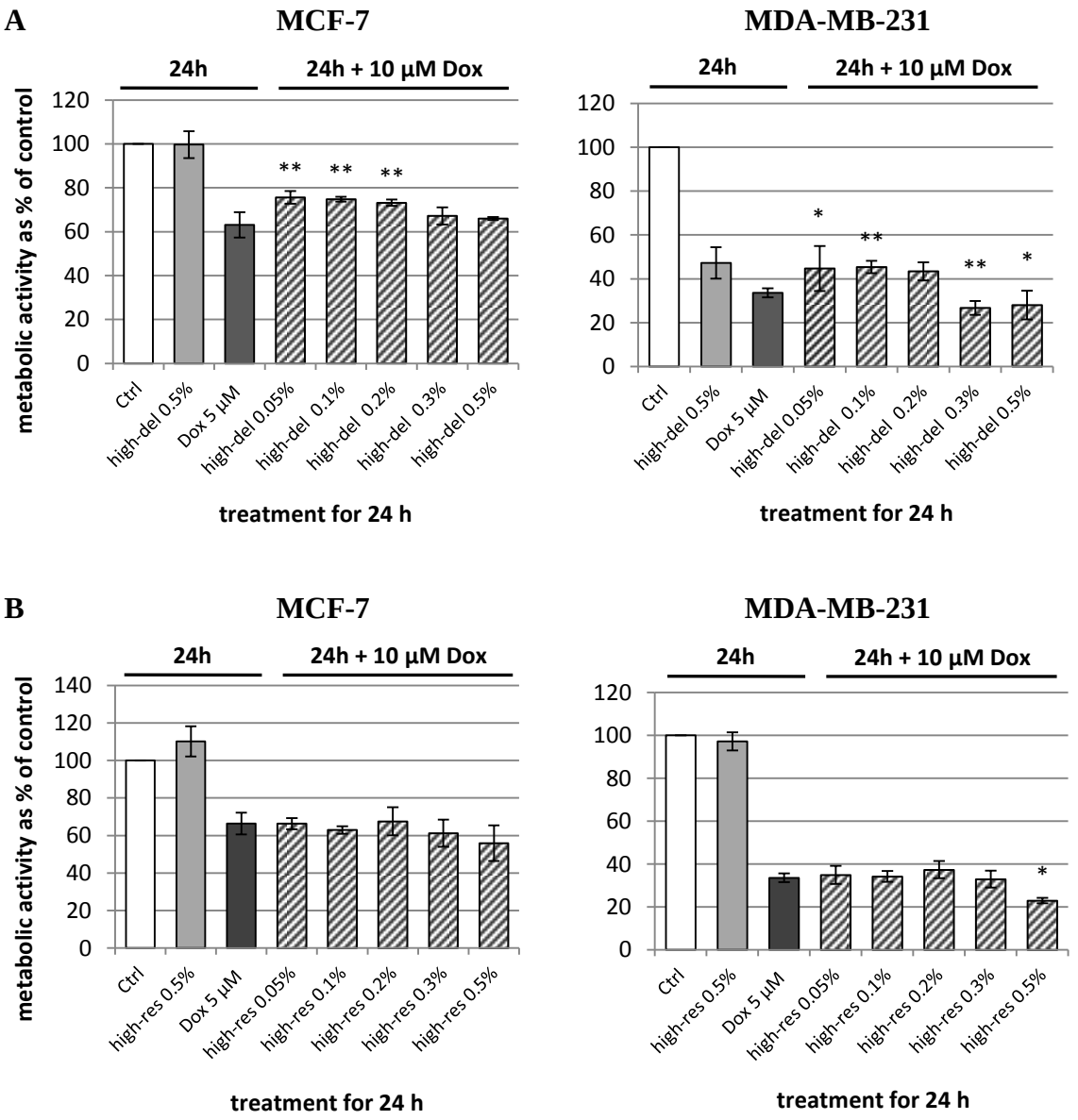

Figure 4.4: Combinatorial effects of doxorubicin (Dox) and (**A**) high-delphinidin tomato extract (high-del) or (**B**) high-resveratrol tomato extract (high-res) on proliferation of MCF-7 and MDA-MB-231 cells were investigated. Cells were exposed to Dox, high-del or high-res alone, or to a combination of Dox and high-del or Dox and high-res to the concentrations indicated. Results are expressed as a percentage of cell metabolic activity after treatment relative to the untreated control. Data shown as mean ± standard error (n=3 technical replicates. Experiments were performed at least twice). The statistical significance of the effect of combined treatment compared to the treatment with 5 µM Dox alone was determined.

* $p<0.05$; ** $p<0.01$.

4.5 Discussion

I investigated the potential co-treatment effects of resveratrol, high-del or high-res tomato extracts and the chemotherapeutic agents, Dox or Rosc. Dox, also known under the brand name Adriamycin, is commonly used to treat certain leukaemias and Hodgkin's lymphoma, as well as cancers of the bladder, breast, stomach, lung, ovaries, thyroid, soft tissue sarcoma and multiple myeloma. Rosc is an experimental drug candidate that is currently undergoing Phase II clinical trials for the treatment of cancers like non-small cell lung cancer and B-cell lymphomas, including multiple myeloma.

Chemotherapeutic drugs are indispensable for the treatment of most cancers and often used in conjunction with radiation and surgery to inhibit or prevent the formation of metastases. Their mode of actions depends on the chemotherapeutic agent but they commonly interfere with DNA and RNA synthesis, including the prevention of DNA replication and translation (e.g. inhibition of topoisomerases such as Doc), DNA intercalation or alteration of the cell cycle (e.g. cyclin-dependent kinase (CDK) inhibitors like Rosc) or mitotic inhibitors such as paclitaxel, which can block the formation of microtubules that is essential angiogenesis and metastasis. As proliferation and growth is de-regulated and up-regulated in cancer cells, they are often more susceptible to cytotoxic agents that interfere with these parameters than normal, non-cancerous cells. However, many of chemotherapy treatment effects are systemic affecting not just aberrant cells as most cytotoxic agents lack the specificity to discriminate between normal and cancerous cells. Fast-dividing cells of the body, such as blood cells and the cells lining the mouth, stomach, and intestines are particularly susceptible to drug-induced damage that may result in the severe side effects commonly associated with chemotherapy such as fatigue, anaemia, suppression of the immune system, gastrointestinal distress, nausea and hair-loss, infertility and organ-damage, particularly cardiotoxicity.

Development and clinical trials of agents that specifically target abnormal cells are currently underway to minimize the effects on non-target tissues. For example, the development of drugs that target molecules only expressed on the surface of tumour cells are amongst the most promising strategies that are currently explored (Maeda et al., 2009, van Rijt and Sadler, 2009, Petros and DeSimone, 2010). Furthermore, there is scope for significant improvements to existing cytotoxic agents like enhanced delivery

of cytotoxic compounds to the tumour cells (e.g. through the use of nanoparticles or tissue-specific antibodies) or the use of adjuvants that increase sensitization of tumours or prevent the development of resistance to cytotoxic agents.

Polyphenolic compounds are among those natural compounds that have received substantial scientific and medical interest due to their anti-cancer and anti-inflammatory properties and their low or minor systemic toxicity. To date, several studies reported the use of polyphenolic compounds as adjuvants in the treatment of cancer cells with chemotherapeutic agents (Węsierska-Gądek et al., 2008, Raffoul et al., 2006, Fukui et al., 2010, Gill et al., 2007, Jazirehi and Bonavida, 2004).

Węsierska-Gądek and colleagues (2008) reported that the addition of non-toxic doses of resveratrol potentiated the antiproliferative effects of Rosc on MCF-7 breast cancer cells. I was able to confirm the results reported by Węsierska-Gądek for MCF-7 cells and performed the same experiment with the MDA-MB-231 breast cancer cell line. Resveratrol alone reduced the metabolic activity of MCF-7 cell by at least 35% but did not inhibit the metabolic activity of MDA-MB-231 cells up to a treatment concentration of 100 µM (Table 4i A). In contrast, treatment with resveratrol alone stimulated the metabolic activity of MDA-MB-231 significantly. A resveratrol-induced stimulation of metabolic activity of MDA-MB-231 was also observed in combination with non-cytotoxic levels of Rosc (5 µM; Figure 4.2 A).

The concomitant use of Dox and resveratrol did not significantly impede the metabolic status of either cell lines but treatment with 5 µM of Dox and non-toxic doses of resveratrol (25 µM) increased the metabolic status of MCF-7 cells (Figure 4.2 B). Several studies have demonstrated that co-treatment with resveratrol can potentiate drug-induced apoptosis in certain cancer cell types (Węsierska-Gądek et al., 2008, Kweon et al., 2010, Komina and Węsierska-Gądek, 2008, Casanova et al., 2012). However, there are some conflicting reports suggesting that resveratrol may promote tumour growth and attenuate drug-induced apoptosis in cancer cells. Delphinidin, for example, induced proliferation and apoptosis in human colon carcinoma cells *in vitro* and inhibited tumour-induced lymph node lymphangiogenesis in tumour-bearing rats *in vivo* but strongly promoted tumour growth and metastasis to the lymph nodes of rats developing tumours derived from rat mammary carcinoma cells (Thiele et al., 2013).

Castillo-Pichardo et al. (2013) also reported increased mammary tumour growth (derived from MDA-MB-231 and the highly metastatic MDA-MB-435 breast cancer cell lines) and metastasis in immunocompromised mice after feed supplementation with resveratrol. Fukui et al. (2010) showed that concomitant use of resveratrol reduced apoptosis of several breast cancer cell lines, including MDA-MB-231, that were treated with paclitaxel, a microtubule-targeting agent that induces G2/M cell cycle arrest as well as apoptosis. However, another study reported the resveratrol-mediated sensitization of non-Hodgkin's lymphoma and multiple myeloma cell lines to paclitaxel-induced apoptosis (Jazirehi and Bonavida, 2004).

To date, publications reporting the chemopreventive and -sensitizing effects of resveratrol, outweigh those reporting any adverse effects associated with resveratrol. However, it is evident that the pharmacological effects associated with resveratrol differ strongly between independent studies and are also highly dependent on the cell type and model used. For example, at 100 µM, I observed resveratrol-mediated inhibition of metabolic activity of MCF-7 breast cancer cells but stimulatory effects on MDA-MB-231 cells. Similarly, Pozo-Guisado et al. (2002) observed resveratrol-mediated apoptosis and alteration of the cell cycle in MCF-7 but not in MDA-MB-231. These cell lines differ in their biochemical characteristics such as the oestrogen dependence of ER^+ MCF-7 cells and the oestrogen independence of ER^- MDA-MB-231 cells which may affect their response and sensitivity to certain pharmacological agents. Some of the contradictory results regarding the chemopreventive and –sensitizing effects of phytochemicals such as resveratrol may be the result of their multiple modes of action that are strongly dependent on dosage and cell type and affect their ability to potentiate or interfere with some cytotoxic agents.

I also investigated the co-treatment effects of the chemotherapeutic compounds, Dox and Rosc, with high-del or high-res tomato extracts on the metabolic status of breast cancer cells. Despite many reports on the protective and inhibitory effects of anthocyanins on different cancer cell lines and tumours, there are no reports on the effects of combinatorial treatments including anthocyanin supplements or anthocyanin-rich extracts and chemotherapeutic agents. I used extracts from the delphinidin-containing high-del tomatoes in combination with Dox and Rosc to identify any synergistic effects affecting the metabolic status of human breast cancer cells.

The addition of low, non-toxic concentrations of high-del extracts increased the metabolic status of cells treated with Dox and Rosc, an effect that was not observed with the addition of the high-res extract. This suggests that at non-toxic concentrations, high-del extracts may be protective leading to attenuation of doxorubicin-mediated toxicity in MDA-MB-231 cells (Figure 4.4 A). I observed the same increase in metabolic activity after treatment with low doses of purified resveratrol indicating that phytochemicals can act as stimulants or inhibitors depending on the concentrations to which the cells are exposed. However, the concomitant use of Dox and Rosc and 0.5% high-del extract potentiated the effects of drug-induced inhibition of the metabolic status of MDA-MB-231 cells but not MCF-7 cells (Figure 4.3 A and 4.4. A). Co-treatment with high-res tomato extract weakly potentiated the inhibition of metabolic activity of Dox and Rosc-treated MCF-7 cells (Figure 4.3 B and 4.4. B). Combinatorial use of 0.5% of high-res tomato extract and Dox reduced the metabolic status of MDA-MB-231 cells by almost 50% compared to the treatment with Dox alone but had little effect on Rosc-treated cells (Figure 4.4 B).

The results from the combinatorial use of tomato extracts and cytotoxic agents highlighted the complex mechanisms that are responsible for chemosensitization and chemoprevention. In the MDA-MB-231 cells, for example, a clear correlation between increasing concentrations of high-del extracts and increased cytotoxic effects of Dox and Rosc was observed suggesting that anthocyanin-containing tomato extracts and chemotherapeutic agents may act synergistically to exert stronger cytotoxic effects than each treatment alone. These synergisms were not observed in the MCF-7 cells which suggest that at least some of the mechanisms responsible for inducing the cytotoxic effects may be associated with targets that are unique to particular cell types. Anthocyanins are thought to exert their anti-cancer activities through modulation of signalling pathways involved in the induction of apoptosis or cell cycle regulation (Chen et al., 2006b, Xia et al., 2009, Lee et al., 2009, Lee et al., 2010, Huang et al., 2011, Afaq et al., 2005). The combination of compounds, which individually target different components of the cancer cell, may partly explain the synergistic or additive effects observed with combinatorial treatment. However, anthocyanins and other polyphenolic compounds may also improve or reverse drug resistance of cancer cells by chemosensitizing them to the cytotoxic drugs. Several plant compounds, including

flavonoids have been shown to inhibit the function of multidrug resistance (MDR) proteins which are present in the majority of human tumours and are strongly associated with tumour resistance and subsequently, therapeutic failure (Molnár et al., 2008, Wink et al., 2012). Co-formulation of Dox and curcumin, for example, suppressed the development of multidrug resistance in human leukaemia (K562) cells (Misra and Sahoo, 2011).

The ability of many phytochemicals to regulate a wide network of different signalling pathways that directly affect the survival of cancer cells through induction of apoptosis, alteration of the cell cycle or indirectly through prevention of resistance development to other cytotoxic agents are likely to explain the chemosensitizing effects observed. The inconsistency in the reports and the variability between different cell lines makes it difficult to interpret the data and make some reliable predictions for further application. More *in vivo* animal studies are required to confirm whether synergistic effects between physiologically relevant concentrations of phytochemicals and chemotherapy drugs also take place in a whole organism. Cells in tissues distal to the gastrointestinal tract are unlikely to be exposed to polyphenol (or their metabolites) concentrations exceeding nanomolar ranges. However, cells lining the gastrointestinal tract may experience much higher concentrations of these bioactives and are actively involved in their uptake and biochemical modification. Novel formulations such as encapsulation of food bioactives, that increase bioavailability or stability of polyphenolic compounds and facilitate controlled release of bioactive food additives are currently being explored (Gandía-Herrero et al., 2010, Kropat et al., 2013). However, it is essential to rule out any combinatorial effects that might interfere with the efficacy of chemotherapy drugs before recommending the use of phytochemicals as adjuvants in chemotherapy treatment. Despite the lack of clear evidence for the efficacy of polyphenols as therapeutic adjuvant, their dietary consumption may still confer substantial health benefits by stimulating the body's immune response and enhance its protection from chemotherapy-induced side effects. Due to their severe systemic toxicity, chemotherapeutic agents are usually delivered in intervals in order to allow the body the recover in between treatments. Plant polyphenolics are natural constituents of the human diet with low or no systemic toxicity and no adverse health effects have been associated with a high intake of fruit and vegetables. These compounds may not be highly effective as single anti-cancer agents but their combinatorial use with

chemotherapeutic agents may open up new avenues for more specific and effective targeting of tumour cells or reduce the systemic effects of chemotherapeutic drug regimes (Younes-Sakr et al., 2012). Dietary chemosensitization is an emerging field in pharmacology but due to the lack of reliable clinical data, no recommendations have been established. However, there is strong evidence from chemoprevention studies that phytochemicals or their food sources can inhibit the proliferation and growth of tumour cells and induce immune responses that may target cancer cells directly or can protect against the systemic effects of cytotoxic agents.

5 Summary and future directions

To date, plant metabolic engineering has been used successfully to enrich different plants, including model species such as *Arabidopsis* as well as important crop species, with essential and health-beneficial nutrients or to reduce the content of toxic or undesirable compounds. The Golden Rice Project development of β-carotene-enriched rice heralded the use of metabolic engineering for the nutritional enhancement of crops with health-promoting or essential dietary components. Golden rice, developed to combat vitamin-A deficiency in developing countries, demonstrated the potential of plant metabolic engineering, where previous conventional breeding approaches had failed.

5.1 Metabolic engineering to control different anthocyanin branches in tomato

Plant polyphenols are the largest and most diverse group of secondary metabolites, and amongst them, anthocyanins are probably the most ubiquitous and conspicuous compounds. To date, more than 600 different anthocyanins have been identified and their structural identity and decoration varies significantly between individual species and clades. Few plants produce all three structural classes of anthocyanins that are defined by the number of hydroxyl groups on the phenyl B-ring (pelargonidin, cyanidin, delphinidin), yet accumulation of anthocyanins of all three classes is found in the fruit of mulberry, pomegranate and black currents (Engmann et al., 2013, Noda et al., 2001, Slimestad and Solheim, 2002). However, the majority of plants accumulate no more than twenty different molecular structures that belong to one or two classes of anthocyanins.

Substrate specificity of late anthocyanin biosynthetic pathway enzymes is often associated with failure to synthesise a particular structural group, while a lack of activation of early biosynthetic genes is linked to the total absence of anthocyanins.

Commercial tomato varieties do not accumulate anthocyanins in the fruit due to the absence of transcriptional activation of the structural genes involved in anthocyanin biosynthesis (Figure 2.1). Introgression with wild relatives that synthesise anthocyanins in fruit resulted in the cold- and light-inducible accumulation of anthocyanins in the

peel of tomatoes (Povero et al., 2011). Conventional breeding strategies have, however, failed to induce production of anthocyanins in the pericarp of the tomato fruit. Metabolic engineering of the tomato flavonoid metabolism using anthocyanin-specific transcription factors from *A. majus*, resulted in the accumulation of high amounts of anthocyanins in the fruit (Butelli et al., 2008). The anthocyanin-enriched tomatoes developed by Butelli accumulated up 3 mg/g FW of anthocyanins, amounts that are comparable to those found in many berries.

The pharmacological properties of anthocyanins are well studied both *in vitro* and *in vivo* and dietary consumption has been associated with a reduced risk of developing CVDs, type 2 diabetes, cancer, inflammatory bowel disease and many other non-communicable diseases (discussed in Chapter 1.6). Butelli's transgenic, anthocyanin-enriched tomatoes significantly prolonged the lifespan of cancer-prone *Trp53*$^{-/-}$ mice by delaying or slowing down the onset of the disease. These observations provided strong evidence that nutritional enhancement of food crops through plant metabolic engineering is a promising and effective strategy to deliver health-promoting compounds and combat dietary-related chronic diseases.

How anthocyanins exert their health-promoting effects remains unclear. Most compounds appear to modulate signalling and regulatory pathways implicated in disease development and progression but there is mounting evidence that they may interact directly with the DNA through modulation of epigenetic modifications. Little is known however, about the impact of structural variation of individual compounds on the biological activity of these compounds and how the food matrix affects their bioavailability and efficacy *in vivo*.

I used metabolic engineering to develop new tomato lines that accumulate mono- and dihydroxylated anthocyanins in their fruit which would allow us to compare the biological activity of different structural classes of anthocyanins to the trihydroxylated anthocyanins of the purple tomatoes in the physicochemical environment of the same food matrix. The transcriptional regulators *Delila* and *Rosea*1, which control anthocyanin biosynthesis in the flowers of *A. majus*, successfully activated the production of trihydroxylated anthocyanins in *Del/Ros*1 tomatoes (Butelli et al., 2008). Substrate specificity of tomato DFR for DHM impeded the formation of mono- and

dihydroxylated anthocyanins in *Del/Ros*1 tomato fruit. I demonstrated that inhibition of F3'5'H and introduction of a substrate-independent DFR from *A. majus* could induce accumulation of pelargonidin- and cyanidin-type anthocyanins in tomato fruit of *AmDfr/Del/Ros*1/*f3'5'h*$^{-/-}$. The total amount of anthocyanins accumulated by the *AmDfr/Del/Ros*1/*f3'5'h*$^{-/-}$ line was, however 2.5 fold below that of the delphinidin-accumulating *Del/Ros*1 line. I hypothesised that failure of *Del* and *Ros*1to upregulate *f3'h* activity in the flesh of *AmDfr/Del/Ros*1/*f3'5'h*$^{-/-}$significantly was responsible for the low level accumulation of cyanidins and the presence of pelargonidins in the fruit flesh.

In order to generate tomato plants accumulating only monohydroxylated anthocyanins, I concomitantly inhibited F3'H and F3'5H activity using *f3'h* RNAi and the *f3'5'h* mutation, which resulted in plants that failed to self-pollinate and develop fruit. The *a* mutant, which lacked F3'5'H activity, was characterised by a reduced amount of fruit development compared to WT plants. The observation that inactivation of F3'5H reduced fertility and loss of both F3'H and F3'5'H resulted in infertile plants suggested that these structural enzymes are involved gametogenesis or pollen tube formation. The engineering of a tomato line that produces only monohydroxylated anthocyanins may not be possible, if the activity of F3'H is an essential requirement for fruit development.

5.2 Accumulation of anthocyanins enhanced the health benefits of tomatoes

The novel anthocyanin tomato line, *AmDfr/Del/Ros*1/*f3'5'h*$^{-/-}$, accumulated, however, substantial amounts of predominantly monohydroxylated anthocyanins. The comparison with the *Del/Ros*1 tomato line revealed that fruit extracts of both anthocyanin tomato lines induced alterations in the cell cycle and strong proapoptotic effects by activating proapoptotic caspases in the human breast cancer cell lines, MCF-7 and MDA-MB-231. Extracts of WT tomato fruit had no biological effects on the breast cancer cell lines suggesting that the anthocyanins, possibly in synergy with other compounds in the extracts of *Del/Ros*1 and *AmDfr/Del/Ros*1/*f3'5'h*$^{-/-}$, exerted the tumoricidal effects. Treatment with purified dietary supplements such as rutin, delphinidin-3-glucose, and anthocyanins purified from *Del/Ros*1 tomato fruit had little or no effect on the metabolic

activity of MCF-7 and MDA-MB-231 cells. These findings indicate that phytochemicals such as anthocyanins are more effective in the physicochemical environment of the food matrix, where their biological effects are potentiated through interaction with other compounds. A number of studies have reported reduced biological effects of dietary supplements compared to their whole food sources (Prior et al., 2008, Titta et al., 2010). The complex interactions between the constituents of food that might explain the potentiating effects of the food matrix on the biological activity of anthocyanins and other phytonutrients remain to be elucidated. It is possible that other components in the food matrix enhance the uptake or tissue delivery of poorly bioavailable compounds such as anthocyanins. On their own, these different dietary compounds may have only weak biological activity, but by acting on multiple targets in the disease pathway their combinatorial effects could be much more powerful. Since phytonutrients such as anthocyanins are always consumed in foods, it is important to define their bioactivities within the context of the food matrix. Anthocyanins in berry extracts, for example, may not have the same bioactivity as anthocyanins in tomato extracts, which could explain much of the incoherent and inconclusive results from epidemiological studies that investigated general dietary patterns rather than individual food groups.

Supplementation of WT tomato extract, which did not display anti-cancer activity, with purified anthocyanins should be performed to test the hypothesis that the food matrix and its different components impact the biological effects observed with the high-anthocyanin tomato lines. If anthocyanin-supplemented WT tomato extracts exerted stronger biological activity than purified anthocyanins, this would provide evidence that food matrix components are implicated in the strong biological effects observed with the high-anthocyanin transgenic tomato extracts.

5.3 How can plant metabolic engineering contribute to human nutrition and health?

Many chronic, non-communicable diseases have been associated with the dietary and habitual changes of a modern Westernized lifestyle. Global incidences of cancer, CVDs and type 2 diabetes are highest in Westernized cultures and on the rise in emerging

economies as they adopt a Westernized lifestyle. Lack of exercise and an unhealthy diet have been identified has the leading factors behind the global obesity epidemic and are associated with most cases of CVDs and certain types of cancer. The 5-a-day campaign, that was introduced to raise awareness for the benefits of a healthier diet and increase intake of fruit and vegetables (Foerster et al., 1995), has, so far, failed to significantly promote healthier eating behaviour across all population groups.

Access to large amounts of different fruit and vegetables that would naturally deliver these bioactives may be difficult for certain population groups and in many countries due to the inaccessibility or high costs associated with them. Malnutrition and deficiency in micronutrients and phytochemicals can be significantly reduced through biofortification of popular crop species such as maize, rice, wheat, potato and tomato using plant metabolic engineering (Zhao and Shewry, 2011). Plant metabolic engineering is a powerful tool that can be used to increase the amount of specific bioactive compounds through upregulation or activation of metabolic pathways (e.g. golden rice, high-flavonol or high-carotenoid tomatoes).

Advances in the fields of pharmacology and epidemiology investigating the mechanisms that govern the biological effects of phytonutrients and understanding of the relationship between dietary habits and the prevalence of certain non-communicable diseases should be considered in future crop improvement strategies. A concerted approach using evidence from clinical studies, nutrition and pharmacology is required to develop novel crop species that meet the nutritional demands of future generations and deliver appropriate amounts of the compounds that are important for maintaining and promoting health.

6 References

ADAMS, K. F., SCHATZKIN, A., HARRIS, T. B., KIPNIS, V., MOUW, T., BALLARD-BARBASH, R., HOLLENBECK, A. & LEITZMANN, M. F. 2006. Overweight, Obesity, and Mortality in a Large Prospective Cohort of Persons 50 to 71 Years Old. *New England Journal of Medicine,* 355**,** 763-778.

AFAQ, F., SALEEM, M., KRUEGER, C. G., REED, J. D. & MUKHTAR, H. 2005. Anthocyanin- and hydrolyzable tannin-rich pomegranate fruit extract modulates MAPK and NF-κB pathways and inhibits skin tumorigenesis in CD-1 mice. *International Journal of Cancer,* 113**,** 423-433.

AHARONI, A., DE VOS, C. H. R., WEIN, M., SUN, Z., GRECO, R., KROON, A., MOL, J. N. M. & O'CONNELL, A. P. 2001. The strawberry FaMYB1 transcription factor suppresses anthocyanin and flavonol accumulation in transgenic tobacco. *The Plant Journal,* 28**,** 319-332.

AMERICAN INSTITUTE FOR CANCER RESEARCH, 1997. Food, nutrition, and the prevention of cancer: A global perspective. *Washington, DC: American Institute for Cancer Research*.

ANAND, P., KUNNUMAKKARA, A. B., SUNDARAM, C., HARIKUMAR, K. B., THARAKAN, S. T., LAI, O. S., SUNG, B. & AGGARWAL, B. B. 2008. Cancer is a preventable disease that requires major lifestyle changes. *Pharm Res,* 25**,** 2097-116.

ANDERSEN, Ø. M. & JORDHEIM, M. (eds.) 2006. *The Anthocyanins,* Boca Raton, Florida: CRC Press.

ARMSTRONG, B. & DOLL, R. 1975. Environmental factors and cancer incidence and mortality in different countries, with special reference to dietary practices. *Int J Cancer,* 15**,** 617-31.

ASHKENAZI, A. 2002. Targeting death and decoy receptors of the tumour-necrosis factor superfamily. *Nature Reviews Cancer,* 2**,** 420-430.

AURA, A. M., MARTIN-LOPEZ, P., O'LEARY, K. A., WILLIAMSON, G., OKSMAN-CALDENTEY, K. M., POUTANEN, K. & SANTOS-BUELGA, C. 2005. In vitro metabolism of anthocyanins by human gut microflora. *European Journal of Nutrition,* 44**,** 133-142.

BACKHED, F., DING, H., WANG, T., HOOPER, L. V., KOH, G. Y., NAGY, A., SEMENKOVICH, C. F. & GORDON, J. I. 2004. The

gut microbiota as an environmental factor that regulates fat storage. *Proc Natl Acad Sci U S A,* 101**,** 15718-23.

BAI, C., TWYMAN, R. M., FARRE, G., SANAHUJA, G., CHRISTOU, P., CAPELL, T. & ZHU, C. F. 2011. A golden era-pro-vitamin A enhancement in diverse crops. *In Vitro Cellular & Developmental Biology-Plant,* 47**,** 205-221.

BAI, Y., MAO, Q.-Q., QIN, J., ZHENG, X.-Y., WANG, Y.-B., YANG, K., SHEN, H.-F. & XIE, L.-P. 2010. Resveratrol induces apoptosis and cell cycle arrest of human T24 bladder cancer cells in vitro and inhibits tumor growth in vivo. *Cancer Science,* 101**,** 488-493.

BAUDRY, A., HEIM, M. A., DUBREUCQ, B., CABOCHE, M., WEISSHAAR, B. & LEPINIEC, L. 2004. TT2, TT8, and TTG1 synergistically specify the expression of BANYULS and proanthocyanidin biosynthesis in Arabidopsis thaliana. *The Plant Journal,* 39**,** 366-380.

BELD, M., MARTIN, C., HUITS, H., STUITJE, A. R. & GERATS, A. G. M. 1989. Flavonoid synthesis in Petunia hybrida: partial characterization of dihydroflavonol-4-reductase genes. *Plant Molecular Biology,* 13**,** 491-502.

BENETOU, V., TRICHOPOULOU, A., ORFANOS, P., NASKA, A., LAGIOU, P., BOFFETTA, P. & TRICHOPOULOS, D. 2008. Conformity to traditional Mediterranean diet and cancer incidence: the Greek EPIC cohort. *Br J Cancer,* 99**,** 191-5.

BISSELL, M. J., RADISKY, D. C., RIZKI, A., WEAVER, V. M. & PETERSEN, O. W. 2002. The organizing principle: microenvironmental influences in the normal and malignant breast. *Differentiation,* 70**,** 537-546.

BOFFETTA, P., COUTO, E., WICHMANN, J., FERRARI, P., TRICHOPOULOS, D., BUENO-DE-MESQUITA, H. B., VAN DUIJNHOVEN, F. J. B., BÜCHNER, F. L., KEY, T., BOEING, H., NÖTHLINGS, U., LINSEISEN, J., GONZALEZ, C. A., OVERVAD, K., NIELSEN, M. R. S., TJØNNELAND, A., OLSEN, A., CLAVEL-CHAPELON, F., BOUTRON-RUAULT, M.-C., MOROIS, S., LAGIOU, P., NASKA, A., BENETOU, V., KAAKS, R., ROHRMANN, S., PANICO, S., SIERI, S., VINEIS, P., PALLI, D., VAN GILS, C. H., PEETERS, P. H., LUND, E., BRUSTAD, M., ENGESET, D., HUERTA, J. M., RODRÍGUEZ, L., SÁNCHEZ, M.-J., DORRONSORO, M., BARRICARTE, A., HALLMANS, G., JOHANSSON, I., MANJER, J., SONESTEDT, E., ALLEN, N. E., BINGHAM, S., KHAW, K.-T., SLIMANI, N., JENAB, M., MOUW, T., NORAT, T., RIBOLI, E. & TRICHOPOULOU, A. 2010. Fruit and Vegetable Intake and Overall Cancer Risk in the European

Prospective Investigation Into Cancer and Nutrition (EPIC). *Journal of the National Cancer Institute,* 102**,** 529-537.
BORKOWSKI, T., SZYMUSIAK, H., GLISZCZYNSKA-SWIGLO, A. & TYRAKOWSKA, B. 2005. The effect of 3-O-[beta]-glucosylation on structural transformations of anthocyanidins. *Food Research International,* 38**,** 1031-1037.
BOULTON, R. 2001. The Copigmentation of Anthocyanins and Its Role in the Color of Red Wine: A Critical Review. *Am. J. Enol. Vitic.,* 52**,** 67-87.
BOVY, A., DE VOS, R., KEMPER, M., SCHIJLEN, E., ALMENAR PERTEJO, M., MUIR, S., COLLINS, G., ROBINSON, S., VERHOEYEN, M., HUGHES, S., SANTOS-BUELGA, C. & VAN TUNEN, A. 2002. High-Flavonol Tomatoes Resulting from the Heterologous Expression of the Maize Transcription Factor Genes LC and C1. *Plant Cell,* 14**,** 2509 - 2526.
BOYA, P., GONZÁLEZ-POLO, R.-A., CASARES, N., PERFETTINI, J.-L., DESSEN, P., LAROCHETTE, N., MÉTIVIER, D., MELEY, D., SOUQUERE, S., YOSHIMORI, T., PIERRON, G., CODOGNO, P. & KROEMER, G. 2005. Inhibition of Macroautophagy Triggers Apoptosis. *Molecular and Cellular Biology,* 25**,** 1025-1040.
BROUILLARD, R. (ed.) 1988. *Flavonoids and flower colour,* London: Chapman and Hall Ltd.
BROUILLARD, R. & DELAPORTE, B. 1977. Chemistry of anthocyanin pigments. 2. Kinetic and thermodynamic study of proton transfer, hydration, and tautomeric reactions of malvidin 3-glucoside. *Journal of the American Chemical Society,* 99**,** 8461-8468.
BURBULIS, I. E., IACOBUCCI, M. & SHIRLEY, B. W. 1996. A Null Mutation in the First Enzyme of Flavonoid Biosynthesis Does Not Affect Male Fertility in Arabidopsis. *Plant Cell,* 8**,** 1013-1025.
BUTELLI, E., TITTA, L., GIORGIO, M., MOCK, H.-P., MATROS, A., PETEREK, S., SCHIJLEN, E. G. W. M., HALL, R. D., BOVY, A. G., LUO, J. & MARTIN, C. 2008. Enrichment of tomato fruit with health-promoting anthocyanins by expression of select transcription factors. *Nat Biotech,* 26**,** 1301-1308.
CAI, H., MARCZYLO, T. H., TELLER, N., BROWN, K., STEWARD, W. P., MARKO, D. & GESCHER, A. J. 2010. Anthocyanin-rich red grape extract impedes adenoma development in the ApcMin mouse: Pharmacodynamic changes and anthocyanin levels in the murine biophase. *European Journal of Cancer,* 46**,** 811-817.
CALLE, E. E. & KAAKS, R. 2004. Overweight, obesity and cancer: epidemiological evidence and proposed mechanisms. *Nat Rev Cancer,* 4**,** 579-91.

CALLE, E. E., RODRIGUEZ, C., WALKER-THURMOND, K. & THUN, M. J. 2003. Overweight, Obesity, and Mortality from Cancer in a Prospectively Studied Cohort of U.S. Adults. *New England Journal of Medicine,* 348**,** 1625-1638.

CARMELIET, P. 2005. Angiogenesis in life, disease and medicine. *Nature,* 438**,** 932-6.

CARMICHAEL, A. R. 2006. Obesity and prognosis of breast cancer. *Obesity Reviews,* 7**,** 333-340.

CARRERA-BASTOS, P. 2011. The western diet and lifestyle and diseases of civilization. *Research Reports in Clinical Cardiology,* 2**,** 11.

CASANOVA, F., QUARTI, J., DA COSTA, D. C., RAMOS, C. A., DA SILVA, J. L. & FIALHO, E. 2012. Resveratrol chemosensitizes breast cancer cells to melphalan by cell cycle arrest. *J Cell Biochem,* 113**,** 2586-96.

CASTAÑEDA-OVANDO, A., PACHECO-HERNÁNDEZ, M. D. L., PÁEZ-HERNÁNDEZ, M. E., RODRÍGUEZ, J. A. & GALÁN-VIDAL, C. A. 2009. Chemical studies of anthocyanins: A review. *Food Chemistry,* 113**,** 859-871.

CASTILLO-PICHARDO, L., CUBANO, L. A. & DHARMAWARDHANE, S. 2013. Dietary grape polyphenol resveratrol increases mammary tumor growth and metastasis in immunocompromised mice. *BMC Complement Altern Med,* 13**,** 6.

CHAI, T. T., PANIRCHELLVUM, E., ONG, H. C. & WONG, F. C. 2012. Phenolic contents and antioxidant properties of Stenochlaena palustris, an edible medicinal fern. *Botanical Studies,* 53**,** 439-446.

CHEN, P.-N., CHU, S.-C., CHIOU, H.-L., KUO, W.-H., CHIANG, C.-L. & HSIEH, Y.-S. 2006a. Mulberry anthocyanins, cyanidin 3-rutinoside and cyanidin 3-glucoside, exhibited an inhibitory effect on the migration and invasion of a human lung cancer cell line. *Cancer Letters,* 235**,** 248-259.

CHEN, P.-N., KUO, W.-H., CHIANG, C.-L., CHIOU, H.-L., HSIEH, Y.-S. & CHU, S.-C. 2006b. Black rice anthocyanins inhibit cancer cells invasion via repressions of MMPs and u-PA expression. *Chemico-Biological Interactions,* 163**,** 218-229.

CHOE, Y. J., HA, T. J., KO, K. W., LEE, S. Y., SHIN, S. J. & KIM, H. S. 2012. Anthocyanins in the black soybean (Glycine max L.) protect U2OS cells from apoptosis by inducing autophagy via the activation of adenosyl monophosphate-dependent protein kinase. *Oncol Rep,* 28**,** 2049-56.

COOKE, D., SCHWARZ, M., BOOCOCK, D., WINTERHALTER, P., STEWARD, W. P., GESCHER, A. J. & MARCZYLO, T. H. 2006. Effect of cyanidin-3-glucoside and an anthocyanin mixture from bilberry on adenoma development in the ApcMin mouse model of

intestinal carcinogenesis—Relationship with tissue anthocyanin levels. *International Journal of Cancer,* 119**,** 2213-2220.
CORDAIN, L., EATON, S. B., SEBASTIAN, A., MANN, N., LINDEBERG, S., WATKINS, B. A., O'KEEFE, J. H. & BRAND-MILLER, J. 2005. Origins and evolution of the Western diet: health implications for the 21st century. *The American Journal of Clinical Nutrition,* 81**,** 341-354.
CORDAIN, L., MILLER, J. B., EATON, S. B., MANN, N., HOLT, S. H. & SPETH, J. D. 2000. Plant-animal subsistence ratios and macronutrient energy estimations in worldwide hunter-gatherer diets. *The American Journal of Clinical Nutrition,* 71**,** 682-692.
DAVIES, K. M. 2010. *Metabolic Engineering of Bioactive Phenylpropanoids in Crops*.
DAVIES, K. M. & SCHWINN, K. E. (eds.) 2006. *Molecular Biology and Biotechnology of Flavonoid Biosynthesis,* Boca Raton, Florida: CRC Press.
DAVULURI, G. R., VAN TUINEN, A., FRASER, P. D., MANFREDONIA, A., NEWMAN, R., BURGESS, D., BRUMMELL, D. A., KING, S. R., PALYS, J., UHLIG, J., BRAMLEY, P. M., PENNINGS, H. M. & BOWLER, C. 2005. Fruit-specific RNAi-mediated suppression of DET1 enhances carotenoid and flavonoid content in tomatoes. *Nat Biotechnol,* 23**,** 890-5.
DE JONG, W. S., EANNETTA, N. T., JONG, D. M. & BODIS, M. 2004. Candidate gene analysis of anthocyanin pigmentation loci in the Solanaceae. *Theoretical and Applied Genetics,* 108**,** 423-432.
DE LORGERIL, M., SALEN, P., MARTIN, J. L., MONJAUD, I., BOUCHER, P. & MAMELLE, N. 1998. Mediterranean dietary pattern in a randomized trial: prolonged survival and possible reduced cancer rate. *Arch Intern Med,* 158**,** 1181-7.
DEAPEN, D., LIU, L., PERKINS, C., BERNSTEIN, L. & ROSS, R. K. 2002. Rapidly rising breast cancer incidence rates among Asian-American women. *International Journal of Cancer,* 99**,** 747-750.
DELUC, L., BARRIEU, F., MARCHIVE, C., LAUVERGEAT, V., DECENDIT, A., RICHARD, T., CARDE, J.-P., MÉRILLON, J.-M. & HAMDI, S. 2006. Characterization of a Grapevine R2R3-MYB Transcription Factor That Regulates the Phenylpropanoid Pathway. *Plant Physiology,* 140**,** 499-511.
DEWS, M., HOMAYOUNI, A., YU, D., MURPHY, D., SEVIGNANI, C., WENTZEL, E., FURTH, E. E., LEE, W. M., ENDERS, G. H., MENDELL, J. T. & THOMAS-TIKHONENKO, A. 2006. Augmentation of tumor angiogenesis by a Myc-activated microRNA cluster. *Nat Genet,* 38**,** 1060-5.

DIXON, R. A. 2005. Engineering of plant natural product pathways. *Current Opinion in Plant Biology,* 8**,** 329-336.

DOLARA, P., LUCERI, C., FILIPPO, C. D., FEMIA, A. P., GIOVANNELLI, L., CADERNI, G., CECCHINI, C., SILVI, S., ORPIANESI, C. & CRESCI, A. 2005. Red wine polyphenols influence carcinogenesis, intestinal microflora, oxidative damage and gene expression profiles of colonic mucosa in F344 rats. *Mutation Research/Fundamental and Molecular Mechanisms of Mutagenesis,* 591**,** 237-246.

EARNSHAW, W. C., MARTINS, L. M. & KAUFMANN, S. H. 1999. MAMMALIAN CASPASES: Structure, Activation, Substrates, and Functions During Apoptosis. *Annual Review of Biochemistry,* 68**,** 383-424.

ENGMANN, N. F., MA, Y., YING, X. & QING, Y. 2013. Investigating the effect of high hydrostatic pressure processing on anthocyanins composition of mulberry (Morus moraceae) juice. *Czech Journal of Food Sciences,* 31**,** 72-80.

EWALD, P. & SWAIN EWALD, H. 2012. Infection, mutation, and cancer evolution. *Journal of Molecular Medicine,* 90**,** 535-541.

FALCHETTI, R., FUGGETTA, M. P., LANZILLI, G., TRICARICO, M. & RAVAGNAN, G. 2001. Effects of resveratrol on human immune cell function. *Life Sciences,* 70**,** 81-96.

FELGINES, C., TEXIER, O., BESSON, C., LYAN, B., LAMAISON, J. L. & SCALBERT, A. 2007. Strawberry pelargonidin glycosides are excreted in urine as intact glycosides and glucuronidated pelargonidin derivatives in rats. *Br J Nutr,* 98**,** 1126-31.

FELGINES, C., TEXIER, O., GARCIN, P., BESSON, C., LAMAISON, J.-L. & SCALBERT, A. 2009. Tissue distribution of anthocyanins in rats fed a blackberry anthocyanin-enriched diet. *Molecular Nutrition & Food Research,* 53**,** 1098-1103.

FENG, R., NI, H.-M., WANG, S. Y., TOURKOVA, I. L., SHURIN, M. R., HARADA, H. & YIN, X.-M. 2007. Cyanidin-3-rutinoside, a Natural Polyphenol Antioxidant, Selectively Kills Leukemic Cells by Induction of Oxidative Stress. *Journal of Biological Chemistry,* 282**,** 13468-13476.

FERNANDES, I., FARIA, A., CALHAU, C., DE FREITAS, V. & MATEUS, N. Bioavailability of anthocyanins and derivatives. *Journal of Functional Foods*.

FERNANDES, I., NAVE, F., GONÇALVES, R., DE FREITAS, V. & MATEUS, N. 2012. On the bioavailability of flavanols and anthocyanins: Flavanol–anthocyanin dimers. *Food Chemistry,* 135**,** 812-818.

FERRARA, N. & KERBEL, R. S. 2005. Angiogenesis as a therapeutic target. *Nature,* 438**,** 967-74.

FOERSTER, S. B., KIZER, K. W., DISOGRA, L. K. & BAL, D. G. 1995. California's "5 a Day —for Better Healthp" Campaign: An innovative population-based effort to effect large-scale dietary change. *American Journal of Preventive Medicine,* 11**,** 124-131.

FORD, D., EASTON, D. F., STRATTON, M., NAROD, S., GOLDGAR, D., DEVILEE, P., BISHOP, D. T., WEBER, B., LENOIR, G., CHANG-CLAUDE, J., SOBOL, H., TEARE, M. D., STRUEWING, J., ARASON, A., SCHERNECK, S., PETO, J., REBBECK, T. R., TONIN, P., NEUHAUSEN, S., BARKARDOTTIR, R., EYFJORD, J., LYNCH, H., PONDER, B. A. J., GAYTHER, S. A., BIRCH, J. M., LINDBLOM, A., STOPPA-LYONNET, D., BIGNON, Y., BORG, A., HAMANN, U., HAITES, N., SCOTT, R. J., MAUGARD, C. M., VASEN, H., SEITZ, S., CANNON-ALBRIGHT, L. A., SCHOFIELD, A. & ZELADA-HEDMAN, M. 1998. Genetic Heterogeneity and Penetrance Analysis of the BRCA1 and BRCA2 Genes in Breast Cancer Families. *The American Journal of Human Genetics,* 62**,** 676-689.

FORKMANN, G. 1991. Flavonoids as Flower Pigments: The Formation of the Natural Spectrum and its Extension by Genetic Engineering. *Plant Breeding,* 106**,** 1-26.

FUKUI, M., YAMABE, N. & ZHU, B. T. 2010. Resveratrol attenuates the anticancer efficacy of paclitaxel in human breast cancer cells in vitro and in vivo. *Eur J Cancer,* 46**,** 1882-91.

FULDA, S. & DEBATIN, K. M. 2004. Sensitization for anticancer drug-induced apoptosis by the chemopreventive agent resveratrol. *Oncogene,* 23**,** 6702-11.

FUNG, T. T., HU, F. B., HOLMES, M. D., ROSNER, B. A., HUNTER, D. J., COLDITZ, G. A. & WILLETT, W. C. 2005. Dietary patterns and the risk of postmenopausal breast cancer. *Int J Cancer,* 116**,** 116-21.

FURUTA, K. 1986. Host preference and population dynamics in an autumnal population of the maple aphid, Periphyllus californiensis Shinji (Homoptera, Aphididae). *Journal of Applied Entomology,* 102**,** 93-100.

GALLUS, S., BOSETTI, C. & VECCHIA, C. L. 2004. Mediterranean diet and cancer risk. *European Journal of Cancer Prevention,* 13**,** 447-452.

GANDÍA-HERRERO, F., JIMÉNEZ-ATIÉNZAR, M., CABANES, J., GARCÍA-CARMONA, F. & ESCRIBANO, J. 2010. Stabilization of the Bioactive Pigment of Opuntia Fruits through Maltodextrin Encapsulation. *Journal of Agricultural and Food Chemistry,* 58**,** 10646-10652.

GILL, C., WALSH, S. E., MORRISSEY, C., FITZPATRICK, J. M. & WATSON, R. W. G. 2007. Resveratrol sensitizes androgen independent prostate cancer cells to death-receptor mediated apoptosis through multiple mechanisms. *The Prostate,* 67**,** 1641-1653.

GOFF, S. A., CONE, K. C. & CHANDLER, V. L. 1992. Functional analysis of the transcriptional activator encoded by the maize B gene: evidence for a direct functional interaction between two classes of regulatory proteins. *Genes Dev,* 6**,** 864-75.

GOLSTEIN, P. & KROEMER, G. 2007. Cell death by necrosis: towards a molecular definition. *Trends in Biochemical Sciences,* 32**,** 37-43.

GOODRICH, J., CARPENTER, R. & COEN, E. S. 1992. A common gene regulates pigmentation pattern in diverse plant species. *Cell,* 68**,** 955-964.

GOULD, K. S., DUDLE, D. A. & NEUFELD, H. S. 2010. Why some stems are red: cauline anthocyanins shield photosystem II against high light stress. *Journal of Experimental Botany,* 61**,** 2707-2717.

GOULD, K. S., MCKELVIE, J. & MARKHAM, K. R. 2002. Do anthocyanins function as antioxidants in leaves? Imaging of H2O2 in red and green leaves after mechanical injury. *Plant, Cell & Environment,* 25**,** 1261-1269.

GRAY, J., CAPARRÓS-RUIZ, D. & GROTEWOLD, E. 2012. Grass phenylpropanoids: Regulate before using! *Plant Science,* 184**,** 112-120.

GREAVES, M. & MALEY, C. 2012. Clonal evolution in cancer. *Nature,* 481**,** 306-313.

GREEN, D. R. & KROEMER, G. 2004. The Pathophysiology of Mitochondrial Cell Death. *Science,* 305**,** 626-629.

GROSSMANN, M., RAY, A., NKHATA, K., MALAKHOV, D., ROGOZINA, O., DOGAN, S. & CLEARY, M. 2010. Obesity and breast cancer: status of leptin and adiponectin in pathological processes. *Cancer and Metastasis Reviews,* 29**,** 641-653.

HADI, S. M., BHAT, S. H., AZMI, A. S., HANIF, S., SHAMIM, U. & ULLAH, M. F. 2007. Oxidative breakage of cellular DNA by plant polyphenols: a putative mechanism for anticancer properties. *Semin Cancer Biol,* 17**,** 370-6.

HALLIWELL, B. 2008. Are polyphenols antioxidants or pro-oxidants? What do we learn from cell culture and in vivo studies? *Archives of Biochemistry and Biophysics,* 476**,** 107-112.

HALLIWELL, B., RAFTER, J. & JENNER, A. 2005. Health promotion by flavonoids, tocopherols, tocotrienols, and other phenols: direct or indirect effects? Antioxidant or not? *The American Journal of Clinical Nutrition,* 81**,** 268S-276S.

HANAHAN, D. & WEINBERG, R. 2000. The Hallmarks of Cancer. *Cell,* 100**,** 57-70.
HANAHAN, D. & WEINBERG, R. 2011. Hallmarks of Cancer: The Next Generation. *Cell,* 144**,** 646-674.
HARBORNE, J. 1965. Anthocyanins in ferns. *Nature,* 207**,** 1.
HAVAUX, M. & KLOPPSTECH, K. 2001. The protective functions of carotenoid and flavonoid pigments against excess visible radiation at chilling temperature investigated in Arabidopsis npq and tt mutants. *Planta,* 213**,** 953-966.
HIDALGO, M., ORUNA-CONCHA, M. J., KOLIDA, S., WALTON, G. E., KALLITHRAKA, S., SPENCER, J. P. E., GIBSON, G. R. & DE PASCUAL-TERESA, S. 2012. Metabolism of Anthocyanins by Human Gut Microflora and Their Influence on Gut Bacterial Growth. *Journal of Agricultural and Food Chemistry,* 60**,** 3882-3890.
HILLMAN, G. G., WANG, Y., KUCUK, O., CHE, M., DOERGE, D. R., YUDELEV, M., JOINER, M. C., MARPLES, B., FORMAN, J. D. & SARKAR, F. H. 2004. Genistein potentiates inhibition of tumor growth by radiation in a prostate cancer orthotopic model. *Molecular Cancer Therapeutics,* 3**,** 1271-1279.
HO, M.-L., CHEN, P.-N., CHU, S.-C., KUO, D.-Y., KUO, W.-H., CHEN, J.-Y. & HSIEH, Y.-S. 2010. Peonidin 3-Glucoside Inhibits Lung Cancer Metastasis by Downregulation of Proteinases Activities and MAPK Pathway. *Nutrition and Cancer,* 62**,** 505-516.
HOSHINO, A., MORITA, Y., CHOI, J.-D., SAITO, N., TOKI, K., TANAKA, Y. & IIDA, S. 2003. Spontaneous Mutations of the Flavonoid 3′-hydroxylase Gene Conferring Reddish Flowers in the Three Morning Glory Species. *Plant and Cell Physiology,* 44**,** 990-1001.
HUANG, H.-P., CHANG, Y.-C., WU, C.-H., HUNG, C.-N. & WANG, C.-J. 2011. Anthocyanin-rich Mulberry extract inhibit the gastric cancer cell growth in vitro and xenograft mice by inducing signals of p38/p53 and c-jun. *Food Chemistry,* 129**,** 1703-1709.
HUI, C., BIN, Y., XIAOPING, Y., LONG, Y., CHUNYE, C., MANTIAN, M. & WENHUA, L. 2010. Anticancer Activities of an Anthocyanin-Rich Extract From Black Rice Against Breast Cancer Cells In Vitro and In Vivo. *Nutrition and Cancer,* 62**,** 1128-1136.
HÜTTEMANN, M., PECINA, P., RAINBOLT, M., SANDERSON, T. H., KAGAN, V. E., SAMAVATI, L., DOAN, J. W. & LEE, I. 2011. The multiple functions of cytochrome c and their regulation in life and death decisions of the mammalian cell: From respiration to apoptosis. *Mitochondrion,* 11**,** 369-381.

HWANG, Y. P., CHOI, J. H., HAN, E. H., KIM, H. G., WEE, J.-H., JUNG, K. O., JUNG, K. H., KWON, K.-I., JEONG, T. C., CHUNG, Y. C. & JEONG, H. G. 2011a. Purple sweet potato anthocyanins attenuate hepatic lipid accumulation through activating adenosine monophosphate–activated protein kinase in human HepG2 cells and obese mice. *Nutrition Research,* 31**,** 896-906.

HWANG, Y. P., CHOI, J. H., YUN, H. J., HAN, E. H., KIM, H. G., KIM, J. Y., PARK, B. H., KHANAL, T., CHOI, J. M., CHUNG, Y. C. & JEONG, H. G. 2011b. Anthocyanins from purple sweet potato attenuate dimethylnitrosamine-induced liver injury in rats by inducing Nrf2-mediated antioxidant enzymes and reducing COX-2 and iNOS expression. *Food and Chemical Toxicology,* 49**,** 93-99.

ISHIGURO, K., TANIGUCHI, M. & TANAKA, Y. 2012. Functional analysis of Antirrhinum kelloggii flavonoid 3'-hydroxylase and flavonoid 3',5'-hydroxylase genes; critical role in flower color and evolution in the genus Antirrhinum. *J Plant Res,* 125**,** 451-6.

JÄNICKE, R. U., SPRENGART, M. L., WATI, M. R. & PORTER, A. G. 1998. Caspase-3 Is Required for DNA Fragmentation and Morphological Changes Associated with Apoptosis. *Journal of Biological Chemistry,* 273**,** 9357-9360.

JAZIREHI, A. R. & BONAVIDA, B. 2004. Resveratrol modifies the expression of apoptotic regulatory proteins and sensitizes non-Hodgkin's lymphoma and multiple myeloma cell lines to paclitaxel-induced apoptosis. *Mol Cancer Ther,* 3**,** 71-84.

JOE, A. K., LIU, H., SUZUI, M., VURAL, M. E., XIAO, D. & WEINSTEIN, I. B. 2002. Resveratrol Induces Growth Inhibition, S-phase Arrest, Apoptosis, and Changes in Biomarker Expression in Several Human Cancer Cell Lines. *Clinical Cancer Research,* 8**,** 893-903.

JOHNSON, E., RYU, S., YI, H., SHIN, B., CHEONG, H. & CHOI, G. 2001a. Alteration of a single amino acid changes the substrate specificity of dihydroflavonol 4-reductase. *The Plant Journal,* 25**,** 325 - 333.

JOHNSON, E. T., RYU, S., YI, H., SHIN, B., CHEONG, H. & CHOI, G. 2001b. Alteration of a single amino acid changes the substrate specificity of dihydroflavonol 4-reductase. *The Plant Journal,* 25**,** 325-333.

JONES, C. M., MES, P. & MYERS, J. R. 2003. Characterization and Inheritance of the Anthocyanin fruit (Aft) Tomato. *Journal of Heredity,* 94**,** 449-456.

JÖNSSON, T., GRANFELDT, Y., AHRÉN, B., BRANELL, U. C., PÅLSSON, G., HANSSON, A., SÖDERSTRÖM, M. & LINDEBERG, S. 2009. Beneficial effects of a Paleolithic diet on

cardiovascular risk factors in type 2 diabetes: a randomized cross-over pilot study. *Cardiovascular diabetology,* 8**,** 35.
JORGENSEN, R. A., QUE, Q. D. & NAPOLI, C. A. 2002. Maternally-controlled ovule abortion results from cosuppression of dihydroflavonol-4-reductase or flavonoid-3 ',5 '-hydroxylase genes in Petunia hybrida. *Functional Plant Biology,* 29**,** 1501-1506.
KANG, S.-Y., SEERAM, N. P., NAIR, M. G. & BOURQUIN, L. D. 2003. Tart cherry anthocyanins inhibit tumor development in ApcMin mice and reduce proliferation of human colon cancer cells. *Cancer Letters,* 194**,** 13-19.
KATO, I., TOMINAGA, S. & KUROISHI, T. 1987. Relationship between westernization of dietary habits and mortality from breast and ovarian cancers in Japan. *Jpn J Cancer Res,* 78**,** 349-57.
KAUSAR, H., JEYABALAN, J., AQIL, F., CHABBA, D., SIDANA, J., SINGH, I. P. & GUPTA, R. C. 2012. Berry anthocyanidins synergistically suppress growth and invasive potential of human non-small-cell lung cancer cells. *Cancer Letters,* 325**,** 54-62.
KENNY, P. A., LEE, G. Y., MYERS, C. A., NEVE, R. M., SEMEIKS, J. R., SPELLMAN, P. T., LORENZ, K., LEE, E. H., BARCELLOS-HOFF, M. H., PETERSEN, O. W., GRAY, J. W. & BISSELL, M. J. 2007. The morphologies of breast cancer cell lines in three-dimensional assays correlate with their profiles of gene expression. *Mol Oncol,* 1**,** 84-96.
KERR, J. F., WYLLIE, A. H. & CURRIE, A. R. 1972. Apoptosis: a basic biological phenomenon with wide-ranging implications in tissue kinetics. *Br J Cancer,* 26**,** 239-57.
KING, M.-C., MARKS, J. H., MANDELL, J. B. & GROUP, T. N. Y. B. C. S. 2003. Breast and Ovarian Cancer Risks Due to Inherited Mutations in BRCA1 and BRCA2. *Science,* 302**,** 643-646.
KOMINA, O. & WĘSIERSKA-GĄDEK, J. 2008. Action of resveratrol alone or in combination with roscovitine, a CDK inhibitor, on cell cycle progression in human HL-60 leukemia cells. *Biochemical Pharmacology,* 76**,** 1554-1562.
KONG, J.-M., CHIA, L.-S., GOH, N.-K., CHIA, T.-F. & BROUILLARD, R. 2003. Analysis and biological activities of anthocyanins. *Phytochemistry,* 64**,** 923-933.
KROON, P. A., CLIFFORD, M. N., CROZIER, A., DAY, A. J., DONOVAN, J. L., MANACH, C. & WILLIAMSON, G. 2004. How should we assess the effects of exposure to dietary polyphenols in vitro? *The American Journal of Clinical Nutrition,* 80**,** 15-21.
KROPAT, C., BETZ, M., KULOZIK, U., LEICK, S., REHAGE, H., BOETTLER, U., TELLER, N. & MARKO, D. 2013. Effect of Microformulation on the Bioactivity of an Anthocyanin-rich Bilberry

Pomace Extract (Vaccinium myrtillus L.) in Vitro. *Journal of Agricultural and Food Chemistry,* 61**,** 4873-4881.
KUBASEK, W. L., SHIRLEY, B. W., MCKILLOP, A., GOODMAN, H. M., BRIGGS, W. & AUSUBEL, F. M. 1992. Regulation of Flavonoid Biosynthetic Genes in Germinating Arabidopsis Seedlings. *Plant Cell,* 4**,** 1229-1236.
KWEON, S. H., SONG, J. H. & KIM, T. S. 2010. Resveratrol-mediated reversal of doxorubicin resistance in acute myeloid leukemia cells via downregulation of MRP1 expression. *Biochemical and Biophysical Research Communications,* 395**,** 104-110.
LA VECCHIA, C. 2004. Mediterranean diet and cancer. *Public Health Nutr,* 7**,** 965-8.
LAMBERT, J. D., SANG, S. & YANG, C. S. 2007. Possible Controversy over Dietary Polyphenols: Benefits vs Risks. *Chemical Research in Toxicology,* 20**,** 583-585.
LAMY, S., BLANCHETTE, M., MICHAUD-LEVESQUE, J., LAFLEUR, R., DUROCHER, Y., MOGHRABI, A., BARRETTE, S., GINGRAS, D. & BÉLIVEAU, R. 2006. Delphinidin, a dietary anthocyanidin, inhibits vascular endothelial growth factor receptor-2 phosphorylation. *Carcinogenesis,* 27**,** 989-996.
LAZZE, M. C., SAVIO, M., PIZZALA, R., CAZZALINI, O., PERUCCA, P., SCOVASSI, A. I., STIVALA, L. A. & BIANCHI, L. 2004. Anthocyanins induce cell cycle perturbations and apoptosis in different human cell lines. *Carcinogenesis,* 25**,** 1427-1433.
LEE, S. H., PARK, S. M., PARK, S. M., PARK, J. H., SHIN, D. Y., KIM, G. Y., RYU, C. H., SHIN, S. C., JUNG, J. M., KANG, H. S., LEE, W. S. & CHOI, Y. H. 2009. Induction of apoptosis in human leukemia U937 cells by anthocyanins through down-regulation of Bcl-2 and activation of caspases. *Int J Oncol,* 34**,** 1077-83.
LEE, Y. K., LEE, W. S., KIM, G. S. & PARK, O. J. 2010. Anthocyanins are novel AMPKalpha1 stimulators that suppress tumor growth by inhibiting mTOR phosphorylation. *Oncol Rep,* 24**,** 1471-7.
LEVINE, A. J. 1997. p53, the Cellular Gatekeeper for Growth and Division. *Cell,* 88**,** 323-331.
LEWIS, C. E., WALKER, J. R. L., LANCASTER, J. E. & SUTTON, K. H. 1998. Determination of anthocyanins, flavonoids and phenolic acids in potatoes. I: Coloured cultivars of Solanum tuberosum L. *Journal of the Science of Food and Agriculture,* 77**,** 45-57.
LI, Y., AHMED, F., ALI, S., PHILIP, P. A., KUCUK, O. & SARKAR, F. H. 2005. Inactivation of Nuclear Factor κB by Soy Isoflavone Genistein Contributes to Increased Apoptosis Induced by Chemotherapeutic Agents in Human Cancer Cells. *Cancer Research,* 65**,** 6934-6942.

LINDEBERG, S. 2012. Paleolithic diets as a model for prevention and treatment of western disease. *American Journal of Human Biology,* 24**,** 110-115.

LINDEBERG, S., JÖNSSON, T., GRANFELDT, Y., BORGSTRAND, E., SOFFMAN, J., SJÖSTRÖM, K. & AHRÉN, B. 2007. A Palaeolithic diet improves glucose tolerance more than a Mediterranean-like diet in individuals with ischaemic heart disease. *Diabetologia,* 50**,** 1795-1807.

LINK, A., BALAGUER, F. & GOEL, A. 2010. Cancer chemoprevention by dietary polyphenols: Promising role for epigenetics. *Biochemical Pharmacology,* 80**,** 1771-1792.

LIU, A. G., VOLKER, S. E., JEFFERY, E. H. & ERDMAN, J. W. 2009. Feeding Tomato and Broccoli Powders Enriched with Bioactives Improves Bioactivity Markers in Rats. *Journal of Agricultural and Food Chemistry,* 57**,** 7304-7310.

LIU, X., LI, P., WIDLAK, P., ZOU, H., LUO, X., GARRARD, W. T. & WANG, X. 1998. The 40-kDa subunit of DNA fragmentation factor induces DNA fragmentation and chromatin condensation during apoptosis. *Proc Natl Acad Sci U S A,* 95**,** 8461-6.

LIU, X., ZOU, H., SLAUGHTER, C. & WANG, X. 1997. DFF, a Heterodimeric Protein That Functions Downstream of Caspase-3 to Trigger DNA Fragmentation during Apoptosis. *Cell,* 89**,** 175-184.

LIVASY, C. A., KARACA, G., NANDA, R., TRETIAKOVA, M. S., OLOPADE, O. I., MOORE, D. T. & PEROU, C. M. 2006. Phenotypic evaluation of the basal-like subtype of invasive breast carcinoma. *Mod Pathol,* 19**,** 264-71.

LORD, C. J. & ASHWORTH, A. 2012. The DNA damage response and cancer therapy. *Nature,* 481**,** 287-94.

LU, J. N., LEE, W. S., YUN, J. W., KIM, M. J., KIM, H. J., KIM, D. C., JEONG, J.-H., CHOI, Y. H., KIM, G.-S., RYU, C. H. & SHIN, S. C. 2013. Anthocyanins from Vitis coignetiae Pulliat Inhibit Cancer Invasion and Epithelial-Mesenchymal Transition, but These Effects Can Be Attenuated by Tumor Necrosis Factor in Human Uterine Cervical Cancer HeLa Cells. *Evidence-Based Complementary and Alternative Medicine,* 2013**,** 11.

LUO, J., BUTELLI, E., HILL, L., PARR, A., NIGGEWEG, R., BAILEY, P., WEISSHAAR, B. & MARTIN, C. 2008. AtMYB12 regulates caffeoyl quinic acid and flavonol synthesis in tomato: expression in fruit results in very high levels of both types of polyphenol. *The Plant Journal,* 56**,** 316-326.

LUO, J., SOLIMINI, N. L. & ELLEDGE, S. J. 2009. Principles of Cancer Therapy: Oncogene and Non-oncogene Addiction. *Cell,* 136**,** 823-837.

MAEDA, H., BHARATE, G. Y. & DARUWALLA, J. 2009. Polymeric drugs for efficient tumor-targeted drug delivery based on EPR-effect. *European Journal of Pharmaceutics and Biopharmaceutics,* 71**,** 409-419.

MALIK, M., ZHAO, C., SCHOENE, N., GUISTI, M. M., MOYER, M. P. & MAGNUSON, B. A. 2003. Anthocyanin-Rich Extract From Aronia meloncarpa E. Induces a Cell Cycle Block in Colon Cancer but Not Normal Colonic Cells. *Nutrition and Cancer,* 46**,** 186-196.

MANACH, C., WILLIAMSON, G., MORAND, C., SCALBERT, A. & RÉMÉSY, C. 2005. Bioavailability and bioefficacy of polyphenols in humans. I. Review of 97 bioavailability studies. *The American Journal of Clinical Nutrition,* 81**,** 230S-242S.

MANSON, M. M. 2003. Cancer prevention -- the potential for diet to modulate molecular signalling. *Trends Mol Med,* 9**,** 11-8.

MARKWICK, N. P., POULTON, J., ESPLEY, R. V., ROWAN, D. D., MCGHIE, T. K., WADASINGHE, G., WOHLERS, M., JIA, Y. & ALLAN, A. C. 2013. Red-foliaged apples affect the establishment, growth, and development of the light brown apple moth, Epiphyas postvittana. *Entomologia Experimentalis et Applicata,* 146**,** 261-275.

MARTIN, C., BUTELLI, E., PETRONI, K. & TONELLI, C. 2011. How Can Research on Plants Contribute to Promoting Human Health? *Plant Cell,* 23**,** 1685-1699.

MARTIN, C. & GERATS, T. 1993. Control of Pigment Biosynthesis Genes during Petal Development. *Plant Cell,* 5**,** 1253-1264.

MARTIN, C. & PAZ-ARES, J. 1997. MYB transcription factors in plants. *Trends in Genetics,* 13**,** 67-73.

MARTIN, C., PRESCOTT, A., MACKAY, S., BARTLETT, J. & VRIJLANDT, E. 1991. Control of anthocyanin biosynthesis in flowers of Antirrhinum majus. *The Plant Journal,* 1**,** 37-49.

MARTIN, C., ZHANG, Y., TONELLI, C. & PETRONI, K. 2013. Plants, Diet, and Health. *Annual Review of Plant Biology,* 64**,** 19-46.

MARTINS, C. P., BROWN-SWIGART, L. & EVAN, G. I. 2006. Modeling the therapeutic efficacy of p53 restoration in tumors. *Cell,* 127**,** 1323-34.

MASTERS, R. K., POWERS, D. A. & LINK, B. G. 2013. Obesity and US Mortality Risk Over the Adult Life Course. *American Journal of Epidemiology,* 177**,** 431-442.

MATHEWS, H., CLENDENNEN, S. K., CALDWELL, C. G., LIU, X. L., CONNORS, K., MATHEIS, N., SCHUSTER, D. K., MENASCO, D. J., WAGONER, W., LIGHTNER, J. & WAGNER, D. R. 2003. Activation Tagging in Tomato Identifies a Transcriptional Regulator of Anthocyanin Biosynthesis, Modification, and Transport. *Plant Cell,* 15**,** 1689-1703.

MATSUI, K., UMEMURA, Y. & OHME-TAKAGI, M. 2008. AtMYBL2, a protein with a single MYB domain, acts as a negative regulator of anthocyanin biosynthesis in Arabidopsis. *The Plant Journal,* 55**,** 954-967.

MAZZA, G. & BROUILLARD, R. 1987. Recent developments in the stabilization of anthocyanins in food products. *Food Chemistry,* 25**,** 207-225.

MAZZA, G. & MINIATI, E. (eds.) 1993. *Anthocyanins in Fruits, Vegetables, and Grains,* Boca Rato, USA.

MES, P. J., BOCHES, P., MYERS, J. R. & DURST, R. 2008. Characterization of Tomatoes Expressing Anthocyanin in the Fruit. *Journal of the American Society for Horticultural Science,* 133**,** 262-269.

MESSINA, M. & HILAKIVI-CLARKE, L. 2009. Early Intake Appears to Be the Key to the Proposed Protective Effects of Soy Intake Against Breast Cancer. *Nutrition and Cancer,* 61**,** 792-798.

MEYER, P., HEIDMANN, I., FORKMANN, G. & SAEDLER, H. 1987. A new petunia flower colour generated by transformation of a mutant with a maize gene. *Nature,* 330**,** 677-678.

MICHELS, K. B., MOHLLAJEE, A. P., ROSET-BAHMANYAR, E., BEEHLER, G. P. & MOYSICH, K. B. 2007. Diet and breast cancer: a review of the prospective observational studies. *Cancer,* 109**,** 2712-49.

MISRA, R. & SAHOO, S. K. 2011. Coformulation of doxorubicin and curcumin in poly(D,L-lactide-co-glycolide) nanoparticles suppresses the development of multidrug resistance in K562 cells. *Mol Pharm,* 8**,** 852-66.

MOLNÁR, J., ENGI, H., GYÉMÁNT, N., SCHELZ, Z., SPENGLER, G., OCSOVSKI, I., SZÜCS, M., HOHMANN, J., SZABO, M., TANÁCS, L., MOLNÁR, P., DELI, J., KRENN, L., KAWASE, M., WAKABAYASHI, H., KURIHARA, T., SHIRATAKI, Y., SAKAGAMI, H., MOTOHASHI, N. & DIDIZIAPETRIS, R. 2008. Multidrug Resistance Reversal on Cancer Cells by Selected Carotenoids, Flavonoids and Anthocyanins. *In:* MOTOHASHI, N. (ed.) *Bioactive Heterocycles VI.* Springer Berlin Heidelberg.

MUIR, S. R., COLLINS, G. J., ROBINSON, S., HUGHES, S., BOVY, A., RIC DE VOS, C. H., VAN TUNEN, A. J. & VERHOEYEN, M. E. 2001. Overexpression of petunia chalcone isomerase in tomato results in fruit containing increased levels of flavonols. *Nat Biotech,* 19**,** 470-474.

NAIR, S. K. & BURLEY, S. K. 2000. Recognizing DNA in the library. *Nature,* 404**,** 715, 717-8.

NIELSEN, S. L. & SIMONSEN, A. M. 2011. Photosynthesis and photoinhibition in two differently coloured varieties of Oxalis triangularis — the effect of anthocyanin content. *Photosynthetica,* 49**,** 346-352.

NODA, Y., KANEYUKI, T., MORI, A. & PACKER, L. 2001. Antioxidant Activities of Pomegranate Fruit Extract and Its Anthocyanidins: Delphinidin, Cyanidin, and Pelargonidin. *Journal of Agricultural and Food Chemistry,* 50**,** 166-171.

NOMURA, A. M., WILKENS, L. R., MURPHY, S. P., HANKIN, J. H., HENDERSON, B. E., PIKE, M. C. & KOLONEL, L. N. 2008. Association of vegetable, fruit, and grain intakes with colorectal cancer: the Multiethnic Cohort Study. *The American Journal of Clinical Nutrition,* 88**,** 730-737.

O'KEEFE JR, J. H. & CORDAIN, L. 2004. Cardiovascular Disease Resulting From a Diet and Lifestyle at Odds With Our Paleolithic Genome: How to Become a 21st-Century Hunter-Gatherer. *Mayo Clinic Proceedings,* 79**,** 101-108.

OVASKAINEN, M.-L., TÖRRÖNEN, R., KOPONEN, J. M., SINKKO, H., HELLSTRÖM, J., REINIVUO, H. & MATTILA, P. 2008. Dietary Intake and Major Food Sources of Polyphenols in Finnish Adults. *The Journal of Nutrition,* 138**,** 562-566.

PAGE, J. E. & TOWERS, G. H. 2002. Anthocyanins protect light-sensitive thiarubrine phototoxins. *Planta,* 215**,** 478-84.

PAINE, J. A., SHIPTON, C. A., CHAGGAR, S., HOWELLS, R. M., KENNEDY, M. J., VERNON, G., WRIGHT, S. Y., HINCHLIFFE, E., ADAMS, J. L., SILVERSTONE, A. L. & DRAKE, R. 2005. Improving the nutritional value of Golden Rice through increased pro-vitamin A content. *Nature Biotechnology,* 23**,** 482-487.

PARK, E. J. & PEZZUTO, J. M. 2002. Botanicals in cancer chemoprevention. *Cancer Metastasis Rev,* 21**,** 231-55.

PARK, S. H., HANNING, I., GILBERT, W., MUNRO, M., DEVAREDDY, L. & RICKE, S. C. 2013. Feeding mice aged and fresh blackberries powder supplements result in shifts in the gastrointestinal microflora. *Food Bioscience,* 1**,** 66-72.

PARKAR, S. G., STEVENSON, D. E. & SKINNER, M. A. 2008. The potential influence of fruit polyphenols on colonic microflora and human gut health. *International Journal of Food Microbiology,* 124**,** 295-298.

PETRONI, K. & TONELLI, C. 2011. Recent advances on the regulation of anthocyanin synthesis in reproductive organs. *Plant Science,* 181**,** 219-229.

PETROS, R. A. & DESIMONE, J. M. 2010. Strategies in the design of nanoparticles for therapeutic applications. *Nature Reviews Drug Discovery,* 9**,** 615-627.

PIERCE, J. P., NATARAJAN, L., CAAN, B. J., PARKER, B. A., GREENBERG, E. R., FLATT, S. W., ROCK, C. L., KEALEY, S., AL-DELAIMY, W. K., BARDWELL, W. A., CARLSON, R. W., EMOND, J. A., FAERBER, S., GOLD, E. B., HAJEK, R. A., HOLLENBACH, K., JONES, L. A., KARANJA, N., MADLENSKY, L., MARSHALL, J., NEWMAN, V. A., RITENBAUGH, C., THOMSON, C. A., WASSERMAN, L. & STEFANICK, M. L. 2007. Influence of a diet very high in vegetables, fruit, and fiber and low in fat on prognosis following treatment for breast cancer: the Women's Healthy Eating and Living (WHEL) randomized trial. *JAMA,* 298**,** 289-98.

POLLAK, P. E., HANSEN, K., ASTWOOD, J. D. & TAYLOR, L. P. 1995. Conditional male fertility in maize. *Sexual Plant Reproduction,* 8**,** 231-241.

POMMIER, Y., SORDET, O., ANTONY, S., HAYWARD, R. L. & KOHN, K. W. 2004. Apoptosis defects and chemotherapy resistance: molecular interaction maps and networks. *Oncogene,* 23**,** 2934-2949.

POP, C. & SALVESEN, G. S. 2009. Human Caspases: Activation, Specificity, and Regulation. *Journal of Biological Chemistry,* 284**,** 21777-21781.

POVERO, G., GONZALI, S., BASSOLINO, L., MAZZUCATO, A. & PERATA, P. 2011. Transcriptional analysis in high-anthocyanin tomatoes reveals synergistic effect of Aft and atv genes. *Journal of Plant Physiology,* 168**,** 270-279.

POZO-GUISADO, E., ALVAREZ-BARRIENTOS, A., MULERO-NAVARRO, S., SANTIAGO-JOSEFAT, B. & FERNANDEZ-SALGUERO, P. M. 2002. The antiproliferative activity of resveratrol results in apoptosis in MCF-7 but not in MDA-MB-231 human breast cancer cells: cell-specific alteration of the cell cycle. *Biochemical Pharmacology,* 64**,** 1375-1386.

PRENTICE, R. L., CAAN, B., CHLEBOWSKI, R. T. & ET AL. 2006. Low-fat dietary pattern and risk of invasive breast cancer: The women's health initiative randomized controlled dietary modification trial. *Journal of the American Medical Association,* 295**,** 629-642.

PRIOR, R. L., WU, X., GU, L., HAGER, T. J., HAGER, A. & HOWARD, L. R. 2008. Whole berries versus berry anthocyanins: interactions with dietary fat levels in the C57BL/6J mouse model of obesity. *J Agric Food Chem,* 56**,** 647-53.

PRITCHARD, J. K. 2010. How we are evolving. *Sci Am,* 303**,** 40-7.

PROTANI, M., COORY, M. & MARTIN, J. 2010. Effect of obesity on survival of women with breast cancer: systematic review and meta-analysis. *Breast Cancer Research and Treatment,* 123**,** 627-635.
QUATTROCCHIO, F., WING, J., WOUDE, K., MOL, J. & KOES, R. 1998. Analysis of bHLH and MYB domain proteins: species-specific regulatory differences are caused by divergent evolution of target anthocyanin genes. *The Plant Journal,* 13**,** 475 - 488.
RAFFOUL, J., WANG, Y., KUCUK, O., FORMAN, J., SARKAR, F. & HILLMAN, G. 2006. Genistein inhibits radiation-induced activation of NF-kappaB in prostate cancer cells promoting apoptosis and G2/M cell cycle arrest. *BMC Cancer,* 6**,** 107.
RAHMAN, I., BISWAS, S. K. & KIRKHAM, P. A. 2006. Regulation of inflammation and redox signaling by dietary polyphenols. *Biochem Pharmacol,* 72**,** 1439-52.
RAUSHER, M. D. 2008. Evolutionary Transition in Floral Color. *International Journal of Plant Sciences,* 169**,** 14.
REDDIVARI, L., VANAMALA, J., CHINTHARLAPALLI, S., SAFE, S. H. & MILLER, J. C., JR 2007. Anthocyanin fraction from potato extracts is cytotoxic to prostate cancer cells through activation of caspase-dependent and caspase-independent pathways. *Carcinogenesis,* 28**,** 2227-2235.
ROBERTS, C. K. & BARNARD, R. J. 2005. Effects of exercise and diet on chronic disease. *Journal of Applied Physiology,* 98**,** 3-30.
ROBINSON, G. M. & ROBINSON, R. 1931. A survey of anthocyanins. I. *Biochemistry Journal,* 25**,** 1687-1705.
ROSATI, C., AQUILANI, R., DHARMAPURI, S., PALLARA, P., MARUSIC, C., TAVAZZA, R., BOUVIER, F., CAMARA, B. & GIULIANO, G. 2000. Metabolic engineering of beta-carotene and lycopene content in tomato fruit. *The Plant Journal,* 24**,** 413-420.
SAHARA, S., AOTO, M., EGUCHI, Y., IMAMOTO, N., YONEDA, Y. & TSUJIMOTO, Y. 1999. Acinus is a caspase-3-activated protein required for apoptotic chromatin condensation. *Nature,* 401**,** 168-73.
SALAMONE, F., LI VOLTI, G., TITTA, L., PUZZO, L., BARBAGALLO, I., LA DELIA, F., ZELBER-SAGI, S., MALAGUARNERA, M., PELICCI, P. G., GIORGIO, M. & GALVANO, F. 2012. Moro orange juice prevents fatty liver in mice. *World journal of gastroenterology,* 18**,** 3862-3868.
SALAS-SALVADÓ, J., BULLÓ, M., BABIO, N., MARTÍNEZ-GONZÁLEZ, M. Á., IBARROLA-JURADO, N., BASORA, J., ESTRUCH, R., COVAS, M. I., CORELLA, D., ARÓS, F., RUIZ-GUTIÉRREZ, V., ROS, E. & INVESTIGATORS, F. T. P. S. 2011. Reduction in the Incidence of Type 2 Diabetes With the

Mediterranean Diet: Results of the PREDIMED-Reus nutrition intervention randomized trial. *Diabetes Care,* 34**,** 14-19.
SATOH, H., NISHIKAWA, K., SUZUKI, K., ASANO, R., VIRGONA, N., ICHIKAWA, T., HAGIWARA, K. & YANO, T. 2003. Genistein, a soy isoflavone, enhances necrotic-like cell death in a breast cancer cell treated with a chemotherapeutic agent. *Res Commun Mol Pathol Pharmacol,* 113-114**,** 149-58.
SAURA-CALIXTO, F., SERRANO, J. & GOÑI, I. 2007. Intake and bioaccessibility of total polyphenols in a whole diet. *Food Chemistry,* 101**,** 492-501.
SCALBERT, A. & WILLIAMSON, G. 2000. Dietary Intake and Bioavailability of Polyphenols. *The Journal of Nutrition,* 130**,** 2073S-2085S.
SCHAART, J. G., DUBOS, C., ROMERO DE LA FUENTE, I., VAN HOUWELINGEN, A. M. M. L., DE VOS, R. C. H., JONKER, H. H., XU, W., ROUTABOUL, J.-M., LEPINIEC, L. & BOVY, A. G. 2013. Identification and characterization of MYB-bHLH-WD40 regulatory complexes controlling proanthocyanidin biosynthesis in strawberry (Fragaria × ananassa) fruits. *New Phytologist,* 197**,** 454-467.
SCHIJLEN, E., VOS, C. H. R. D., JONKER, H., BROECK, H. V. D., MOLTHOFF, J., TUNEN, A. V., MARTENS, S. & BOVY, A. 2006. Pathway engineering for healthy phytochemicals leading to the production of novel flavonoids in tomato fruit. *Plant Biotechnology Journal,* 4**,** 433-444.
SCHIJLEN, E. G. W. M., DE VOS, C. H. R., MARTENS, S., JONKER, H. H., ROSIN, F. M., MOLTHOFF, J. W., TIKUNOV, Y. M., ANGENENT, G. C., VAN TUNEN, A. J. & BOVY, A. G. 2007. RNA Interference Silencing of Chalcone Synthase, the First Step in the Flavonoid Biosynthesis Pathway, Leads to Parthenocarpic Tomato Fruits. *Plant Physiol.,* 144**,** 1520-1530.
SCHIJLEN, E. G. W. M., RIC DE VOS, C. H., VAN TUNEN, A. J. & BOVY, A. G. 2004. Modification of flavonoid biosynthesis in crop plants. *Phytochemistry,* 65**,** 2631-2648.
SCHILMILLER, A. L., STOUT, J., WENG, J. K., HUMPHREYS, J., RUEGGER, M. O. & CHAPPLE, C. 2009. Mutations in the cinnamate 4-hydroxylase gene impact metabolism, growth and development in Arabidopsis. *Plant Journal,* 60**,** 771-782.
SCHULZE, A. & HARRIS, A. L. 2012. How cancer metabolism is tuned for proliferation and vulnerable to disruption. *Nature,* 491**,** 364-73.
SCHWINN, K., VENAIL, J., SHANG, Y., MACKAY, S., ALM, V., BUTELLI, E., OYAMA, R., BAILEY, P., DAVIES, K. & MARTIN, C. 2006. A Small Family of MYB-Regulatory Genes

Controls Floral Pigmentation Intensity and Patterning in the Genus Antirrhinum. *Plant Cell,* 18**,** 831-851.
SERRA, A., MACIÀ, A., ROMERO, M.-P., PIÑOL, C. & MOTILVA, M.-J. 2011. Rapid methods to determine procyanidins, anthocyanins, theobromine and caffeine in rat tissues by liquid chromatography-tandem mass spectrometry. *Journal of Chromatography B,* 879**,** 1519-1528.
SHERRATT, H. S. A. 1958. The relationship between anthocyanidins and flavonols in different genotypes ofAntirrhinum majus. *Journal of Genetics,* 56**,** 28-36.
SHIH, P.-H., YEH, C.-T. & YEN, G.-C. 2005. Effects of anthocyanidin on the inhibition of proliferation and induction of apoptosis in human gastric adenocarcinoma cells. *Food and Chemical Toxicology,* 43**,** 1557-1566.
SHIN, D. Y., LEE, W. S., LU, J. N., KANG, M. H., RYU, C. H., KIM, G. Y., KANG, H. S., SHIN, S. C. & CHOI, Y. H. 2009. Induction of apoptosis in human colon cancer HCT-116 cells by anthocyanins through suppression of Akt and activation of p38-MAPK. *Int J Oncol,* 35**,** 1499-504.
SHIN, D. Y., LU, J. N., KIM, G. Y., JUNG, J. M., KANG, H. S., LEE, W. S. & CHOI, Y. H. 2011. Anti-invasive activities of anthocyanins through modulation of tight junctions and suppression of matrix metalloproteinase activities in HCT-116 human colon carcinoma cells. *Oncol Rep,* 25**,** 567-72.
SIRITUNGA, D. & SAYRE, R. 2003. Generation of cyanogen-free transgenic cassava. *Planta,* 217**,** 367-373.
SLEE, E. A., HARTE, M. T., KLUCK, R. M., WOLF, B. B., CASIANO, C. A., NEWMEYER, D. D., WANG, H. G., REED, J. C., NICHOLSON, D. W., ALNEMRI, E. S., GREEN, D. R. & MARTIN, S. J. 1999. Ordering the cytochrome c-initiated caspase cascade: hierarchical activation of caspases-2, -3, -6, -7, -8, and -10 in a caspase-9-dependent manner. *J Cell Biol,* 144**,** 281-92.
SLIMESTAD, R. & SOLHEIM, H. 2002. Anthocyanins from black currants (Ribes nigrum L.). *J Agric Food Chem,* 50**,** 3228-31.
SMITH, T. F., GAITATZES, C., SAXENA, K. & NEER, E. J. 1999. The WD repeat: a common architecture for diverse functions. *Trends in Biochemical Sciences,* 24**,** 181-185.
SOFI, F., CESARI, F., ABBATE, R., GENSINI, G. F. & CASINI, A. 2008. Adherence to Mediterranean diet and health status: meta-analysis. *BMJ,* 337**,** a1344.
STEPHENS, P., GREENMAN, C., FU, B., YANG, F., BIGNELL, G., MUDIE, L., PLEASANCE, E., LAU, K., BEARE, D., STEBBINGS, L., MCLAREN, S., LIN, M.-L., MCBRIDE, D., VARELA, I., NIK-

ZAINAL, S., LEROY, C., JIA, M., MENZIES, A., BUTLER, A., TEAGUE, J., QUAIL, M., BURTON, J., SWERDLOW, H., CARTER, N., MORSBERGER, L., IACOBUZIO-DONAHUE, C., FOLLOWS, G., GREEN, A., FLANAGAN, A., STRATTON, M., FUTREAL, A. & CAMPBELL, P. 2011. Massive Genomic Rearrangement Acquired in a Single Catastrophic Event during Cancer Development. *Cell,* 144**,** 27-40.

STONER, G. D. 2009. Foodstuffs for Preventing Cancer: The Preclinical and Clinical Development of Berries. *Cancer Prevention Research,* 2**,** 187-194.

STRATTON, M. R., CAMPBELL, P. J. & FUTREAL, P. A. 2009. The cancer genome. *Nature,* 458**,** 719-24.

SUN, J. & HAI LIU, R. 2006. Cranberry phytochemical extracts induce cell cycle arrest and apoptosis in human MCF-7 breast cancer cells. *Cancer Letters,* 241**,** 124-134.

SURH, Y. J. 2003. Cancer chemoprevention with dietary phytochemicals. *Nat Rev Cancer,* 3**,** 768-80.

SUZUKI, K.-I., XUE, H.-M., TANAKA, Y., FUKUI, Y., FUKUCHI-MIZUTANI, M., MURAKAMI, Y., KATSUMOTO, Y., TSUDA, S. & KUSUMI, T. 2000. Flower color modifications of Torenia hybrida by cosuppression of anthocyanin biosynthesis genes. *Molecular Breeding,* 6**,** 239-246.

SYED, D. N., AFAQ, F., SARFARAZ, S., KHAN, N., KEDLAYA, R., SETALURI, V. & MUKHTAR, H. 2008. Delphinidin inhibits cell proliferation and invasion via modulation of Met receptor phosphorylation. *Toxicology and Applied Pharmacology,* 231**,** 52-60.

TANAKA, T., KOJIMA, T., KAWAMORI, T., YOSHIMI, N. & MORI, H. 1993. CHEMOPREVENTION OF DIETHYLNITROSAMINE-INDUCED HEPATOCARCINOGENESIS BY A SIMPLE PHENOLIC-ACID PROTOCATECHUIC ACID IN RATS. *Cancer Research,* 53**,** 2775-2779.

TANAKA, Y., SASAKI, N. & OHMIYA, A. 2008. Biosynthesis of plant pigments: anthocyanins, betalains and carotenoids. *The Plant Journal,* 54**,** 733-749.

TANG, L. K., CHU, H., YIP, W. K., YEUNG, E. C. & LO, C. 2009. An anther-specific dihydroflavonol 4-reductase-like gene (DRL1) is essential for male fertility in Arabidopsis. *New Phytologist,* 181**,** 576-587.

TAYLOR, L. P. & GROTEWOLD, E. 2005. Flavonoids as developmental regulators. *Current Opinion in Plant Biology,* 8**,** 317-323.

TCHERNOF, A. & DESPRÉS, J. P. 2000. Sex Steroid Hormones, Sex Hormone-Binding Globulin, and Obesity in Men and Women. *Horm Metab Res,* 32**,** 526-536.

THIELE, W., ROTHLEY, M., TELLER, N., JUNG, N., BULAT, B., PLAUMANN, D., VANDERHEIDEN, S., SCHMAUS, A., CREMERS, N., GÖPPERT, B., DIMMLER, A., ESCHBACH, V., QUAGLIATA, L., THALER, S., MARKO, D., BRÄSE, S. & SLEEMAN, J. P. 2013. Delphinidin is a novel inhibitor of lymphangiogenesis, but promotes mammary tumor growth and metastasis formation in syngeneic experimental rats. *Carcinogenesis*.

TITTA, L., TRINEI, M., STENDARDO, M., BERNIAKOVICH, I., PETRONI, K., TONELLI, C., RISO, P., PORRINI, M., MINUCCI, S., PELICCI, P. G., RAPISARDA, P., RECUPERO, G. R. & GIORGIO, M. 2010. Blood orange juice inhibits fat accumulation in mice. *Int J Obes,* 34**,** 578-588.

TOLEDO-ORTIZ, G., HUQ, E. & QUAIL, P. H. 2003. The Arabidopsis basic/helix-loop-helix transcription factor family. *Plant Cell,* 15**,** 1749-70.

TORRES, C. A., DAVIES, N. M., YANEZ, J. A. & ANDREWS, P. K. 2005. Disposition of selected flavonoids in fruit tissues of various tomato (lycopersicon esculentum mill.) Genotypes. *J Agric Food Chem,* 53**,** 9536-43.

TREMAROLI, V. & BACKHED, F. 2012. Functional interactions between the gut microbiota and host metabolism. *Nature,* 489**,** 242-9.

TRICHOPOULOU, A., COSTACOU, T., BAMIA, C. & TRICHOPOULOS, D. 2003. Adherence to a Mediterranean Diet and Survival in a Greek Population. *New England Journal of Medicine,* 348**,** 2599-2608.

TRICHOPOULOU, A., LAGIOU, P., KUPER, H. & TRICHOPOULOS, D. 2000. Cancer and Mediterranean Dietary Traditions. *Cancer Epidemiology Biomarkers & Prevention,* 9**,** 869-873.

TROCK, B. J., HILAKIVI-CLARKE, L. & CLARKE, R. 2006. Meta-Analysis of Soy Intake and Breast Cancer Risk. *Journal of the National Cancer Institute,* 98**,** 459-471.

TSENG, T. H., HSU, J. D., LO, M. H., CHU, C. Y., CHOU, F. P., HUANG, C. L. & WANG, C. J. 1998. Inhibitory effect of Hibiscus protocatechuic acid on tumor promotion in mouse skin. *Cancer Letters,* 126**,** 199-207.

TSUDA, H., TAKARABE, T., HASEGAWA, F., FUKUTOMI, T. & HIROHASHI, S. 2000. Large, central acellular zones indicating myoepithelial tumor differentiation in high-grade invasive ductal carcinomas as markers of predisposition to lung and brain metastases. *Am J Surg Pathol,* 24**,** 197-202.

TSUDA, T., HORIO, F. & OSAWA, T. 1999. Absorption and metabolism of cyanidin 3-O-β-D-glucoside in rats. *FEBS Letters,* 449**,** 179-182.

TSUGANE, S. & SASAZUKI, S. 2007. Diet and the risk of gastric cancer: review of epidemiological evidence. *Gastric Cancer,* 10**,** 75-83.
TUNG, H. T., TSUKUMA, H., TANAKA, H., KINOSHITA, N., KOYAMA, Y., AJIKI, W., OSHIMA, A. & KOYAMA, H. 1999. Risk Factors for Breast Cancer in Japan, with Special Attention to Anthropometric Measurements and Reproductive History. *Japanese Journal of Clinical Oncology,* 29**,** 137-146.
VAN DER MEER, I. M., STAM, M. E., VAN TUNEN, A. J., MOL, J. N. & STUITJE, A. R. 1992. Antisense inhibition of flavonoid biosynthesis in petunia anthers results in male sterility. *Plant Cell,* 4**,** 253-62.
VAN RIJT, S. H. & SADLER, P. J. 2009. Current applications and future potential for bioinorganic chemistry in the development of anticancer drugs. *Drug Discovery Today,* 14**,** 1089-1097.
VANDEN BERGHE, W. 2012. Epigenetic impact of dietary polyphenols in cancer chemoprevention: Lifelong remodeling of our epigenomes. *Pharmacological Research,* 65**,** 565-576.
VENTURA, A., KIRSCH, D. G., MCLAUGHLIN, M. E., TUVESON, D. A., GRIMM, J., LINTAULT, L., NEWMAN, J., RECZEK, E. E., WEISSLEDER, R. & JACKS, T. 2007. Restoration of p53 function leads to tumour regression in vivo. *Nature,* 445**,** 661-5.
VERBERNE, L., BACH-FAIG, A., BUCKLAND, G. & SERRA-MAJEM, L. 2010. Association Between the Mediterranean Diet and Cancer Risk: A Review of Observational Studies. *Nutrition and Cancer,* 62**,** 860-870.
VITAGLIONE, P., DONNARUMMA, G., NAPOLITANO, A., GALVANO, F., GALLO, A., SCALFI, L. & FOGLIANO, V. 2007. Protocatechuic Acid Is the Major Human Metabolite of Cyanidin-Glucosides. *The Journal of Nutrition,* 137**,** 2043-2048.
VODUC, K. D., CHEANG, M. C. U., TYLDESLEY, S., GELMON, K., NIELSEN, T. O. & KENNECKE, H. 2010. Breast Cancer Subtypes and the Risk of Local and Regional Relapse. *Journal of Clinical Oncology,* 28**,** 1684-1691.
WANG, H., CAO, G. & PRIOR, R. L. 1997. Oxygen Radical Absorbing Capacity of Anthocyanins. *Journal of Agricultural and Food Chemistry,* 45**,** 304-309.
WANG, L.-S., KUO, C.-T., CHO, S.-J., SEGUIN, C., SIDDIQUI, J., STONER, K., WENG, Y.-I., HUANG, T. H. M., TICHELAAR, J., YEARSLEY, M., STONER, G. D. & HUANG, Y.-W. 2013. Black Raspberry-Derived Anthocyanins Demethylate Tumor Suppressor Genes Through the Inhibition of DNMT1 and DNMT3B in Colon Cancer Cells. *Nutrition and Cancer,* 65**,** 118-125.

WANG, Q., CHEN, Q., HE, M., MIR, P., SU, J. & YANG, Q. 2011. Inhibitory Effect of Antioxidant Extracts From Various Potatoes on the Proliferation of Human Colon and Liver Cancer Cells. *Nutrition and Cancer-an International Journal,* 63**,** 1044-1052.

WĘSIERSKA-GĄDEK, J., KRAMER, M. P. & MAURER, M. 2008. Resveratrol modulates roscovitine-mediated cell cycle arrest of human MCF-7 breast cancer cells. *Food and Chemical Toxicology,* 46**,** 1327-1333.

WILLETT, W. C. 2010. Fruits, Vegetables, and Cancer Prevention: Turmoil in the Produce Section. *Journal of the National Cancer Institute,* 102**,** 510-511.

WILLIAMS, D. H., STONE, M. J., HAUCK, P. R. & RAHMAN, S. K. 1989. Why Are Secondary Metabolites (Natural Products) Biosynthesized? *Journal of Natural Products,* 52**,** 1189-1208.

WILLIAMS, R., SPENCER, J. & RICE-EVANS, C. 2004. Flavonoids: antioxidants or signalling molecules? *Free Radical Biology and Medicine,* 36**,** 838 - 849.

WILLIAMSON, G., BARRON, D., SHIMOI, K. & TERAO, J. 2005. In vitro biological properties of flavonoid conjugates found in vivo. *Free Radic Res,* 39**,** 457-69.

WILLSTÄTTER, R. & EVEREST, A. E. 1913. Untersuchungen über die Anthocyane. I. Über den Farbstoff der Kornblume. *Justus Liebigs Annalen der Chemie,* 401**,** 189-232.

WINK, M., ASHOUR, M. L. & EL-READI, M. Z. 2012. Secondary Metabolites from Plants Inhibiting ABC Transporters and Reversing Resistance of Cancer Cells and Microbes to Cytotoxic and Antimicrobial Agents. *Front Microbiol,* 3**,** 130.

XIA, M., LING, W., ZHU, H., MA, J., WANG, Q., HOU, M., TANG, Z., GUO, H., LIU, C. & YE, Q. 2009. Anthocyanin attenuates CD40-mediated endothelial cell activation and apoptosis by inhibiting CD40-induced MAPK activation. *Atherosclerosis,* 202**,** 41-47.

YI, W., AKOH, C. C., FISCHER, J. & KREWER, G. 2006. Absorption of Anthocyanins from Blueberry Extracts by Caco-2 Human Intestinal Cell Monolayers. *Journal of Agricultural and Food Chemistry,* 54**,** 5651-5658.

YOUNES-SAKR, L., SENESSE, P., LAURENT, C., ROUANET, J. M., RUGANI, N., CRISTOL, J. P. & GAILLET, S. 2012. Validation of a Surgical Technique for Rat Intestinal Irradiation: Potential Side Effects Prevention by Dietary Grape Phenolics. *Digestive Diseases and Sciences,* 57**,** 2562-2570.

YUN, J. M., AFAQ, F., KHAN, N. & MUKHTAR, H. 2009. Delphinidin, an anthocyanidin in pigmented fruits and vegetables, induces

apoptosis and cell cycle arrest in human colon cancer HCT116 cells. *Mol Carcinog,* 48**,** 260-70.

YUN, J. W., LEE, W. S., KIM, M. J., LU, J. N., KANG, M. H., KIM, H. G., KIM, D. C., CHOI, E. J., CHOI, J. Y., KIM, H. G., LEE, Y.-K., RYU, C. H., KIM, G., CHOI, Y. H., PARK, O. J. & SHIN, S. C. 2010. Characterization of a profile of the anthocyanins isolated from Vitis coignetiae Pulliat and their anti-invasive activity on HT-29 human colon cancer cells. *Food and Chemical Toxicology,* 48**,** 903-909.

ZENG, X.-Q., CHOW, W. S., SU, L.-J., PENG, X.-X. & PENG, C.-L. 2010. Protective effect of supplemental anthocyanins on Arabidopsis leaves under high light. *Physiologia Plantarum,* 138**,** 215-225.

ZHANG, X. Y., LI, W. G., WU, Y. J., ZHENG, T. Z., LI, W., QU, S. Y. & LIU, N. F. 2005a. Proanthocyanidin from grape seeds potentiates anti-tumor activity of doxorubicin via immunomodulatory mechanism. *Int Immunopharmacol,* 5**,** 1247-57.

ZHANG, Y., VAREED, S. K. & NAIR, M. G. 2005b. Human tumor cell growth inhibition by nontoxic anthocyanidins, the pigments in fruits and vegetables. *Life Sciences,* 76**,** 1465-1472.

ZHAO, F.-J. & SHEWRY, P. R. 2011. Recent developments in modifying crops and agronomic practice to improve human health. *Food Policy,* 36, Supplement 1**,** S94-S101.

ZHU, H.-F., FITZSIMMONS, K., KHANDELWAL, A. & KRANZ, R. G. 2009. CPC, a Single-Repeat R3 MYB, Is a Negative Regulator of Anthocyanin Biosynthesis in Arabidopsis. *Molecular Plant,* 2**,** 790-802.

ZIEGLER, R. G., HOOVER, R. N., PIKE, M. C., HILDESHEIM, A., NOMURA, A. M., WEST, D. W., WU-WILLIAMS, A. H., KOLONEL, L. N., HORN-ROSS, P. L., ROSENTHAL, J. F. & HYER, M. B. 1993. Migration patterns and breast cancer risk in Asian-American women. *J Natl Cancer Inst,* 85**,** 1819-27.

ZUFALL, R. A. & RAUSHER, M. D. 2004. Genetic changes associated with floral adaptation restrict future evolutionary potential. *Nature,* 428**,** 847-50.

Appendix

Chapter 2 related:

Tomato transformation growth media and supplements

Regeneration medium contained 1x MS salts, myo-inositol 100 mg/L, 1x Nitsch's vitamins, Sucrose 20 g/L, Agargel 4 g/L and was adjusted to pH 6.0 with KOH. After autoclaving the shoot-inducing cytokinin trans-zeatin riboside was added to the medium at 2mg/L. The antibiotics, augmentin and kanamycin, were added at 500 µg/mL and 100 µg/mL, respectively, to select for the T-DNA transformation markers.

Table 2.1: Nitsch's Vitamins composition and concentration

Compound	**Final concentration mg/L**	**1000x stock (mg/100ml)**
Thiamine	0.5	50
Glycine	2.0	200
Nicotinic acid	5.0	500
Pyridoxine HCl	0.5	50
Folic acid	0.5	50
Biotin	0.05	5

Shooting medium contained 0.5x MS medium, Sucrose at 5g/L, Gelrite at 2.25g/L and was adjusted to pH 6.0 with KOH. The antibiotics, timentin at 320 mg/L and kanamycin at 50 mg/L, were added to the medium to kill the *Agrobacterium* and select for transformed shoots, respectively.